Distribution Agreement

In presenting this thesis or dissertation as a partial fulfillment of the requirements for an advanced degree from Emory University, I hereby grant to Emory University and its agents the nonexclusive license to archive, make accessible, and display my thesis or dissertation in whole or in part in all forms of media, now or hereafter known, including display on the world wide web. I understand that I may select some access restrictions as part of the online submission of this thesis or dissertation. I retain all ownership rights to the copyright of the thesis or dissertation. I also retain the right to use in future works (such as articles or books) all or part of this thesis or dissertation.

Signature:

_____ _____

Akram Salam Date

Development of a novel antibiotic adjuvant strategy against hypervirulent Community-Associated Methicillin-Resistant *Staphylococcus aureus*

By
Akram Salam
Doctor of Philosophy

Graduate Division of Biological and Biomedical Science
Molecular and Systems Pharmacology

_____
Cassandra L. Quave, Ph.D.
Advisor

_____
Christine M. Dunham, Ph.D.
Committee Member

_____
Haian Fu, Ph.D.
Committee Member

_____
Bruce R. Levin, M.D, Ph.D.
Committee Member

_____
Edward T. Morgan, Ph.D.
Committee Member

_____
Timothy D. Read, Ph.D.
Committee Member

Accepted:

_____
Lisa A. Tedesco, Ph.D.
Dean of the James T. Laney School of Graduate Studies

_____
Date

Development of a novel antibiotic adjuvant strategy against hypervirulent Community-Associated Methicillin-Resistant *Staphylococcus aureus*

By

Akram Salam
B.S., University of Rochester

Advisor: Cassandra Quave, Ph.D.

An abstract of
A dissertation submitted to the Faculty of the
James T. Laney School of Graduate Studies of Emory University
in partial fulfillment of the requirements for the degree of
Doctor of Philosophy
in the Graduate Division of Biological and Biomedical Sciences,
Molecular and Systems Pharmacology
2020

Abstract

Development of a novel antibiotic adjuvant strategy against hypervirulent Community-Associated Methicillin-Resistant *Staphylococcus aureus*

By Akram Salam

Methicillin-resistant *Staphylococcus aureus* (MRSA) represents one of the most serious infectious disease concerns worldwide, with the CDC labeling it a “serious threat” in 2019. The current arsenal of antibiotics works by targeting growth and survival, which exerts great selective pressure for the development of resistance. The development of novel anti-infectives that inhibit virulence in MRSA has been recurrently proposed as a promising therapeutic approach. In order to discover drug leads that work, we looked to nature. Previous studies on rural Italian traditional medicine confirm that select extracts of plants used in traditional medicinal preparations for the treatment of dermatological ailments exert antivirulence activity against MRSA. In a follow-up of a study examining the *S. aureus* quorum sensing inhibitory activity of Italian plants used in local traditional medicine, extract 224C-F2 was reported as a bioactive fraction of a *Castanea sativa* (European chestnut) extract. The fraction demonstrated high quorum sensing inhibitory activity against MRSA *in vitro* and effective attenuation of pathogenicity in a mouse model of skin infection.

Through further bioassay-guided fractionation using reverse-phase high performance liquid chromatography, a novel hydroperoxy cycloartane triterpenoid, castaneroxy A, was isolated. Its structure was confirmed by X-ray crystallography, mass spectrometry, and nuclear magnetic resonance. An isomer of castaneroxy A was also detected in an adjacent fraction, with a possible third isomer as a minor constituent. The castaneroxys are unique in that they possess not only a hydroperoxy group but also a cyclopropyl group, both of which are rare. In a series of assays assessing inhibition of markers of *S. aureus* virulence, castaneroxy A

exerted activities in the low micromolar range. Castaneroxy A inhibited *agr*::P3 activation (IC_{50} = 31.72 µM), δ-toxin production (IC_{50} = 31.72 µM in NRS385), supernatant cytotoxicity to HaCaT human keratinocytes (IC_{50} = 7.93 µM in NRS385), and rabbit erythrocyte hemolytic activity (IC_{50} = 7.93 µM in LAC). Castaneroxy A also demonstrated no effect on biofilm production and no cytotoxicity to HaCaTs at 31.72 µM and below. Finally, castaneroxy A was shown to abate MRSA-induced dermonecrosis in a mouse model of skin infection. The results establish castaneroxy A as a promising antivirulence drug lead for development against *S. aureus* and at the same time validate the ethnobotanical anti-infective value of *C. sativa* leaves.

Development of a novel antibiotic adjuvant strategy against hypervirulent Community-Associated Methicillin-Resistant *Staphylococcus aureus*

By

Akram Salam
B.S., University of Rochester

Advisor: Cassandra Quave, Ph.D.

An abstract of
A dissertation submitted to the Faculty of the
James T. Laney School of Graduate Studies of Emory University
in partial fulfillment of the requirements for the degree of
Doctor of Philosophy
in the Graduate Division of Biological and Biomedical Sciences,
Molecular and Systems Pharmacology
2020

Acknowledgements

Thank you, Dr. Cassandra Quave, for your mentorship over the years. It is thanks to you that I developed the work ethic and technical skills to do high-quality research. I came into the lab with a love for chemistry and the diversity and complexity of the natural products that plants make. Now I leave the lab not only with a deeper love for the chemistry but also with a profound love for the plants themselves and the field of ethnobotany.

I spent by far the most time with you, Dr. James Lyles. The culture of warmth and excellence you affected in the phytochemistry lab helped me and really all of us grow into sharper and more collaborative scientists. From the very beginning I saw you as a role model for being kind, analytical, hardworking, and quick on my feet. Thanks for teaching me so much and being there for me, James.

Since you arrived in the later part of my doctoral work, you have been a very important mentor, Dr. Gina Porras. I learned a lot more from you than just NMR. Thanks for all the times you went above and beyond to help me, Gina.

I extend a big thank you to you, my dissertation committee: Dr. Christine Dunham, Dr. Haian Fu, Dr. Bruce Levin, Dr. Edward Morgan, and Dr. Timothy Read. You all greatly improved the quality of this dissertation, and you were each very supportive of me over the years. I spent the most time with you, Eddie, especially as a teaching assistant, and I am so grateful to have had you as a pharmacology mentor and as someone to reach out to.

And to my dear friends who I spent a lot of time with during my time as a PhD candidate: Rozenn, Faraz, Jessica, Sarah, Fabien, Vika, Olya, Diana, Rahmat, Elena Yurevna, Kevin, Sasha, Natasha, Lewis, Cate, and Natalia. My life became so much richer with you guys. And when times got rough I could keep going thanks to you.

Finally, I could not have achieved what I achieved without the most loving mother in the world and the smartest and coolest sister in the world. There were many stretches of weeks when we could not spend so much time together, and you guys were steadfastly supportive in those times. There were also many stretches of weeks where we spent a lot of time together, and those were the best times of all.

Table of Contents

Contents

List of Figures and Tables

List of Abbreviations

AI	artificial intelligence
AIP	autoinducing peptide
APCI	atmospheric-pressure chemical ionization
ASE	accelerated solvent extraction
ATCC	American Type Culture Collection
BALB	Bagg Albino
CA	community-associated
CASE	computer-assisted structure elucidation
CFM-ID	Competitive Fragmentation Modeling-ID
CFU	colony-forming units
ChEMBL	database of bioactive molecules
CHIKV	chikungunya virus
CLIME	clustering by inferred models of evolution
COSY	correlation spectroscopy
CSA	chemical shift anisotropy
DC	dipolar coupling
DEPT	distortionless enhancement by polarization transfer
DESI	desorption electrospray ionization
DFT	density functional theory
DMSO	dimethylsulfoxide
DNA	deoxyribonucleic acid
DNP	Dictionary of Natural Products
DSF	diffusible signal factor
ELSD	evaporative light scattering detector
cryo-EM	cryo-electron microscopy
EMSA	electrophoretic mobility shift assay
ESI	electrospray ionization
FDA	Food and Drug Administration
FID	flame ioization detector
FID	free induction decay
FT	Fourier transform
FT-IR	Fourier Transform-Infrared
GACP	Good Agricultural and Collection Practices
GC	gas chromatography
GNPS	Global Natural Product Social Networking
GOT	geranylpyrophosphate:olivetolate geranyltransferase
HETCOR	heteronuclear correlation
HILIC	hydrophilic interaction chromatography
HMBC	heteronuclear multiple bond correlation
HMQC	heteronuclear multiple quantum coherence
HPLC	high performance liquid chromatography
HRMS	high resolution mass spectrometry
HRESIMS	high resolution electrospray ionization mass spectrometry
HSQC	heteronuclear single quantum correlation

HTS	high throughput screening
IBM	International Business Machines
IMS	imaging mass spectrometry
ISBN	International Standard Book Number
KEGG	Kyoto Encyclopedia of Genes and Genomes
LAC	Los Angeles colony
LAESI	laser ablation electrospray ionization
LC	liquid chromatography
LDH	lactate dehydrogenase
LNA	locked nucleic acid
LTQ-FT	Linear Trap Quadrupole-Fourier Transform
MADByTE	Metabolomics And Dereplication By Two-dimensional Experiments
MAE	microwave-assistaed extraction
MALDI	matrix assisted laser desorption ionization
MIC	minimum inhibitory concentration
microED	microcrystal electron diffraction
ML	machine learning
MN	molecular networking
MRS	magnetic resonance spectroscopy
MRSA	methicillin-resistant Staphylococcus aureus
MS	mass spectrometry
MSI	mass spectrometry imagining
MSSA	methicillin-sensitive Staphylococcus aureus
NAPRALERT	Natural Products Alert
NIAID	National Institute of Allergy and Infectious Diseases
NIH	National Institutes of Health
NMR	nuclear magnetic resonance
NOE	nuclear Overauser effect
NOESY	nuclear Overhauser effect spectroscopy
NORINE	database of nonribosomal peptides
4-OH-ICN	4-hydroxyindole-3carbonyl nitrile
OHM	ω-hydroxyemodin
OXA	oxacillin
PCA	principle component analysis
PCR	polymerase chain reaction
PDA	photodiode array
PMCID	PubMed Central Identification
PMN	polymorphonuclear leukocytes
PQS	Pseudomonas quinolone signal
PSM	phenol-soluble modulin
QQ	quorum quenching
QS	quorum sensing
RCSA	residual chemical shift anisotropy
RDC	residual dipolar coupling
RF	radio frequency
RIP	RNAIII inhibiting peptide

RNA	ribonucleic acid
RP	reverse phase
RXR	retinoid X receptor
SCF	supercritical fluid
SFC	supercritical fluid chromatography
SFE	supercritical fluid extraction
antiSMASH	antibiotics & Secondary Metabolite Analysis SHell
SMILES	simplified molecular-input line-entry system
SPE	solid phase extraction
SPiDER	self-organizing map-based prediction of drug equivalence relationships
SSTI	skin and soft tissue infection
TCD	thermal conductivity detector
TOCSY	total correlation spectroscopy
TOF	time-of-flight
UAE	ultrasound-assisted extraction
UPLC	ultra-performance liquid chromatography
US	United States
USA	United States of America
UV	ultraviolet
WHO	World Health Organization
XCMS	bioinformatics software for statistical analysis of mass spectrometry data
YFP	yellow fluorescent protein

CHAPTER I

Introduction

This dissertation serves to add to the body of scientific knowledge concerning bioactive compounds from nature by applying the principles of pharmacology to two fields: ethnobotany and microbiology. While to many it may at first glance seem that these two fields are unrelated, at least one concept does connect them: by leveraging existing human knowledge of the medicinal uses of plants, plant chemicals can be discovered that represent promising anti-infective candidates. These two fields, then, are connected by chemistry; specifically, phytochemistry encompasses the knowledge of extracting, isolating, and identifying plant compounds via chromatography and spectroscopic techniques. Indeed, the Quave Research Group necessarily works within all three spheres of research in order to discover plant natural products with promising antibiotic or anti-infective activity for drug development. Not only is this line of research unique due to its interdisciplinary nature, but also because it connects some of the most ancient human knowledge – the knowledge of traditional medicine – to the most cutting edge knowledge in drug discovery that man possesses today. This line of research is not new, however. “The interdisciplinary scientific exploration of biologically active agents traditionally employed or observed by man” is called ethnopharmacology (1).

The research compiled into this dissertation represents a continuation of a study that my mentor Dr. Cassandra Quave began, and our research has its roots in traditional medicine (2). Since time immemorial, humans, as well as our ancestors and even other animals, have looked to Nature for medicines for the ailments that befell them. For example, eating a particular type of mushroom could relieve a malady of the gut, as was deduced from a mummified corpse of Ötzi the Iceman in northern Italy. At the time of his death sometime between 3400 and 3100 B.C., Ötzi, who was suffering from intestinal worms, was carrying birch fungus, a fungus now known to have antihelminthic properties (3). Throughout history,

all civilizations developed their own systems of medicine using the plants and other organisms around them (4). Even today, in most countries traditional medicine plays a major role in primary health care (5). While over the centuries and especially recently some traditional medicinal knowledge has been forgotten, these systems have been optimized through trial and error. One need only look to the profound knowledge of the identities and medicinal effects of plants possessed by different peoples, such as those of the Amazon Rainforest (6).

When ethnobotanists travel to communities across the world and engage with their traditional medicinal practices, one of their goals is to identify which plants have been confirmed by the people as having a therapeutic effect when prepared as a medicine. Using this knowledge, and with the necessary permissions and agreements with the community visited, an ethnobotanist may further study plants of interest in order to discover medicinal chemicals contained within. If, for example, the leaves of a tree have been used to prepare a wash that heals skin inflammations, there is a high likelihood that those leaves contain at least one anti-inflammatory or anti-infective compound to which the therapeutic effects can be attributed. This is where the knowledge of phytochemistry and microbiology enter the research workflow, allowing for the ethnopharmacological study of the plant's chemistry and its effects on bacteria.

The first step is the extraction of chemicals from the plant part of interest (7). There are many different types of extraction techniques, the one perhaps most familiar to the non-scientist being the infusion, which is how tea is made by extracting the chemicals from tea leaves into hot water. After an extract is made, phytochemical and microbiological studies – and great effort – hopefully lead to the identification and isolation of an anti-infective compound. The

basic framework for performing these studies is bioassay-guided fractionation of the plant extract. Through bioassay-guided fractionation, a crude plant extract, usually containing hundreds of unique chemicals, is iteratively fractionated by chromatographic techniques to separate its constituents into fractions based on chemical properties such as hydrophobicity. The fractions are then assayed for a particular bioactivity in a screen; the most bioactive fraction, considered to be enriched for bioactive natural products for the activity of interest, is selected for further fractionation. This process is repeated for a number of iterations until compound isolation is achieved and confirmed through spectroscopic analysis. New technologies and techniques such as pre-fractionation, metabolomics, and molecular networking aid in streamlining this workflow. If a compound was isolated from a plant used in traditional medicine to treat skin infections, this compound may represent a hit for a particular anti-infective indication. That hit can be further studied for assessment of its pharmacodynamics, such as mechanism of action and potency, and pharmacokinetics, such as metabolic stability and plasma protein binding.

In this dissertation, I have continued the ethnopharmacological work of Dr. Cassandra Quave on the anti-infective activity of an extract of the leaves of *Castanea sativa*, the European Chestnut, against the Gram-positive bacterial pathogen *Staphylococcus aureus* (8). This research presents two layers of innovation: (1) it looks to plant chemicals for the discovery of new anti-infective agents, and (2) it seeks to identify chemistry that specifically inhibits virulence, or infective ability, in *S. aureus* rather than growth, as conventional antibiotics do. This second layer of innovation is especially valuable, as the literature on antibiotic resistance cites growth inhibition of bacteria by conventional antibiotics as the key driver of resistance, and it also cites inhibition of virulence as a new, promising strategy for slowing or even circumventing resistance (9; 10).

Antibiotics have revolutionized medicine since their introduction in the early 1900s (9). Not only have more infants and children been able to survive into adulthood, but lifespans in general in the past century have nearly doubled thanks in large part to antibiotics. Antibiotics allow for the treatment of infections that once had extremely high morbitity rates in patients, and they allow for invasive surgical operations to be done safely. Although there are numerous classes of antibiotics in the clinic today, all of them exert their antibiotic activity through either a bactericidal or bacteriostatic mechanism (11). Bactericidal antibiotics kill specific target bacteria while bacteriostatic antibiotics prevent the further growth of target bacteria. Both mechanisms involve the inhibition of bacterial growth. Due to their growth inhibitory effects, continued use antibiotics eventually leads to antibiotic resistance (12). Bacterial growth occurs by cell division, and because bacteria rapidly divide, cells can be found in a population of bacteria with genetic mutations. Antibiotics place selective pressure for the development of resistance in bacteria by targeting biological processes in bacterial cells essential for survival, thus inhibiting growth. Cells that become resistant to an antibiotic are those that develop particular mutations in genes involved in the mechanism of action of an antibiotic. If the essential biological process that the antibiotic perturbs is no longer affected by treatment due to the mutation, those cells can continue to grow and enrich the population of bacteria in the presence of the antibiotic. The increase in the spread of antibiotic resistance is monitored by numerous organizations, at the forefront of which are the Centers for Disease Control and Prevention and the World Health Organization (12; 13). In 2019, both organizations have designation methicillin-resistant *S. aureus* (MRSA) as a serious threat to public health, with new therapeutic strategies urgently needed (14; 15).

In order to target virulence in MRSA, I have targeted the *agr* system, one of the key governors of virulence in the pathogen (16). The *agr* system makes up the quorum sensing system of *S. aureus*. Quorum sensing is a system of stimuli and response between cells in a bacterial population that coordinates certain behaviors such as virulence, antibiotic resistance, and biofilm formation based on the local population density (16).

Many bacteria have several systems that contribute to quorum sensing; as for *S. aureus*, the accessory gene regulator (*agr*) system coordinates the majority of virulence factors and is thus the main target of antivirulence compounds (17; 18). The *agr* system is encoded in the *agr* chromosomal locus which determines two divergent transcripts: RNAII, which is an operon of four genes, agrBDCA, that encode factors required to synthesize the autoinducer protein (AIP) and activate the regulatory cascade; and RNAIII, which yields a regulatory RNA molecule that acts as the primary effector of the *agr* system by up-regulating extracellular virulence factors and down-regulating cell surface protein expression (19; 20). Four allelic groups of *agr* have been identified within *S. aureus*, categorized as *agr* Types I-IV (21). Through *agr*, *S. aureus* produces an array virulence factors including enzymes, superantigens, adhesins, and hemolysins which serve a wide scope of purposes in the infection process (22-28). Skin and soft tissue infections (SSTIs) are the most common type of infection caused by *S. aureus*; most of these cases are associated with the formation of abscesses, whether they are minor inflammatory conditions or more invasive infections (29; 30). The *agr* system's importance to abscess formation has been confirmed via genetic and *agr*-inhibiting tools (31-35). Studies on sterile supernatants from wild type and *agr* mutant demonstrated that the bulk of the phenotype is due to virulence factors secreted in an *agr*-dependent manner (34; 36; 37). Abscess formation was shown to be hindered by interference with the *agr* system via competing AIPs or AIP-sequestering antibodies (31; 33; 34). These

observations directly support for the notion that *agr*-targeted therapies are highly promising skin infection treatments. Inhibition of virulence in *S. aureus* has been recurrently been proposed as strategy to either enhance antibiotic efficacy or to work as standalone therapy in some cases (16). The enhancing of antibiotic efficacy may allow for lower doses of antibiotic to be used, possible reducing the spread of antibiotic resistance, and in a standalone therapy, targeted bacteria would be eliminated not by the antiviruelence treatment but by the immune system.

In prior ethnobotanical work on Italian traditional medicine, Quave, *et al*, identified *C. sativa* as a medicinal plant (38; 39). Chestnut leaves had been previously reported in an ethnography of Italian folk medicine as being used to prepare a boiled leaf compress applied topically to treat pustulent wounds, rashes, and burns (40). In preliminary screening of extracts of various Italian plants, Quave, *et al*, determined that the extract of *C. sativa* leaves does not exert its anti-infective effect by killing *S. aureus*, but by inhibiting its quorum sensing (41). Quorum sensing is a form of communication between bacterial cells that governs the production of virulence factors (42). In 2015, Quave, *et al*, published their findings on the quorum sensing inhibitory effects against *S. aureus* of an enriched fraction of *C. sativa* leaves, 224C-F2 (8).

I continue Dr. Cassandra Quave's look to nature as a source of potential antivirulence compounds. My starting point was with enriched extract 224C-F2, which exerted non-bacteriostatic/bactericidal quorum sensing inhibitory activity against methicillin-resisatnt *Staphylococcus aureus* (MRSA) and no detectable resistance after 15 days of drug passaging (8). In a mouse skin infection model, co-administration of the extract with MRSA impaired pathogenesis without manifesting local or systemic toxicity. Ethnobotanical studies on the traditional uses of plants for the management of skin and soft tissue infections and general

skin care in Italy formed the original basis for laboratory analyses of chestnut and maybe other species, for their anti-infective potential (38-41; 43). A key revelation of these studies was that many of the extracts, and particularly that of *C. sativa* leaves, exerted anti-infective activity not by inhibiting *S. aureus* growth, but by inhibition of *S. aureus* quorum sensing.

The goal of my doctoral research has been to identify compounds present in 224C-F2 that exert quorum sensing inhibitory activity against *S. aureus*. From the microbiological point of view, the aim is to demonstrate that a quorum sensing inhibitory compound can inhibit markers of virulence, giving preclinical evidence for the therapeutic efficacy of this strategy. From the ethnobotanical point of view, the aim is to demonstrate that *C. sativa* is yet another source of antivirulence compounds, further confirming the plant's use in Italian traditional medicine. Phytochemistry provides many of the tools to perform this research, while finally, pharmacology allows for the study of the drugs obtained.

The following three chapters in this dissertation address all aspects of my doctoral research that bring new knowledge to ethnopharmacology. Chapter II discusses the isolation of a novel compound from the leaves of *C. sativa*: castaneroxy A. This hydroperoxy cycloartane triterpenoid was isolated via a bioassay-guided fractionation approach from the 224C-F2 enriched fraction reported by Quave *et al* in 2015. It was given the name "castaneroxy" due to its being isolated from ***Castan****ea sativa* and its being distinguished chemically by its hydrop**eroxy** functional group. The bioassay-guided fractionation of the 224C-F2c portion by two iterations of reverse phase HPLC led to the isolation of castaneroxy A. Spectroscopic data of a fraction adjacent to the castaneroxy A fraction suggested the presence of two isomers thereof. The discovery of the castaneroxys contributes to the literature on unsaturated

sterols and especially to the hydroperoxy cycloartane literature, as it addresses questions related to synthesis and stereochemistry.

The bioassay employed during fractionation was a panel of yellow fluorescent protein (YFP) reporter strains of *agr*::P3 activation, acting as the preliminary screen for quorum sensing inhibitory activity against *S. aureus*. The *agr* gene encodes for the machinery of quorum sensing in *S. aureus* as well as a regulatory RNA, RNAIII transcribed as a result of the activation of this machinery; this regulatory RNA is responsible for the modulation of genes implicated in virulence (44). Therefore, inhibition of reporter strain YFP output is a preliminary indicator – though not a conclusive one, alone – of inhibition of quorum sensing, the main modulator of virulence in *S. aureus*.

In Chapter III, the antivirulence activity of castaneroxy A against MRSA is confirmed through an array of pharmacological experiments that assay *S. aureus* virulence factors. In the literature, a plethora of assays have been used to establish a treatment's effect on markers of virulence, from qRT-PCR of relevant gene transcripts to Western blots of relevant proteins (45; 46). While I employ the *agr*::P3 reporter strain assay to measure a transcriptional product of virulence, I also employ a number of assays to look at translational products: δ-toxin quantification by HPLC, α-toxin quantification by rabbit blood hemolysis, and supernatant toxicity against human keratinocytes. Finally, a collaborator studying the effects of castaneroxy A *in vivo* found that it abates dermonecrosis in a mouse model of MRSA skiun infection. Chapter IV elaborates on the significance of my dissertation work to the field of ethnopharmacology. I discuss possible future directions for my work with castaneroxy A and my perspectives on how the field of ethnopharmacology will continue to evolve.

In order to introduce the subject matter relevant to my research, I will summarize four published review works of mine, which are available in the appendices. The first review in Appendix I, “Opportunities for plant natural products in infection control”, discusses the foundational premises of ethnobotanical antibiotic drug discovery (47). These begin with the fact that plants produce a vast array of secondary metabolites due to their sessile nature. A note on terminology is needed at this point: “plant secondary metabolites” refers to non-primary metabolites (nucleic acids, fatty acids, etc.) produced by plants, and the term is synonymous with “plant natural product” and “phytochemical.”

Indeed, because they are unable to move to interact with their environment, plants have evolved the production of secondary metabolites to perform such tasks as attracting pollinators and killing infectious microbes. A plant thus contains hundreds of unique secondary metabolites with different functions. When a plant is prepared in a traditional medicinal practice to treat a disease, it is one or a combination of these secondary metabolites that are mediating the therapeutic effect. Practitioners of traditional medicine throughout the world possess knowledge of the preparations of plants effective against various diseases; in effect, they understand which plants contain secondary metabolites with specific bioactivities. It is in consulting the already collected traditional medicinal knowledge and in interviewing new informants that an ethnobotanist can determine which plants to explore for drug leads. And in this approach lies a key advantage of ethnobotanical drug discovery: its targeted nature. For even before screening against a given indication is performed, the plants collected and extracted are chosen based on prior human knowledge of effectiveness against that indication.

There are many examples of plant extracts and fractions thereof that exert their bioactivity in a synergistic fashion (48-53). This presents an interesting situation: whereas several drugs isolated from plants or derived from plant natural products are effective on their own, improved pharmacodynamics and/or pharmacokinetics can sometimes be observed when the drug is administered as a component of an extract. Plant natural products are receiving more attention for drug discovery now, at least from academic laboratories, than in the 90s and 00s due to increased accessibility. This increased accessibility can be attributed to several factors, including advances in high throughput screening that improve compatibility with plant natural products and advances in the bioassay-guided fractionation workflow that minimize bottlenecks. A growing area in both ethnobotanical drug discovery and in antibiotic drug discovery is antivirulence lead identification and validation. Both fields are concerned with generating a pipeline of drug leads that inhibit bacterial virulence rather than growth. To this extent, there are several examples in the literature of promising leads.

The second review in Appendix II, “Methods in the Extraction and Chemical Analysis of Medicinal Plants”, reviews deeply the phytochemical techniques that bridge ethnobotany to drug discovery (54). There are many methods of extraction of phytochemicals from plants, some requiring little equipment, like macerations and decoctions, and others requiring more sophisticated equipment, such as accelerated solvent extraction. Extractions are usually performed in liquid phase, and the resulting filtered liquid extracts are concentrated *in vacuo* by rotary evaporation and lyophilization to yield dry powders. Each dry powder, or crude extract, represents a chemical library—hundreds of unique phytochemicals that dissolved into the solvent under the extraction parameters. In order to then isolate from this extract the compounds contributing to any bioactivity, the extract is put through bioassay-guided fractionation. Under this framework, a panel of extracts is screened for a given bioactivity;

one or more hits are selected for a fractionation process wherein iterations of increasingly high resolution chromatography are used to separate the sample into fractions based on chemical properties, each fraction then being screened again for a new hit. The process is repeated (i.e. fractions are themselves fractionated) until a pure compound is isolated. Such a fractionation process may begin with a low resolution but high-sample-load chromatographic technique such as liquid-liquid partitioning, performed in separatory funnels. Following this, increasingly high resolution techniques may be used, such as column chromatography, flash chromatography, and high-performance liquid chromatography (HPLC).

At all points in the bioassay-guided fractionation framework, it is beneficial to employ spectroscopic techniques for the analysis of extracts, fractions, and isolated compounds. Two of the most valuable spectroscopic techniques are mass spectrometry (MS) and nuclear magnetic resonance (NMR). Mass spectrometry offers detection of the mass of compounds in a sample as well as their fragmentation fingerprints (via tandem mass spectrometry, or MS/MS). Nuclear magnetic resonance provides spectra that give information as to the local electronic environment of atoms in a sample, crucial information for understanding the chemical makeup of a sample or elucidating the structure of a pure compound. Major advances in these techniques have occurred over the past two decades that allow for higher resolution detection with lower amounts of sample. Often, these spectroscopic techniques are coupled to automated liquid chromatography to speed up the workflow. For example, in LC/MS-MS, a sample being fractionated via HPLC is immediately directed to a mass spectrometer after exiting the detector. This way, the fractions made are simultaneously analyzed by mass spectrometry. When MS, MS/MS and NMR data are available for a sample, this data can be used to undertake metabolomics and molecular networking studies to verify whether compounds with similar masses, fragmentation fingerprints, or NMR spectra

have been reported in the past. This allows researchers to better identify which samples are likely to contain compounds that have not yet been discovered.

The third review in Appendix III, "Targeting Virulence in *Staphylococcus aureus* by Chemical Inhibition of the Accessory Gene Regulator System *In Vivo,"* delves into the problem my research addresses: targeting *S. aureus* by chemical inhibition of its Agr system (16). *Staphylococcus aureus*, including methicillin-resistant *S. aureus* (MRSA), remains a pathogen of great concern in the United States and across the world. In 2019 the Centers for Disease Control and Prevention (CDC) designated *S. aureus* as a "serious threat" due to its having caused 323,700 hospitalizations, 10,600 deaths, and $1.7 billion in healthcare costs in 2017 alone (14). *S. aureus* has the ability to both rapidly develop antibiotic resistance and to infect numerous types of tissue (55; 56). The common types of infections that *S. aureus* causes are vascular catheter-related infections, skin and soft tissue infections, pleuropulmonary infections, osteoarticular infections, and infective endocarditis (57). *S. aureus* is a leading cause of bacteremia, and the mortality rate of *S. aureus* bacteremia is 20%, remaining constant since the 1990s (58). Additionally, reductions in hospital cases of MRSA bacteremia have stalled; an estimated 17% decline each year from 2005 to 2016 was seen, whereas no change occurred from 2013 to 2016. *S. aureus* relies on a suite of virulence mechanisms in order to successfully cause infection. A chief governor of *S. aureus* virulence is quorum sensing, the components of which are coded for by the *agr* locus and are collectively called the a*gr* system (**Figure 1.1**) (59; 60). Since staphylococcal virulence factors are expressed under the control of quorum sensing, inhibition of virulence can be achieved by chemical inhibition of quorum sensing.

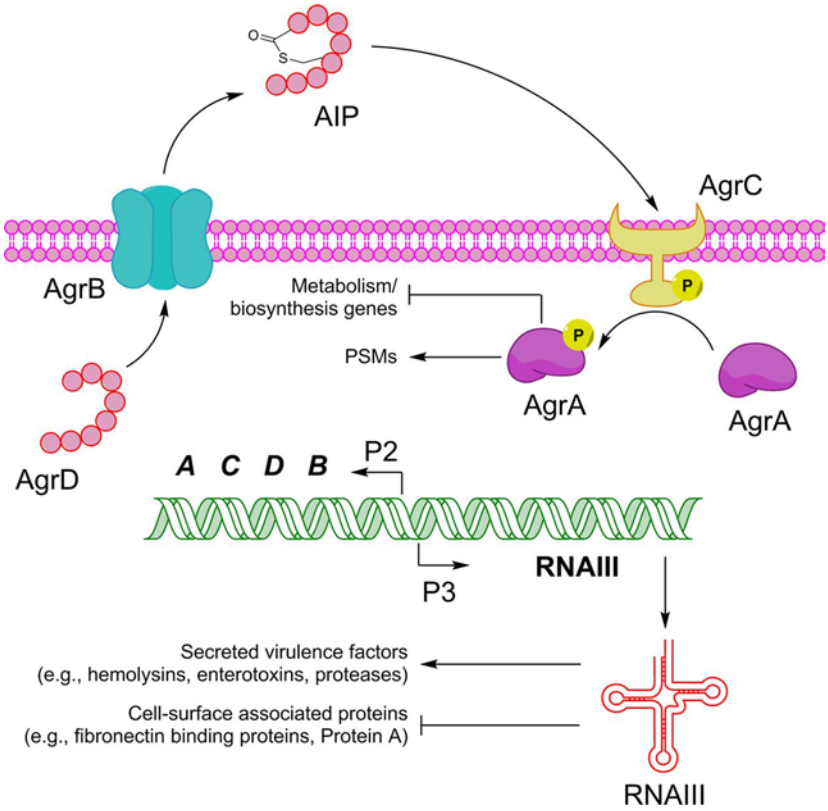

Fig. 1.1. Schematic of the *S. aureus* accessory gene regulatory (Agr) system. This is a reproduction of Fig. A3.1.

Quorum sensing is a system of stimuli and response between cells in a bacterial population that coordinates the gene expression of pathways that contribute to virulence, the capacity to infect a host, in a population-density fashion (60). The machinery of quorum sensing in *S. aureus* (**Figure 1.1**) includes an autoinducer peptide termed AIP (AgrD) that is secreted by an integral membrane endopeptidase (AgrB) and recognized by a membrane-bound receptor histidine kinase (AgrC), which subsequently phosphorylates a response regulator (AgrA) in the cytosol of the bacterium (44). These four components comprise the Agr machinery and are coded for by the P2 promotor-controlled portion of the *agr* gene locus. The P3 promotor, on the other hand, controls the expression of RNAIII, a small RNA molecule that acts as the primary effector of the quorum sensing system by upregulating virulence factor expression and downregulating cell surface protein expression (61). While phosphorylated AgrA (p-AgrA) binds to the P2 promotor with high affinity, it binds to P3 with low affinity, hence the population-density dependence of *S. aureus* virulence (62). This is because the low affinity of p-AgrA for P3 necessitates, by the law of mass action, that a higher concentation of p-AgrA is required for there to occur binding sufficient for the activation of P3. This higher concentration of p-AgrA would come about when enough AIP is available to sufficiently activate AgC; this in turn would occur when a population density threshold of *S. aureus* cells in the population has been reached.

Four allelic variants of the *agr* system exists across all *S. aureus* strains, differing in amino acid sequence (63). Reports are available on the schematic of the *agr* system and tools for the discovery of inhibitors (16; 64). The importance of *agr* to abscess formation has been confirmed via genetic and *agr*-inhibiting tools (31-35). Studies on sterile supernatants from wild type and *agr* mutant strains demonstrated that the virulent phenotype is due to virulence factors secreted in an *agr*-dependent manner (34; 36; 37), and abscess formation is hindered

by interference with *agr* competing AIPs or AIP-sequestering antibodies (31; 33; 34). Based on these findings, a number of quorum sensing inhibitors against *S. aureus* have been developed, and some have demonstrated the ability to retard *S. aureus* pathogenesis in prophylactic mouse models of MRSA skin infection (8; 34; 65-74).

Finally, Appendix IV is an excerpt I wrote for a review article, “Ethnobotany and the Role of Plant Natural Products in Antibiotic Drug Discovery.” There, I discuss cutting-edge technologies with particular applicability to ethnobotanical anti-infective drug discovery. Such technologies include machine learning, molecular networking, ethnophytotechnology, anisotropic NMR, and cryo-EM (cryogenic electron microscopy)/microED (microcrystal electron diffraction). Drug discovery in general faces a number of challenges; these include improving the quality of drug libraries, enhancing screen hit rates, and optimizing the drug lead optimization process. In plant natural products drug discovery, other unique challenges are also faced, such as dereplication (the rapid identification of known secondary metabolites) (75-77). Many of the new technologies reported serve to alleviate such bottlenecks in the drug discovery process.

CHAPTER II

Isolation of castaneroxy A from the leaves of *Castanea sativa*

The results are being assembled for submission to *Frontiers in Pharmacology*.

Introduction

With the spread of antibiotic resistance on the rise, new approaches are sought for treating drug-resistant bacterial infections. Methicillin-resistant *Staphylococcus aureus* (MRSA) represents a serious threat to global health, and we have looked to nature for the discovery of plant natural products that inhibit MRSA virulence. *Castanea sativa* leaves were reported in Italian traditional medicine for the preparation of a boiled leaf compress applied topically to treat pustulant wounds, rashes, and burns (40). Further study of a *C. sativa* leaf extract for effects on *S. aureus* established its quorum sensing inhibitory activity against MRSA (38; 41).We subsequently reported the non-bacteriostatic/bactericidal quorum sensing inhibitory activity of an enriched *C. sativa* leaf extract, 224C-F2 (8). Extract 224C-F2 demonstrated high bioactivity against MRSA *in vitro* and no detectable resistance after 15 days of drug passaging (8). In a mouse skin infection model, co-administration of the extract with MRSA impaired pathogenesis without manifesting local or systemic toxicity.

C. sativa, commonly called the European chestnut or sweet chestnut, is a large deciduous tree belonging to the Fagaceae (beech) family. It is native to elevated forests from Iran to the Balkans, and its fruit, the chestnut, has been eaten by humans for millennia. *C. sativa* has been reported to be used by many communities around in the world in their traditional medicines. In the Kosovar Albanian Alps, decoctions are prepared from the fruits, and they are taken internally to treat headaches and externally to treat hemorrhoids (78). In the Marches region of Central-Eastern Italy, decoctions of the fruits are used as a hair wash to give light-colored hair a brown gloss (43), and a compress is made of the boiled fruit pulp to whiten facial skin (43). In parts of Turkey, chestnut flower tea is used to treat hemorrhoids (79). And going back to Pietro Andrea Mattioli's 1554 commentary on Dioscorides's *De*

materia medica, chestnuts roasted with salt and pepper are attributed with aphrodisiac properties (80).

The aim of the current study was to isolate antivirulence compounds against MRSA from *C. sativa* leaves that contribute to the plant's ethnobotanical anti-infective value. The bioassay-guided fractionation of the previously reported active fraction 224C-F2 led to the isolation and structure elucidation of a novel hydroperoxy cycloartane triterpenoid, castaneroxy A (**1**), and detection of two isomers thereof: the major product, compound **2a** (called castaneroxy B), and the minor product, compound **2b**. The structure of **1** was determined by X-ray crystallography, NMR, and MS. A crystal structure was also obtained for **2a**, and the presence of **2b** as a minor product with it was suggested by NMR spectral data. The castaneroxys are hydroperoxy cycloartane triterpenoids, and they are likely biosynthesized by a photooxygenation of a precursor compound.

Results

Bioassay-guided isolation of castaneroxy compounds

The isolation of castaneroxy A (**1**) from the leaves of *C. sativa* followed a bioassay-guided fractionation scheme (**Fig. 2.1**). In brief, a double methanolic maceration of dried *C. sativa* ground leaves was performed, and the resulting filtered and dried crude extract was designated “224.” Crude extract 224 was sequentially partitioned against hexanes and ethyl acetate; the ethyl acetate partition, 224C, was fractionated as previously described via silica gel flash chromatography with three mobile phases: hexanes, ethyl acetate, and methanol. Flash fractions of 224C were produced, all given the prefix “F”. In order to determine which fraction was most likely to contain quorum sensing inhibitory compounds against *S. aureus*, a preliminary screen of the fractions was performed using a panel of four yellow fluorescent protein (YFP) *agr*::P3 reporter strains representing the four *agr* subtypes (81).

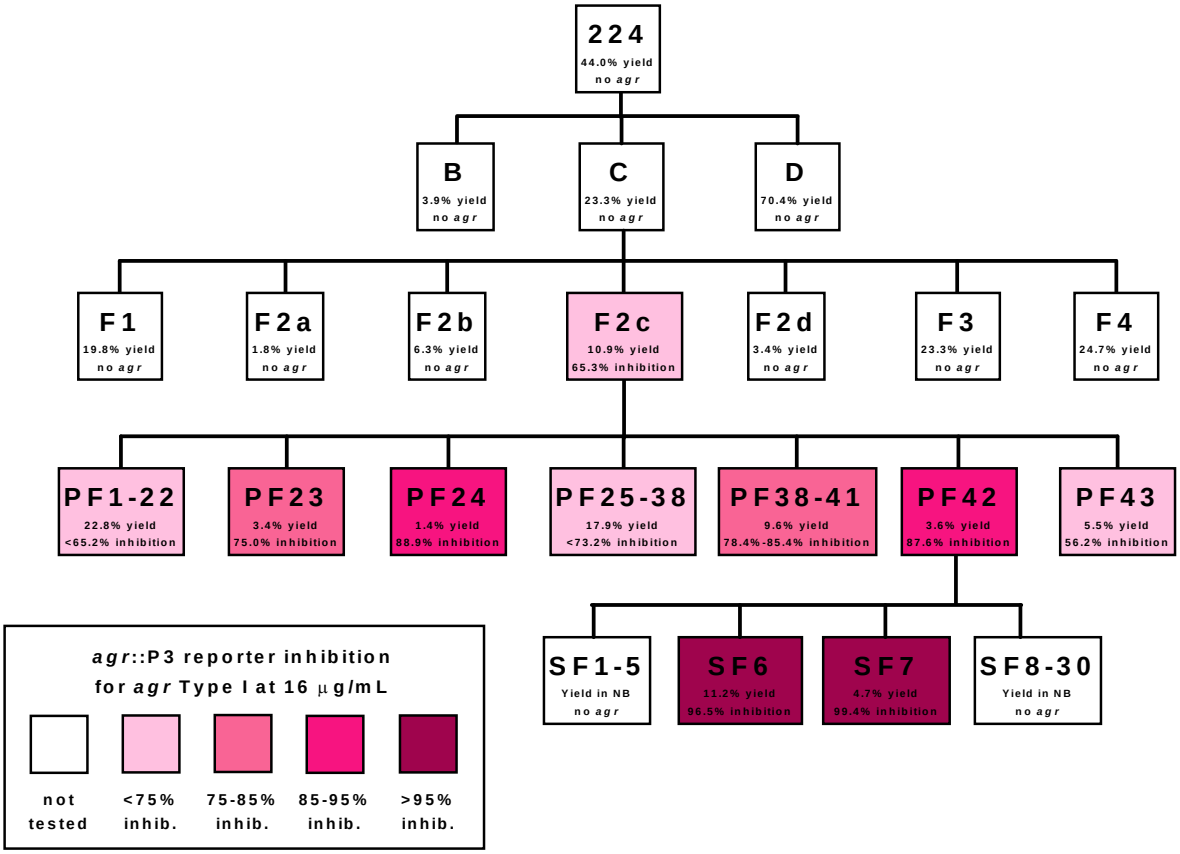

Fig. 2.1. Fractionation scheme of methanolic extract of *C. sativa* leaves. The fractionation of the crude methanolic extract of *C. sativa* leaves, 224, was done in four rounds using different methods: liquid-liquid partitioning was performed first, then normal phase flash chromatography, and then two iterations of reverse phase HPLC. Percent yield values are indicated as well as percent vehicle values for *agr*::P3 activation in 16 µg/mL treatment in AH1677 (*agr* Type I).

The fraction 224C-F2c exhibited the highest efficacy at quenching the reporter and was thus selected for further fractionation. Fraction 224C-F2c was fractionated by C-18 reverse phase high-performance liquid chromatography (HPLC) to produce 43 “preparative fractions,” all given the prefix “PF.” The 43 PFs were screened in the YFP *agr*::P3 reporter strain panel, which revealed that PF22-28 and 39-42 were the most bioactive (**Fig. 2.2**). Of these, fraction 224C-F2c-PF42 was selected for further fractionation via reverse phase HPLC, and this yielded 30 “subfractions,” all given the prefix “SF.” 224C-F2c-PF42-SF7 was compound **1**, and its structure and absolute configuration was determined by Nuclear Magnetic Resonance (NMR), Mass Spectrometry (MS), and X-ray crystallography data. From 224C-F2c-PF42-SF6, a mixture of isomers of **1** (compounds **2a**, **2b**) was detected. Compound **2a** (major component) was crystallized and its structure was determined by X-ray diffraction analyses. Similar compounds to **1** and **2a**, **2b** have been reported previously (82-84). Herein, the structure elucidation and MRSA antivirulence bioactivities of the castaneroxy compounds are described.

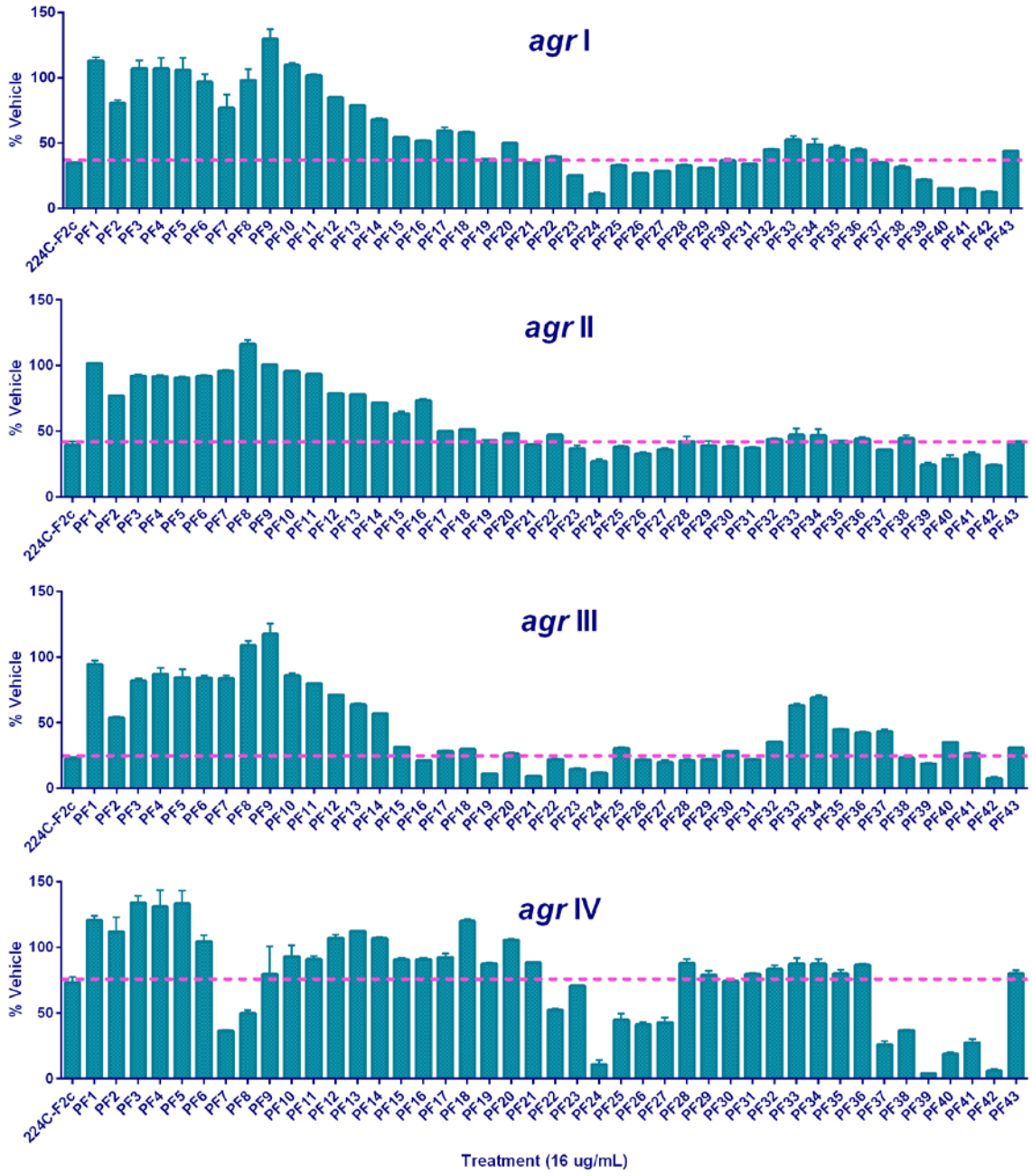

Fig. 2.2. Reporter strain screen of *agr*::P3 expression indicates fraction 224C-F2c and PF42 are potential sources of quorum sensing inhibitors. *S. aureus* reporter strains of AIP-induced *agr*::P3 activation representing the four *agr* subtypes were used to screen the fractions of 224C-F2c at 16 µg/mL. The pink dashed lines indicate the level of activity of the parent fraction, 224C-F2c. None of the treatments affected optical density of culture at the test concentration; therefore, culture growth was not impacted by any of the treatments.

Subtypes of *agr* represented by each graph are shown. All assays were performed in duplicate. The following MRSA strains were used: AH1677 (*agr* I), AH430 (*agr* II), AH1747 (*agr* III), and AH1872 (*agr* IV). Incubation was done for 18 h. “% Vehicle” refers to the raw fluorescence value at 18 h minus the raw fluorescence value at 0 h and then normalized to the raw fluorescence value obtained by DMSO treatment alone.

Structure elucidation of castaneroxy compounds

Castaneroxy A (**1**) was obtained as a white amorphous solid and the molecular formula was deduced to be $C_{30}H_{48}O_6$ on the basis of HRESIMS (high resolution electrospray ionization mass spectrometry) data (*m/z* 503.3381, calculated for $C_{30}H_{47}O_6$, $[M - H]^-$) (**Supplementary Fig. 2.1**), indicating seven degrees of unsaturation (**Fig. 2.3**). Analysis of the ^{13}C NMR data, DEPT (Distortionless Enhancement by Polarization Transfer)-135, and HSQC (Hetereonuclear Single Quantum Correlation) spectra (**Supplementary Figs. 2.2-2.4**) revealed the presence of 30 carbons including three sp^2 carbons (two olefinic carbons at δ_C 146.1 and δ_C 114.0 ppm and one carboxylic acid at δ_C 182.6 ppm) and 27 sp^3 carbons, of which there were five methyls, ten methylenes, seven methines (three are oxygenated) and five quaternary carbons. The above satisfied two degrees of unsaturation, indicating the presence of a pentacyclic core.

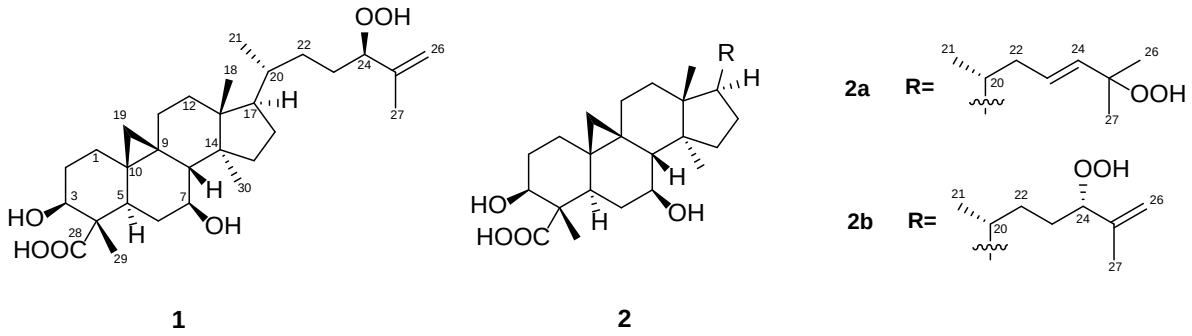

Figure 2.3. Structures of the isolated compounds (**1** and **2a**,**2b**).

The ^{1}H NMR spectrum of **1** (**Table 2.1**, **Supplementary Fig. 2.5**) displayed signals for five methyl groups at δ 1.71 (s), 1.10 (s), 1.00 (s), 0.95 (s), 0.90 (d, *J* = 6.4 Hz), one *exo*-methylene group at δ 4.91 (m) and 4.93 (dq, *J* = 1.6, 1.6 Hz), three oxymethine protons at δ 4.16 (dd , *J* = 6.8, 6.8 Hz), 4.01 (m) and 3.53 (brs), and two methylene protons with high-field resonances at δ 0.80 (d, *J* = 4.5 Hz) and 0.30 (d, *J* = 4.4 Hz), characteristic of a cyclopropyl group and in accordance with a cycloartane-type triterpenoid skeleton. The 1D NMR data of **1** were similar to those of the known compound musambin A (82), differing only in the position of one hydroxyl group, attached at C-7 (δ_H 3.53, brs; δ_C 70.8) in **1** instead of C-1 (δ_H 3.54, dd, *J* = 3.2, 2.8; δ_C 73.6) in musambin A.

Table 1. ^{1}H and ^{13}C NMR data (δ, in ppm) for compounds **1** and **2a**, **2b**.

Position	**1**		**2a** (major)		**2b** (minor)	
	δ_C, type	δ_H, mult. (*J* in Hz)	δ_C, type	δ_H, mult. (*J* in Hz)	δ_C, type	δ_H, mult. (*J* in Hz)
1a	31.9, CH_2	1.65, m	31.9, CH_2	1.67, m		
1b		1.37, m		1.39, m		
2a	30.2, CH_2	1.73, m	30.2, CH_2	1.75, m		
2b		1.29, m		1.30, m		
3	76.4, CH	4.01, m	76.2, CH	4.01, dd (11.6, 4.0)		
4	55.8, C[a]	--	55.3, C	--		
5	43.3, CH	2.13, m	43.4, CH	2.13, dd (13.2, 3.7)		
6a	33.3, CH_2	1.45, m	33.3, CH_2	1.41, m		
6b		1.11, m		1.14, m		
7	70.7, CH	3.53, brs	70.5, CH	3.53, brs		
8	54.5, CH	1.73, m	54.5, CH	1.74, m		
9	29.3, C	--	29.2, C	--		
10	21.3, C	--	21.4, C	--		
11a	28.1, CH_2	1.78, m	28.1, CH_2	1.78, m		
11b		1.43, m		1.46, m		
12	33.9, CH_2	1.60, m	33.6, CH_2	1.60, m		
13	46.7, C	--	46.7, C	--		
14	49.9, C	--	49.8, C	--		
15a	36.9, CH_2	1.59, m	37.0, CH_2	1.59, m		
15b		1.46, m		1.47, m		
16a	29.2, CH_2	1.30, m	29.1, CH_2	1.95, m		
16b		1.30, m		1.33, m		
17	52.8, CH	1.56, m	52.5, CH	1.56, m		
18	17.2, CH_3	1.00, s	17.3, CH_3	1.02, s		
19a	27.1, CH_2	0.80, d (4.5)	27.5, CH_2	0.80, d (4.7)		
19b		0.30, d (4.4)		0.30, d (4.6)		
20	37.4, CH	1.42, m	37.7, CH	1.51, m		
21	19.0, CH_3	0.90, d (6.4)	19.0, CH_3	0.90, d (6.4)		
22a	33.7, CH_2	1.60, m	40.5, CH_2	2.21, m		
22 b		1.60, m		1.81, m		
23a	28.7, CH_2	1.89, m	129.7, CH	5.62, ddd (16.0, 7.8, 2.6)		
23b		1.31, m				
24	90.9, CH	4.16, dd (6.8, 6.8)	137.1, CH	5.57, d (16.0)	91.0, CH	4.17, dd (6.8, 6.8)
25	146.1, C	--	82.5, C	--	145.7, C	--
26a	114.0, CH_2	4.93, dq (1.6, 1.6)	24.9, CH_3	1.29, s	114.4, CH_2	4.94, dq (1.6, 1.6)
26b		4.91, m				4.91, m
27	17.1, CH_3	1.71, s	25.1, CH_3	1.29, s	16.8, CH_3	1.71, s
28	182.6, C[a]	--	180.9, C	--		

29	10.3, CH_3	1.10, s	9.8, CH_3	1.10, s
30	19.2, CH_3	0.95, s	19.2, CH_3	0.94, s

Detailed analysis of COSY (Correlated Spectroscopy) and HMBC (Heteronuclear Multiple Bond Correlation) experiments (**Supplementary Fig. 2.6 and 2.7**) established the planar structure of **1** (**Figure 2.4A**). ^{1}H-^{1}H COSY spectral data revealed the presence of four spin systems (**a-d**): System **a** (–CH_2–CH_2–CH(OH)–), system **b** (–CH–CH_2–CH(OH)–CH–), system **c** (–CH_2–CH_2–), and system **d** (–CH–CH_2–CH–CH(CH_3)–CH_2–CH_2–CH(OH)–) (**Figure 2.4A**). The HMBC correlations of H_3-29 with C-3, C-5, and C-28 place H_3-29 and a carboxylic acid at C-4 and connect systems **a** and **b**, while the correlations between H_2-19 and C-1, C-5, and C-8 locate the cyclopropane ring at C-9 and C-10. Additionally, the HMBC cross peaks from H_3-18 to C-12 and C-17 connect systems **c** and **d**, and the linkage of systems **d** and **b** was established on the basis of HMBC correlations from H_3-30 to C-8 and C-15. Regarding the side chain, HMBC correlations observed from H-24 to C-26 and C-27 permit the lengthening of fragment **d** and confirm the presence of a hydroperoxide group at C-24, in agreement with the characteristic chemical shift value of this carbon at δ_C 90.9 ppm (84-86).

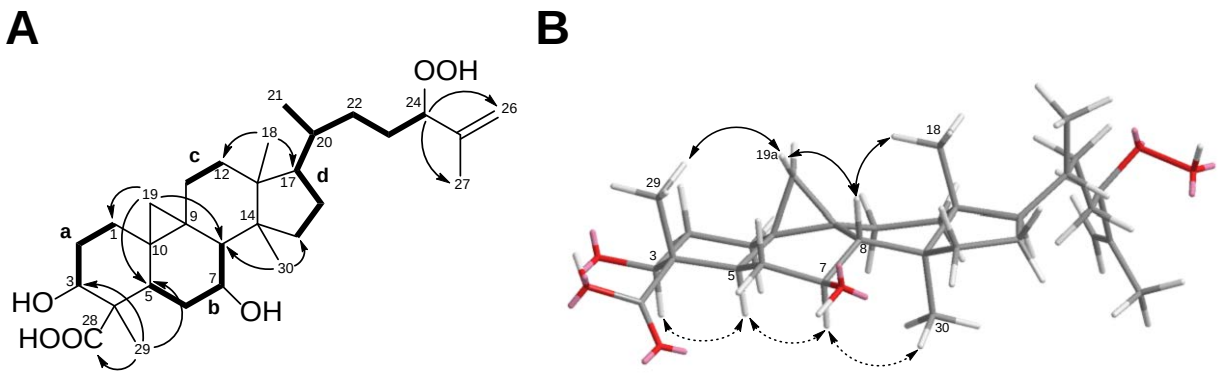

Figure 2.4. **(A)** $^{1}H-^{1}H$ COSY correlations and key HMBC correlations for compound **1**. **(B)** Key NOESY correlations of **1** (double-headed arrows). Solid arrows denote effects on the top face of the pentacyclic structure as shown; dashed arrows denote effects on the bottom face.

The relative configuration of **1** (**Figure 2.4B**) was established based on NOESY (Nuclear Overhauser Effect Spectroscopy) experiments (**Supplementary Fig. 2.8**). NOE correlations observed from H-5 to H-3/H-7, H-7 to H_3-30 indicate that these protons are on the same face of the molecule, arbitrarily assigned to be alpha-oriented, whereas the NOEs between Ha-19 and H_3-29/H-8 and between H-8 and H_3-18 suggested that these protons are on the beta side of the molecule. To support the above deductions and determine the absolute configuration of **1**, an X-ray crystal structure was obtained (**Figure 2.5A, Supplementary Information S1**). The crystallographically determined torsional angles between the $^{1}H–^{1}H$ hydrogens corroborate the COSY correlations shown in Figure 2A. The absolute configuration of **1** was assigned as 3*S*, 4*S*, 5*R*, 7*S*, 8*S*, 9*S*, 10*R*, 13*R*, 14*S*, 17*R*, 20*R*, 24*R*, and this compound was named castaneroxy A (3β,7β-dihydroxy-24-hydroperoxy-cycloart-26-en-28-oic acid).

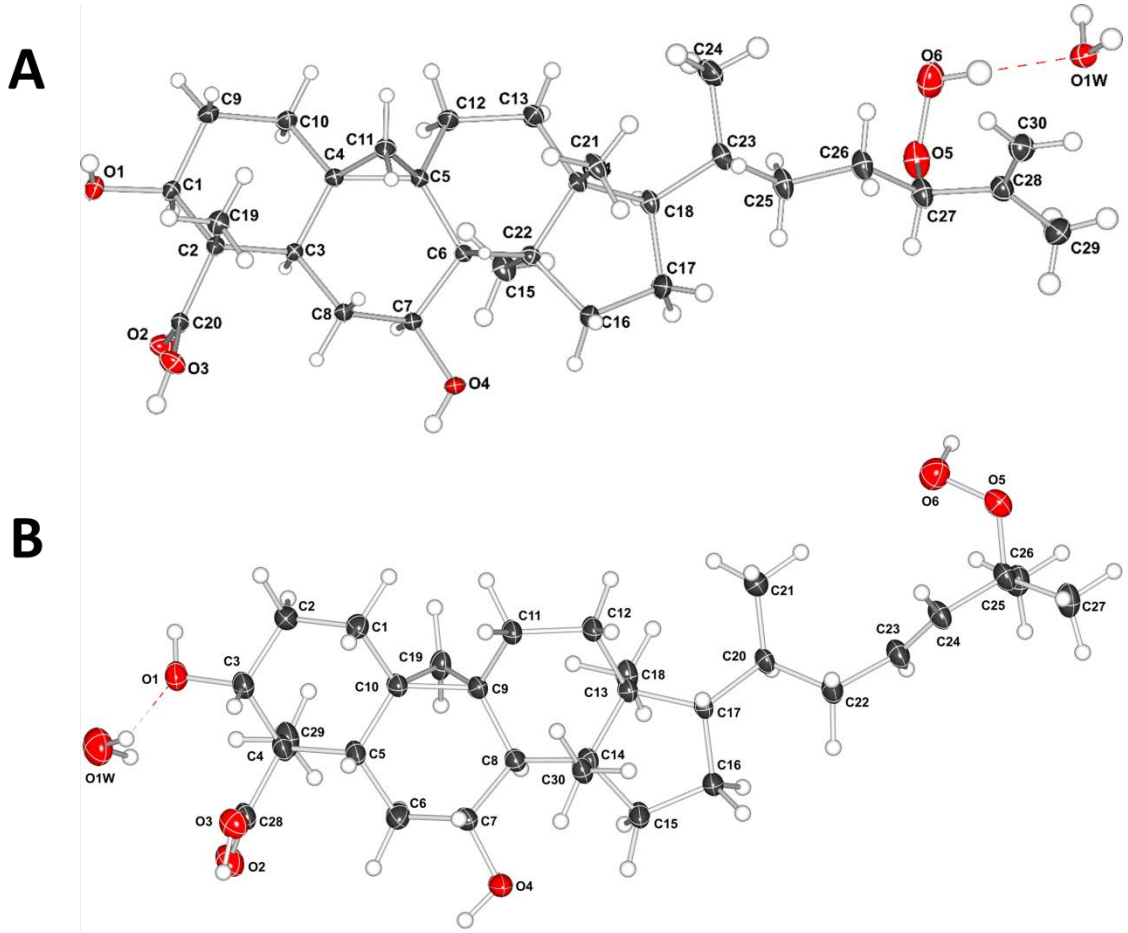

Figure 2.5. X-ray crystal structures of compound **1** (A) and compound **2a** (B).

Compounds **2a** and **2b** were identified as an inseparable mixture of coeluting compounds (**Figure 2.3**). Exhaustive efforts to separate the mixture by several optimized conditions were unsuccessful. Thus, structure elucidation was performed on the mixture. HRESIMS data of **2a**/**2b** showed the same molecular formula as **1** ($C_{30}H_{47}O_6$, $[M - H]^-$, *m/z* 503.3392), suggesting the presence of isomers (**Supplementary Fig. 2.9**). Comparison of ^1H and ^{13}C NMR for **2a**/**2b** (**Table 2.1**, **Supplementary Fig. 2.10-12**) with those for **1** showed that they shared the same cycloartane-type triterpenoid skeleton and suggested that the main differences are in the side chain. Detailed analysis of 1&2D NMR spectroscopic data allowed them to be identified and considered separately as two groups of signals, **2a** and **2b**.

The side chain structure of **2a** was determined based on its ^1H-^1H COSY and HMBC correlation data (**Supplementary Fig. 2.13 and 2.14**) and comparison of ^1H and ^{13}C chemical shifts with **1**. The most significant differences were the presence of olefinic signals (δ_H 5.57 and 5.62; δ_C 137.1 and 129.7 ppm) in **2a**, suggesting that a 1,2-disubstituted double bond replaced the *exo*-methylene moiety ($\delta_{H\text{-}26}$ 4.93 and 4.91, $\delta_{C\text{-}25}$ 146.1 and $\delta_{C\text{-}26}$ 114.0 ppm) in **1**, and suggesting the presence of a quaternary oxygenated carbon ($\delta_{C\text{-}25}$ 82.5 ppm) in **2a** instead of an oxymethine group ($\delta_{H\text{-}24}$ 4.16, 1H, dd, J = 6.8, 6.8 Hz; δ_c 90.9 ppm) in **1**. The position of the double bond was placed between C-23 and C-24 by the HMBC correlations from H-23 to C-25 and from H_3-26/H_3-27 to C-24. The downfield shift of C-25 confirmed that a hydroperoxy group was attached in this carbon (87). Slow evaporation of a CH_3OH solution of the mixture **2a**/**2b**, allowed to obtain suitable crystals of **2a**, and a single-crystal X-ray diffraction study confirmed its structure and assigned the absolute configuration as 3*S*, 4*S*, 5*R*, 7*S*, 8*S*, 9*S*, 10*R*, 13*R*, 14*S*, 17*R*, 20*R* (**Figure 2.5B, Supplementary Information S2**). Compound **2a** was named castaneroxy B.

The NMR spectroscopic group of signals attributed to **2b** was almost identical to that of **1**, suggesting that they may be a pair of epimers. When comparing the ^{1}H and ^{13}C chemical shifts of both, the signals attributable to the side chains were found to be slightly different (**Table 2.1**), indicating that **2b** had to be the C-24 epimer of **1**. However, the structure and stereochemistry of **2b** could not be confirmed since the physical separation of mixture **2a**/**2b** was not achieved.

The origin of compounds **1** and **2a**/**2b** can be understood by analyzing their biosynthetic pathway (**Figure 2.6**). Cabrera *et al.* proposed that these compounds might be generated via a naturally sensitized photooxygenation of olefinic precursors in the plant (88). The reaction involves the formation of an allylic hydroperoxide from an olefin by a process involving abstraction of an allylic proton along with migration of the carbon-carbon double bond (89; 90). Other studies have shown that in the presence of light, chlorophylls, due to their porphyrin sub-structures, are strong oxidation promotors and can act as photosensitizers to catalyze the photooxygenation of olefins to produce hydroperoxides (91-95). Previously, $\Delta^{25(26)}$-unsaturated hydroperoxy cycloartanes similar to **1** have been reported (82-85), and in all such studies isomers thereof are concurrently reported. Additionally, Banskota *et al.* propose a possible pathway for the formation of hydroperoxy cycloartane isomers which occurs by the photooxygenation of a hypothetical precursor with a cycloartane-type skeleton (83). As the reaction is non-stereoselective, product mixtures are commonly obtained.

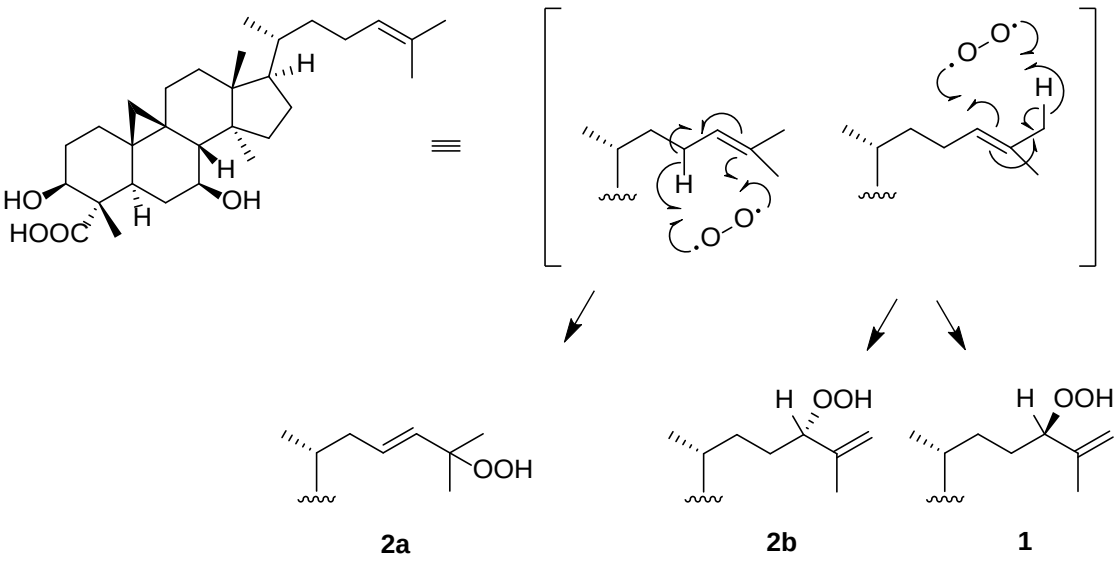

Figure 2.6. Proposed pathway for the formation of the castaneroxys from the hypothetical precursor. Based on the pathway proposed by Banskota et al. (83).

The compound proposed as the hypothetical precursor of the castaneroxys has been previously reported (96). Its ^{1}H spectrum exhibited a signal for one olefinic proton at δ_H 5.13 (t, *J* = 7.0 Hz, H-24) very similar to that observed in the ^{1}H NMR data of the parent fraction 224C-F2c-PF42 (δ_H 5.09, t, *J* = 7.3 Hz), suggesting the presence of this precursor in the fraction studied and its possible participation in the biosynthetic pathway (**Supplementary Fig. 2.15)**.

Discussion

Hydroperoxy functionalization is rare, and the hydroperoxy nature of the castaneroxys was further confirmed by a hydroperoxy clock reaction of 224C-F2c-PF42-SF6 (**Fig. 2.7**). In this reaction, compounds containing a peroxide will quickly turn the solution brown; starch intensifies this color (97). The solution alone with no compound added will turn brown over the course of several hours due to the oxygen in the air. Briefly, 100 mg KI was placed into a microcentrifuge tube and mixed with 0.5 mL acetic acid. 1 mg fraction SF6 was dissolved into 0.5 mL of MeOH and added to the microcentrifuge tube. Immediately, the solution turned brown. Adding a few drops of saturated aqueous starch solution intensified the brown color. When this experiment was performed with empty MeOH (no compound dissolved into it), a faint yellow color developed over the course of 5 minutes, which was not immediately intensified by starch solution. When the experiment was performed with empty MeOH followed by a few drops of H_2O_2, the solution immediately became a very intense brown.

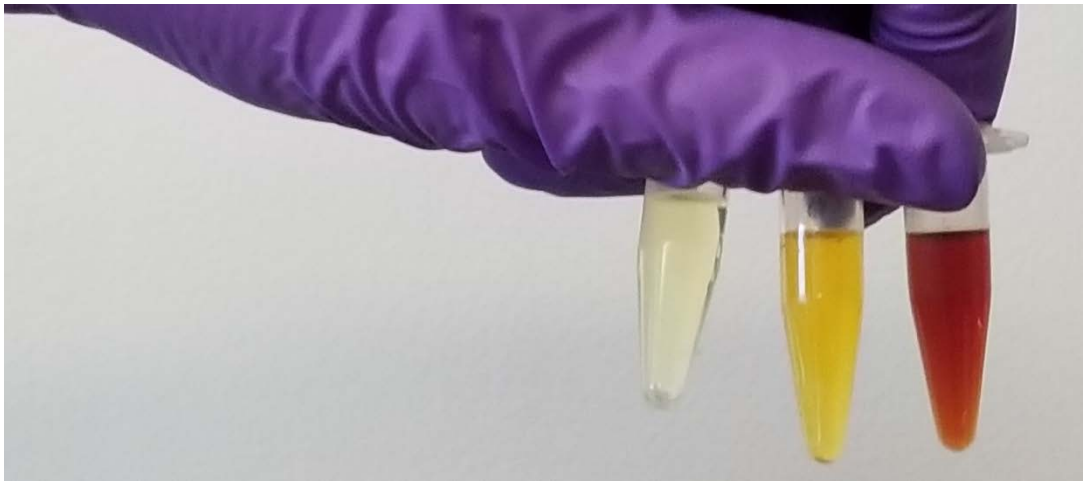

From left to right: MeOH solvent (negative control), fraction SF6 dissolved in MeOH, H_2O_2 dissolved in MeOH (positive control) – all at 15 min post-reaction.

Fig. 2.7. Hydroperoxy clock reaction confirms that fraction SF6 has hydroperoxy functionality. The following peroxide reaction was performed:

$3\ I^-\ (aq) + H_2O_2\ (aq) + 2\ H^+\ (aq) \rightarrow I_3^-\ (aq) + 2\ H_2O\ (l)$ (slow)

$I_3^-\ (aq) + 2\ S_2O_3^{2-}\ (aq) \rightarrow 3\ I^-\ (aq) + S_4O_6^{2-}\ (aq)$ (fast)

$2\ I_3^-\ (aq) + \text{starch}\ (aq) \rightarrow \text{starch-}I_5^-\ \text{complex}\ (aq) + I^-\ (aq)$

The hydroperoxy functionalization is a result of a photooxygenation reaction from an alkene precursor. As mentioned earlier, ^{1}H NMR data suggests that this precursor is present in 224C-F2c-PF42. Its presence can be confirmed; if incubated in photooxygenative conditions, the ^{1}H NMR signals corresponding to the precursor would diminish while those corresponding to the castaneroxys would amplify proportionally as the photooxygenation took place. Indeed, it has long been established that molecular oxygen can react with olefins to produce allylic hydroperoxides (89; 98-100). While light and molecular oxygen are proposed by Banskota *et al.* to be the sole requirements for this olefin photooxygenation, a photosensitizer is likely required as a catalyst as well, as previously stated; otherwise, photooxygenations would always rapidly occur at accessible olefins in the presence of light and molecular oxygen (91; 92). PF42 is dark green in color, indicating the presence of chlorophylls from the leaves. In the presence of light, chlorophylls, due to their porphyrin sub-structures, are strong oxidation promotors by their behavior as photosensitizers of molecular oxygen in photooxygenative reactions (101; 102). HPLC-FTMS of 224C-F2c-PF42 in positive mode revealed the presence of an ion with an *m/z* of 907.77, indicative of chlorophyll b (**Fig. 2.8**) (103-105). Indeed, chlorophylls have been shown to function as photosensitizers to catalyze the photooxygenation of olefins to produce hydroperoxides (93-95).

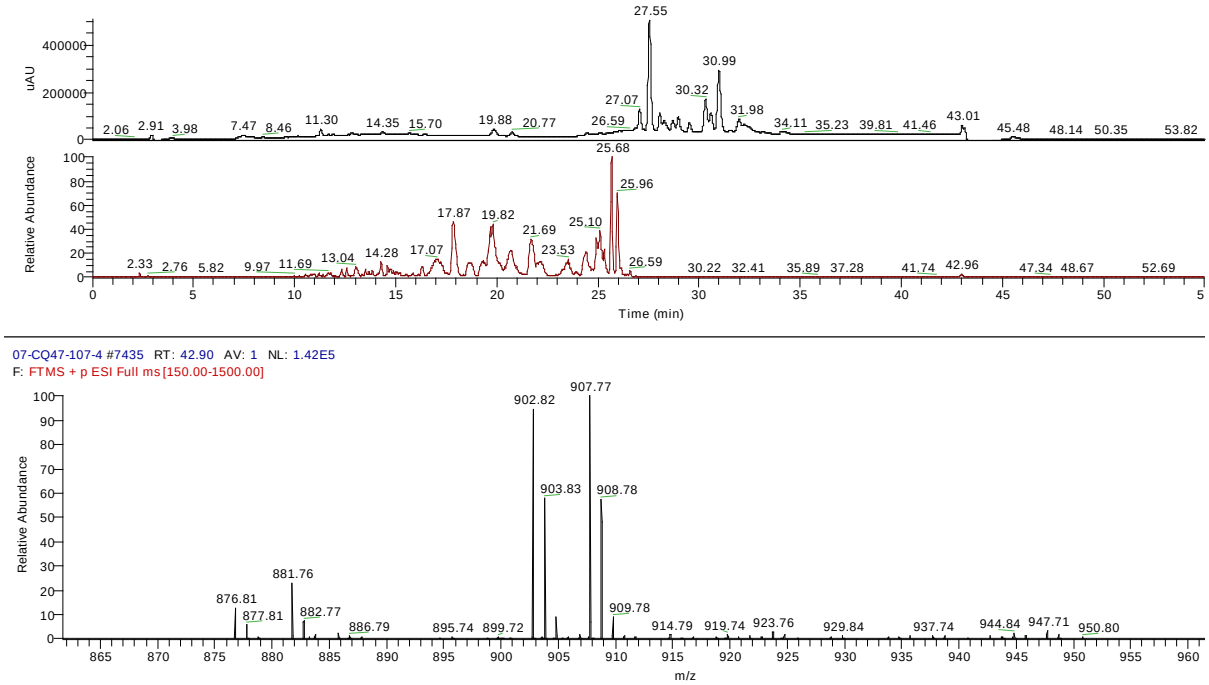

Fig. 2.8. Chlorophyll b detected in 224C-F2c-PF42 by LC-FTMS. (*Top panel*) A UV chromatogram of the run is stacked on top of a base peak chromatogram in positive ion mode. (*Bottom panel*) The mass spectrum at 42.90 minutes reveals the $[M+H]^+$ ion with an *m/z* of 907.77, which corresponds to chlorophyll b.

The ^{1}H NMR experiment described above was performed to test the hypothesis that the hypothetical precursor is indeed present in fraction PF42 and that the ^{1}H signal at δ_H 5.10 ppm corresponds to its H_1-24. Two samples of PF42 were incubated aerobically, one in light and the other in the dark, and the ^{1}H NMR spectrum of each was taken every 24 h for three days. Over the course of the three days, the δ_H 5.10 ppm signal depleted in the fraction PF42 incubated aerobically and exposed to light, while no change in the ^{1}H spectrum occurred in the fraction PF42 incubated aerobically in the dark (**Fig. 2.9**). Furthermore, the depletion in signal in the former sample was accompanied by a proportional amplification of signals corresponding to the unsaturated protons of the castaneroxys. This observation strongly implies the depletion under photooxygenative conditions of the species that is the source of the δ_H 5.10 ppm signal, which is likely the hypothetical precursor, and the simultaneous and proportional formation of the castaneroxys. While the above results speak as to the ability of the precursor to be photooxygenized *ex vivo*, they do not speak as to its ability to do so *in vivo*. In all PF42 samples studied under ^{1}H NMR, castaneroxy signals were observed, and similar photooxygenations have been confirmed to occur in the plant itself by fractionation processes done in dark conditions (88).

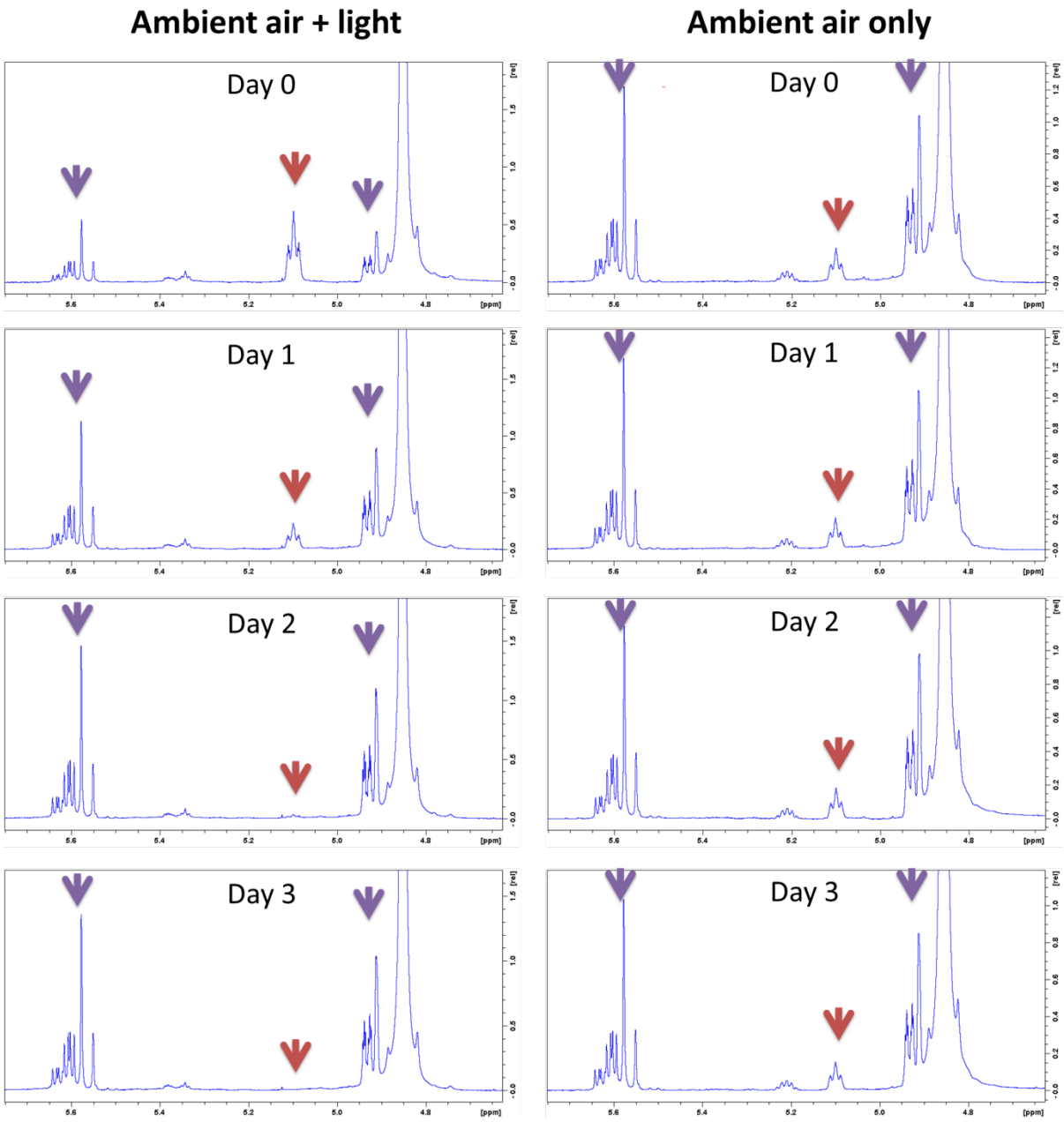

Fig. 2.9. Hypothetical precursor in PF42 diminishes in the presence of oxygen and light over the course of three days, giving rise to castaneroxys. Zoomed-in ^{1}H NMR spectra of PF42 are shown with purple arrows indicating signal clusters corresponding to the unsaturated alkyl chain protons of the castaneroxys and red arrows indicating the signal corresponding to the hypothetical precursor's unsaturated alkyl chain proton. Reactions occurred in 5 mm NMR tubes.

An unexpected observation is that the physical separation of castaneroxy A from its C-24 epimer and C-25 hydroperoxy isomer castaneroxy B was achieved while the latter two remained inseparable. Indeed, they remained inseparable despite exhaustive efforts (**Fig. 2.10 and 2.11**). Previous reports of hydroperoxy cycloartane triterpenoids report, in fact, the physical separation of the C-25 hydroperoxy isomer from the inseparable mixture of the C-24 epimers (82; 84; 85). The reason we have achieved an alternative result is unclear. Furthermore, while three hydroperoxy cycloartanes are detected in this study, many more could be formed by photooxygenation and were indeed isolated by Banskota et al (83). These other photooxygention products were not achieved likely because photooxygenation of the precursor *ex vivo* was not allowed more time.

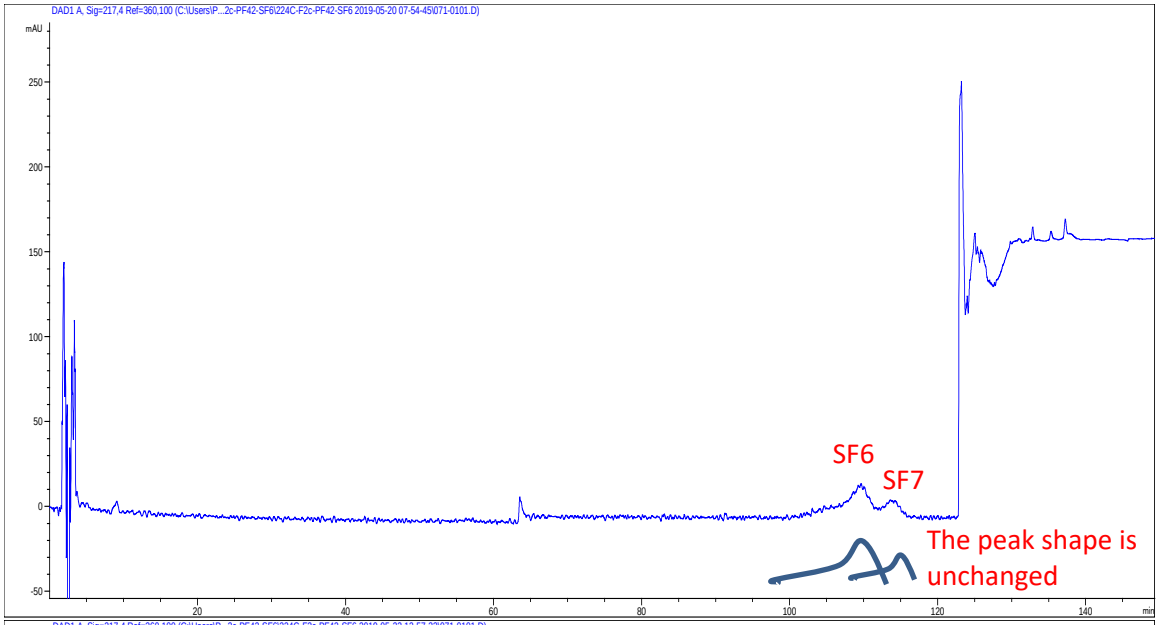
DAD1 A, Sig=217,4 Ref=360,100 (C:\Users\P...2c-PF42-SF6\224C-F2c-PF42-SF6 2019-05-20 07-54-45\071-0101.D)
mAU
250
200
150
100
50
0
-50
20
40
60
80
100
120
140
min
SF6
SF7
The peak shape is unchanged

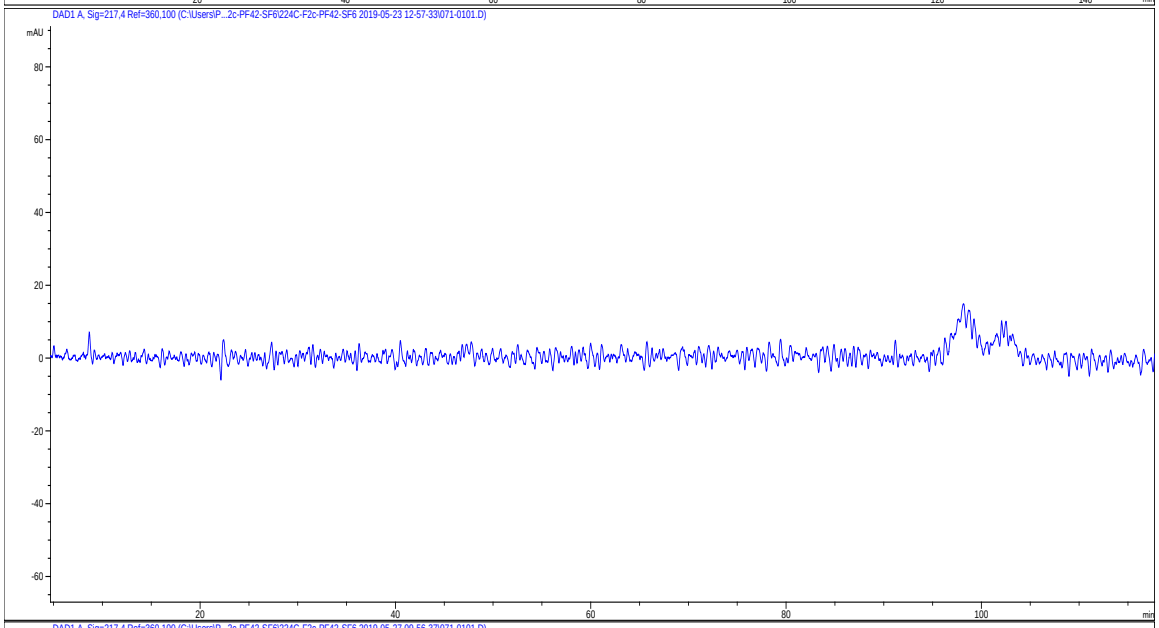
DAD1 A, Sig=217,4 Ref=360,100 (C:\Users\P...2c-PF42-SF6\224C-F2c-PF42-SF6 2019-05-23 12-57-33\071-0101.D)
mAU
80
60
40
20
0
-20
-40
-60
20
40
60
80
100
min

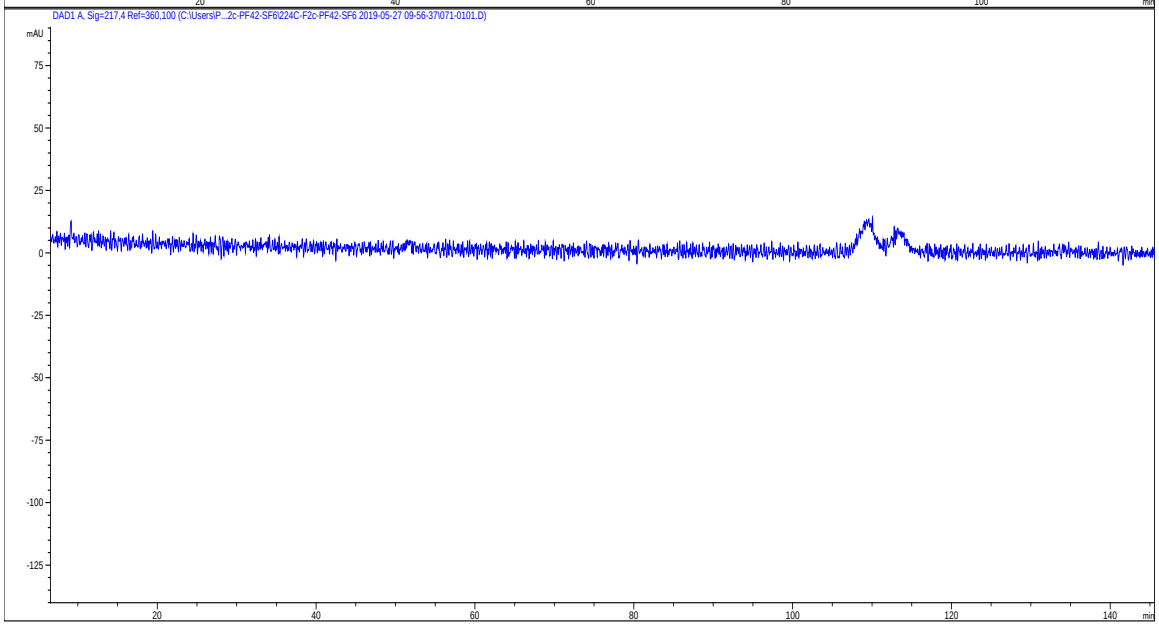
DAD1 A, Sig=217,4 Ref=360,100 (C:\Users\P...2c-PF42-SF6\224C-F2c-PF42-SF6 2019-05-27 09-56-37\071-0101.D)
mAU
75
50
25
0
-25
-50
-75
-100
-125
20
40
60
80
100
120
140
min

Fig. 2.10. Attempts to further fractionate fraction SF6 by HPLC failed. In all runs, fraction SF6 was run on an extended gradient. (*Top panel*) Column: Agilent XDB-C18 5 μm, 4.6 x 250 mm. Mobile phase (A) 0.1% formic acid in water, (B) 0.1% formic acid in acetonitrile, flow rate: 43 mL/min. Gradient is 35% B 0-60 min, 36% 60-120 min, 100% B 120-150 min. (*Middle panel*) Column: Agilent Eclipse XDB-C18 5 μm, 4.6 x 250 mm. Mobile phase (A) 0.1% formic acid in water, (B) 0.1% formic acid in acetonitrile, flow rate: 1 mL/min. Isocratic gradient at 36% B. (*Bottom panel*) Column: Agilent Eclipse XDB-C18 5 μm, 9.4 x 250 mm. Mobile phase (A) 0.1% formic acid in water, (B) 0.1% formic acid in acetonitrile, flow rate: 4 mL/min. Isocratic gradient at 36% B. This was a semi-preparative run. Interestingly, running only fraction SF6 seemed to yield both SF6 and SF7 peaks, confirming that trace castaneroxy A (fraction SF7) is present in fraction SF6 and can be further purified from it. In the semi-preparative run, fractions were manually collected from the two peaks. ^{1}H NMR data showed that all fractions of the SF6 peak were the same; no further resolution was achieved. This strongly suggests that the analytical columns similarly did not achieve further resolution. Meanwhile, ^{1}H NMR data of fractions of the SF7 peak confirmed that it was indeed fraction SF7.

Fig. 2.11. Preparative SISN (silica impregnated with silver nitrate) TLC failed to further resolve fraction SF6. SISN TLC was selected due to the reported resolving power of SISN for isomeric alkenes. A 40:10:50 IPA:EtOAc:Hex mobile phase was selected after method development. (*Left panel*) After the run, spray reagent (vanillin and sulfuric acid in ethanol) was used to visualize a portion of the plate in order to divide the length into fragments for cutting. (*Right panel*) Cuts were made according to the markings shown, with four major fragments being specified. After cutting, the SISN of each fragment was scraped onto aluminum foil and individually extracted by methanol. Subsequent ^{1}H NMR data collected from the evaporated products revealed that no bands showed substantially increased resolution over what is observed in fraction SF6.

Methods

General Experimental Procedures. Optical rotations were measured using a Perkin-Elmer 341 polarimeter (concentration in g/100mL) with methanol as a solvent. IR spectra were recorded on a Nicolet iS10 FT-IR spectrometer and the absorption peaks were reported in cm^{-1}. Nuclear magnetic resonance (NMR) data were recorded on a Bruker 600 Ascend (600 MHz for ^{1}H NMR and 150 MHz for ^{13}C NMR) instrument equipped with CryoProbe™ Prodigy. NMR spectra were recorded in solutions of deuterated methanol (MeOD) with the residual methanol (3.31 ppm for ^{1}H NMR and 49.15 ppm for ^{13}C NMR) taken as the internal standard; they were reported in parts per million (ppm) relative to tetramethylsilane (TMS) at 0 ppm. Mass spectrometric data was acquired in MS1 mode scanning from a *m/z* of 150–1500 on a Thermo Scientific LTQ-FT Ultra MS in negative ESI mode and processed with Thermo Scientific Xcalibur 2.2 SP1.48 software (San Jose, CA). Samples were directly injected. The capillary temperature was 275.0°C, sheath gas of 60, source voltage and current were 5.0 kV and 100.0 μA, and the capillary voltage was -49.0 V. 3D molecular modeling was performed using ChemBioDraw Ultra and Chem3D. All solvents were acquired from Fisher Chemical, Certified ACS. Target compounds and side products are labeled with Arabic numerals.

Collection and processing of plant materials. Fresh leaves of wild *Castanea sativa* Mill. (European chestnut) of the Fagaceae family were collected in the months of May-July in the years 2012-2014 in the Rionero-Alto Bradano region of the Basilicata Province in southern Italy. Standard guidelines for collection of wild specimens were followed (106). Collections were made on private land with the landowner's consent. The voucher specimen for the collections of *C. sativa* (CQ-309) is viewable online on the SERNEC web portal (107); they were deposited at both the *Herbarium Lucanum* (HLUC) at the *Universitá della Basilicata* in Potenza, Italy and at the Emory University Herbarium (GEO) in Atlanta, GA, USA. Initial

specimen identification was done using the standard Italian Flora (108), and this was confirmed at HLUC. *C. sativa* leaves were dried in the shade, ground with a blender, and vacuum sealed with silica packets before shipment to the US (under USDA permit P587-120409-008). At the laboratory, the leaf powder was further ground with a Thomas Wiley Mill at a 2 mm mesh size (Thomas Scientific).

Extraction and isolation. 224C-F2 was obtained as previously described (8). Briefly, ground, dried leaves of *C. sativa* were macerated in MeOH at room temperature for two successive periods of 72 h with daily agitation. Filtered extracts were concentrated *in vacuo*, lyophilized, then partitioned in sequentially against hexanes then ethyl acetate. The resulting non-aqueous partitions were dried over anhydrous Na_2SO_4, concentrated *in vacuo*, and lyophilized before testing for activity. The ethyl acetate partition (224C) was subjected to further fractionation using a CombiFlash Rf+ (Teledyne ISCO) flash chromatography system using a RediSep Rf Gold silica column. Extract 224C was bonded to Celite 545 (Acros Organics) at a 1:4 ratio and dry-loaded via RediSep dry load cartridge. Three mobile phases were employed: hexane (A), ethyl acetate (B), and methanol (C). The mobile phase gradient starts at 100% A (0% B), which is held for 6.3 column volumes (CV). From 6.3 CV to 25.3 CV, this is increased to 50% B, and from 25.3 CV to 63.3 CV, this is further increased to 100% B. 100% B held until 69.9 CV. From 69.9 CV to 88.6 CV, the gradient changes to 70:30 B:C, and 30% C is held until 94.9 CV. The wavelengths monitored were 254 and 280 nm. 224C-F2c represents the portion of 224C-F2 that elutes from 28.5 CV to 37.1 CV.

Method development for the fractionation of 224C-F2c via HPLC was performed on analytical HPLC. An Agilent 1260 Infinity system running OpenLab CDS ChemStation (Agilent Technologies, Santa Clara, CA, USA) was used with an Agilent XDB-C18 (250 mm

x 4.6 mm, 5 μm) column with compatible guard column at a column temperature of 25°C. Mobile phase reagents were HPLC-grade and purchased from Fisher Scientific except for the Type 1 water, which was obtained from an EMD Millipore MILLI-Q water system (Billerica, MA). The mobile phases were 0.1% formic acid in acetonitrile (A) and 0.1% formic acid in water (B); the flow rate was 1 mL/min. Production of 224C-F2c fractions was performed on an Agilent 1260 Infinity II system running the same software. The column used was an Agilent XDB-C18 (250 mm x 30 mm, 5 μm) column. 224C-F2c was dissolved in MeOH and 2 mL injections were made. Chromatograms were monitored at 254 nm and 314 nm. Initial conditions were 98:2 (A:B), held for 5.5 min, changing to 43:57 (A:B) at 14.5 min and held till 23.5 min, changing to 2:98 (A:B) at 26.5 min and held until 45 min. A total of 43 "preparative fractions" (PFs) were obtained using this method. PF42 eluted from 35.0 - 35.5 min, and due to its activity in the *S. auereus agr* reporter strain panel, it was chosen for further fractionation.

A second round of preparative HPLC fractionation to split 224C-F2c-PF42 into "subfractions" (SFs) utilized an Agilent XDB-C18 (50 mm x 30 mm, 5 μm) column. Method development was performed on the analytical system cited above, and a custom-built open-bed fraction collector was used for preparative HPLC (109). Initial conditions were 70:30 (A:B), held for 9.00 min, changing to 43:57 (A:B) at 12.00 min and held until 14.00 min, changing to 0:100 (A:B) at 14.01 min and held until 16 min. 224C-F2c-PF42 was dissolved in MeOH and 1 mL injections were made. Chromatograms were monitored at 217 nm and 254 nm. 224C-F2C-PF42-SF6, containing compounds **2a/2b**, eluted from 2.5-3.0 min; one run yielded 1.12 mg (11.2% yield). 224C-F2c-PF42-SF7, containing compound **1** (castaneroxy A), eluted from 3.0-3.5 min; one run yielded 0.47 mg (4.7% yield).

Castaneroxy A (**1**): white amorphous solid; $[\alpha]^{23}_{D}$ +51.0 (c 0.003, MeOH); UV (MeOH) λ_{max} (log ε) 210 (1.04) nm; IR υ_{max} 3352, 2932, 2866, 1696, 1558, 1443, 1374, 1260, 1077, 996, 925, 902, 846, 768, 750 cm^{-1}; HRESIMS m/z 503.3381 $[M - H]^-$ (calc. for 503.3367 $C_{30}H_{47}O_6$); ^1H and ^{13}C NMR data (**Table 2.1**).

Single Crystal X-ray Diffraction. Colorless crystals were initially obtained by evaporating the fractions 224C-F2c-PF42-SF6 and 224C-F2c-PF42-SF7 under a barvap. Larger crystals suitable for X-ray crystallographic analysis of castaneroxy A were later obtained by slow evaporation from a chloroform-hexane mixture. Slow evaporation of a CH_3OH solution of the mixture **2a/2b** yielded crystals of **2a** suitable for a single-crystal X-ray diffraction study. Suitable crystals were mounted on a loop with paratone. X-ray diffraction data were collected on a Rigaku XtaLAB Synergy-S diffracrometer with a HyPix-6000HE detector. The crystals were cooled to 100 K with an Oxford Cryosystems low-temperature device during the collections. Data were measured using ω scans of 0.5° per frame for variable scan times using CuK_α radiation (micro-focus sealed X-ray tube, 50 kV, 1.0 mA). The total number of runs and images was based on the strategy calculation from the program CrysAlisPro (Rigaku, V1.171.39.35c, 2017). Data reduction, scaling and absorption corrections were performed using CrysAlisPro (Rigaku, V1.171.40.76a, 2020). All non-hydrogen atoms were refined anisotropically. Hydrogen atom positions were either located from electron density maps and refined freely (or with restraints) using the non-spherical scattering factors or hydrogen atom positions were calculated geometrically and refined using the riding model.

Crystallographic data for compounds **1** and **2a** have been deposited with the Cambridge Crystallographic Data Centre, 12 Union Road, CB2 1EZ, UK (fax: +44-1223-336033; e-mail:

deposit@ccdc.cam.ac.uk) and are available on request quoting the deposition number CCDC: 2046240 (compound **1**) and 2046241 (compound **2a**).

Crystallographic data of **1**. ($C_{30}H_{48}O_6$). (H_2O), M_r = 522.70, monoclinic, $P2_1$ (No. 4), a = 7.54880(14) Å, b = 11.2160(2) Å, c = 16.9599(3) Å, β = 102.5498(18)°, $\alpha = \gamma$ = 90°, V = 1401.64(5) Å^3, T = 100.0(4) K, Z = 2, Z' = 1, μ(Mo K$_\alpha$) = 0.086 mm^{-1}, 30323 reflections measured, 12736 unique (R_{int} = 0.0291) which were used in all calculations. The final wR_2 was 0.1258 (all data) and R_1 was 0.0460 (I > 2σ(I)).

Crystallographic data of **2a**. ($C_{30}H_{48}O_6$). 2 (H_2O), M_r = 540.72, monoclinic, $P2_1$ (No. 4), a = 6.7500(3) Å, b = 12.2578(7) Å, c = 17.4707(12) Å, β = 98.740(6)°, $\alpha = \gamma$ = 90°, V = 1428.75(15) Å^3, T = 110.1(8) K, Z = 2, Z' = 1, μ(CuK$_\alpha$) = 0.723 mm^{-1}, 9232 reflections measured, 3582 unique (R_{int} = 0.0776) which were used in all calculations. The final wR_2 was 0.1689 (all data) and R_1 was 0.0648 (I > 2σ(I)).

Spectra

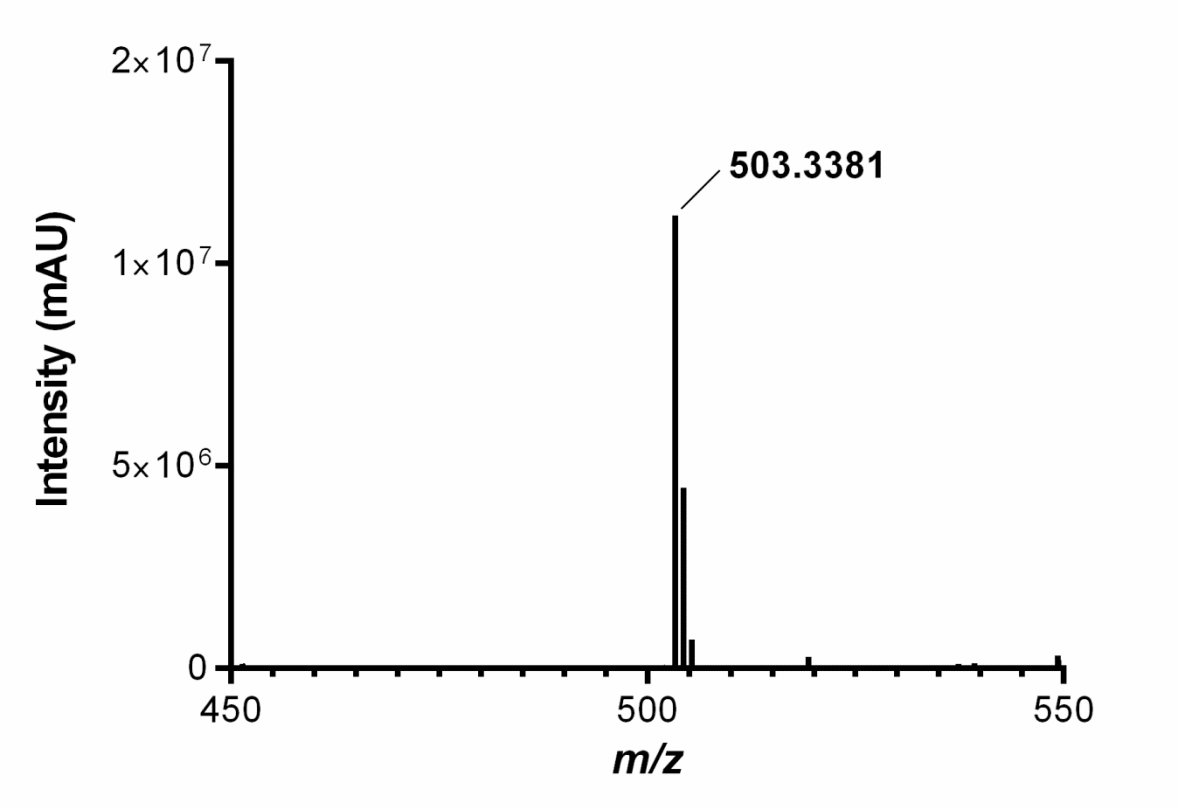

Peak mass	Display formula	RDB	Delta [ppm]	Theoretical mass	Combined Score	MS Cov. [%]
503.33809	$C_{30}H_{47}0_6$	7.50	2.72	503.33672	89.45	92.54

Supplementary Fig. 2.1. ESI-MS negative mode spectrum and empirical formula calculations of compound **1**.

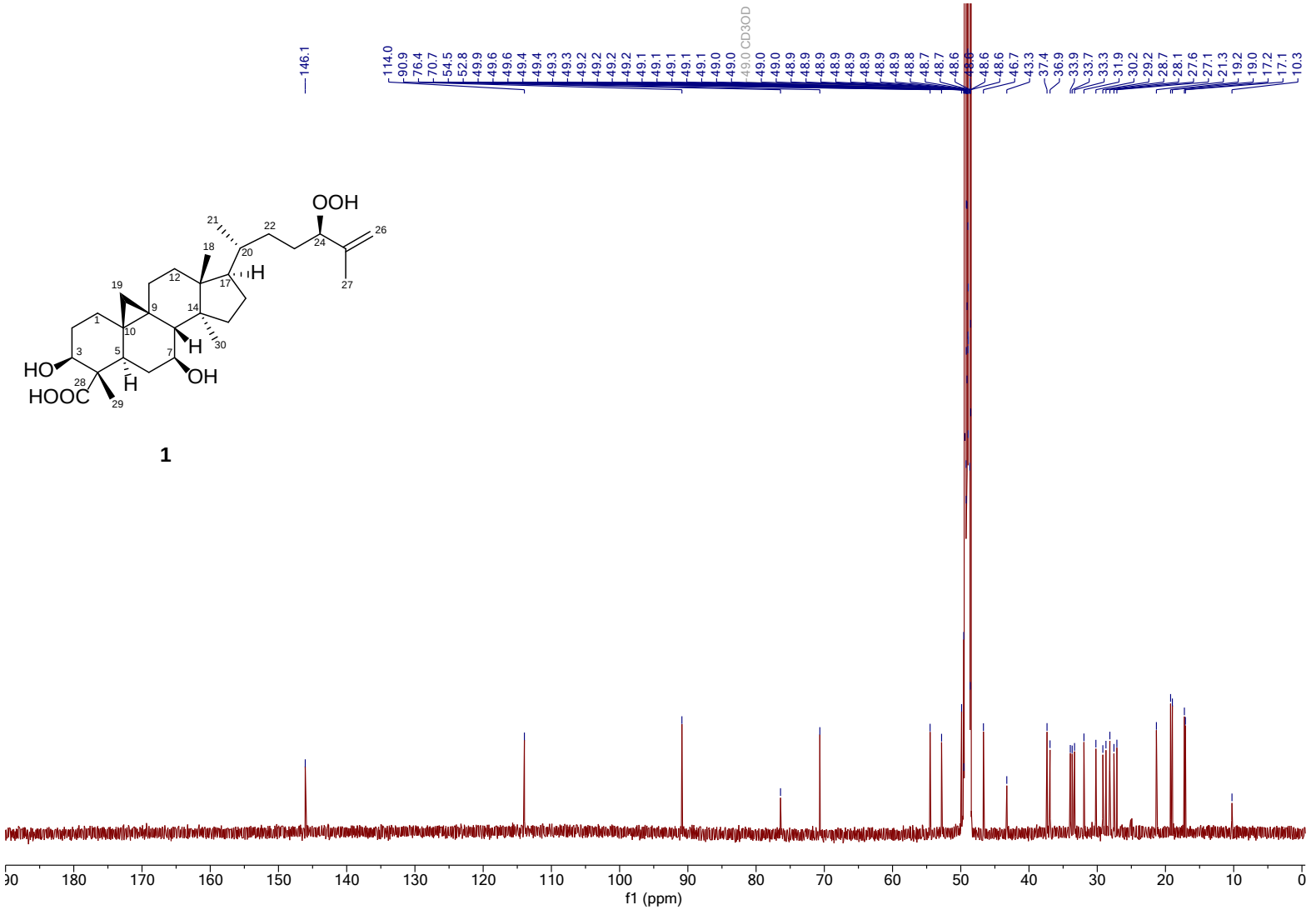

1

Supplementary Fig. 2.2. ^{13}C NMR spectrum of **1** in CD_3OD.

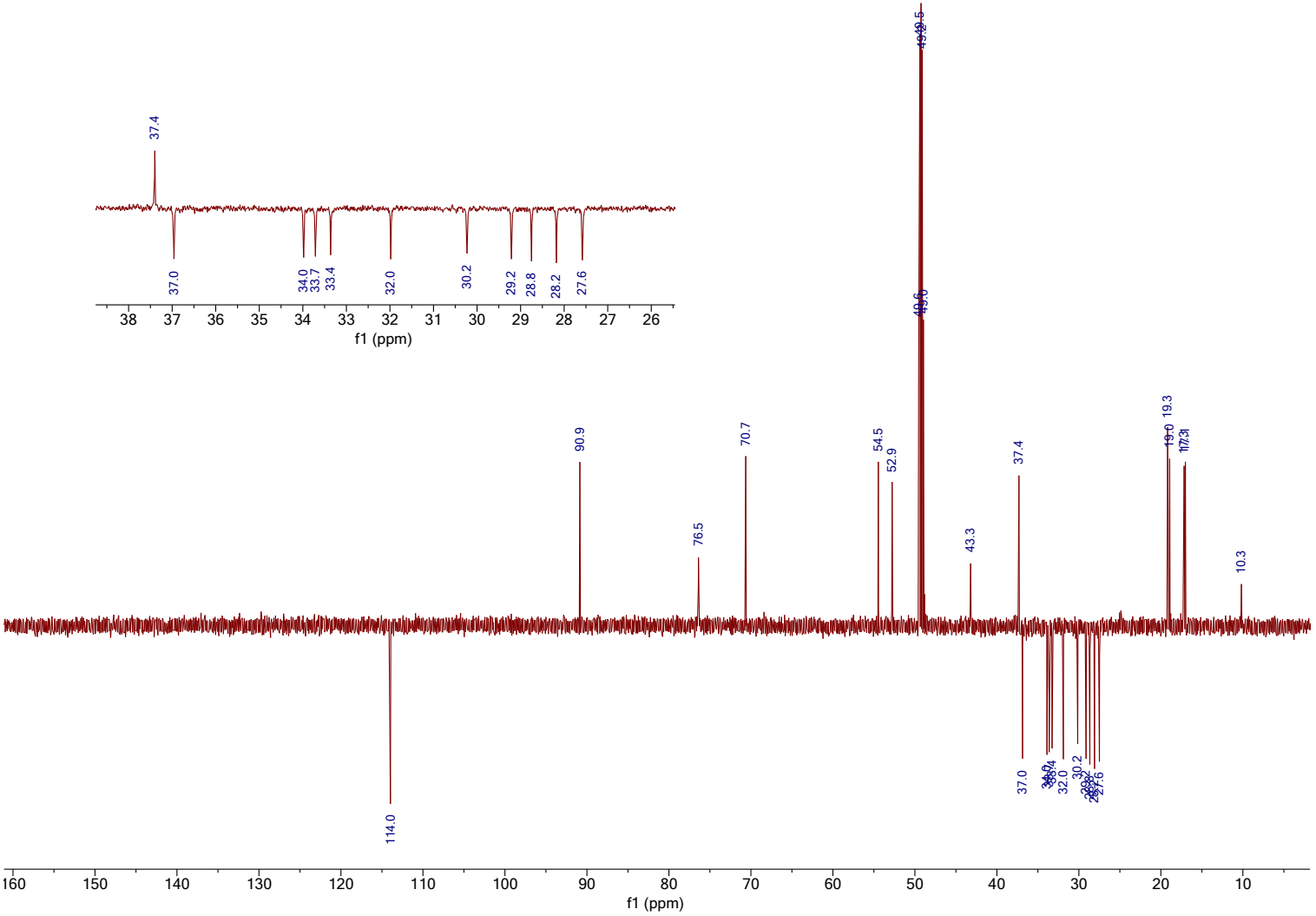

Supplementary Fig. 2.3. DEPT-135 spectrum of **1** in CD_3OD.

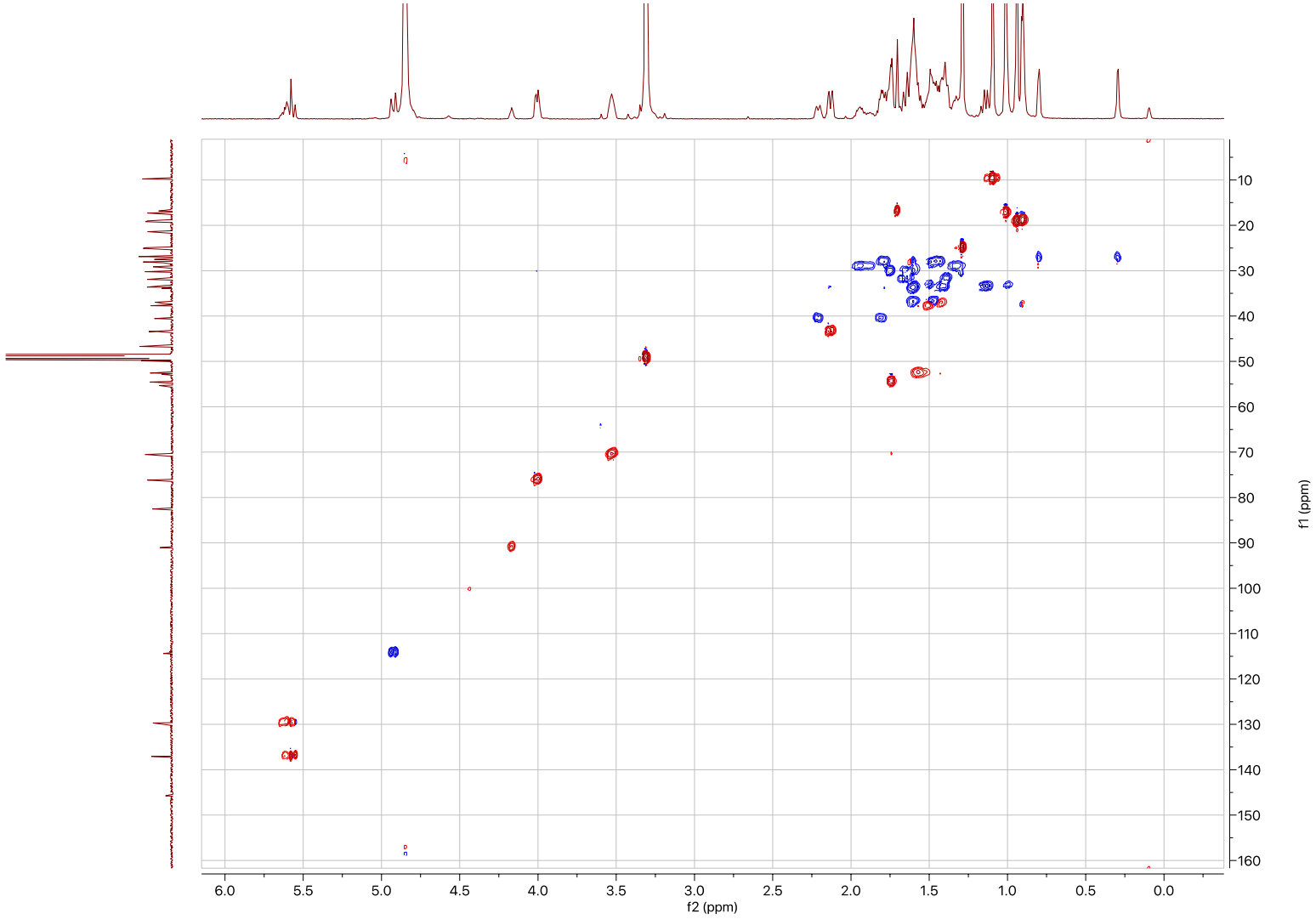

Supplementary Fig. 2.4. HSQC spectrum of **1** in CD_3OD.

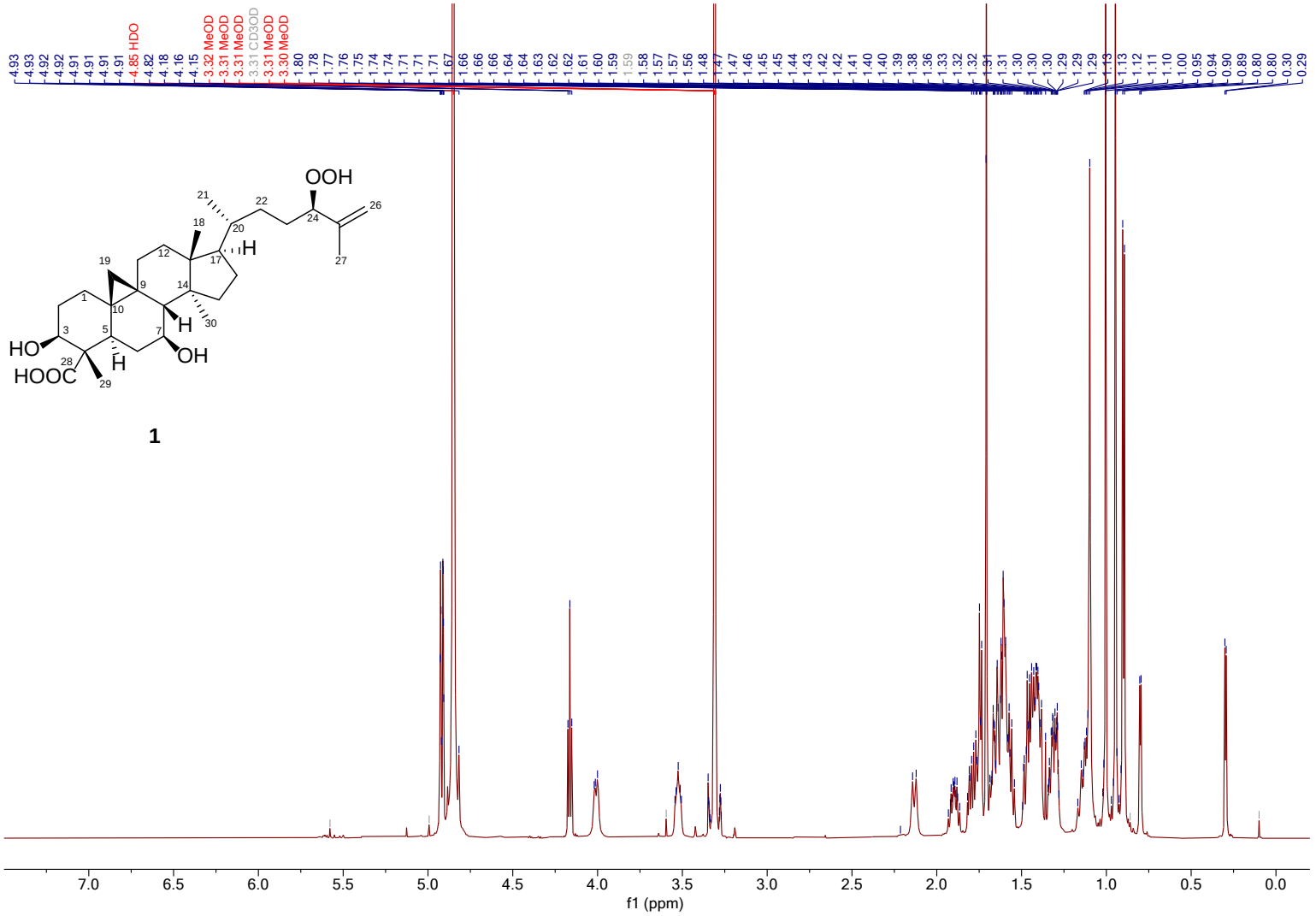

Supplementary Fig. 2.5. ^{1}H NMR spectrum of **1** in CD_3OD.

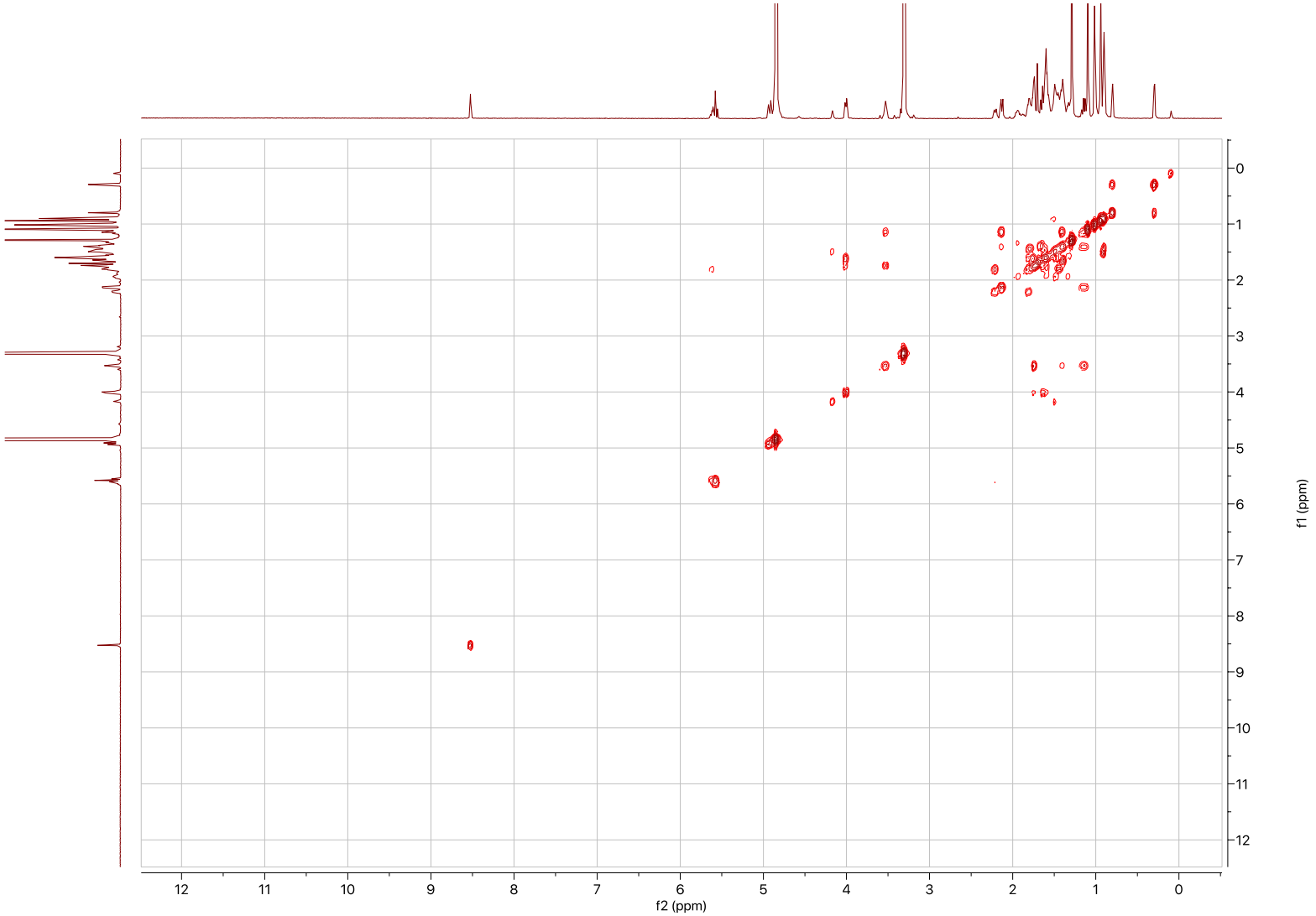

Supplementary Fig. 2.6. COSY spectrum of **1** in CD_3OD.

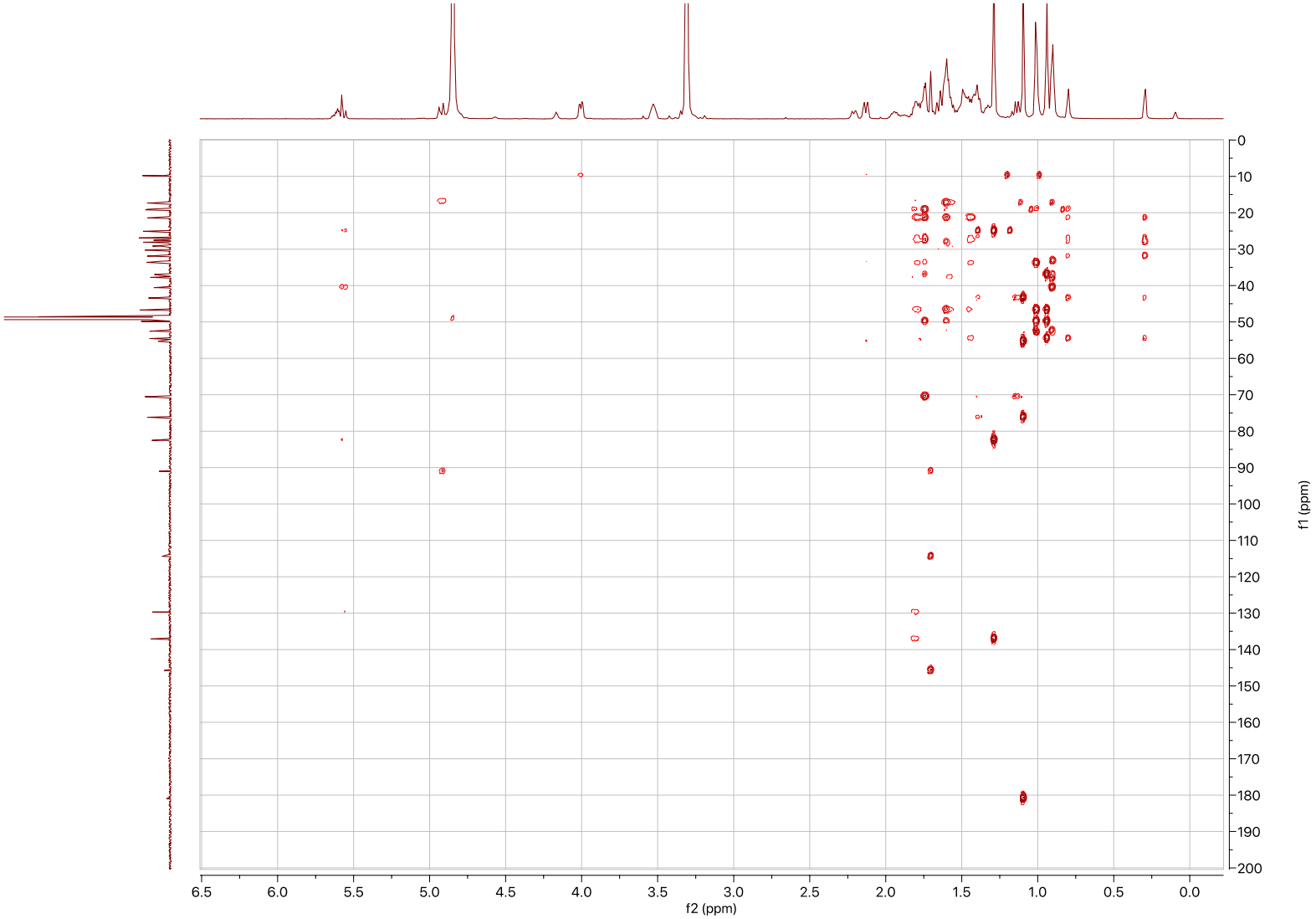

Supplementary Fig. 2.7. HMBC spectrum of **1** in CD_3OD.

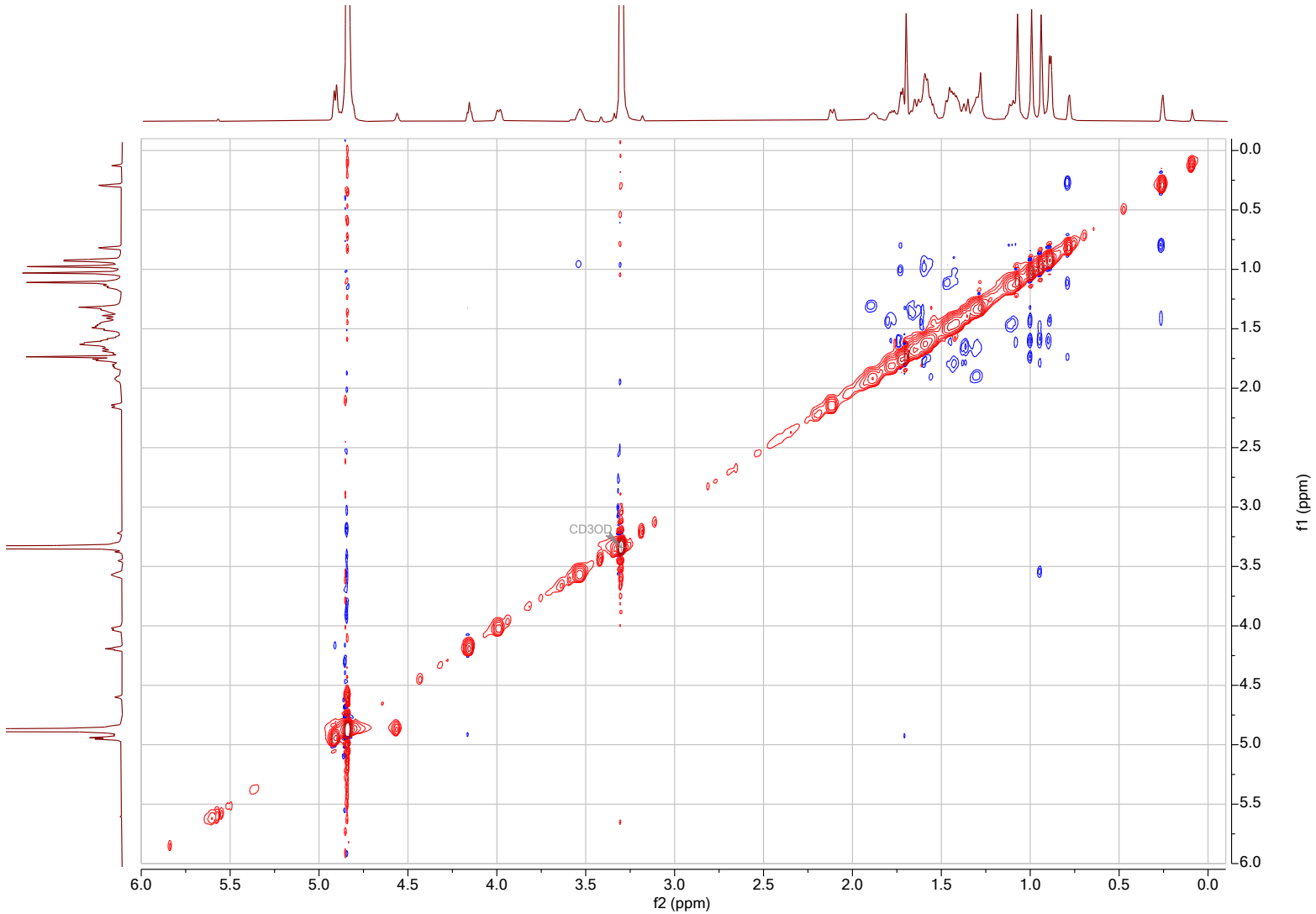

Supplementary Fig. 2.8. NOESY spectrum of **1** in CD_3OD.

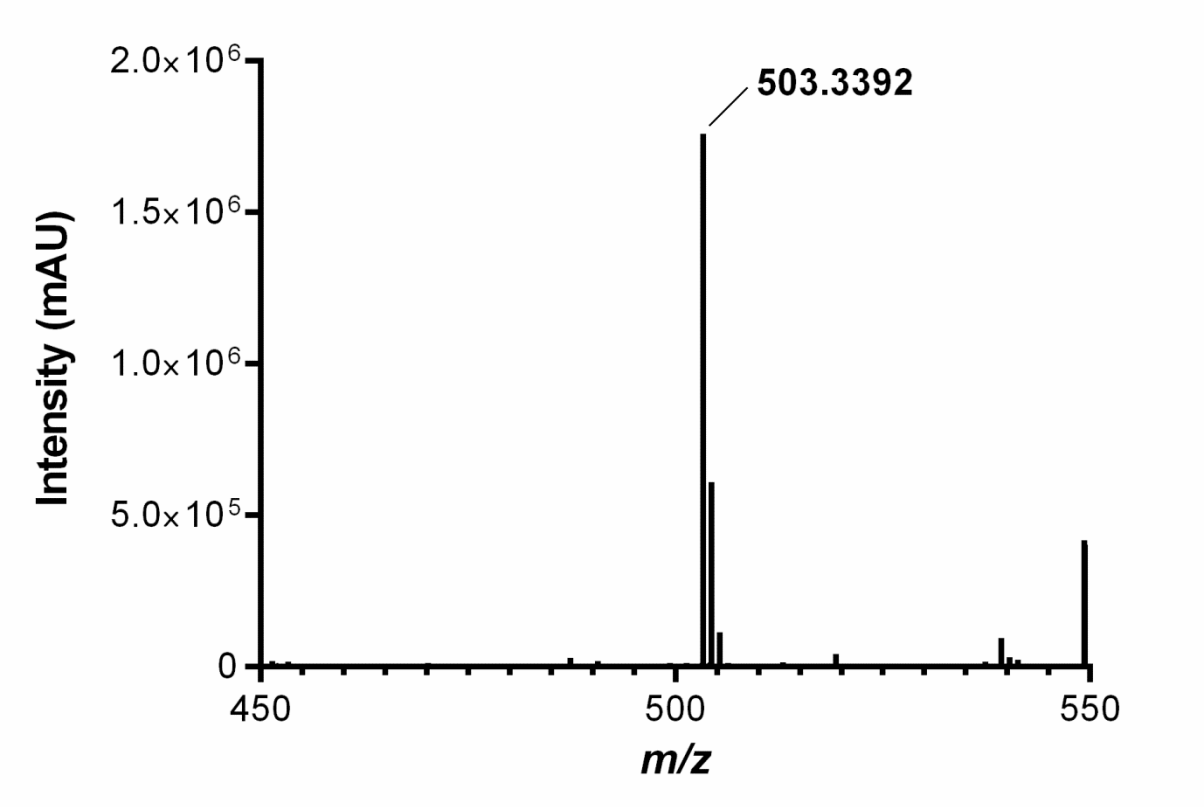

Peak mass	Display formula	RDB	Delta [ppm]	Theoretical mass	Combined Score	MS Cov. [%]
503.33918	$C_{30}H_{47}0_6$	7.50	4.90	503.33672	82.78	86.61

Supplementary Fig. 2.9. ESI-MS negative mode spectrum and empirical formula calculations of compounds **2a, 2b**.

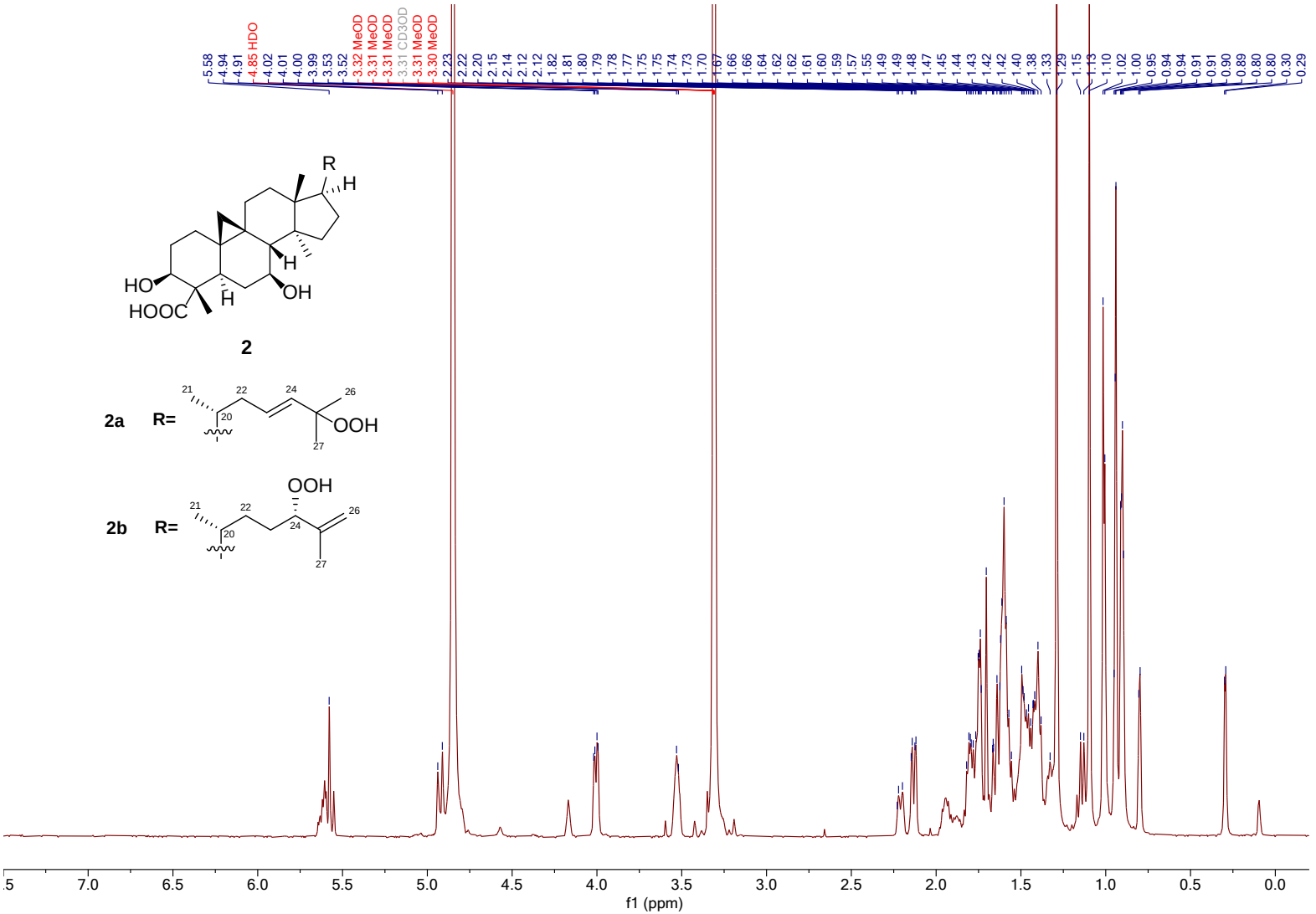

Supplementary Fig. 2.10. ^{1}H NMR spectrum of compounds **2a, 2b** in CD_3OD.

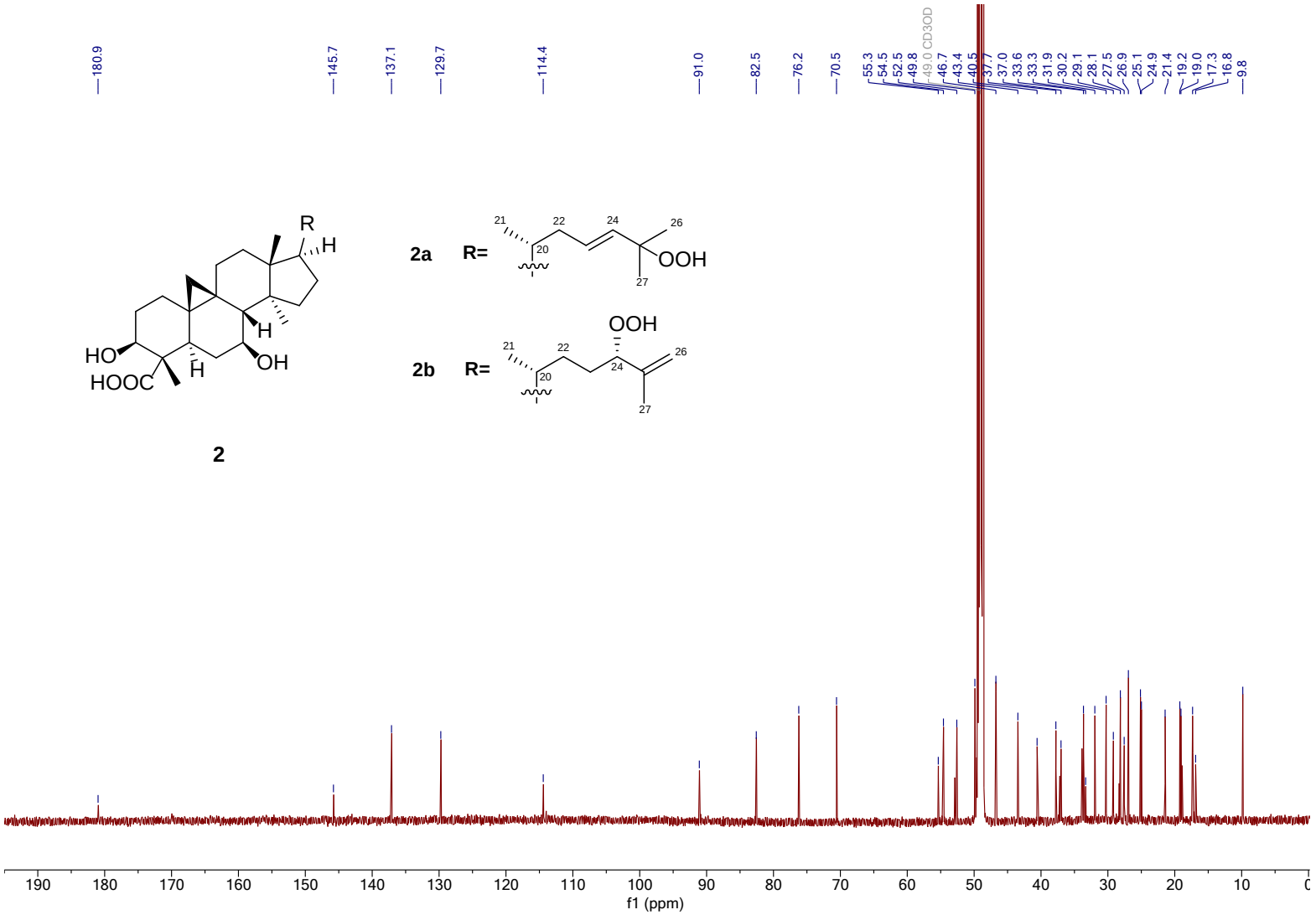

Supplementary Fig. 2.11. ^{13}C NMR spectrum of compounds **2a, 2b** in CD_3OD.

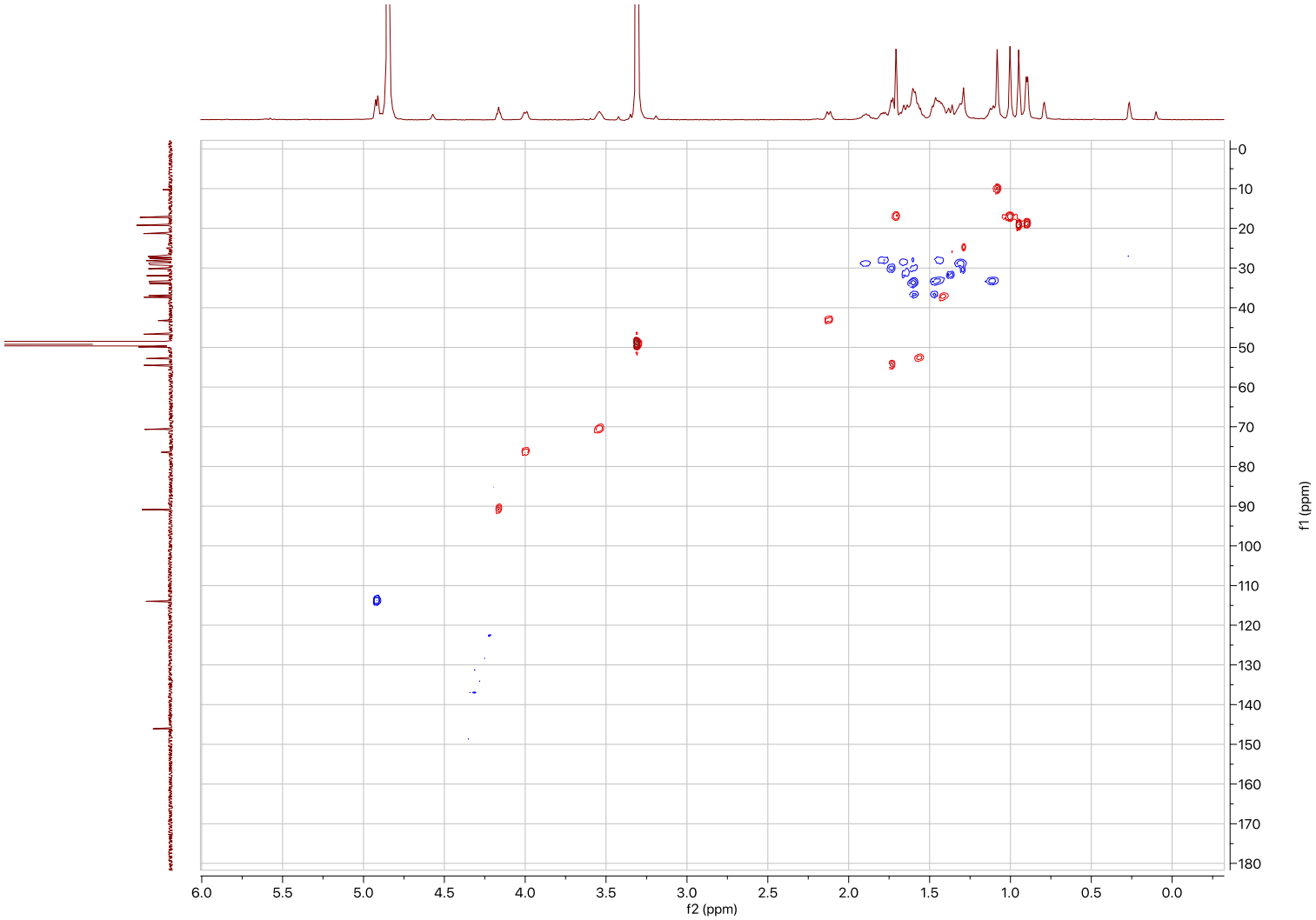

Supplementary Fig. 2.12. HSQC spectrum of compounds **2a, 2b** in CD_3OD.

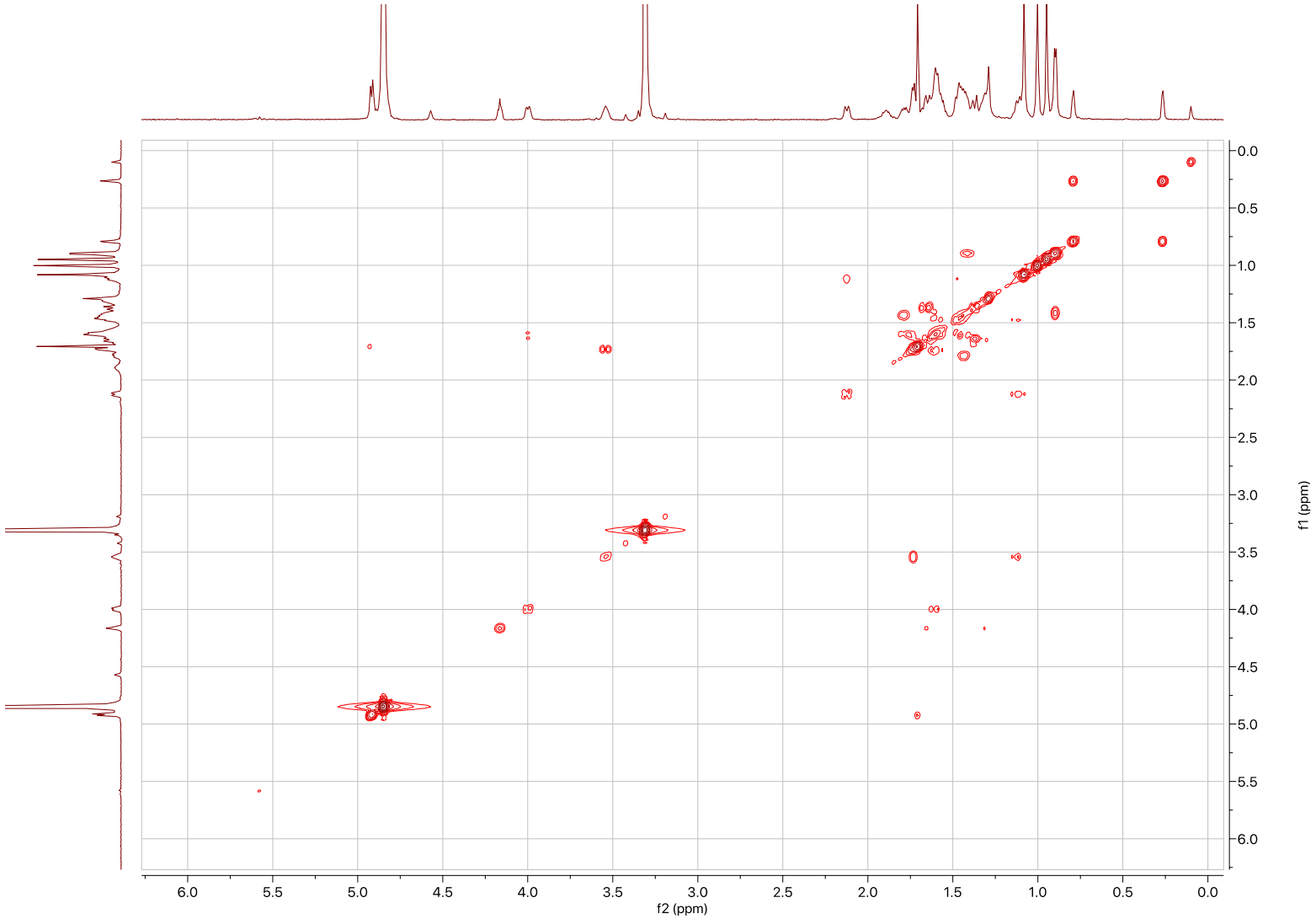

Supplementary Fig. 2.13. COSY spectrum of compounds **2a, 2b** in CD_3OD.

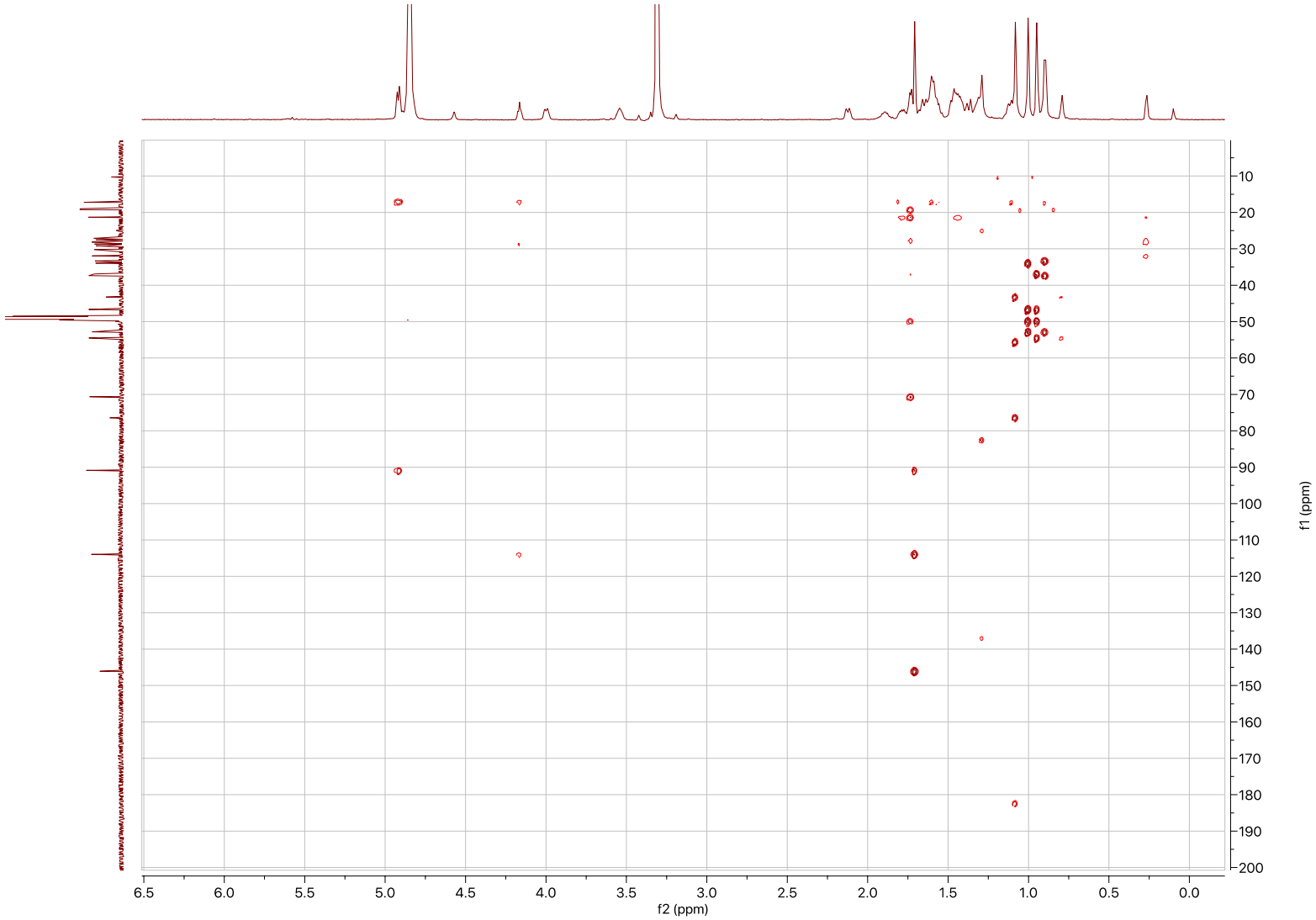

Supplementary Fig. 2.14. HMBC spectrum of compounds **2a, 2b** in CD_3OD.

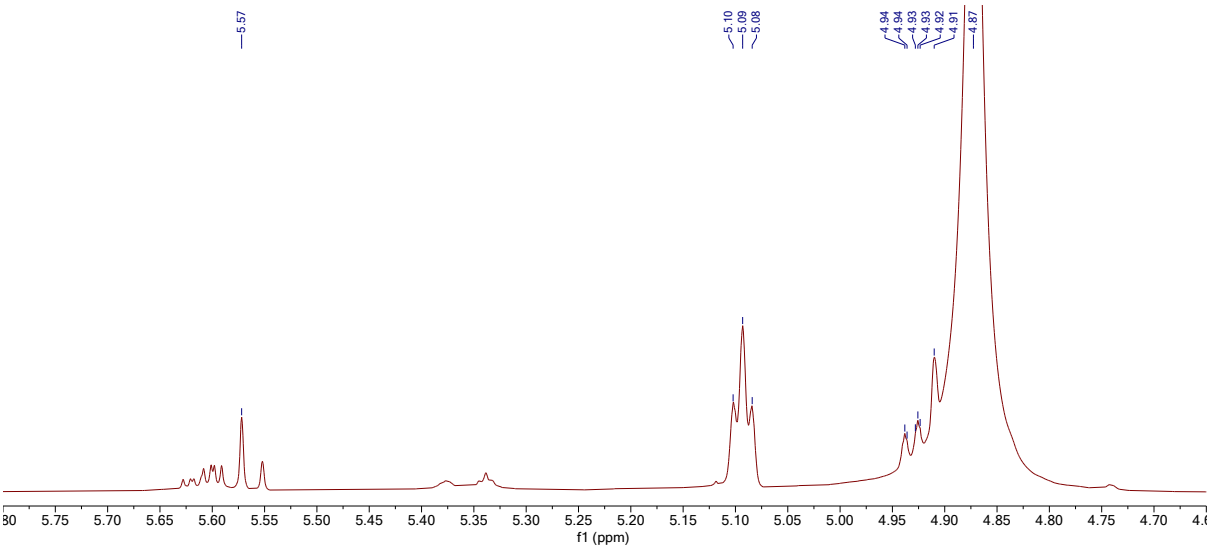

Supplementary Fig. 2.15. Zoomed in ^{1}H spectrum of 224C-F2c-PF42. The triplet signal δ_H 5.10 ppm is suggested to correspond to H_1-24 of the proposed castaneroxy precursor, reported by Popova, *et al* (96).

CHAPTER III

Castaneroxy A inhibits quorum sensing and virulence in methicillin-resistant *Staphylococcus aureus* (MRSA)

The results are being assembled for submission to *Frontiers in Pharmacology*.

Introduction

Staphylococcus aureus, including methicillin-resistant *S. aureus* (MRSA), remains a pathogen of great concern in the United States and across the world. In 2019, the Centers for Disease Control and Prevention (CDC) labeled *S. aureus* as a "serious threat," and in 2017 alone *S. aureus* caused 323,700 hospitalizations, 10,600 deaths, and $1.7 billion in healthcare costs (14). The World Health Organization (WHO) has designated *S. aureus*, including MRSA, as a leading international pathogen of concern both in the community and in hospitals, and in 2017 it cited *S. aureus* a high priority pathogen for which new antibiotics are urgently needed (15; 110). Both organizations cite antibiotic resistance in *S. aureus* as one of its most threatening characteristics. In the face of spreading antibiotic resistance, the world is in need of new anti-infective drugs (111). All currently approved antibiotic treatments exert their activity via bacteriostatic or bactericidal mechanisms (112). While many efforts are being made to discover and develop new growth-inhibiting drugs that target new pathways, much research is also being devoted to targeting bacterial virulence as an alternative approach (113; 114). Indeed, the inhibition of virulence has been recurrently cited and demonstrated in the literature as a promising anti-infective strategy against *S. aureus*, including MRSA (115-117).

S. aureus is a Gram-positive bacterium that is unique in that it is capable of infecting numerous tissue types and has demonstrated a rapid ability to develop antibiotic resistance (55; 56). In order to successfully infect a host, *S. aureus* depends on a variety of virulence mechanisms largely controlled by the Accessory Gene Regulator (*agr*) quorum sensing system (59; 60). In the establishment of infection, capsular polysaccharides on the cell surface enhance tissue colonization and protect from phagocytosis (118) while cell wall-anchored proteins play roles in

nutrient uptake, biofilm formation, immune evasion, and tissue adhesion and invasion (119). Later in the infection cycle, during stationary phase growth, exotoxins such as α-toxin and δ-toxin target host cells for destruction to aid in immunity disruption, nutrient acquisition, and dissemination (59; 120-122). Since staphylococcal virulence factors are expressed under the control of quorum sensing, inhibition of virulence can be achieved by chemical inhibition of quorum sensing. Quorum sensing is a system of stimuli and response between cells in a bacterial population that coordinates the gene expression of pathways that contribute to virulence, the capacity to infect a host, in a population-density fashion (60). The machinery of quorum sensing in *S. aureus* forms the *agr* system, the organism's most well-studied virulence regulatory system (44; 64; 117).

In an effort to develop a novel therapeutic strategy against methicillin-resistant *Staphylococcus aureus* (MRSA), an enriched extract of *Castanea sativa* leaves, 224C-F2, was identified as containing compounds that inhibit MRSA virulence. Castaneroxy A (**1**), a hydroperoxy cycloartane triterpenoid, was subsequently isolated from 224C-F2 by bioassay-guided fractionation utilizing reverse-phase HPLC. The bioassay employed in this process was a set *S. aureus* reporter strains of *agr*::P3 activation (123). Since the assay provides a measure of inhibition of the *agr* system, **1** was identified as a potential MRSA antivirulence compound. A series of bioassays were employed to confirm whether **1** does indeed inhibit markers of virulence in MRSA. Castaneroxy A displays a concentration-dependent inhibition of *agr*::P3 activation in all *S. aureus agr* subtypes. In assays measuring δ-toxin production, MRSA supernatant toxicity, and MRSA supernatant hemolytic acitivity, **1** exerts IC_{50} values in the low micromolar range. Additionally, the biofilm inhibitory activity and potential for human cytotoxicity of **1** were

assessed. Finally, **1** demonstrates the ability to abate MRSA-induced dermonecrosis in a mouse model of skin infection. In comparison to other recently reported inhibitors of MRSA virulence, **1** exerts comparable activities *in vitro*. These data confirm **1** both as a promising MRSA antivirulence drug candidate and as a contributor to the ethnobotanical anti-infective value of *C. sativa* leaves.

Results

Castanaroxy A acts on the *agr* system to inhibit virulence in MRSA

To confirm the quorum sensing inhibitory activity of **1**, its concentration-dependent effects were examined on a number of *S. aureus* markers of virulence: *agr*::P3 activation, α-toxin and δ-toxin production, and culture supernatant toxicity to human cells. The IC_{50} of castaneroxy A on all strains to be examined was first determined in order to ensure subsequent testing at sub-IC_{50} concentrations (**Table 3.1**). The IC_{50} of castaneroxy A for the *S. aureus* strains UAMS-1, AH1263, AH1292, AH1589, and NRS835 is 126.90 µM (64 µg/mL) (124-127). Therefore, the following assays were performed using castaneroxy A and its parent fractions at concentrations of up to 32 µg/mL (63.45 µM for castaneroxy A).

Table 3.1. IC_{50} and MIC values of castaneroxy A against various *S. aureus* strains, based on optical density of growth cultures.

Strain ID	IC	Castaneroxy A (uM)
UAMS-1	IC_{50}	126.90
	MIC	126.90
AH1263	IC_{50}	126.90
	MIC	253.80
AH1292	IC_{50}	126.90
	MIC	253.80
AH1589	IC_{50}	126.90
	MIC	253.80
NRS385	IC_{50}	126.90
	MIC	253.80

To confirm whether **1** targets the *agr* system in MRSA, it was assayed along with its parent fractions in the *agr*::P3 reporter strain panel (**Figure 3.1**). Castaneroxy A exhibited a concentration-dependent inhibition of YFP production in all strains in the panel, as did its parent fractions 224C-F2, 224C-F2c, and 224C-F2c-PF42 (referred to henceforth as F2, F2c, PF42). The results are summarized in **Table 3.2**. Across all *agr* types, the dose response curves of F2 and F2c closely align with each other, suggesting that F2c contains most of the compounds that contribute to the effects of F2 in *agr*::P3 inhibition. The dose response curves of PF42 and castaneroxy A are similarly closely aligned with each other in each reporter strain. One possible implication of this is that the castaneroxys in PF42 each exert similar activities on the *agr* system despite their differences in structure. Unlike F2 and F2c, PF42 and castaneroxy A exhibit growth inhibitory activity at higher concentrations in *agr* Types I and II. At these concentrations, then, a portion of the apparent reporter inhibition is due to growth inhibition.

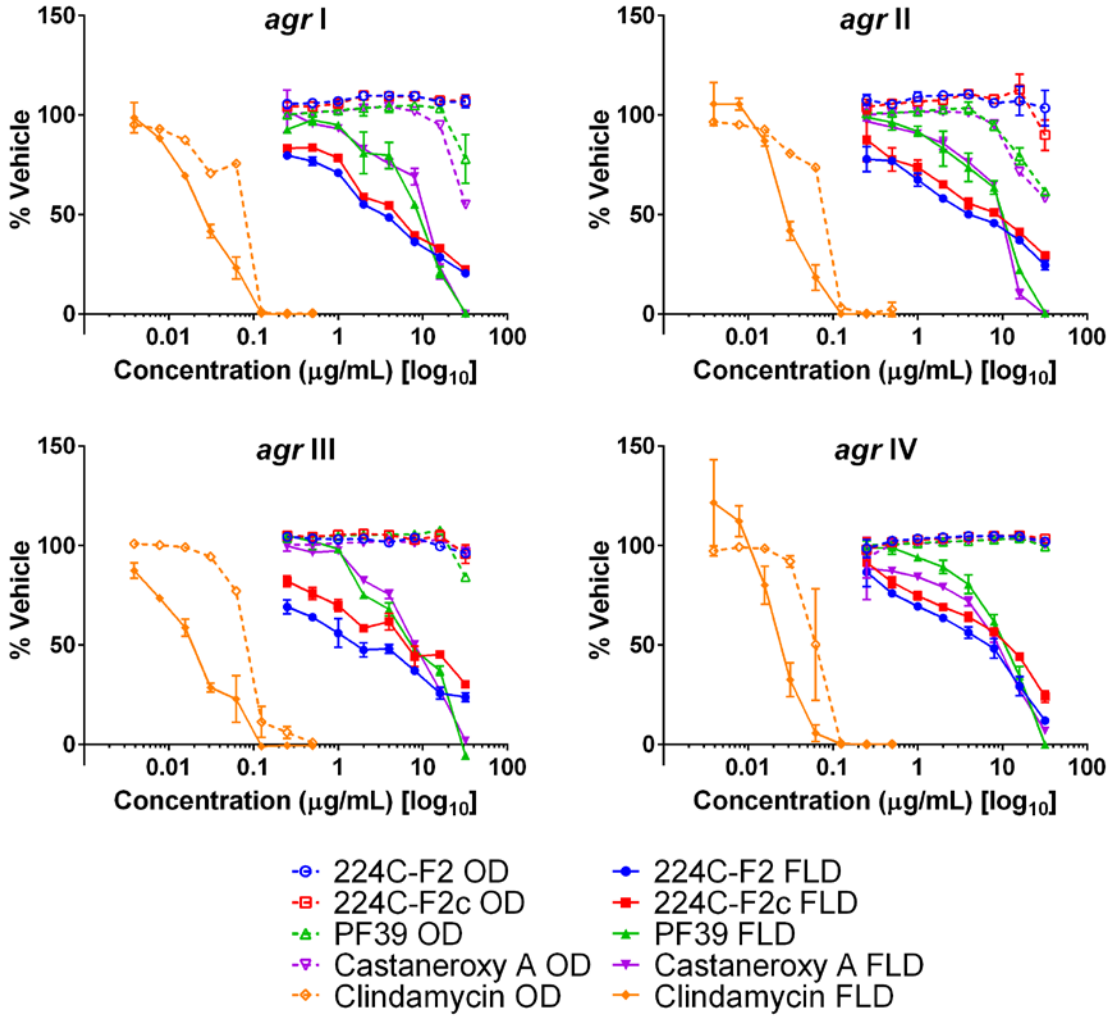

Fig. 3.1. Castaneroxy A and its parents exert selective concentration-dependent inhibition of *agr*::P3 activation in all *agr* sub-types. Castaneroxy A and its parent fractions were tested from 0.25-32 µg/mL on four *S. aureus agr*::P3 reporter strains: AH1677 (*agr* I), AH430 (*agr* II), AH1747 (*agr* III), AH1872 (*agr* IV). All dashed curves represent optical density (OD) values, indicating growth; all solid curves represent fluorescence detection (FLD) values, indicating intensity of YFP detection as a result of *agr*::P3 activation. Clindamycin was used as a control to demonstrate reporter inhibition due solely to growth inhibition.

Table 3.2. IC values of castaneroxy A and parent fractions on *agr* reporter strain fluorescence detection.

Strain ID	***agr* group**	**IC**	**Test agent (µg/mL)**				
			224C-F2	224C-F2c	224C-F2c-PF42	Castaneroxy A	Castaneroxy A (µM)
AH1677	I	IC_{50}	4	8	16	16	31.72
		IC_{90}	ND	ND	32	32	63.45
AH430	II	IC_{50}	8	16	16	16	31.72
		IC_{90}	ND	ND	32	32	63.45
AH1747	III	IC_{50}	2	8	8	16	31.72
		IC_{90}	ND	ND	32	32	63.45
AH1872	IV	IC_{50}	8	16	16	16	31.72
		IC_{90}	ND	ND	32	32	63.45

ND: IC not detected at the concentration range tested (0.25-32 ug/mL)

With the ability of castaneroxy A established to inhibit transcriptional products of the *agr* system in MRSA, key translational products of *agr* were interrogated next. δ-toxin is a member of the phenol-soluble modulin (PSM) family of secreted peptides, and it is encoded by the *hld* gene (hemolysin delta), which is located within the RNAIII portion of the *agr* operon (121; 128). Amphipathic and alpha-helical in structure, δ-toxin possesses a moderate capacity to lyse human neutrophils and contributes to synergistic hemolysis and PSM-mediated phenotypes such as bacteremia; a dedicated target of δ-toxin has yet to be determined (128; 129). Effects of castaneroxy A on δ-toxin production were assessed in three high toxin producers: AH1263, an erythromycin (Erm) sensitive variant of USA300 strain LAC, NRS385, a USA500 *agr* I HA-MRSA isolate, and NRS249, an *agr* I isolate. In all three strains, culturing in the presence of increasing concentrations of castaneroxy A yields a concentration-dependent inhibition of δ-toxin production, as assessed by HPLC analysis of the culture supernatants (**Figure 3.2A**). At 32 μg/mL, castaneroxy A exerts mild growth inhibitory activity and complete inhibition of δ-toxin production across the three strains. Since *hld* is located on RNAIII, inhibition of δ-toxin production represents a direct layer of evidence that castaneroxy A acts on the *agr* system, either directly or via an upstream regulator thereof.

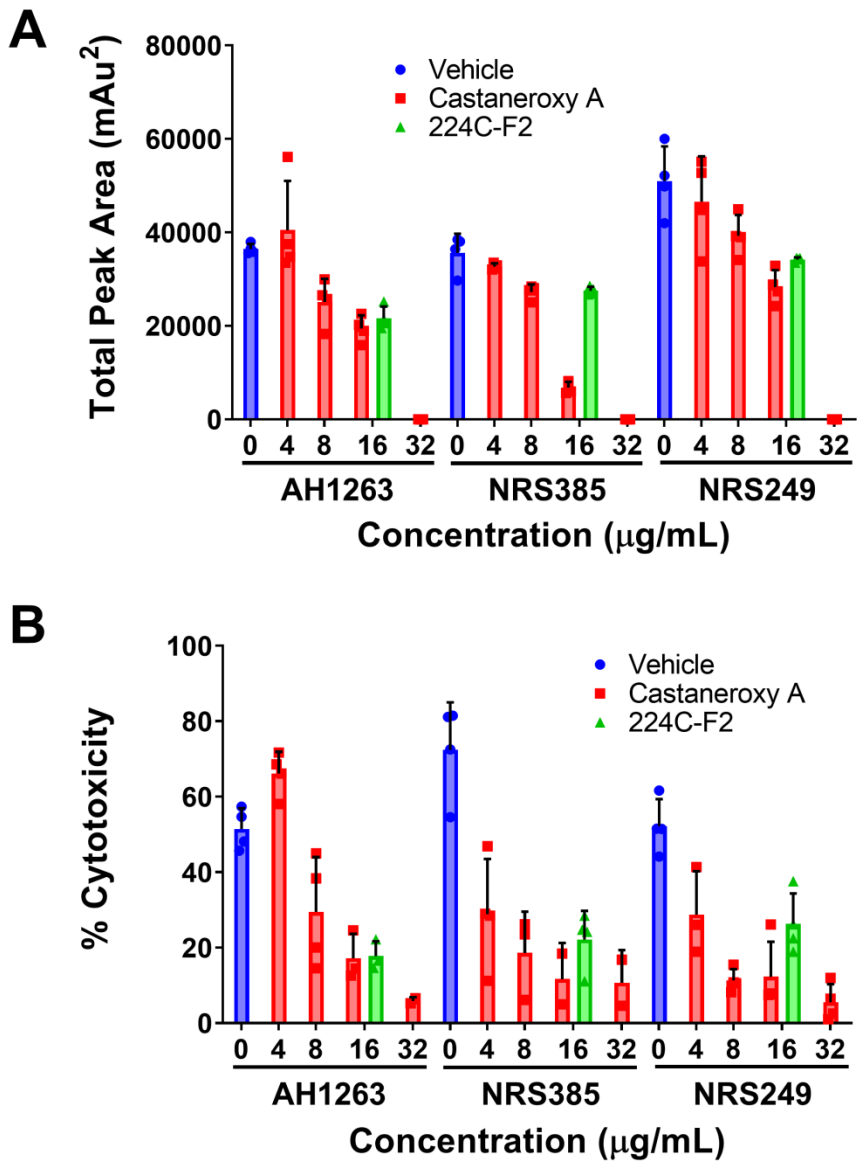

Figure 3.2. Castaneroxy A inhibits MRSA toxin production in a concentration-dependent manner. The strains AH1263 (LAC), NRS385, and NRS249, were cultured in the presence of increasing concentrations of castaneroxy A. **(A)** Supernatants from 15-hour cultures were analyzed by HPLC for the detection of δ-toxin. **(B)** HaCaT human keratinocytes were incubated in the presence of filtered culture supernatants (the same supernatants from part A) for 24 h; cytotoxicity was subsequently assessed by LDH assay. In both graphs, the dark-colored symbols represent the response of each replicate of a treatment-concentration. Each treatment-

concentration was performed in quadruplicate; each experiment was performed in duplicate on separate days. Shown are the results of one of the duplicates of each experiment. Error bars represent SD.

In order to probe the inhibition of exotoxin production in general, HaCaT immortalized human keratinocytes were incubated in the presence of the same supernatants as utilized above, sterile-filtered, from AH1263, NRS385, and NRS249. Assessment of cytotoxicity by a lactate dehydrogenase (LDH) assay reveals that in all strains, supernatants treated with increasing concentrations of castaneroxy A exert decreasing cytotoxicity on HaCaTs (**Figure 3.2B**). This observation indicates a concentration-dependent inhibition of exotoxin production by castaneroxy A. Different trends are observed between the three strains. In AH1263, the concentration-dependent decrease in HaCaT cytotoxicity mirrors very closely the concentration-dependent decrease in δ-toxin production. In both NRS385 and NRS249, however, the concentration-dependent effects between δ-toxin production and HaCaT cytotoxicity trends differ. At 4 μg/mL, a concentration at which no significant decrease in δ-toxin production is affected, supernatant cytotoxicity to HaCaTs decreases significantly, indicating that inhibition of the production of toxins besides δ-toxin is achieved. The disproportional inhibition of HaCaT cytotoxicity as compared to δ-toxin production is also observable at 8 μg/mL. Finally, in all strains, at 32 μg/mL, a concentration at which δ-toxin production is completely shut down, some cytotoxic effect are still observed in HaCaTs, confirming that the production of other toxins persists.

Given the ability of castaneroxy A to inhibit the production of δ-toxin and other exotoxins, effects of castaneroxy A on α-toxin production were next assessed. Perhaps the best-studied *S. aureus* toxin, α-toxin has a mostly beta-sheet structure and is a member of the pore-forming beta-barrel toxin family (121). It is encoded by the *hla* gene (hemolysin alpha) and possesses lytic activity for erythrocytes and a number of leukocytes, but not for neutrophils (121). The

expression of the *hla* gene is controlled by the *agr* system (61). To interrogate treatment effects on α-toxin production, we assessed the hemolytic activity of treated *S. aureus* culture supernatants on rabbit erythrocytes, which are extraordinarily sensitive to α-toxin (130). Three strains were treated with increasing concentrations of castaneroxy A: AH1263 (LAC), here designated as "wild type," AH1589, an *hla::Tn551* mutant of AH1263, and AH1292, an *Δagr::tetM* mutant of AH1263 (**Figure 3.3**).

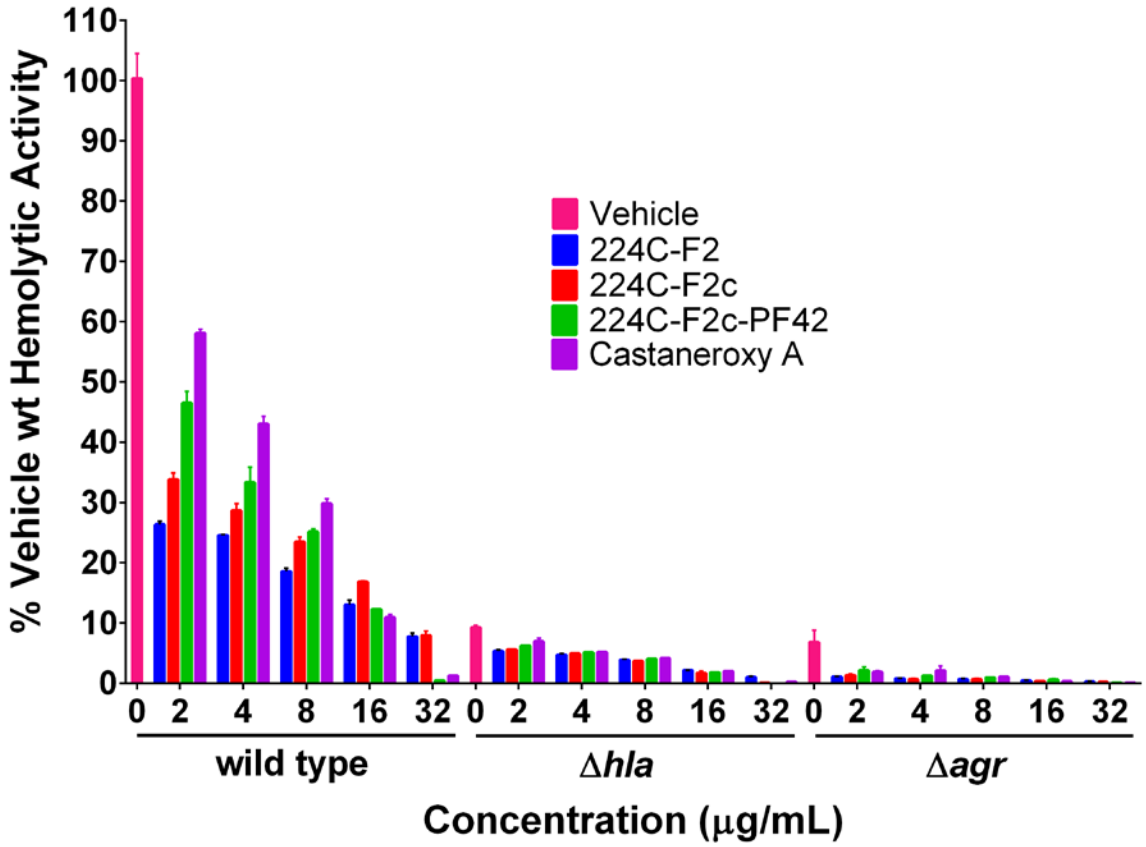

Figure 3.3. Castaneroxy A and its parent fractions inhibit *S. aureus* hemolytic activity in wild-type, Δ*hla* and Δ*agr* strains. The supernatants of treated cultures of three *S. aureus* strains were assessed for hemolytic activity against rabbit erythrocytes. Each treatment-concentration was performed in quadruplicate; the experiment was performed in duplicate on separate days. Shown is the result of one of the duplicates. Error bars represent SD.

In order to evaluate the role of chemical complexity in affecting hemolytic activity, the parent fractions of castaneroxy A were also tested. In the wild type strain, increasing concentrations of all treatments result in a concentration-dependent inhibition of hemolytic activity. A pattern is readily discernable, which also carries over to the other strains in a less pronounced fashion: increasing chemical complexity of the treatment results in increased inhibition of hemolytic activity. At 2, 4, and 8 µg/mL, 224C-F2 is more active than 224C-F2c, which is more active than 224C-F2c-PF42, which in turn is more active than castaneroxy A alone. This pattern breaks down at 16 and 32 µg/mL due to mild growth inhibitory effects of the latter two treatments, which increase apparent hemolytic activity. Increasing concentrations of treatment also cause an increasing inhibition of hemolytic activity of the Δ*hla* and Δ*agr* strains relative to vehicle treatment. Approximately 90% of hemolytic activity is negated by a deletion of either of these genes, confirming the extraordinary sensitivity of rabbit erythrocytes to α-toxin. That hemolytic activity is further inhibited in the Δ*hla* strain by treatment is evidence for the background production of other hemolytic toxins such as the PSMs. Further inhibition in the Δ*agr* strain by treatment suggests that other systems besides *agr* might be targeted to some degree. The Sae system is one possible alternative target that could explain these phenotypes (44).

Assessment of other effects of castaneroxy A

With several lines of evidence presented for the inhibition of the *agr* system in MRSA, other effects were examined. The first was biofilm production. In staphylococci, the *agr* system controls the production of two groups of proteins involved in the structuring and dispersal of biofilms: PSMs and proteases (131-133). In both *S. aureus* and *S. epidermidis*, *agr* mutants were

shown to produce biofilms in an unstructured and extended fashion (134; 135). We sought to determine the concentration-dependent effect of **1** on biofilms of UAMS-1, a PFGE USA200 osteomyelitis *agr* III isolate, and its isogenic *sarA* mutant, UAMS-929, which is biofilm deficient. At concentrations ranging from 0.5-32 µg/mL, **1** and its parent fractions demonstrated no effect on biofilm production as assessed by crystal violet staining (**Figure 8A**).

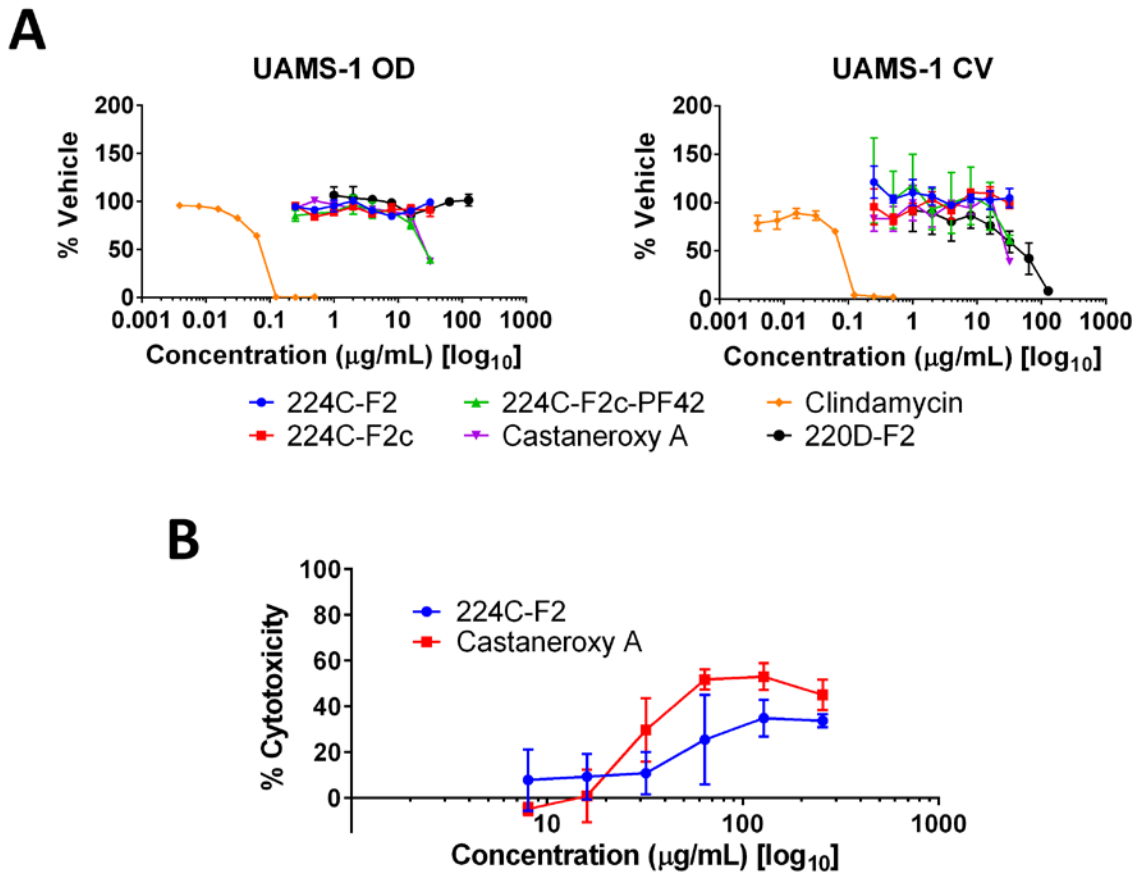

Figure 3.4. Other effects of castaneroxy A. **(A) 1** and its parent fractions do not inhibit biofilm formation in UAMS-1. Clindamycin was used as a control to demonstrate biofilm inhibition due to growth inhibition. The left graph shows optical density (OD), indicating growth as a result of treatment; the right graph shows crystal violet (CV) stain density retained by biofilms after

treatment as a measure of biofilm production. **(B)** Dose response curves demonstrate mild cytotoxicity of castaneroxy A and 224C-F2 against human keratinocytes (HaCaT cells).

Next, potential toxicity of **1** was investigated by incubation in cell culture with HaCaT human keratinocytes at concentrations from 8-256 µg/mL. After 24 h of incubation, **1** exerted cytotoxic activity greater than that of 224C-F2, as assessed by LDH assay (**Figure 8B**). Maximal cytotoxicity was achieved at 64 µg/mL (126.90 µM), a concentration at and beyond which it remained below 60%. At 32 µg/mL, or (63.45 µM), approximately 30% cytotoxicity is observed; no cytotoxicity is observed at lower concentrations. This data suggests that at the concentrations at which **1** inhibits the *agr* system in MRSA it exerts little to no cytotoxicity on mammalian cells. At higher concentrations, however, the cytotoxicity of **1** is significant.

Castaneroxy A abates dermonecrosis *in vivo*

The antivirulence activity of castaneroxy A *in vitro* led us to assess its efficacy as an *in vivo* anti-infective. Using a previously established murine model of dermonecrosis (136), BALB/c mice were intradermally challenged with MRSA (USA300) and a 50 µg or 10 µg dose of castaneroxy A or DMSO vehicle control at the time of infection. Compared to the vehicle control (DMSO), castaneroxy A reduced MRSA-mediated skin damage and animal morbidity in a dose-dependent manner (**Figure 3.5A, B**). Moreover, either dose of castaneroxy A was sufficient to significantly reduce dermonecrotic lesion size throughout the 2-week course of MRSA infection. Finally, a single 50 µg dose of castaneroxy A effectively reduced the dermonecrotic lesion area to nearly undetectable levels, similar to the MRSA *agr*-null mutant (**Figure 3.5C**). Taken together, these

results demonstrate that a single dose of castaneroxy A can protect murine skin from MRSA infection-associated dermonecrotic injury and morbidity.

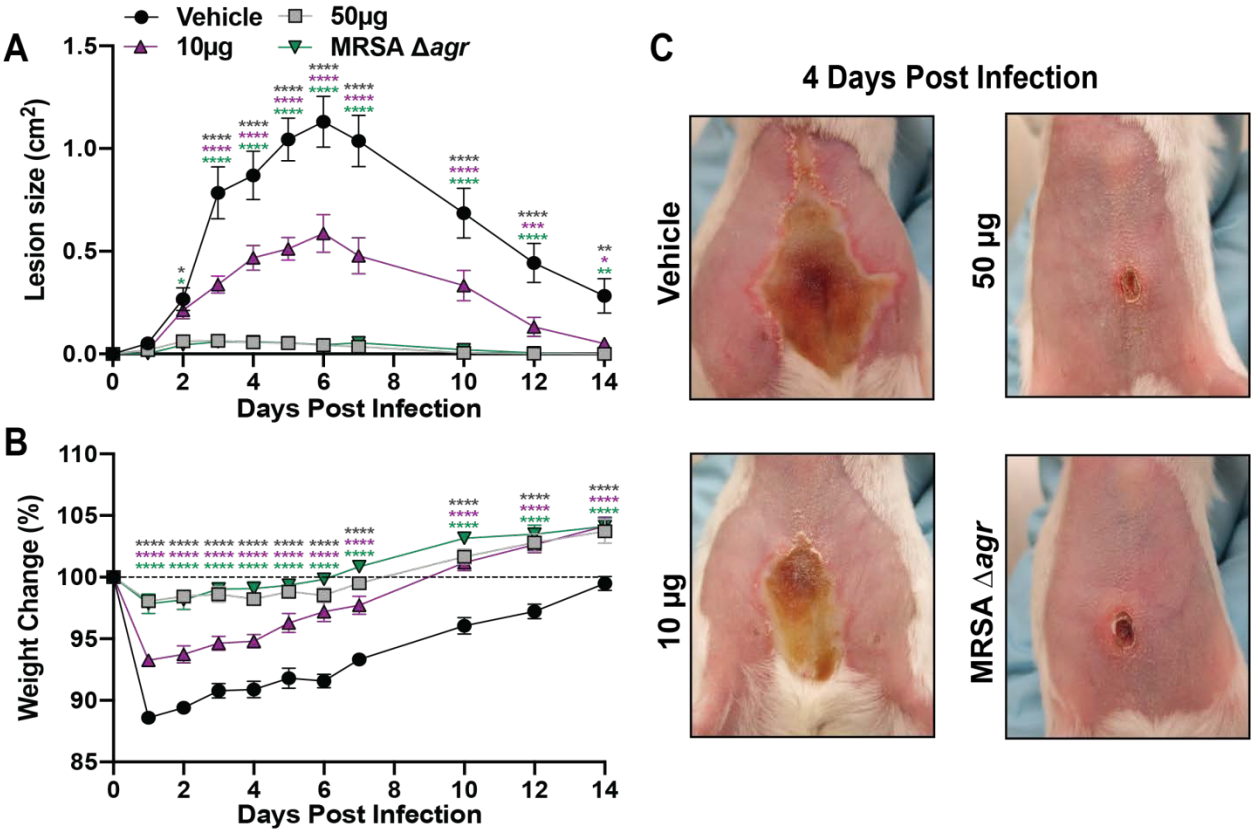

Figure 3.5. Castaneroxy A protects murine skin from MRSA-mediated dermonecrotic injury and morbidity. **(A)** Dermonecrotic lesion size over time for mice challenged with MRSA and a 10 µg or 50 µg dose of castaneroxy A (or vehicle control) or MRSA Δ*agr* at the time of infection. **(B)** Weight change for indicated groups over the two-week infection period. **(C)** Representative images of dermonecrotic lesion size and severity at day 4 post infection. Data are pooled from two independent experiments (n=10 per group). Mean and SEM values are shown. Two-way ANOVA with Dunnett's multiple comparison test was performed comparing the mean of the vehicle control to the mean of each test group for each day of measurements. A p-value <0.05 was considered significant. (*p≤0.0332, **p≤0.0021, ***p≤0.0002, ****p≤0.0001). NOTE: This experiment was performed by a collaborator and not by Akram or his laboratory.

Discussion

We have taken the ethnobotanical drug discovery approach from the discovery of a bioactive enriched extract of a plant used in traditional medicine in the Mediterranean and Balkans to the isolation of a bioactive cycloartane-type triterpenoid, castaneroxy A (**1**) (2). Cycloartane triterpenoids have previously been reported with a range of activities including moderate to high antibacterial and anti-cancer activity (137). Castaneroxy A is reported here for the first time and represents the first cycloartane triterpenoid reported to possess quorum sensing inhibitory activity against MRSA. Until now, hydroperoxy cycloartanes have only been reported with antimicrobial and anti-cancer activity (138). In comparison to its parent extract 224C-F2, **1** demonstrates similar activities across a range of assays assessing inhibition of MRSA *agr* transcriptional and translational products *in vitro*. While **1** shows slightly lower potency in the inhibition of *agr*::P3 activation and hemolytic activity, it shows similar potency in the inhibition of δ-toxin production and supernatant toxicity in MRSA.

Given that the *hld* gene is on RNAIII portion of the *agr* operon, which is transcribed upon activation of the P3 promotor on *agr*, it is expected that concentration-dependent effects would match between inhibition of *agr*::P3 activation and δ-toxin production. Indeed, at the IC_{50} (31.72 µM; 16 µg/mL) and IC_{90} (63.45 µM; 32 µg/mL) of **1** for *agr*::P3 inhibition in *agr* I, **1** inhibits *agr* I δ-toxin production by about half and by 100%, respectively, across the three strains assayed. Another notable trend is that observed in the inhibition of hemolytic activity by **1** and its parent fractions. In the case of this bioassay, decreasing chemical complexity led to decreased activity over a concentration range. While **1** exhibits similar potency to 224C-F2 in the inhibition of δ-toxin production and supernatant toxicity, a difference in potencies is pronounced in the

agr::P3 activation screen which guided fractionation. While in some cases fractionation enriches the abundance of bioactive compounds, fractionation may also cause decreases in bioactivity, particularly in chemical compositions in which synergy between compounds is responsible for bioactivity (48; 49). In the immediate case, what is seen is a decrease in activity against some markers of MRSA virulence but not others due to fractionation. This points to a number of possibilities, including the potential of the more chemically complex fractions to contain chemistries inhibit other virulence regulators, such as SarA, which regulates the *agr* system by activating *agr* P2 expression, or SaeRS, which like *agr* also regulates α-toxin production (44).

Castaneroxy A demonstrates comparable bioactivity to recently-discovered *S. aureus* quorum sensing inhibitor leads that have been tested in mice (45; 46; 116; 139-141), as summarized in **Table 3.3**. Compared to the natural products apicidin and OHM, **1** generally demonstrated higher potency in the *agr*::P3 reporter panel (46; 140). Compound **1** also demonstrated higher toxicity than apicidin, OHM, and ambuic acid to the reporter panel and LAC (46; 140; 141). Like the castaneroxys, another set of *agr* system inhibitor leads were identified in an enriched plant extract: the triterpenoid acids 3-oxo-olean-12-en-28-oic acid, 3-oxotirucalla-7,24Z-dien-26-oic acid, and 3α-hydroxytirucalla-7,24Z-dien-27-oic acid (139). Compared to **1**, these triterpenoid acids generally exhibit lower toxicities against a panel of MRSA strains, higher potencies against the *agr*::P3 reporter panel, lower potencies at δ-toxin inhibition, and lower or equal efficacies in a mouse model of MRSA skin infection.

Table 3.3. Comparison of select activities of other *S. aureus* quorum sensing inhibitors.

Compound name	**Assay**	**IC**	**Value (μM)**	**Ref.**
3-oxo-olean-12-en-28-oic acid	*agr*::P3 reporter panel	IC_{50}	4-64	(139)
Apicidin	*agr*::P3 reporter panel	IC_{50}	6.3-50	(140)
ω-Hydroxyemodin	*agr*::P3 reporter panel	IC_{50}	25-50	(46)
Savirin	Rabbit erythrocyte hemolysis	IC_{90}	13.6	(45)
PLNA34	Rabbit erythrocyte hemolysis	IC_{90}	12.5	(116)
Ambuic acid	LAC AIP inhibition	IC_{50}	2.5	(141)

Savirin is another quorum sensing inhibitor that exerts similar activity to that of castaneroxy A both *in vitro* and *in vivo* (45). A unique set of experiments performed in the savirin study are those assessing *S. aureus* membrane integrity and membrane potential upon treatment. These are properties known to be alterable by antibiotics and thus lead to decreased *agr* expression (142; 143). In fact, a recent study reports that the membrane-active lipopeptide, $C_{10}OOc_{12}O$, at sub-growth inhibitory concentrations to MRSA causes mild membrane depolarization with an accompanying reduction of lipase and α-toxin outputs and resensitization to oxacillin (144). Another study on oxacillin showed that sub-growth inhibitory concentrations of the β-lactam antibiotic caused an altered cell membrane architecture in MRSA while also downregulating *agr*, resulting in reduced virulence *in vitro* and *in vivo* and enhanced killing *in vivo* (145). While the mechanism by which **1** inhibits MRSA quorum sensing has not been probed in this study, its relatively low IC_{50} values across assays measuring virulence inhibition justify future inspection of cell membrane effects. Other possible targets not connected directly to the *agr* system are two-component systems and other regulators that impact *agr* P2 and P3 activation (44).

Further development of **1** as a MRSA quorum sensing inhibitor would entail elucidating mechanism of action and chemical modification to improve pharmacodynamics and pharmacokinetic properties. Indeed, given the moderate growth inhibitory activity against MRSA, there is a narrow range of concentrations at which **1** functions specifically as a quorum sensing inhibitor, and this range must be improved. While medicinal chemistry could improve this as well as pharmacokinetic parameters, the process for modifying a compound as stereochemically complex as **1** is particularly challenging (146; 147). Mechanism of action

studies and preliminary pharmacokinetic studies to assess bioavailability and metabolic stability would inform as to the potential of **1** for lead optimization as a clinical drug.

The proposed precursor of castaneroxy A has been reported to be first isolated from Cretan propolis with an MIC against *S. aureus* ATCC 25923 of 700 µg/mL. This precursor may also contribute to the ethnobotanical anti-infective value of *C. sativa* leaves in Italian traditional medicine. In screening the PFs of 224C-F2c against the *agr*::P3 reporters (**Supplementary Fig. S2**), another set of PFs (PF22-28) also proved active and may contain further compounds that contribute to—perhaps by synergy—to the anti-infective value of the plant.

The *C. sativa* leaves from which the castaneroxys were identified were collected in Italy. *Castanea* species are also found in the United States, and the question of whether these same hydroperoxy cycloartane triterpenoids or their precursors are produced in them and contribute to their ethnobotanical anti-infective value merits investigation. Native Americans in North America have historically utilized the leaves of various *Castanea* species in traditional medicinal preparations for a host of indications, infection-related and otherwise. For example, the Cherokee have used the leaves of *C. dentata* in preparations for treating coughs, sores, and heart troubles (148); they have also used the leaves of *C. pumila* to treat headaches, fevers, chills, and cold sweats (148; 149). The Mohegan people have used the leaves of *C. dentata* in preparations for treating rheumatism, colds, and whooping cough (150; 151).

We have demonstrated the isolation of **1** from the leaves of *C. sativa* as well as its confirmation as an inhibitor of the *S. aureus agr* system. Our findings both identify **1** as potential lead for

MRSA antivirulence drug development and confirm the ethnobotanical anti-infective value of *C. sativa* as used in Italian traditional medicine. We have followed the classical framework of ethnobotanical drug discovery (2). Under this framework, traditional ethnobotanical knowledge focuses plant extract screening to extracts of plants with proven bioactivities of interest, and subsequent bioassay-guided fractionation of extract hits leads to the isolation of bioactive constituent compounds. Following this framework, we were able to tap into underexplored natural chemistries used by people for generations for the treatment of infections. Using state-of-the-art bioassays such as the *agr*::P3 reporter strain panel, those natural chemistries were screened for the innovative antivirulence bioactivity against MRSA as an anti-infective alternative to classical growth inhibition, which inevitably leads to antibiotic resistance. Whether **1** and other products of such screenings can successfully improve therapeutic outcomes in the treatment of MRSA infections—either alone or as an adjuvant to antibiotics—remains to be determined.

Methods

Bacterial Strains. Strain details are compiled in **Table 3.4**. Four strains were used for the *S. aureus agr* reporter panel: AH1677 (*agr* I), AH430 (*agr* II), AH1747 (*agr* III), and AH1872 (*agr* IV). These strains are respectively from the strains AH845, SA502A, MW2, and MN EV; each strain contains the plasmid pDB59, which encodes the *agr* yellow fluorescent protein reporter. Three *S. aureus* strains were used in the hemolysis assay: AH1263 (Erm sensitive USA300 LAC), AH1589 (the *hla::Tn551* mutant of AH1263), and AH1292 (the Δa*gr::tetM* mutant of AH1263). Three *S. aureus* strains were used in the δ-toxin quantification assay: NRS385, AH1263, and NRS249. Two *S. aureus* strains were used for biofilm studies: the clinical isolate UAMS-1 and its isogenic *ΔsarA* mutant UAMS-929, the biofilm production of which is severely retarded. All experiments were performed with treatments measured in µg/mL, and for castaneroxy A these values were then converted to µM. Therefore, the decimal places in the µM measurements of castaneroxy A are not meant to reflect the accuracy of the measurements.

Table 3.4. Profiles of *S. aureus* strains used in this study.

Strain ID	Other Characteristics	Ref.
AH1677	AH845 + pDB59 Cm^R, yfp reporter, *agr* type I	(81)
AH430	SA502a + pDB59 Cm^R, yfp reporter, *agr* type II	(81)
AH1747	MW2 + pDB59 Cm^R, yfp reporter, *agr* type III	(81)
AH1872	MN EV(407) + pDB59 Cm^R, yfp reporter, *agr* type IV	(81)
AH1263 (LAC)	CA-MRSA, PFT USA300, *agr* type I	(124)
AH1589	*hla::Tn551* mutant of AH1263	
AH1292	*Δagr::tetM* mutant of AH1263	
NRS385	HA-MRSA, PFT USA500, MLST ST8, SCC mecIV, sea+, seb+, *agr* type I	(126)
NRS249	sea+, (lukE-lukD)+, hlgv+, associated with native valve endocarditis; SCCmec type IV, agr type I	
UAMS-1	MSSA, osteomyelitis isolate, strong biofilm producer	(152)
UAMS-929	Isogenic *sarA* mutant of UAMS-1, biofilm production is deficient	

Minimum inhibitory concentration (MIC). Clinical Laboratory Standards Institute (CLSI) M100-S23 guidelines for microtiter broth dilution testing were followed (153). Briefly, overnight cultures in TSB were standardized by optical density (OD) to an OD_{600} of 0.0006, which corresponds to 5 x 10^5 CFU/mL. Plate reading was done in a Cytation 3 multimode plate reader (Biotek). After treatment, plates were incubated at 37 °C for 18 h under static conditions. Plates were read at an OD 600nm at 0 and 18 h post-inoculation. All concentrations were tested in triplicate, and experiments were performed at least twice on different days to account for two biological replicates. The IC_{50} value of a treatment in a bacterial strain is defined as the lowest test concentration at which at least 50% growth inhibition was observed by culture optical density measurements. The MIC is defined as the lowest test concentration at which at least 90% growth inhibition is observed, equivalent to no visible growth in the wells.

Reporter strains of inhibition of *agr* expression. Fractions were tested for quorum sensing inhibitory activity against all four *agr* subtypes using previously described (81) *agr*::P3 YFP reporter strains AH1677 (type I), AH430 (type II), AH1747 (type III), and AH1872 (type IV) (154). Overnight cultures in TSB and 10 µg/mL chloramphenicol were standardized to an OD_{600} of 0.0006 for working cultures. After treatment in 96-well black plates (Costar 3603), the plates were incubated at 37°C with shaking (1000 rpm) in a humidified Stuart SI505 incubator (Bibby Scientific, Burlington, NJ). OD_{600} and Fluorescence (top reading, 493 nm excitation, 535 nm emission, gain 60) readings were taken at 0 h and 18 h post-inoculation.

Hemolytic activity by red blood cell lysis assay. The ability of castaneroxy A to inhibit quorum sensing in *S. aureus* was assessed by measuring the toxicity of treated culture supernatants to

rabbit erythrocytes, as previously described (8). Briefly, overnight cultures of strain AH1263 (Erm sensitive USA300 LAC), AH1589 (the *hla::Tn551* mutant of AH1263), and AH1292 (the Δa*gr::tetM* mutant of AH1263) were inoculated 1:500 into TSB to make working cultures. Working cultures were transferred to a 96-well plate to receive treatment in quadruplicates. The three strains received one of four treatments—224C-F2, 224C-F2c, 224C-F2c-PF42, and **1**—at five concentrations: 2, 4, 8, 16, 32 µg/mL (equivalent to 3.97, 7.93, 15.86, 31.72, 63.45 µM for **1**). Vehicle control and untreated wells were included for all strains. The final well volume was 250 µL. After 8 h of incubation in a Stuart shaker (37 °C, 1250 rpm), well contents were transferred to 96-well filter plates, which were centrifuged stacked onto new plates at 2000 *g* for 5 min. Supernatants (filtrates) were diluted 2-fold in triplicate 7x in new 96-well plates in 1.2x PBS with a final well volume of 30 µL.

Rabbit erythrocytes, obtained from defibrinated rabbit blood (Hemostat Laboratories, Dixon, CA) washed 3x in 1.2x PBS, were resuspended in 1.2x PBS and were added 70 µL per well to the 96-well plates of supernatant dilutions. The plates were moved in circles by hand for mixing and then incubated statically at room temperature for 1.5 h. The plates were then read on a plate reader at OD_{630} for the detection of hemolysis. For each treatment-concentration in each strain, a 4-parameter logistic (4PL) fit was fit to the dilution vs OD data points using GraphPad Prism, and the midpoints of these curves were determined. The ratio of AH1263 vehicle 4PL midpoint to each treatment-concentration's midpoint was determined and multiplied by 100.

Quantification of δ-toxin by HPLC. Inhibition of δ-toxin production in NRS385, a USA500 *agr* I HA-MRSA isolate, AH1263, a USA300 LAC isolate, and NRS249, an *agr* I isolate was

tested, as reported previously(155). In brief, 1.5 mL working cultures standardized to an OD_{600} of 0.0006 received sub-MIC_{50} concentrations of treatment. Supernatants were collected 15 h post-incubation at 37 °C and shaking at 275 rpm; they were transferred to HPLC vials and stored at -20 °C until HPLC testing. Samples were run on an Agilent 1260 Infinity system using a Resource PHE 1-mL (GE Healthcare, Uppsala, Sweden) analytical column, as previously described (8; 155). Two mobile phases were used: (A) 0.1% trifluoroacetic acid (TFA) in water, (B) 0.1% TFA in acetonitrile. The injection volume was 500 µL and the flow rate 2 mL/min. The 214 nm chromatograms were used for data processing. Two peaks corresponding to deformylated and formylated δ-toxin were integrated and their areas summed as a relative quantitative measure of δ-toxin presence.

Human keratinocyte toxicity. Human immortalized keratinocytes (HaCaT cell line) were maintained as described previously (8). Upon reaching suitable confluency (90–95%), cells were standardized to 4×10^4 cells/mL using a hemocytometer and 200 µL were seeded per well in a 96-well tissue culture-treated microtiter plate (Falcon 35–3075). Plates were incubated for 48 h prior to media aspiration. Media was then added along with treatment. For the chemical cytotoxicity assay, treatment was an enriched extract or compound. For the supernatant toxicity assay, treatment was spent bacterial supernatant (which was added as 20% of the well volume). After 24 h incubation, treatment-induced cytotoxicity was assessed by the CytoScan™ LDH Cytotoxicity Assay (G-Biosciences) following the manufacturer's protocol.

Animal Studies. A previously described murine model of MRSA skin infection was used to determine the efficacy of castaneroxy A as an anti-infective (136). All animal experiments

described herein were approved by and conducted in accordance with the recommendations of the Animal Care and Use Committee at the University of Colorado Anschutz Medical Campus (IACUC protocol number 117217). One day prior to inoculation, the abdominal hair of 8-week-old female BALB/c mice was shaved and chemically removed with topical application of Nair for 1 minute. LAC (USA300, AH1263) and its deletion mutant (LACΔ*agr*, AH1292) were grown in TSB media overnight at 37 °C in a shaking incubator (200 rpm). Overnight LAC and Δ*agr* cultures were diluted 1:50 in fresh TSB media and allowed to grow to early log phase (~2 hr to OD_{600} nm = 1.0). Cells were washed in sterile PBS and resuspended to achieve an inoculum of 1×10^8 CFU. Groups were inoculated intradermally into the abdominal skin with 63 μL suspensions of either (1) 1×10^8 CFU LAC and castaneroxy A (50 μg or 10 μg dissolved in DMSO), (2) LAC + DMSO vehicle control, or (3) $1x10^8$ CFU LACΔ*agr* + DMSO. Baseline body weights of the mice were taken prior to injection and each following day. For determination of lesion size, digital photos of skin lesions were taken with a Canon PowerShot ELPH180 camera and analyzed with ImageJ software for Mac. Inoculum CFU was verified by serial dilution, plating, and colony counting after overnight incubation of the plate. As no signs of distress were observed in the present study, all animals were euthanized *via* continuous administration of 100% CO_2 at the experimental end point.

CHAPTER IV

Discussion and Perspective

Discussion

This dissertation represents a synthesis of ethnopharmacological knowledge connecting ethnobotany to anti-infective drug discovery via phytochemistry while adding new knowledge to all the fields. It presents the rationale for ethnobotanical anti-infective drug discovery, the phytochemical techniques that link ethnobotany to microbiology, the *agr* system of *S. aureus* as an attractive anti-infective target, the state-of-the-art technology in pursuing such targets, and my own work in discovering a plant natural product that successfully targets the *agr* system.

In the past five years, plant natural products have received more attention than ever as potential sources of new drugs, particularly for infectious diseases. Indeed, plant natural products account for a large portion of all contributions to drugs in the clinic (156; 157) and have countless times been demonstrated as effective drugs for infectious diseases and a vast array of other indications, binding to biological macromolecules to produce therapeutic effects (158). The recent attention stands in contrast to that paid to plant plant natural products in the prior three decades, where work on plant natural products faced many challenges: the embracing of combinatorial chemistry and microbial natural products isolation, incompatibility with many HTS (high throughput screening) assays, difficulty of compound isolation from complex plant extracts, re-isolation of known compounds, difficulty of lead optimization due to numerous stereocenters and functional groups, and difficulty of acquiring foreign plant material (159-162). These challenges have largely been addressed, and increasingly innovative solutions continue to emerge. HTS assays are increasingly being designed to accommodate natural products and complex compositions thereof (163; 164). Additionally, pre-fractionation has been shown to increase the hit rate in

natural product HTS (165; 166). Several of the bottlenecks in plant natural products drug discovery include resolution of separation and structure elucidation, which have and continue to be improved by advances in chromatography and spectroscopy (167). These advances include: smaller columns with smaller particle sizes that can achieve very high resolution separation on ultra-performance liquid chromatography (UPLC) systems, more powerful NMR instrumentation capable of generating higher resolution spectra of smaller sample masses in much shorter times, and innovations ionization, mass accelerating, and detection in mass spectrometers for mass spectrometry. The re-isolation of known compounds is addressed by various methods of dereplication, which include molecular networking and comparison of tandem-MS and NMR data to those in online spectral databases (75; 168; 169). In lead optimization, advances in medicinal chemistry allow for easier structural modifications of natural products than ever before, though the process remains challenging (162; 170). And now international protocols exist for the acquisition of foreign plants, including the Nagoya Protocol, which affirms the sovereign rights of nations over their traditional medicines and stipulates that they receive equitable benefits for sharing them and for consequent successes of that sharing (171).

Targeting bacterial virulence has been recurrently cited in the literature in recent years as a promising as therapeutic approach worth further investigation (172-176). The current anti-infective paradigm consists, on one hand, of a reality where all clinically approved therapeutics are bacteriostatic or bactericidal and, on the other hand, a crescendo of attention on the importance of developing non-growth-targeting therapeutics as antibiotic resistance steadily proliferates (12; 14; 15; 110). Indeed, need is the driver of new trends. There have been countless trends in drug discovery in the past decades that have promised breakthroughs in the way we

treat diseases. In the case of targeting bacterial virulence, the approach is not new, but the large volume of attention directed at it is a phenomenon of only the last few years, especially in the case of *S. aureus*.

Castaneroxy A, then, represents an important contribution to both plant natural product drug discovery and antivirulence drug discovery. It was isolated thanks in large part of some of the advanced instrumentation and techniques available, which circumvent many of the aforementioned challenges: medium-throughput screening with a cellular YFP reporter strain assay, powerful HPLC, NMR, and MS instrumentation, dereplication, and adherence to the Nagoya Protocol. The uncovering of isomers of castaneroxy A adds to the knowledge on unsaturated sterols and hydroperoxy cycloartanes, especially as it relates to synthesis and stereochemistry. Furthermore, castaneroxy A represents one of the few antivirulence compounds isolated from plants. While none of these compounds have completed preclinical drug development, the identification of such activity in plant metabolites increases in the promise that plants harbor anti-infectives with various specificities and mechanisms of action and that plants have evolved multiple and likely synergistic mechanisms for self-defense against infection.

A number of further studies can be planned for castaneroxy A. It is first important to realize that while the pharmacological studies on castaneroxy A do show that the *agr* system is affected, they do not reveal much more about the mechanism of action, which I suggest be next studied. To begin with the simplest aspect of mechanism, it is not established that castaneroxy A enters the *S. aureus* cell, as the bioactivity could be affected by binding, for instance, to the extracellular domain of a membrane protein such as AgrC, the receptor histidine kinase that recognizes the

signal peptide, autoinducing peptide (AIP). There are four possibilities: castaneroxy A does not enter the cell, it enters the cell by phospholipid bilayer diffusion, it enters the cell via active transport, or it enters the cell by both of the latter two ways (177). An LC-MS method to quantify the intracellular concentration of drug in bacteria represents a promising first step to revealing if drug entry occurs (178; 179). It is also not established that a component of the *agr* system itself is targeted; the bioactivity after all could be explained by the inhibition of activity of a regulator of *agr*, such as sarA. To explore which virulence-related systems may be targeted by castaneroxy A, quantitative real-time polymerase chain reaction (qRT-PCR) may be used to determine whether a decrease in their transcriptional outputs occurs upon treatment of *S. aureus*.

The MRSA *agr*::P3 reporter strain assay confirms that castaneroxy A causes a decrease in P3 activation. Another assay could confirm this before probing for which component of *agr* upstream of P3 is perturbed by castaneroxy A. A simple experiment confirms whether the likely target is indeed upstream of P3. LC-MS quantification of levels of dimerized (phosphorylated) AgrA would reveal whether a reduction in dimerized AgrA occurs upon treatment (180). AgrA is phosphorylated by the receptor histidine kinase AgrC once it is activated, and reduction in AgrA dimerization would follow a perturbation in the function of AgrA itself, AgrC, AgrB, or even SpsB, a type I signal peptidase that performs the final maturatiom step for agrD (181). These potential targets can then be explored further. With regards to AgrA, it would be informative to use qRT-PCR to assess the ability of casteranoxy A to inhibit RNAIII expression in *S. epidermis*. Since AgrA is not conserved bewteeen the two species, a lack of effect in *S. epidermis* would indicate that AgrA is the likely target (73). If the target is specifically the AgrA DNA-binding domain, quantitative binding studies could be performed to study the ability of the ligand to

inhibit AgrA-DNA complex formation by demonstrating the presence of unbound DNA vs. AgrA-DNA complex (73). In such an experiment, however, there is also the possibility that ligand binding allows for AgrA to bind to DNA and still prevents transcription. If AgrC or A is the target of castaneroxy A, adding increasing [AIP] in the presence of drug in the MRSA reporter strain assay would surmount reporter inhibition, assuming that inhibition of AgrC was reversible. This experiment is best performed if the K_d for the target is known beforehand in order to determine fractional occupancy at a given concentration by the law of mass action. With regards to AgrB, LC-MS quantification of levels of secreted AIP signal peptide ±AIP-II would reveal whether treatment inhibits AIP production; this would indicate that AgrB or SpsB is likely the target (182; 183). If the target protein can be purified, *in silico* docking studies could be performed to assess binding.

More experiments can be done to assess further the effect of castaneroxy A on markers of MRSA virulence. Although one of the markers of virulence tested is hemolytic activity, which is largely a function of α-toxin production, a Western blot could be used to confirm α-toxin level change directly due to treatment. Additionally, qRT-PCR of virulence, metabolism, cell surface, and stress response mRNAs would reveal treatment specificity for the *agr* system (183). *S. aureus* survival in the presence of neutrophils can also be assessed. The results of this experiment, though it has its limitations, would be informative as one of the hypotheses of quorum sensing inhibition as a therapeutic strategy is that leukocytes would have an increased ability to target *S. aureus* cells if their toxin production is inhibited. Neutrophils are mainly lysed by phenol-soluble modulins (PSMs); therefore, this assay would indirectly measure PSM levels (184). *S. aureus* expressing sGFP would be treated with castaneroxy A in the presence of neutrophils. Flow

cytometry measurements of fluorescence would indicate *S. aureus* sensitivity to neutrophil targeting. Castaneroxy A can also be tested for cytotoxicity against a panel of human skin flora. Finally, castaneroxy A can be tested for plasma protein binding and metabolic stability via plasma protein binding equilibrium dialysis for the former and mouse and human microsomes and mouse hepatocytes for the latter.

To begin understanding the role of different functional groups in the activity of castaneroxy A, its isomers can be isolated and their derivatives can be studied for the inhibition of markers of virulence. A more complex medicinal chemistry approach to these structure-activity relationship (SAR) studies can begin with the compound cycloartenol, which is structurally simpler than castaneroxy A and, therefore, more amenable to chemical modification (**Figure 4.1**) (147; 170). If effective, cycloartenol derivatives can be made and tested, which would also allow for complex and highly informative SAR studies. All effective compounds can be put through resistance passaging experiments, after which resistant mutants could be sequenced to identify possible binding targets involved in quorum sensing.

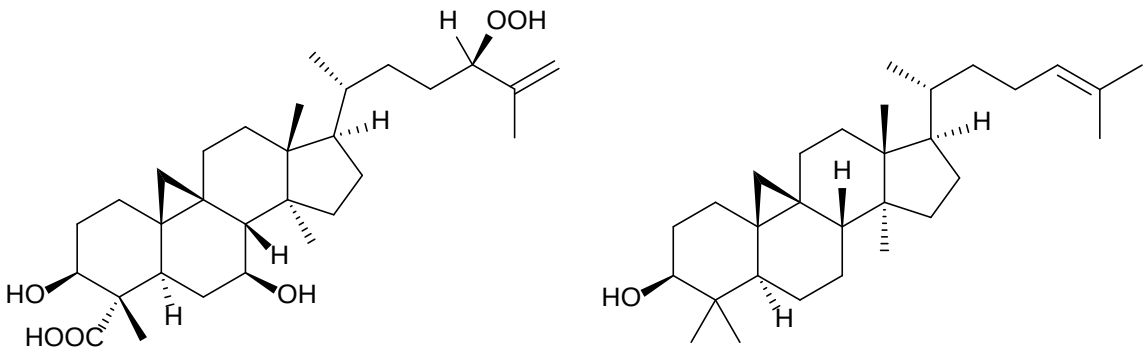

Figure 4.1. Castaneroxy A (left) and cycloartenol (right).

The possibility that castaneroxy A or its isomers may exert their bioactivity synergistically is important to highlight. In cases where a plant extract contains one major bioactive compound, fractionation that enriches for this compounds leads to an increase in the bioactivity. In the case of castaneroxy A, the opposite true. That generally decreased potency for the inhibition of markers of MRSA virulence *in vitro* is observed with fractionation from 224C-2Fc to castaneroxy A suggests that castaneroxy A alone does not account for the total bioactivity of its parent extract. This is most clearly observable in the *agr*::P3 reporter screen on the 43 preparative fractions (PFs) of 224C-F2c. Among the 43 PFs, two loci of activity were identified: the fractions neighboring 224C-F2c-PF42 and those neighboring 224C-F2c-PF24. It is worth studying whether 224C-F2c-PF24 also contains a MRSA antivirulence compound and whether the fraction itself or the compound acts in synergy with 224C-F2c-PF42 or castaneroxy A. This study can be performed via checkerboard assay (185; 186).

❖

"Without urgent, coordinated action by many stakeholders, the world is headed for a post-antibiotic era, in which common infections and minor injuries which have been treatable for decades can once again kill," stated Dr. Keiji Fukuda, the World Health Organization's then-Assistant Director-General for Health Security, in 2014 (13). These common infections are becoming more capable of killing due to the spread of antibiotic resistance across the pathogens of greatest concern, including MRSA, and the subsequent inability of conventional antibiotics to treat them (187). The crisis with MRSA has reached a point where physicians are now turning more than ever to antibiotics of last resort, and even resistance to those antibiotics, such as

linezolid, has begun spreading (188-190). This phenomenon makes sense considering that conventional antibiotics target cellular processes necessary for bacterial survival; as such, great selective pressure is exerted on a population of bacteria, which divide and mutate rapidly, to genetically develop resistance (12; 191). Virulence has been identified as an alternative and highly promising target in *S. aureus* (123; 192). Targeting virulence rather than survival has been proposed to exert less selective pressure for the development of resistance than conventional antibiotics, and it has been proposed to act as an adjuvant to antibiotic therapy or even a standalone therapy, wherein the immune system would eliminate remaining pathogens (175; 192; 193). Indeed, examples of antivirulence agents have emerged where no detectable resistance developed in *S. aureus* after multiple drug passages (8; 73). As such, combining an antivirulence treatment with conventional antibiotics may circumvent the development of resistance by enhancing antibiotic efficacy. Inhibiting virulence represents a strategic approach to disarming *S. aureus* of its pathogenicity, but it is not yet known whether this approach improves antibiotic response in mouse models of established skin abscess infection or bacteremia.

As ongoing studies seek to further mature the field of antivirulence stratgeies against MRSA, an exciting outlook for the future of these compounds is illustrated where they show promise *in vitro* as adjuvants to conventional antibiotic therapy against different pathogenic bacteria (70; 194-196). Looking *in vivo*, there are several examples in the recent literature demonstrating the potential of antivirulence compounds such as savirin, biaryl hydroxyketones, antisense locked nucleic acids, and ω-hydroxyemodin in attenuating MRSA pathogenicity in skin abscess mouse models (71-74). The study on savirin even demonstrates efficacy when administration is delayed to the time of maximal abscess development (73). And in the biaryl hydroxyketones study, the

compounds were shown to not only promote MRSA wound healing in a mouse model when used individually but also to re-sensitize MRSA USA300 to β-lactam antibiotics it was previously resistant to (74).

It is among this small group of MRSA antivirulence compounds where castaneroxy A finds its place and where the process of ethnobotanical drug discovery makes its mark (**Figure 4.2**). While antibiotic resistance in MRSA threatens the efficacy of antibiotics currently in the clinic, antivirulence compounds offer an alternative strategy that aims to circumvent antibiotic resistence, at least to a degree. The successful inhibition of virulence may result in lower doses of antibiotic being needed for therapy, which may contribute to a diminished spread of antibiotic resistance. Alternatively, it may in some cases be appropriate for monotherapy, the immune system subsequently clearing the remaining infecting bacteria. Future studies that explore antivirulence drug candidates past the discovery phase will shed light on if and how antivirulence compounds may be one day suitable for use in patients.

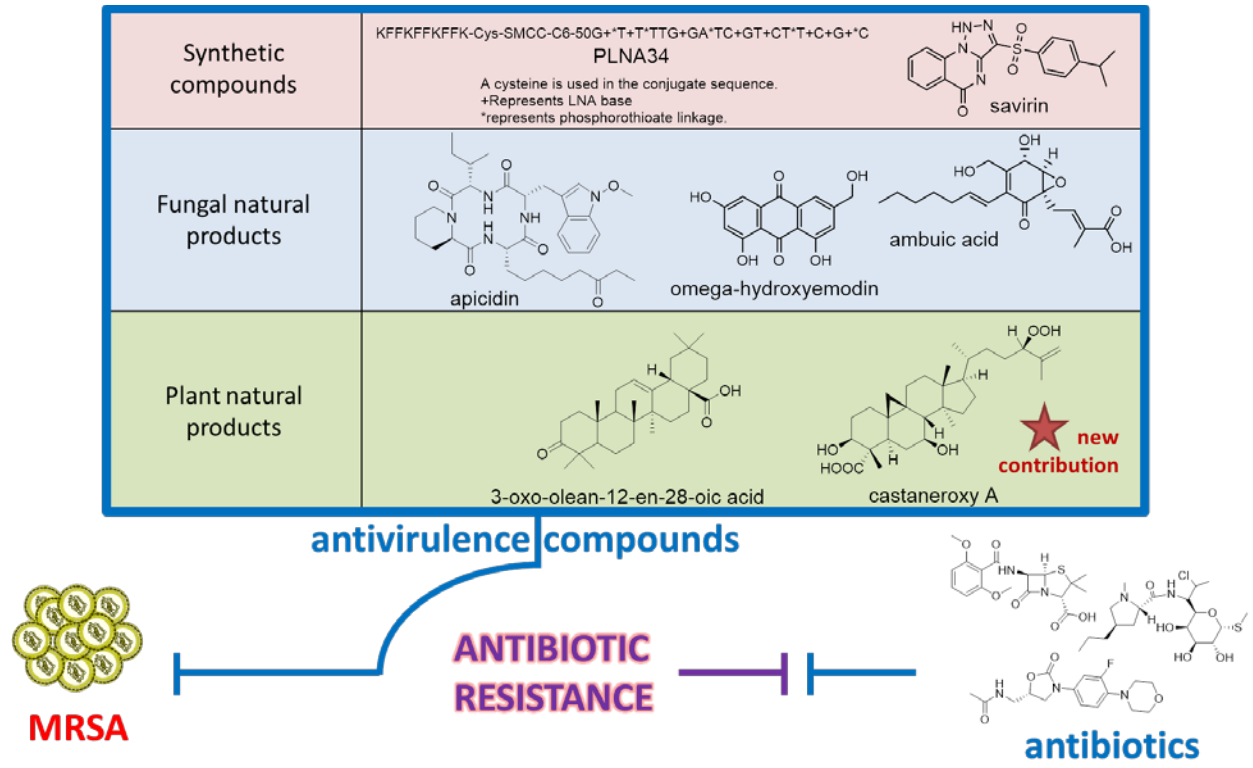

Figure 4.2. Contribuition of castaneroxy A to MRSA antivirulence compounds. Castaneroxy A represents the latest contribution to a small group of compounds, the MRSA antiviruelnce activity of which has been confirmed *in vivo*. Antivirulence compounds aim to circumvent antibiotic resistance to a degree in order to improve anti-infective therapy.

Perspective

The research reported herein represents an account of a successful ethnobotany anti-infective drug discovery approach. It should not be overlooked that the antivirulence compounds reported would not have been discovered were it not for the rural Italian informants who shared their knowledge of the medicinal plants they use for their health. It should also be noted that the anti-infective potential of *C. sativa* natural products would have been overlooked had only traditional growth inhibitory bioactivities been sought in preliminary screens. This highlights the vast importance of laboratory screening capabilities. Indeed, academic laboratories all over the world possess unique collections of plant extracts, fractions, and natural products, and it is up to each laboratory to probe into the therapeutic potential of their own intellectual property. It would behoove each investigator to consider that their natural product libraries possessed an array of bioactive compounds – anti-infective, anti-cancer, anti-Alzheimer's, etc.—and as part of laboratory capability expansion pursue acquiring expertise in different screening assays or forging collaborations with laboratories which could perform these assays.

There is great potential for streamlining the presented workflow by utilizing newer laboratory techniques. Molecular networking expertise, particularly using Global Natural Products Social Molecular Networking (GNPS), has a low barrier for acquisition because it requires free software and training is available. And the benefits it would return are immense, as it would allow for rapid derepelication and identification of novel chemistries. A much more difficult capability to acquire is liquid chromatography-mass spectrometry, as the instrumentation is expensive. In return, high-quality MS and MS/MS data would be obtained on samples, allowing for an expansion of molecular networking capabilities and for the creation of an in-house

database. In time, these techniques and more will become a standard part of the ethnobotanical drug discovery workflow around the world.

In a recent review article, our research group reviewed the literature on the role of ethnobotany on antibacterial drug discovery. In all the literature published in the field from 2012 to 2019, we found that only 12% of the studies actually followed established experimental guidelines (Chassagne, *et al*, in review). Some examples of common poor methodologies include using non-authenticated source material and using of poorly-designed bioassays. One of the main needs lacking in the field, then, is global adherence to established guidelines for ethnopharmacological research. Indeed, the lack of this adherence is a major reason why some view the field of ethnopharmacology negatively. This, coupled with the gradual increase worldwide in access to equipment such as -80°C freezers, microplate readers, flash chromatography, HPLC, NMR, MS, and liquid-handling systems will lead to a surge in results from ethnobotanical drug discovery efforts. And as laboratories around the world progress from discovery projects to drug lead identification, they will acquire the expertise and/or collaborations to perform mechanism of action, pharmacokinetic/pharmacodynamic, medicinal chemistry, and other more advanced preclinical studies. And as such the ethnobotanical drug pipeline will come to play a larger role in worldwide drug discovery efforts.

Supplementary Information S1

checkCIF/PLATON report

Structure factors have been supplied for datablock(s) 224C-F2c-PF42-SF7_nsphera

THIS REPORT IS FOR GUIDANCE ONLY. IF USED AS PART OF A REVIEW PROCEDURE FOR PUBLICATION, IT SHOULD NOT REPLACE THE EXPERTISE OF AN EXPERIENCED CRYSTALLOGRAPHIC REFEREE.

No syntax errors found. CIF dictionary Interpreting this report

Datablock: 224C-F2c-PF42-SF7_nsphera

```
Bond precision:   C-C = 0.0012 A          Wavelength=0.71073

Cell:           a=7.54880(14)    b=11.2160(2)          c=16.9599(3)
alpha=90        beta=102.5498(18)                      gamma=90
Temperature:    100 K

Calculated       Reported Volume           1401.64(4)
                 1401.64(5)
Space group      P 21                      P 1 21 1
Hall group       P 2yb                     P 2yb
Moiety formula   C30 H48 O6, H2 O          C30 H48 O6, H2 O
Sum formula      C30 H50 O7                C30 H50 O7
Mr               522.70                    522.73
Dx,g cm-3        1.238                     1.239
Z                2                         2
Mu (mm-1)        0.086                     0.086
F000             572.0                     572.2
F000'            572.28
h,k,lmax         13,19,29                  12,19,29
Nref             15288[ 7939]              12725
Tmin,Tmax        0.988,0.995               0.553,1.000
Tmin'            0.985

Correction method= # Reported T Limits: Tmin=0.553 Tmax=1.000
AbsCorr = MULTI-SCAN

Data completeness= 1.60/0.83       Theta(max)= 38.010

R(reflections)= 0.0377( 11422)     wR2(reflections)= 0.0953( 12725)

S = 1.051                  Npar= 779
```

The following ALERTS were generated. Each ALERT has the format
test-name_ALERT_alert-type_alert-level.
Click on the hyperlinks for more details of the test.

Alert level A

PLAT355_ALERT_3_A Long O-H (X0.82,N0.98A) O6 - H6 . 1.15 Ang.

Author Response: This is a real experimentally observed distance involving a peroxo hydrogen. This H donates a strong hydrogen bond to a water.

Alert level B

PLAT417_ALERT_2_B Short Inter D-H..H-D H1 ..H1WB . 2.03 Ang.
-1+x,y,1+z = 1_456 Check

Author Response: This is a real experimentally observed distance, with one hydrogen being a strong hydrogen bond donor.

PLAT417_ALERT_2_B Short Inter D-H..H-D H1 ..H3 . 2.09 Ang.
-x,1/2+y,2-z = 2_557 Check

Author Response: This is a real experimentally observed distance, with one hydrogen being a strong hydrogen bond donor.

PLAT926_ALERT_1_B Reported and Calculated R1 Differ by ..... -0.0130 Check

Author Response: Refinement using NoSpherA2, an implementation of NOn-SPHERical Atom-form-factors in Olex2. The calculated R1 is based on spherical form factors.

PLAT927_ALERT_1_B Reported and Calculated wR2 Differ by ..... -0.0363 Check

Author Response: Refinement using NoSpherA2, an implementation of NOn-SPHERical Atom-form-factors in Olex2. The calculated wR2 is based on spherical form factors.

PLAT928_ALERT_1_B Reported and Calculated S value Differ by . -0.400 Check

Author Response: Refinement using NoSpherA2, an implementation of NOn-SPHERical Atom-form-factors in Olex2. The calculated S is based on spherical form factors.

Alert level C

PLAT222_ALERT_3_C NonSolvent Resd 1 H Uiso(max)/Uiso(min) Range 5.4 Ratio
PLAT351_ALERT_3_C Long C-H (X0.96,N1.08A) C7 - H7 . 1.11 Ang.
PLAT351_ALERT_3_C Long C-H (X0.96,N1.08A) C8 - H8A . 1.11 Ang.

```
PLAT351_ALERT_3_C   Long   C-H   (X0.96,N1.08A)   C16   -   H16A      .      1.15   Ang.
PLAT351_ALERT_3_C   Long   C-H   (X0.96,N1.08A)   C18     -   H18     .      1.11   Ang.
PLAT351_ALERT_3_C   Long   C-H   (X0.96,N1.08A)   C25   -   H25B      .      1.12   Ang.
PLAT351_ALERT_3_C   Long   C-H   (X0.96,N1.08A)   C26   -   H26B      .      1.11   Ang.
PLAT351_ALERT_3_C   Long   C-H   (X0.96,N1.08A)   C27     -   H27     .      1.12   Ang.
PLAT351_ALERT_3_C   Long   C-H   (X0.96,N1.08A)   C29   -   H29C      .      1.15   Ang.
PLAT417_ALERT_2_C Short Inter D-H..H-D       H1WB     ..H6       .       2.14 Ang.
x,y,z                                                          =      1_555 Check
```

Author Response: This is a real experimentally observed distance, with one hydrogen being a strong hydrogen bond donor.

```
  PLAT911_ALERT_3_C Missing FCF Refl Between Thmin & STh/L=     0.600          8 Report
  PLAT915_ALERT_3_C No Flack x Check Done: Low Friedel Pair Coverage          71 %
  PLAT975_ALERT_2_C Check Calcd Resid. Dens.   0.60A   From O1              0.41 eA-3
  PLAT976_ALERT_2_C Check Calcd Resid. Dens.   0.48A   From O6             -0.45 eA-3
```

Alert level G

```
 PLAT002_ALERT_2_G Number of Distance or Angle Restraints on AtSite          6 Note
  PLAT003_ALERT_2_G Number of Uiso or Uij Restrained non-H Atoms ...         37 Report
  PLAT068_ALERT_1_G Reported F000 Differs from Calcd (or Missing)...     Please Check
  PLAT172_ALERT_4_G The CIF-Embedded .res File Contains DFIX Records          1 Report
  PLAT173_ALERT_4_G The CIF-Embedded .res File Contains DANG Records          1 Report
  PLAT176_ALERT_4_G The CIF-Embedded .res File Contains SADI Records          1 Report
  PLAT186_ALERT_4_G The CIF-Embedded .res File Contains ISOR Records          2 Report
  PLAT187_ALERT_4_G The CIF-Embedded .res File Contains RIGU Records          2 Report
  PLAT395_ALERT_2_G Deviating   X-O-Y    Angle From 120 for O5            107.7 Degree
  PLAT720_ALERT_4_G Number of Unusual/Non-Standard Labels ..........          2 Note
  PLAT769_ALERT_4_G CIF Embedded explicitly supplied scattering data     Please Note
PLAT790_ALERT_4_G Centre of Gravity not Within Unit Cell: Resd.   #          2 Note
H2 O
PLAT791_ALERT_4_G Model has Chirality at C1           (Sohnke SpGr)          S Verify
PLAT791_ALERT_4_G Model has Chirality at C2           (Sohnke SpGr)          S Verify
PLAT791_ALERT_4_G Model has Chirality at C3           (Sohnke SpGr)          R Verify
PLAT791_ALERT_4_G Model has Chirality at C4           (Sohnke SpGr)          R Verify
PLAT791_ALERT_4_G Model has Chirality at C5           (Sohnke SpGr)          S Verify
PLAT791_ALERT_4_G Model has Chirality at C6           (Sohnke SpGr)          S Verify
PLAT791_ALERT_4_G Model has Chirality at C7           (Sohnke SpGr)          S Verify
PLAT791_ALERT_4_G Model has Chirality at C14          (Sohnke SpGr)          R Verify
PLAT791_ALERT_4_G Model has Chirality at C15          (Sohnke SpGr)          S Verify
PLAT791_ALERT_4_G Model has Chirality at C18          (Sohnke SpGr)          R Verify
PLAT791_ALERT_4_G Model has Chirality at C23          (Sohnke SpGr)          R Verify
PLAT791_ALERT_4_G Model has Chirality at C27          (Sohnke SpGr)          R Verify
PLAT802_ALERT_4_G CIF Input Record(s) with more than 80 Characters           1 Info
PLAT860_ALERT_3_G Number of Least-Squares Restraints .............        792 Note
PLAT883_ALERT_1_G No Info/Value for _atom_sites_solution_primary .      Please Do !
PLAT910_ALERT_3_G Missing # of FCF Reflection(s) Below Theta(Min).          1 Note
PLAT912_ALERT_4_G Missing # of FCF Reflections Above STh/L=   0.600        391 Note
PLAT916_ALERT_2_G Hooft y and Flack x Parameter Values Differ by .         0.41 Check
PLAT933_ALERT_2_G Number of OMIT Records in Embedded .res File ...          13 Note
PLAT941_ALERT_3_G Average HKL Measurement Multiplicity ...........         4.0 Low
PLAT978_ALERT_2_G Number C-C Bonds with Positive Residual Density.          11 Info
PLAT982_ALERT_1_G The   C-f'=    0.0021 Deviates from  IT-value =       0.0033 Check
PLAT982_ALERT_1_G The   O-f'=    0.0079 Deviates from  IT-value =       0.0106 Check
```

---

1 **ALERT level A** = Most likely a serious problem - resolve or explain
5 **ALERT level B** = A potentially serious problem, consider carefully
14 **ALERT level C** = Check. Ensure it is not caused by an omission or oversight
35 **ALERT level G** = General information/check it is not something unexpected

7 ALERT type 1 CIF construction/syntax error, inconsistent or missing data
11 ALERT type 2 Indicator that the structure model may be wrong or deficient
15 ALERT type 3 Indicator that the structure quality may be low
22 ALERT type 4 Improvement, methodology, query or suggestion
0 ALERT type 5 Informative message, check

It is advisable to attempt to resolve as many as possible of the alerts in all categories. Often the minor alerts point to easily fixed oversights, errors and omissions in your CIF or refinement strategy, so attention to these fine details can be worthwhile. In order to resolve some of the more serious problems it may be necessary to carry out additional measurements or structure refinements. However, the purpose of your study may justify the reported deviations and the more serious of these should normally be commented upon in the discussion or experimental section of a paper or in the "special_details" fields of the CIF. checkCIF was carefully designed to identify outliers and unusual parameters, but every test has its limitations and alerts that are not important in a particular case may appear. Conversely, the absence of alerts does not guarantee there are no aspects of the results needing attention. It is up to the individual to critically assess their own results and, if necessary, seek expert advice.

Publication of your CIF in IUCr journals

A basic structural check has been run on your CIF. These basic checks will be run on all CIFs submitted for publication in IUCr journals (*Acta Crystallographica*, *Journal of Applied Crystallography*, *Journal of Synchrotron Radiation*); however, if you intend to submit to *Acta Crystallographica Section C* or *E* or *IUCrData*, you should make sure that full publication checks are run on the final version of your CIF prior to submission.

Publication of your CIF in other journals

Please refer to the *Notes for Authors* of the relevant journal for any special instructions relating to CIF submission.

PLATON version of 18/09/2020; check.def file version of 20/08/2020

Datablock 224C-F2c-PF42-SF7_nsphera - ellipsoid plot

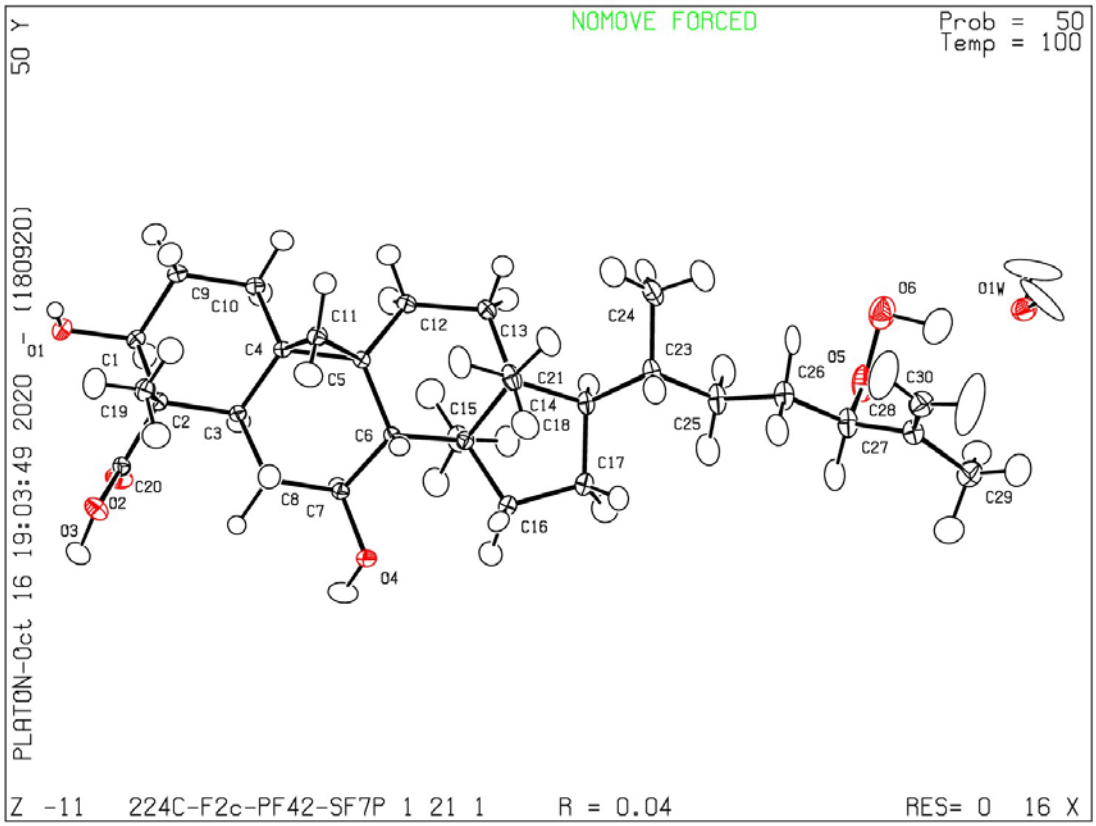

Supplementary Information S2

checkCIF/PLATON report

Structure factors have been supplied for datablock(s) castaneroxy-b

THIS REPORT IS FOR GUIDANCE ONLY. IF USED AS PART OF A REVIEW PROCEDURE FOR PUBLICATION, IT SHOULD NOT REPLACE THE EXPERTISE OF AN EXPERIENCED CRYSTALLOGRAPHIC REFEREE.

No syntax errors found. CIF dictionary Interpreting this report

Datablock: castaneroxy-b

```
Bond precision:   C-C = 0.0068 A          Wavelength=1.54184

 Cell:          a=6.7511(3)  b=12.2548(7)        c=17.4683(12)
                alpha=90     beta=98.733(6)      gamma=90
 Temperature:   110 K

                Calculated       Reported 1428.45(15)
 Volume         1428.46(14)
 Space group    P 21             P 1 21 1
 Hall group     P 2yb            P 2yb
 Moiety formula C30 H48 O6,  2(H2 O)        2(C30 H48 O6), 4(H2 O)
 Sum formula    C30 H52 O8       C60 H104 O16
 Mr             540.72           1081.43
 Dx,g cm-3      1.257            1.257
 Z              2                1
 Mu (mm-1)      0.723            0.723
 F000           592.0            592.0
 F000'          593.81
 h,k,lmax       7,14,20          7,14,20
 Nref           4859[ 2553]      3583
 Tmin,Tmax      0.815,0.927      0.354,1.000
 Tmin'          0.702

Correction method= # Reported T Limits: Tmin=0.354 Tmax=1.000
AbsCorr = GAUSSIAN

Data completeness= 1.40/0.74       Theta(max)= 65.072

R(reflections)= 0.0610( 2898)      wR2(reflections)= 0.1641( 3583)

S = 1.005                  Npar= 364
```

The following ALERTS were generated. Each ALERT has the format
test-name_ALERT_alert-type_alert-level.
Click on the hyperlinks for more details of the test.

Alert level B

```
PLAT355_ALERT_3_B Long     O-H (X0.82,N0.98A)  O6       - H6       .       1.09 Ang.
```

Author Response: This was a freely refined hydrogen atom. It is long because it was refined without restraints.

```
PLAT410_ALERT_2_B Short Intra H...H Contact    H1B      ..H11B     .       1.88 Ang.
x,y,z                                                        =      1_555 Check
```

Author Response: This distance is real and is the distance between two hydrogens of a fused ring system.

```
PLAT915_ALERT_3_B No Flack x Check Done: Low Friedel Pair Coverage          46 %
```

Author Response: Because the Friedel Pair Coverage was low the absolute configuration was assigned using the known absolute configuration of the partner molecule, castaneroxy-a.

Alert level C

```
STRVA01_ALERT_4_C            Flack test results are ambiguous.
From the CIF: _refine_ls_abs_structure_Flack                0.500
From the CIF: _refine_ls_abs_structure_Flack_su                0.400
THETM01_ALERT_3_C   The value of sine(theta_max)/wavelength is less than 0.590
Calculated sin(theta_max)/wavelength =                    0.5882
PLAT089_ALERT_3_C Poor Data / Parameter Ratio (Zmax < 18) ........        6.90 Note
PLAT340_ALERT_3_C Low Bond Precision on   C-C Bonds ..............    0.00679 Ang.
 PLAT351_ALERT_3_C Long    C-H (X0.96,N1.08A) C1       - H1A      .       1.13 Ang.
 PLAT351_ALERT_3_C Long    C-H (X0.96,N1.08A) C1       - H1B      .       1.12 Ang.
 PLAT351_ALERT_3_C Long    C-H (X0.96,N1.08A) C2       - H2A      .       1.12 Ang.
 PLAT351_ALERT_3_C Long    C-H (X0.96,N1.08A) C2       - H2B      .       1.12 Ang.
 PLAT351_ALERT_3_C Long    C-H (X0.96,N1.08A) C5       - H5       .       1.11 Ang.
 PLAT351_ALERT_3_C Long    C-H (X0.96,N1.08A) C6       - H6A      .       1.12 Ang.
 PLAT351_ALERT_3_C Long    C-H (X0.96,N1.08A) C6       - H6B      .       1.12 Ang.
 PLAT351_ALERT_3_C Long    C-H (X0.96,N1.08A) C11      - H11A     .       1.12 Ang.
 PLAT351_ALERT_3_C Long    C-H (X0.96,N1.08A) C11      - H11B     .       1.12 Ang.
 PLAT351_ALERT_3_C Long    C-H (X0.96,N1.08A) C12      - H12A     .       1.12 Ang.
 PLAT351_ALERT_3_C Long    C-H (X0.96,N1.08A) C12      - H12B     .       1.12 Ang.
 PLAT351_ALERT_3_C Long    C-H (X0.96,N1.08A) C15      - H15A     .       1.12 Ang.
 PLAT351_ALERT_3_C Long    C-H (X0.96,N1.08A) C15      - H15B     .       1.12 Ang.
 PLAT351_ALERT_3_C Long    C-H (X0.96,N1.08A) C16      - H16A     .       1.12 Ang.
 PLAT351_ALERT_3_C Long    C-H (X0.96,N1.08A) C16      - H16B     .       1.12 Ang.
 PLAT351_ALERT_3_C Long    C-H (X0.96,N1.08A) C19      - H19A     .       1.12 Ang.
 PLAT351_ALERT_3_C Long    C-H (X0.96,N1.08A) C19      - H19B     .       1.13 Ang.
 PLAT351_ALERT_3_C Long    C-H (X0.96,N1.08A) C20      - H20      .       1.12 Ang.
 PLAT351_ALERT_3_C Long    C-H (X0.96,N1.08A) C22      - H22A     .       1.12 Ang.
```

```
 PLAT351_ALERT_3_C Long    C-H (X0.96,N1.08A) C22       - H22B     .       1.12 Ang.
 PLAT351_ALERT_3_C Long    C-H (X0.96,N1.08A) C23       - H23      .       1.11 Ang.
 PLAT351_ALERT_3_C Long    C-H (X0.96,N1.08A) C24       - H24      .       1.16 Ang.
 PLAT355_ALERT_3_C Long    O-H (X0.82,N0.98A) O1W       - H1WA     .       1.01 Ang.
```

Author Response: This was a freely refined hydrogen atom. It is long because it was refined without restraints.

```
PLAT355_ALERT_3_C Long    O-H (X0.82,N0.98A)  O1W      - H1WB     .       1.01 Ang.
```

Author Response: This was a freely refined hydrogen atom. It is long because it was refined without restraints.

```
PLAT355_ALERT_3_C Long    O-H (X0.82,N0.98A)  O2W      - H2WA     .       1.01 Ang.
```

Author Response: This was a freely refined hydrogen atom. It is long because it was refined without restraints.

```
PLAT355_ALERT_3_C Long    O-H (X0.82,N0.98A)  O2W      - H2WB     .       1.01 Ang.
```

Author Response: This was a freely refined hydrogen atom. It is long because it was refined without restraints.

```
 PLAT751_ALERT_4_C Bond    Calc     0.97000, Rep    0.968(3) ......  Senseless s.u.
             O3      -H3      1.555          1.555 ........     #     2 Check
 PLAT751_ALERT_4_C Bond    Calc     0.97000, Rep    0.966(3) ......  Senseless s.u.
             O1      -H1      1.555          1.555 ........     #     4 Check
 PLAT751_ALERT_4_C Bond    Calc     0.97000, Rep    0.965(3) ......  Senseless s.u.
             O4      -H4      1.555          1.555 ........     #     6 Check
 PLAT751_ALERT_4_C Bond    Calc     1.09000, Rep    1.085(4) ......  Senseless s.u.
             O6      -H6      1.555          1.555 ........     #    10 Check
 PLAT751_ALERT_4_C Bond    Calc     1.12000, Rep    1.123(3) ......  Senseless s.u.
             C6      -H6A     1.555          1.555 ........     #    18 Check
 PLAT751_ALERT_4_C Bond    Calc     1.12000, Rep    1.125(3) ......  Senseless s.u.
             C6      -H6B     1.555          1.555 ........     #    19 Check
 PLAT751_ALERT_4_C Bond    Calc     1.06000, Rep    1.058(5) ......  Senseless s.u.
             C7      -H7      1.555          1.555 ........     #    21 Check
 PLAT751_ALERT_4_C Bond    Calc     1.12000, Rep    1.123(3) ......  Senseless s.u.
             C15     -H15A    1.555          1.555 ........     #    29 Check
 PLAT751_ALERT_4_C Bond    Calc     1.12000, Rep    1.125(3) ......  Senseless s.u.
             C15     -H15B    1.555          1.555 ........     #    30 Check
 PLAT751_ALERT_4_C Bond    Calc     1.12000, Rep    1.124(3) ......  Senseless s.u.
             C16     -H16A    1.555          1.555 ........     #    32 Check
 PLAT751_ALERT_4_C Bond    Calc     1.12000, Rep    1.123(3) ......  Senseless s.u.
             C16     -H16B    1.555          1.555 ........     #    33 Check
 PLAT751_ALERT_4_C Bond    Calc     0.93000, Rep    0.932(5) ......  Senseless s.u.
             C17     -H17     1.555          1.555 ........     #    35 Check
 PLAT751_ALERT_4_C Bond    Calc     1.12000, Rep    1.124(3) ......  Senseless s.u.
             C12     -H12A    1.555          1.555 ........     #    40 Check
 PLAT751_ALERT_4_C Bond    Calc     1.12000, Rep    1.124(3) ......  Senseless s.u.
```

```
               C12      -H12B     1.555          1.555 ........     #    41 Check
  PLAT751_ALERT_4_C Bond    Calc     1.12000, Rep    1.123(3) ......  Senseless s.u.
               C11      -H11A     1.555          1.555 ........     #    43 Check
  PLAT751_ALERT_4_C Bond    Calc     1.12000, Rep    1.123(3) ......  Senseless s.u.
               C11      -H11B     1.555          1.555 ........     #    44 Check
  PLAT751_ALERT_4_C Bond    Calc     1.12000, Rep    1.124(2) ......  Senseless s.u.
               C19      -H19A     1.555          1.555 ........     #    47 Check
  PLAT751_ALERT_4_C Bond    Calc     1.13000, Rep    1.125(2) ......  Senseless s.u.
               C19      -H19B     1.555          1.555 ........     #    48 Check
  PLAT751_ALERT_4_C Bond    Calc     1.00000, Rep    1.005(5) ......  Senseless s.u.
               C3       -H3A      1.555          1.555 ........     #    52 Check
PLAT751_ALERT_4_C Bond    Calc     1.12000, Rep    1.123(3) ......  Senseless s.u.
C2                     -H2A           1.555   1.555 ........     #    54 Check
PLAT751_ALERT_4_C Bond    Calc     1.12000, Rep    1.123(3) ......  Senseless s.u.
C2                     -H2B           1.555   1.555 ........     #    55 Check
PLAT751_ALERT_4_C Bond    Calc     1.13000, Rep    1.126(3) ......  Senseless s.u.
C1                     -H1A           1.555   1.555 ........     #    57 Check
PLAT751_ALERT_4_C Bond    Calc     1.12000, Rep    1.124(3) ......  Senseless s.u.
C1                     -H1B           1.555   1.555 ........     #    58 Check
PLAT751_ALERT_4_C Bond    Calc     1.12000, Rep    1.124(3) ......  Senseless s.u.
C20                    -H20           1.555   1.555 ........     #    62 Check
PLAT751_ALERT_4_C Bond    Calc     1.12000, Rep    1.123(3) ......  Senseless s.u.
C22                    -H22A          1.555   1.555 ........     #    65 Check
PLAT751_ALERT_4_C Bond    Calc     1.12000, Rep    1.124(3) ......  Senseless s.u.
C22                    -H22B          1.555   1.555 ........     #    66 Check
PLAT751_ALERT_4_C Bond    Calc     1.11000, Rep    1.106(5) ......  Senseless s.u.
C23                    -H23           1.555   1.555 ........     #    68 Check
PLAT751_ALERT_4_C Bond    Calc     1.05000, Rep    1.051(4) ......  Senseless s.u.
C27                    -H27A          1.555   1.555 ........     #    74 Check
PLAT751_ALERT_4_C Bond    Calc     1.05000, Rep    1.052(4) ......  Senseless s.u.
C27                    -H27B          1.555   1.555 ........     #    75 Check
PLAT751_ALERT_4_C Bond    Calc     1.05000, Rep    1.050(4) ......  Senseless s.u.
C27                    -H27C          1.555   1.555 ........     #    76 Check
PLAT751_ALERT_4_C Bond    Calc     1.05000, Rep    1.054(4) ......  Senseless s.u.
C26                    -H26A          1.555   1.555 ........     #    77 Check
PLAT751_ALERT_4_C Bond    Calc     1.05000, Rep    1.052(3) ......  Senseless s.u.
C26                    -H26B          1.555   1.555 ........     #    78 Check
PLAT751_ALERT_4_C Bond    Calc     1.05000, Rep    1.051(4) ......  Senseless s.u.
C26                    -H26C          1.555   1.555 ........     #    79 Check
PLAT752_ALERT_4_C Angle   Calc      109.00, Rep    108.5(4) ......  Senseless s.u.
C28                  -O3      -H3         1.555  1.555  1.555     #     1 Check
PLAT752_ALERT_4_C Angle   Calc      109.00, Rep    108.8(4) ......  Senseless s.u.
C3                   -O1      -H1         1.555  1.555  1.555     #     2 Check
PLAT752_ALERT_4_C Angle   Calc      106.00, Rep    105.6(3) ......  Senseless s.u.
C7                   -O4      -H4         1.555  1.555  1.555     #     3 Check
PLAT752_ALERT_4_C Angle   Calc      103.00, Rep    103.3(4) ......  Senseless s.u.
O5                   -O6      -H6         1.555  1.555  1.555     #     5 Check
PLAT752_ALERT_4_C Angle   Calc      114.00, Rep    113.7(4) ......  Senseless s.u.
C5                   -C6      -H6A        1.555  1.555  1.555     #    18 Check
PLAT752_ALERT_4_C Angle   Calc      103.00, Rep    103.1(3) ......  Senseless s.u.
C5                   -C6      -H6B        1.555  1.555  1.555     #    19 Check
PLAT752_ALERT_4_C Angle   Calc      112.00, Rep    111.7(3) ......  Senseless s.u.
H6A                  -C6      -H6B        1.555  1.555  1.555     #    20 Check
PLAT752_ALERT_4_C Angle   Calc      102.00, Rep    101.8(3) ......  Senseless s.u.
C7                   -C6      -H6A        1.555  1.555  1.555     #    22 Check
PLAT752_ALERT_4_C Angle   Calc      118.00, Rep    118.2(4) ......  Senseless s.u.
C7                   -C6      -H6B        1.555  1.555  1.555     #    23 Check
PLAT752_ALERT_4_C Angle   Calc      102.00, Rep    102.3(4) ......  Senseless s.u.
O4                   -C7      -H7         1.555  1.555  1.555     #    25 Check
```

PLAT752_ALERT_4_C Angle   Calc   113.00, Rep   112.9(4) ...... Senseless s.u.
C6   -C7   -H7   1.555 1.555 1.555   #   27 Check
PLAT752_ALERT_4_C Angle   Calc   112.00, Rep   112.0(4) ...... Senseless s.u.
C8   -C7   -H7   1.555 1.555 1.555   #   29 Check
PLAT752_ALERT_4_C Angle   Calc   112.00, Rep   112.0(4) ...... Senseless s.u.
C14   -C15   -H15A   1.555 1.555 1.555   #   42 Check
PLAT752_ALERT_4_C Angle   Calc   107.00, Rep   107.1(4) ...... Senseless s.u.
C14   -C15   -H15B   1.555 1.555 1.555   #   43 Check
PLAT752_ALERT_4_C Angle   Calc   99.00, Rep   98.7(2) ...... Senseless s.u.
H15A   -C15   -H15B   1.555 1.555 1.555   #   45 Check
PLAT752_ALERT_4_C Angle   Calc   118.00, Rep   118.0(3) ...... Senseless s.u.
C16   -C15   -H15A   1.555 1.555 1.555   #   46 Check
PLAT752_ALERT_4_C Angle   Calc   116.00, Rep   115.7(3) ...... Senseless s.u.
C16   -C15   -H15B   1.555 1.555 1.555   #   47 Check
PLAT752_ALERT_4_C Angle   Calc   112.00, Rep   111.6(3) ...... Senseless s.u.
C15   -C16   -H16A   1.555 1.555 1.555   #   48 Check
PLAT752_ALERT_4_C Angle   Calc   108.00, Rep   107.5(3) ...... Senseless s.u.
C15   -C16   -H16B   1.555 1.555 1.555   #   49 Check
PLAT752_ALERT_4_C Angle   Calc   110.00, Rep   109.8(3) ...... Senseless s.u.
H16A   -C16   -H16B   1.555 1.555 1.555   #   50 Check
PLAT752_ALERT_4_C Angle   Calc   110.00, Rep   109.9(4) ...... Senseless s.u.
C17   -C16   -H16A   1.555 1.555 1.555   #   52 Check
PLAT752_ALERT_4_C Angle   Calc   111.00, Rep   110.8(4) ...... Senseless s.u.
C17   -C16   -H16B   1.555 1.555 1.555   #   53 Check
PLAT752_ALERT_4_C Angle   Calc   113.00, Rep   113.4(4) ...... Senseless s.u.
C16   -C17   -H17   1.555 1.555 1.555   #   54 Check
PLAT752_ALERT_4_C Angle   Calc   104.00, Rep   104.5(4) ...... Senseless s.u.
C13   -C17   -H17   1.555 1.555 1.555   #   56 Check
PLAT752_ALERT_4_C Angle   Calc   104.00, Rep   103.9(4) ...... Senseless s.u.
C20   -C17   -H17   1.555 1.555 1.555   #   58 Check
PLAT752_ALERT_4_C Angle   Calc   105.00, Rep   105.3(3) ...... Senseless s.u.
C13   -C12   -H12A   1.555 1.555 1.555   #   66 Check
PLAT752_ALERT_4_C Angle   Calc   107.00, Rep   107.4(3) ...... Senseless s.u.
C13   -C12   -H12B   1.555 1.555 1.555   #   67 Check
PLAT752_ALERT_4_C Angle   Calc   111.00, Rep   111.3(3) ...... Senseless s.u.
H12A   -C12   -H12B   1.555 1.555 1.555   #   69 Check
PLAT752_ALERT_4_C Angle   Calc   110.00, Rep   110.1(3) ...... Senseless s.u.
C11   -C12   -H12A   1.555 1.555 1.555   #   70 Check
PLAT752_ALERT_4_C Angle   Calc   109.00, Rep   109.3(3) ...... Senseless s.u.
C11   -C12   -H12B   1.555 1.555 1.555   #   71 Check
PLAT752_ALERT_4_C Angle   Calc   115.00, Rep   114.8(3) ...... Senseless s.u.
C12   -C11   -H11A   1.555 1.555 1.555   #   72 Check
PLAT752_ALERT_4_C Angle   Calc   113.00, Rep   113.0(3) ...... Senseless s.u.
C12   -C11   -H11B   1.555 1.555 1.555   #   73 Check
PLAT752_ALERT_4_C Angle   Calc   91.00, Rep   91.03(19) ...... Senseless s.u.
H11A   -C11   -H11B   1.555 1.555 1.555   #   74 Check
PLAT752_ALERT_4_C Angle   Calc   109.00, Rep   108.9(4) ...... Senseless s.u.
C9   -C11   -H11A   1.555 1.555 1.555   #   76 Check
PLAT752_ALERT_4_C Angle   Calc   108.00, Rep   107.6(4) ...... Senseless s.u.
C9   -C11   -H11B   1.555 1.555 1.555   #   77 Check
PLAT752_ALERT_4_C Angle   Calc   115.00, Rep   115.2(3) ...... Senseless s.u.
C10   -C19   -H19A   1.555 1.555 1.555   #   85 Check
PLAT752_ALERT_4_C Angle   Calc   110.00, Rep   110.3(3) ...... Senseless s.u.
C10   -C19   -H19B   1.555 1.555 1.555   #   86 Check
PLAT752_ALERT_4_C Angle   Calc   115.00, Rep   114.7(3) ...... Senseless s.u.
C9   -C19   -H19A   1.555 1.555 1.555   #   87 Check
PLAT752_ALERT_4_C Angle   Calc   119.00, Rep   118.6(3) ...... Senseless s.u.
C9   -C19   -H19B   1.555 1.555 1.555   #   88 Check
PLAT752_ALERT_4_C Angle   Calc   121.00, Rep   121.6(3) ...... Senseless s.u.

```
H19A                  -C19     -H19B       1.555  1.555  1.555     #   89 Check
PLAT752_ALERT_4_C Angle    Calc      106.00, Rep    106.2(4) ......  Senseless s.u.
O1                    -C3      -H3A        1.555  1.555  1.555     #   97 Check
PLAT752_ALERT_4_C Angle    Calc       98.00, Rep     98.1(5) ......  Senseless s.u.
C4                    -C3      -H3A        1.555  1.555  1.555     #   99 Check
PLAT752_ALERT_4_C Angle    Calc      118.00, Rep    117.8(5) ......  Senseless s.u.
C2                    -C3      -H3A        1.555  1.555  1.555     #  101 Check
PLAT752_ALERT_4_C Angle    Calc      110.00, Rep    109.5(4) ......  Senseless s.u.
C3                    -C2      -H2A        1.555  1.555  1.555     #  102 Check
PLAT752_ALERT_4_C Angle    Calc      111.00, Rep    110.9(4) ......  Senseless s.u.
C3                    -C2      -H2B        1.555  1.555  1.555     #  103 Check
PLAT752_ALERT_4_C Angle    Calc      106.00, Rep    106.4(3) ......  Senseless s.u.
H2A                   -C2      -H2B        1.555  1.555  1.555     #  105 Check
PLAT752_ALERT_4_C Angle    Calc      114.00, Rep    114.3(4) ......  Senseless s.u.
C1                    -C2      -H2A        1.555  1.555  1.555     #  106 Check
PLAT752_ALERT_4_C Angle    Calc      103.00, Rep    103.5(3) ......  Senseless s.u.
C1                    -C2      -H2B        1.555  1.555  1.555     #  107 Check
PLAT752_ALERT_4_C Angle    Calc      108.00, Rep    107.6(4) ......  Senseless s.u.
C10                   -C1      -H1A        1.555  1.555  1.555     #  109 Check
PLAT752_ALERT_4_C Angle    Calc      109.00, Rep    109.4(4) ......  Senseless s.u.
C10                   -C1      -H1B        1.555  1.555  1.555     #  110 Check
PLAT752_ALERT_4_C Angle    Calc      108.00, Rep    108.5(3) ......  Senseless s.u.
C2                    -C1      -H1A        1.555  1.555  1.555     #  111 Check
PLAT752_ALERT_4_C Angle    Calc      111.00, Rep    111.2(3) ......  Senseless s.u.
C2                    -C1      -H1B        1.555  1.555  1.555     #  112 Check
PLAT752_ALERT_4_C Angle    Calc      111.00, Rep    110.9(3) ......  Senseless s.u.
H1A                   -C1      -H1B        1.555  1.555  1.555     #  113 Check
PLAT752_ALERT_4_C Angle    Calc      108.00, Rep    107.6(4) ......  Senseless s.u.
C17                   -C20     -H20        1.555  1.555  1.555     #  123 Check
PLAT752_ALERT_4_C Angle    Calc      103.00, Rep    102.9(3) ......  Senseless s.u.
C22                   -C20     -H20        1.555  1.555  1.555     #  126 Check
PLAT752_ALERT_4_C Angle    Calc      114.00, Rep    114.4(4) ......  Senseless s.u.
C21                   -C20     -H20        1.555  1.555  1.555     #  128 Check
PLAT752_ALERT_4_C Angle    Calc      108.00, Rep    107.6(3) ......  Senseless s.u.
C20                   -C22     -H22A       1.555  1.555  1.555     #  129 Check
PLAT752_ALERT_4_C Angle    Calc      106.00, Rep    106.3(4) ......  Senseless s.u.
C20                   -C22     -H22B       1.555  1.555  1.555     #  130 Check
PLAT752_ALERT_4_C Angle    Calc      112.00, Rep    112.4(3) ......  Senseless s.u.
H22A                  -C22     -H22B       1.555  1.555  1.555     #  131 Check
PLAT752_ALERT_4_C Angle    Calc      105.00, Rep    105.0(4) ......  Senseless s.u.
C23                   -C22     -H22A       1.555  1.555  1.555     #  133 Check
PLAT752_ALERT_4_C Angle    Calc      111.00, Rep    111.5(4) ......  Senseless s.u.
C23                   -C22     -H22B       1.555  1.555  1.555     #  134 Check
PLAT752_ALERT_4_C Angle    Calc      108.00, Rep    107.9(4) ......  Senseless s.u.
C22                   -C23     -H23        1.555  1.555  1.555     #  135 Check
PLAT752_ALERT_4_C Angle    Calc      127.00, Rep    127.1(5) ......  Senseless s.u.
C24                   -C23     -H23        1.555  1.555  1.555     #  137 Check
PLAT752_ALERT_4_C Angle    Calc      114.00, Rep    114.3(4) ......  Senseless s.u.
C25                   -C27     -H27A       1.555  1.555  1.555     #  147 Check
PLAT752_ALERT_4_C Angle    Calc      115.00, Rep    114.6(4) ......  Senseless s.u.
C25                   -C27     -H27B       1.555  1.555  1.555     #  148 Check
PLAT752_ALERT_4_C Angle    Calc      112.00, Rep    112.4(4) ......  Senseless s.u.
C25                   -C27     -H27C       1.555  1.555  1.555     #  149 Check
PLAT752_ALERT_4_C Angle    Calc      105.00, Rep    104.8(3) ......  Senseless s.u.
H27A                  -C27     -H27B       1.555  1.555  1.555     #  150 Check
PLAT752_ALERT_4_C Angle    Calc      105.00, Rep    104.9(3) ......  Senseless s.u.
H27A                  -C27     -H27C       1.555  1.555  1.555     #  151 Check
PLAT752_ALERT_4_C Angle    Calc      105.00, Rep    104.9(3) ......  Senseless s.u.
H27B                  -C27     -H27C       1.555  1.555  1.555     #  152 Check
```

```
PLAT752_ALERT_4_C Angle    Calc      114.00, Rep    114.4(4) ......  Senseless s.u.
C25                   -C26     -H26A       1.555  1.555  1.555     #  153 Check
PLAT752_ALERT_4_C Angle    Calc      112.00, Rep    112.2(4) ......  Senseless s.u.
C25                   -C26     -H26B       1.555  1.555  1.555     #  154 Check
PLAT752_ALERT_4_C Angle    Calc      115.00, Rep    115.3(4) ......  Senseless s.u.
C25                   -C26     -H26C       1.555  1.555  1.555     #  155 Check
PLAT752_ALERT_4_C Angle    Calc      105.00, Rep    104.5(3) ......  Senseless s.u.
H26A                  -C26     -H26B       1.555  1.555  1.555     #  156 Check
PLAT752_ALERT_4_C Angle    Calc      105.00, Rep    104.6(3) ......  Senseless s.u.
H26A                  -C26     -H26C       1.555  1.555  1.555     #  157 Check
PLAT752_ALERT_4_C Angle    Calc      105.00, Rep    104.8(3) ......  Senseless s.u.
H26B                  -C26     -H26C       1.555  1.555  1.555     #  158 Check
PLAT911_ALERT_3_C Missing FCF Refl Between Thmin & STh/L=     0.588         40 Report
```

Alert level G

```
PLAT002_ALERT_2_G Number of Distance or Angle Restraints on AtSite          61 Note
PLAT007_ALERT_5_G Number of Unrefined Donor-H Atoms ..............           4 Report
PLAT032_ALERT_4_G Std. Uncertainty on Flack Parameter Value High .       0.400 Report
PLAT042_ALERT_1_G Calc. and Reported MoietyFormula Strings   Differ     Please Check
PLAT045_ALERT_1_G Calculated and Reported Z Differ by a Factor ...       2.00 Check
PLAT072_ALERT_2_G SHELXL FirstParameter in WGHT     Unusually Large       0.11 Report
PLAT172_ALERT_4_G The CIF-Embedded .res File Contains DFIX Records        4 Report
PLAT176_ALERT_4_G The CIF-Embedded .res File Contains SADI Records        7 Report
PLAT395_ALERT_2_G Deviating   X-O-Y    Angle From 120 for O5             109.1 Degree
PLAT720_ALERT_4_G Number of Unusual/Non-Standard Labels .........         4 Note
PLAT790_ALERT_4_G Centre of Gravity not Within Unit Cell: Resd.   #          3 Note
H2 O
PLAT791_ALERT_4_G Model has Chirality at C3           (Sohnke SpGr)          S Verify
PLAT791_ALERT_4_G Model has Chirality at C4           (Sohnke SpGr)          S Verify
PLAT791_ALERT_4_G Model has Chirality at C5           (Sohnke SpGr)          R Verify
PLAT791_ALERT_4_G Model has Chirality at C7           (Sohnke SpGr)          S Verify
PLAT791_ALERT_4_G Model has Chirality at C8           (Sohnke SpGr)          S Verify
PLAT791_ALERT_4_G Model has Chirality at C9           (Sohnke SpGr)          S Verify
PLAT791_ALERT_4_G Model has Chirality at C10          (Sohnke SpGr)          R Verify
PLAT791_ALERT_4_G Model has Chirality at C13          (Sohnke SpGr)          R Verify
PLAT791_ALERT_4_G Model has Chirality at C14          (Sohnke SpGr)          S Verify
PLAT791_ALERT_4_G Model has Chirality at C17          (Sohnke SpGr)          R Verify
PLAT791_ALERT_4_G Model has Chirality at C20          (Sohnke SpGr)          R Verify
PLAT860_ALERT_3_G Number of Least-Squares Restraints .............        393 Note
PLAT883_ALERT_1_G No Info/Value for _atom_sites_solution_primary .      Please Do !
PLAT909_ALERT_3_G Percentage of I>2sig(I) Data at Theta(Max) Still         62% Note
PLAT910_ALERT_3_G Missing # of FCF Reflection(s) Below Theta(Min).          1 Note
PLAT941_ALERT_3_G Average HKL Measurement Multiplicity ...........        3.6 Low
PLAT978_ALERT_2_G Number C-C Bonds with Positive Residual Density.         4 Info
```

---

0 **ALERT level A** = Most likely a serious problem - resolve or explain
3 **ALERT level B** = A potentially serious problem, consider carefully
139 **ALERT level C** = Check. Ensure it is not caused by an omission or oversight
28 **ALERT level G** = General information/check it is not something unexpected

3 ALERT type 1 CIF construction/syntax error, inconsistent or missing data
5 ALERT type 2 Indicator that the structure model may be wrong or deficient
36 ALERT type 3 Indicator that the structure quality may be low
125 ALERT type 4 Improvement, methodology, query or suggestion
1 ALERT type 5 Informative message, check

It is advisable to attempt to resolve as many as possible of the alerts in all categories. Often the minor alerts point to easily fixed oversights, errors and omissions in your CIF or refinement strategy, so attention to these fine details can be worthwhile. In order to resolve some of the more serious problems it may be necessary to carry out additional measurements or structure refinements. However, the purpose of your study may justify the reported deviations and the more serious of these should normally be commented upon in the discussion or experimental section of a paper or in the "special_details" fields of the CIF. checkCIF was carefully designed to identify outliers and unusual parameters, but every test has its limitations and alerts that are not important in a particular case may appear. Conversely, the absence of alerts does not guarantee there are no aspects of the results needing attention. It is up to the individual to critically assess their own results and, if necessary, seek expert advice.

Publication of your CIF in IUCr journals

A basic structural check has been run on your CIF. These basic checks will be run on all CIFs submitted for publication in IUCr journals (*Acta Crystallographica*, *Journal of Applied Crystallography*, *Journal of Synchrotron Radiation*); however, if you intend to submit to *Acta Crystallographica Section C* or *E* or *IUCrData*, you should make sure that full publication checks are run on the final version of your CIF prior to submission.

Publication of your CIF in other journals

Please refer to the *Notes for Authors* of the relevant journal for any special instructions relating to CIF submission.

PLATON version of 18/09/2020; check.def file version of 20/08/2020

Datablock castaneroxy-b - ellipsoid plot

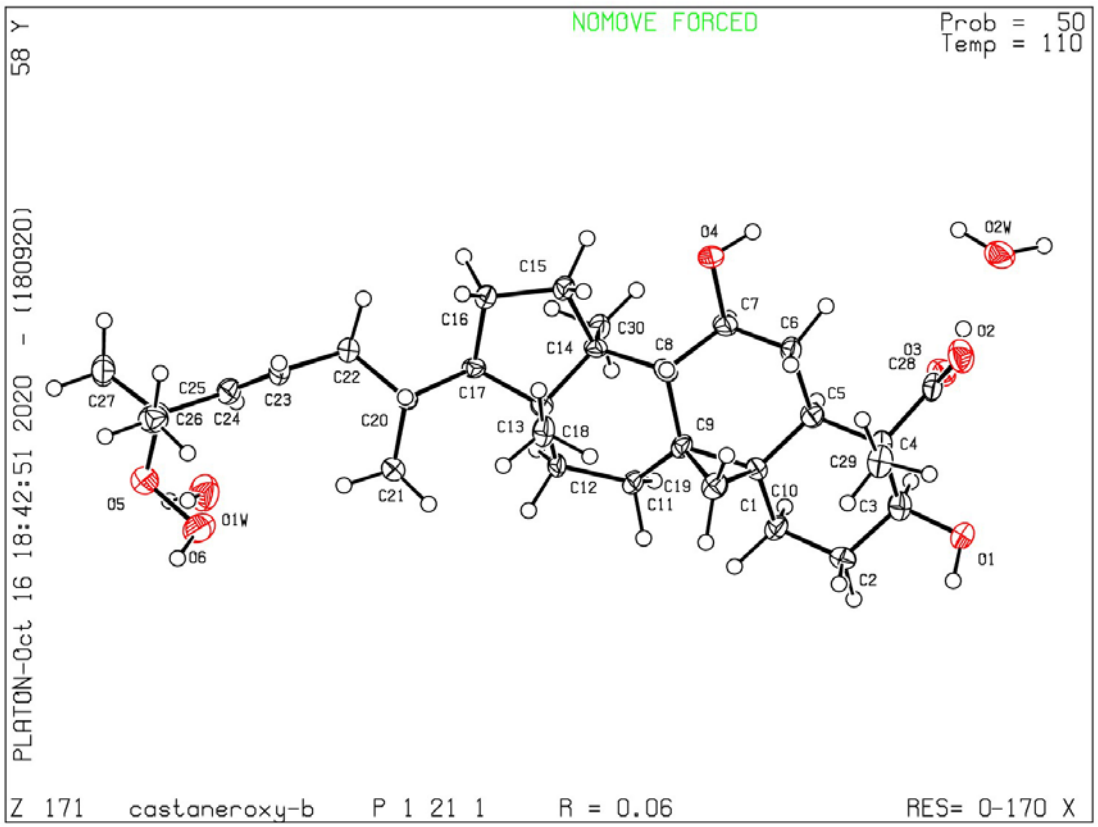

APPENDIX I

Opportunities for plant natural products in infection control

This has been published in *Current Opinion in Microbiology* (2019) 45:189-194. PMCID: PMC6295356

Salam, A.; Quave, C., Opportunities for plant natural products in infection control. *Current Opinion in Microbiology* **2018,** *45*, 189-194.

Opportunities for plant natural products in infection control

Akram M. Salam[1] and Cassandra L. Quave[2,3,4,5*]

[1]Molecular and Systems Pharmacology Program, Laney Graduate School, Emory University, Atlanta, GA, United States

[2]Center for the Study of Human Health, Emory University College of Arts and Sciences, Atlanta, GA, United States

[3]Department of Dermatology, Emory University School of Medicine, Atlanta, GA, United States

[4]Antibiotic Resistance Center, Emory University, Atlanta, GA, United States

[5]Emory University Herbarium, Atlanta, GA, United States

*Corresponding author: Cassandra Quave, cquave@emory.edu

Abstract

The continued spread of antimicrobial resistance represents one of the most serious infectious disease threats to global health. There is consensus that a key component of addressing this threat is to replenish the waning pipeline of antimicrobials, with attention being paid to novel mechanisms of action. This includes the development of new classes of classic bacteriostatic and bactericidal antibiotics as well as antivirulence drugs, and it is especially in these areas where plant natural products demonstrate great potential. To this end, we discuss the unique characteristics of plant natural products, the advantages of plants as a resource for anti-infective drug discovery, and recent technologies that have further enabled this path of inquiry. As a result of emerging realization of their advantages, plant natural products have recently enjoyed increased scrutiny in antimicrobial lead discovery, and they will continue to serve as a source of leads. We conclude that plant natural products represent a promising and largely untapped source of new chemical entities from which novel anti-infectives can be discovered.

Introduction

As antimicrobial resistant infections become more and more common, the need for new drugs that circumvent resistance arises as one of the main challenges in combatting this global health phenomenon (197). Indeed, numerous voices in the literature have cited innovation in anti-infective drug discovery as one of the most important aspects of infection control moving forward (159; 198). This innovation includes the development of drugs that inhibit microbial growth through novel mechanisms of action as well as drugs that work otherwise to attenuate pathogenicity, such as by inhibiting virulence factor production. The latter category of drugs is largely projected to serve as a source of adjuvants to antibiotics that may enhance potency and delay the onset of antimicrobial resistance (199; 200). This projection has received much attention in the literature, with much *in vivo* evidence supporting the effectiveness of adjuvants in infection treatment (16; 201). Herein we elaborate as to how natural products are especially well-positioned to help fill this gap in the anti-infective pipeline.

Plant secondary metabolites

Most plants produce hundreds if not thousands of unique compounds as an adaptation to their environment for the purpose of self-defense and interaction with other organisms in the environment; these are collectively referred to as plant secondary metabolites, or natural products (**Fig. A1.1**). The set of total compounds contained in any plant tissue in fact represents a chemical library from which bioactive compounds may be mined (202). Such libraries possess many characteristics highly favorable for drug discovery. Chief among these

is their chemical and structural diversity, which stands in excess of many synthetic small molecule libraries (160). With this diversity, plant natural products largely belong to the biologically relevant chemical space, which represents the subset of all chemicals that

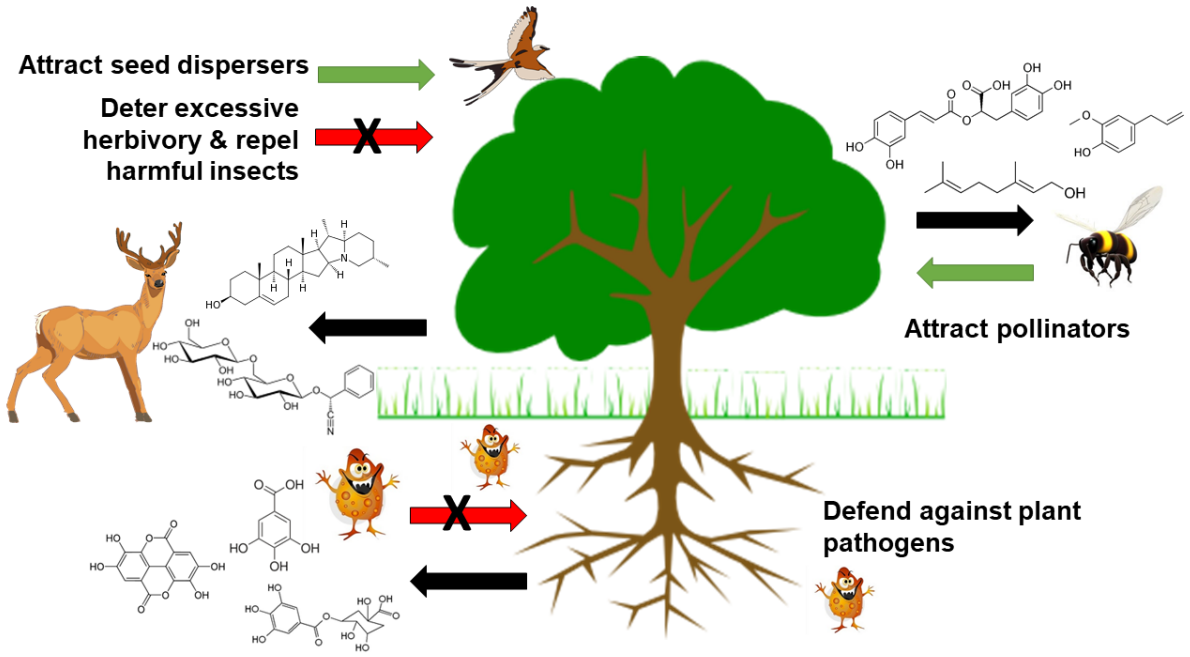

Fig. A1.1. The role of secondary metabolites in plants. Plants are sessile and individuals cannot physically move toward resources or away from threats in the environment. Instead, plants produce secondary metabolites – also known as natural products – as chemical communication tools in response to environmental cues. These metabolites are differentiated from the ubiquitous primary metabolites – which include carbohydrates, lipids, proteins, and nucleic acids – and are used for the basic processes involved in maintaining plant life. Secondary metabolites also come at an additional energy cost to the plant, and thus are not produced without reason. Some of the purposes that these compounds serve are in defense against predation and herbivory, attraction of pollinators and seed dispersers, and competition with other organisms in the environment. Secondary metabolites are responsible for the colors, flavors and odors of plant species.

possess bioactivity (**Fig. A1.2**); they are also largely metabolite-like, thus largely allowing for recognition by transport systems for entry into tissue (159; 203-205). Lead discovery efforts over the last two decades have shifted toward the screening of less structurally complex synthetic compounds, and while there have been many success stories from these campaigns, infectious diseases remain one of the areas that often require chemically and structurally complex molecules (206).

Of the plant natural products explored to date, those tested for microbial growth inhibiton have tended to exhibit weaker potency and selectivity than microbial natural products (207), with some exceptions. Acylphloroglucinols from S. Johns Wort species (*Hypericum* spp.) have demonstrated MICs in the range 0.5-1 µg/mL in methicillin resistant *Staphylococcus aureus* (MRSA) isolates (208). At the same time, plant natural products are very clearly rich in anti-virulence properties, with numerous single compounds currently in development to this end (10; 192; 207). Epigallocatechin gallate, a major component of green tea catechins, was identified as a promising non-bactericidal antivirulence agent against *Streptococcus pneumoniae* (209). Hamamelitannin, a tannin found in the bark and leaves of American witch hazel (*Hamamelis virginiana*), and derivatives thereof are being actively studied for the potentiation of vancomycin in biofilm-associated MRSA infections (210; 211). INP1855 is a derivative of 8-hydroxyquinoline, synthesized in roots of the diffuse knapweed (*Centaurea diffusa*) and was identified in a screen of a synthetic small molecule library (212; 213). It was confirmed to inhibit the injectisome and flagellar type III secretion systems in *Pseudomonas aeruginosa*, thereby impairing virulence (214). There are also examples of synthetic small molecule antivirulence compounds that resemble plant natural product pharmacophores. One

example is Compound 22, an isoquinolone mannoside that targets the type 1 pilus adhesin FimH in *Escherichia coli*

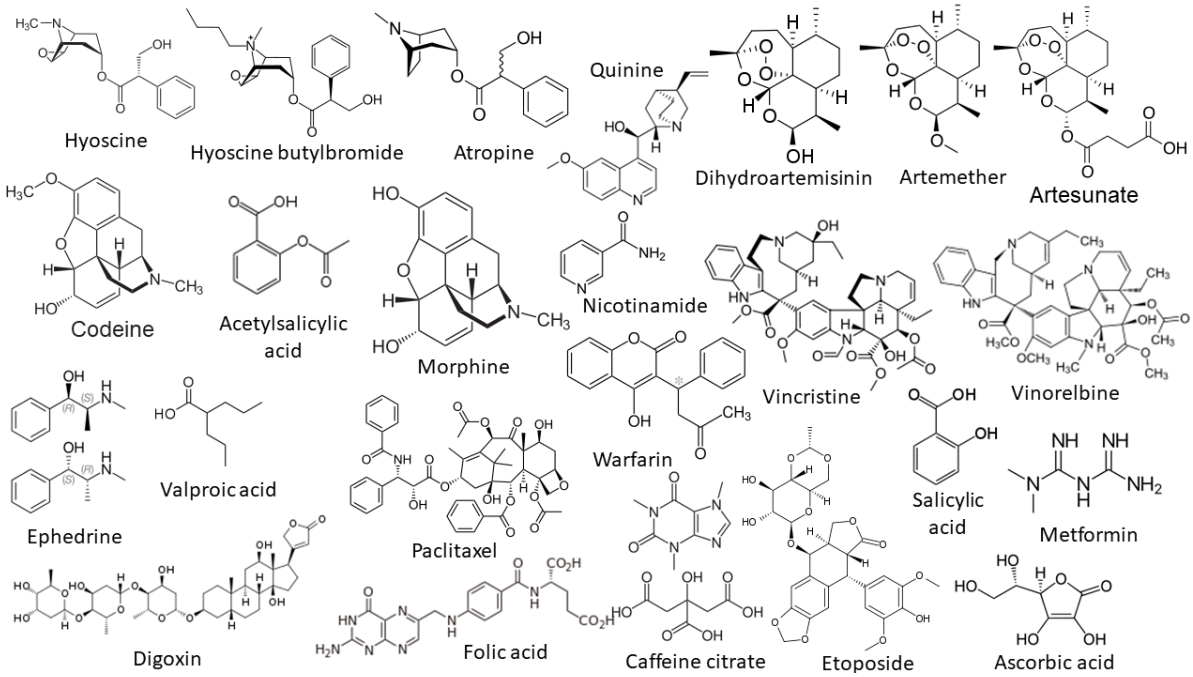

Fig. A1.2. Plants produce a diversity of bioactive natural products. What do these compounds share in common? They are all included in the 2017 WHO List of Essential Medicines and they were all originally discovered in – or modeled after chemical scaffolds discovered in – plants. Today, many of these are mass-produced using tools from plant biotechnology and synthetic chemistry.

(215). Another example is virstatin, an isoquinoline that targets pili biogenesis in *Acinetobacter baumannii* (216; 217).

Ethnobotany as a drug discovery tool

In addition to the diversity and drug-like chemical character of plant natural products, the ability to explore this chemical space in a targeted fashion using the lens of ethnobotany – the study of how people use plants – represents a major advantage. This is made possible by the centuries-old practices of traditional medicine in societies across the world, which have identified indications for countless different plant preparations. A recent report on the State of the World's Plants noted that there are at least 28,187 species that have been documented as being used in traditional medicine (218). While there is no accurate report of how many of these have been investigated to date for their pharmacologic potential, it could be estimated that only a few hundred have been subjected to in depth pharmacologic analysis for bioactivity and chemical composition.

An example of where ethnobotany has guided the discovery of antimicrobial compounds is the immensely successful antimalarial, artemisinin. Malaria is a mosquito-borne infectious disease caused by parasitic protozoans belonging to the *Plasmodium* genus. In 1967, a plant screening research program under the name *Project 523* was set up by the Chinese government with the goal of discovering novel antimalarial chemicals (219). Tu Youyou was part of a group working on the isolation of antimalarial candidates from plants used in traditional Chinese medicine. Initially, an extract of sweet wormwood (*Artemesia annua*) yielded promising antimalarial activity in a mouse model of infection, though the results were

not reproducible. Following preparation for malaria symptoms found in the 4th Century book *The Handbook of Prescriptions for Emergency Treatments* by Ge Hong, Tu Youyou prepared an *A. annua* extract consistently effective in the mouse model of malarial infection. It was through this extraction method that artemisinin was subsequently isolated.

Of the hundreds of compounds contained in different plants, it is small subsets of these compounds, if not single compounds, that are responsible for the therapeutic effects of these plant preparations. As such, by consulting traditional medicinal practices, plants can be identified that potentially contain chemicals of interest for development against a given disease state, and it is this set of plants on which drug discovery efforts can be focused (220). The identified plants must first be collected and processed for chemical extraction (167). There are numerous methods of chemical extraction, most of which make use of a solvent as the vehicle through which chemicals are dissolved from the plant material into a liquid phase that can then be separated and dried into a powder (221). Yet another advantage of plants as a chemical library source is the relative ease of generating large quantities of chemicals, which only requires collecting and processing more plant material. The dried plant extracts are then subject to the drug discovery framework of bioassay-guided fractionation, in which bioactive compounds are isolated by iterative rounds of chromatographic fractionation followed by assessment of biological activities of the fractions. Once natural products of interest are identified, more efficient chromatographic methods may be developed for their isolation.

Synergy among natural products

Another advantage of plant natural products for infection control is the potential for discovering highly effective synergies between different compounds in a given plant extract (222). Such synergies may lead to increased efficacy and a diminished tendency for the evolution of resistance (223). Artemisinin and its plant of origin, *A. annua*, can also serve as an example that illustrates this potential. In a rodent model of malarial infection, oral delivery of the plant's dried leaves was compared to treatment with a dose of pure artemisinin matching the whole plant content (50). The dried leaf treatment was found not only to be more efficacious at attenuating parasitemia, but also to result in a 40-fold increase in artemisinin bioavailability in the rodents. A later study, also in a rodent model of malarial infection, showed both that oral delivery of the dried leaves overcame existing resistance to artemisinin and that stable resistance to the whole plant treatment took three times longer to develop than stable resistance to artemisinin alone (51). Although the mechanism of action is not known, it could be that other chemicals present in the whole leaves target at least one other pathway important for the plasmodial life cycle, making the development of a resistant strain less likely to occur.

Indeed, there are a number of examples in the literature where multiple metabolites in the same plant have been identified and shown to synergistically exert a pharmacological effect. For instance, through synergy-directed fractionation, three flavonoids from goldenseal (*Hydrastis canadensis*) were identified, each of which capable of enhancing the antimicrobial efficacy of berberine, also present in *H. canadensis* (52). It was shown that all three flavonoids possessed no inherent antimicrobial activity against *S. aureus*, but rather functioned as inhibitors of the NorA multidrug resistance pump. With such multi-component defense systems being identified in plants, the possibility of developing plant natural product

fractions that exhibit more favorable activity and resistance profiles is highly attractive. To accommodate such botanical compositions, the United States Food and Drug Administration (US FDA) has a botanical drug track that requires them to be well-characterized (224). Natural product synergies can be highly complex and difficult to define, and we will discuss avenues for deconvoluting such complexities.

Drug discovery from plant natural products

Performing classical drug discovery from plant natural products is more accessible than ever before. In decades past, natural products in general had received diminished attention in favor of combinatorial and synthetic chemical libraries. More recently, difficulties that would have hindered plant natural products research have been overcome, such as improved compatibility with high throughput screening (HTS) and improvements in foreign plant acquisition, dereplication, compound isolation, and medicinal chemistry (159-162). Moving forward, the field of metabolomics stands as one of the strongest enablers of plant natural product discovery, allowing scientists to effectively mine the extremely chemical diversity available (225).

Metabolomics transforms the classical framework of bioassay-guided fractionation into a much shorter process of rapid identification of valuable plant natural products. In its most general sense, metabolomics is the analysis of all the known and/or unknown metabolites in a given biological sample. From such a dataset, very complex analyses can be undertaken to ask questions such as “which pharmacophores tend to be present in the most bioactive

fractions of this extract" and "which compounds are necessary for any possible synergism in fractions with the best resistance profiles" (226).

For metabolomics studies in plant natural product drug discovery, the acquisition of high quality data from a sample has been facilitated by technological advancements in chromatography, which separates the metabolites of a sample over time, and spectroscopy, which provides chemical data on said metabolites (227). Liquid chromatography-mass spectrometry (LC-MS) represents the most useful platform for profiling natural product compositions, and high-quality data is particularly achievable with ultra-performance liquid chromatography-high-resolution mass spectrometry (UPLC-HRMS) (228; 229).

From MS data, molecular features (molecular ions, adducts, in-source fragments, etc.) can be grouped and putative molecular formulae of metabolites can be determined (225). An MS data organization tool can then use MS fragmentation (MS/MS) data to link metabolites based on attributes such as similarity in spectrum or structure or presence of a particular structural moiety. More layers of information can then be mapped to the organized data, such as bioactivities, taxonomy, and gene sequences. This way, the MS/MS data can be organized as a molecular network of features that can then be annotated, ideally by unambiguously linking unique identifiers to a single molecular structure. Once a molecular network is annotated, it becomes possible to apply different types of scoring to refine the annotation results. As such, valuable natural products are identified from plant extracts or fractions thereof while at the same time massive metadata sets are constructed for these samples, which can be mined under various criteria. For example, such a metabolomics approach was used to focus isolation efforts on previously undescribed compounds from the leaves of

Palicourea sessilis (230). An alkaloid fraction of the leaves was analyzed, and MS/MS data were organized as molecular networks (231). The metabolites were then grouped in clusters of similar scaffolds, and the data was annotated against *in silico* spectra of natural products present in the *Dictionary of Natural Products* (75). Following this, compounds that did not match any known natural products were not annotated, indicating the presence of novel compounds.

Success in anti-virulence approaches

Demonstrating the strong potential for plant natural products in anti-infective drug discovery is the sheer volume of isolated compounds with confirmed anti-virulence activities, covered in recent review articles (10; 192). The state of the literature truly demonstrates that anti-virulence is the main category of bioactivity exerted by plant natural products, and that a vast number of different pharmacophores have been identified in this domain. This is the case, even though plants as a source of chemical diversity remain largely untapped (232). Only an estimated 15% of approximately 300,000 higher plant species have been investigated phytochemically, and only a nominal fraction of these has been investigated for anti-infective potential (233). As metabolomics has yet to enjoy widespread use in plant natural product drug discovery laboratories across the world, the promise for infection control seems even greater. Additionally, advances in bioreactor technology and metabolic engineering have and continue to improve the production, manipulation, and scientific understanding of both single molecule and synergistic mixtures of therapeutic plant natural products (220). These advances have culminated in the birth of ethnophytotechnology, defined as “the use of plant

biotechnology to improve or enhance the inherent economic or culturally valuable traits of plants as described and influenced by ethnobotany (220)."

Conclusions

We have summarized the advantages and potential that plant natural products present for anti-infective drug discovery. The field is in need of novel pharmacophores, and to this end, plant natural products represent an underinvestigated region of the chemical space where targeted exploration can be undertaken with the aid of new technologies such as metabolomics. It is important to note that while plant natural products hold such potential, synthetic approaches are being increasingly utilized to construct chemical scaffolds bearing the complexity of natural products, traversing into regions of the chemical space beyond the scope of nature (170). Within the realm of what nature can synthesize, microbial and marine natural products will continue to be studied for new chemical entities. It is ultimately this expansion into the yet underexplored chemical space where plant natural products will play a unique and critical role in the discovery of the next generation of anti-infectives.

Conflicts of interest

None.

Acknowledgements

Work in the Quave Research Group is funded by the National Institutes of Health, National Institute of Allergy and Infectious Disease (R21 AI136563, PI: CLQ). The content is solely the responsibility of the authors and does not necessarily reflect the official views of the NIH

or NIAID. The funding agency had no role in study design, data collection and analysis, decision to publish, or preparation of the manuscript. Our sincere apologies to authors, whose publications could not be cited due to the article length constraints.

APPENDIX II

Methods in the Extraction and Chemical Analysis of Medicinal Plants

This has been published in *Methods and Techniques in Ethnobiology and Ethnoecology* (2019) pp 257-283. Print ISBN: 978-1-4939-8918-8

Salam, A.; Lyles, J.; Quave, C., Methods in the Extraction and Chemical Analysis of Medicinal Plants. In *Methods in the Extraction and Chemical Analysis of Medicinal Plants*, Albuquerque, U. P.; Lucena, R. F. P. d.; Cunha, L. V. F. C. d.; Alves, R. R. N., Eds. Springer: 2019; pp 257-283.

Methods in the Extraction and Chemical Analysis of Medicinal Plants

Akram M. Salam[1], James T. Lyles[2], Cassandra L. Quave[2,3,4,5*]

[1]Molecular and Systems Pharmacology Program, Laney Graduate School, Emory University, Atlanta, GA, United States

[2]Center for the Study of Human Health, Emory University College of Arts and Sciences, Atlanta, GA, United States

[3]Department of Dermatology, Emory University School of Medicine, Atlanta, GA, United States

[4]Antibiotic Resistance Center, Emory University, Atlanta, GA, United States

[5]Emory University Herbarium, Atlanta, GA, United States

*Corresponding author: Cassandra Quave, cquave@emory.edu

Abstract

This chapter aims to give an overview of advanced techniques for the extraction, isolation, and analysis of natural products from medicinal plants. It is of great pharmacological interest to isolate and study bioactive natural products. Although sometimes the plants selected for study are chosen based on their traditional medicinal uses, this need not be the case as other attributes may justify study, such as chemical diversity and lack of previous study. Extraction techniques represent one of the earliest steps in natural products isolation, and as such can greatly impact results. Once a crude extract is obtained, compound isolation is achieved through the framework of bioassay-guided fractionation. Under this framework, chromatographic separations are used to iteratively generate fractions, each enriched with a compound or set of compounds of a certain attribute, until finally single compounds are isolated. Analysis of extracts, fractions, and single compounds is performed via spectroscopy, through which the chemical character of fractions and structural attributes of compounds of interest can be elucidated.

Keywords: extract, flash chromatography, mass spectrometry, high-performance liquid chromatography, nuclear magnetic resonance

Introduction

Extraction is the process of releasing natural products from a biomass (221). The biomass is often a pulverized plant or plant part, but may also be a preparation of a fungus or other microorganism. It is important to begin with good quality starting material that meets the standards of the World Health Organization's guidelines on Good Agricultural and Collection Practices (GACP) for medicinal plants (234). For example, collection of certain plants specimens should be avoided, such as those subjected to agrochemical runoff, those that are in close proximity to roadsides, and those that belong to threatened or endangered species. Furthermore, international collections need to incorporate consideration of appropriate collection and import/export permits and adhere to the principles of the Nagoya protocol (171). After plant collection, a chief consideration is whether to dry the plant material. Dried material lasts longer at ambient temperature and can easily be shipped without decay, though drying may result in loss of some volatile compounds. If fresh material is to be extracted, freezing may be necessary for shipping. For all collected plants, a herbarium voucher specimen must be made.

Extraction of a biomass is usually undertaken with a liquid solvent, the polarity of which being one of the key determinants of the types of natural products that migrate and dissolve into the liquid (235). Another key determinant is the length of time the biomass and solvent are in contact and the degree and type of agitation exerted. The initial extraction of a given biomass yields a crude extract, referred to as such because it is yet unrefined by chromatographic techniques. A crude extract may contain anywhere from a few to hundreds or even thousands of unique compounds and isomers. To isolate compounds from this composition, chromatographic methods are employed, such as partitioning, column

chromatography, and high performance liquid chromatography (HPLC). The goal of chromatography is the separation of compounds in a sample based on attributes such as polarity, size, and chemical functionalization (167). Fractions of a crude extract may be referred to as enriched extracts since they are enriched for chemicals with a certain set of attributes or simply “fractions”.

Extracts and isolated compounds are analyzed via spectroscopic techniques such as ultraviolet–visible spectroscopy (UV-Vis), mass spectrometry (MS) and nuclear magnetic resonance (NMR). While only mass spectrometry is capable of providing the masses of analytes, both MS and NMR can be used to elucidate the structure and connectivity of functional groups, with NMR being more capable in this respect (236). Compounds do not necessarily have to be isolated before analysis. With hyphenated techniques, separation and analysis of compounds can be coupled into one procedure (237). This has made the quick identification of natural products possible and has opened many doors to the analysis of complex chemical samples. Nevertheless, the vast majority of natural products isolation and structural elucidation is performed without the aid of these hyphenated techniques, often due to the expense of the instrumentation. **Fig. A2.1** provides an example of a general workflow for identifying single compounds from plant material.

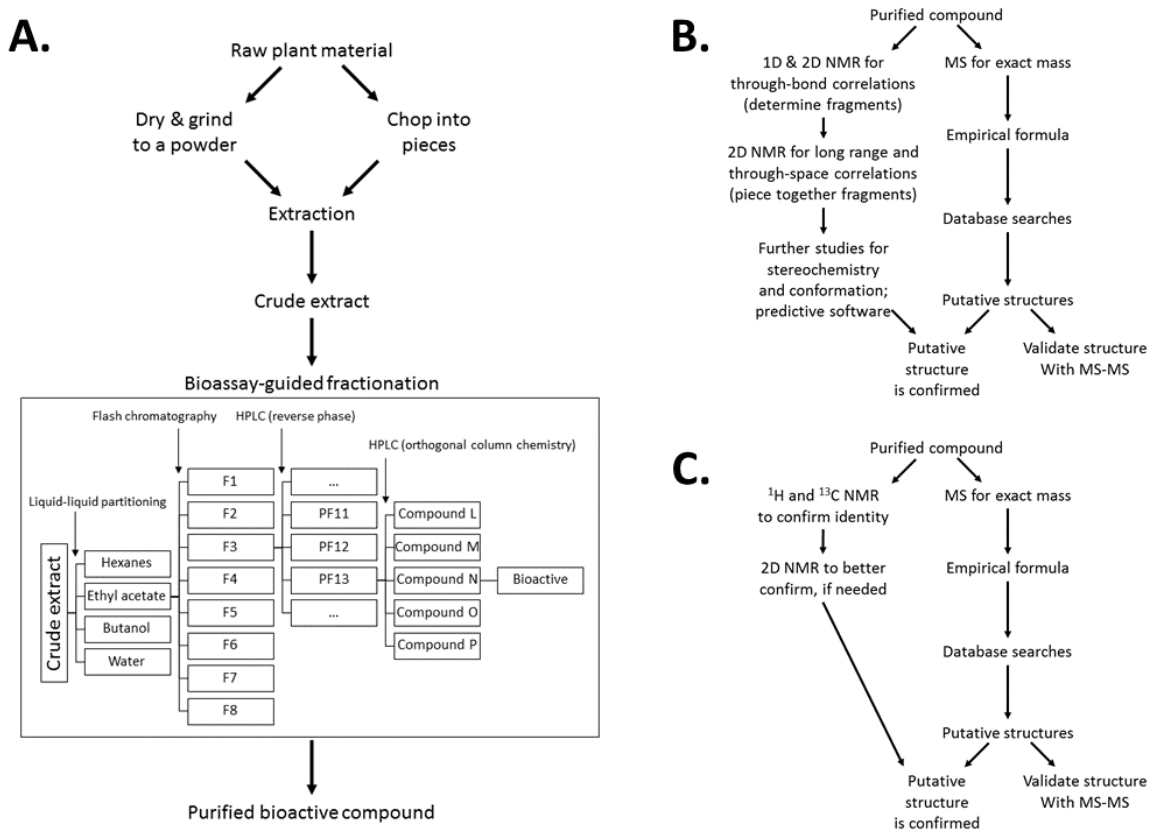

Fig. A2.1. Example of a general workflow for the identification of natural products from plants. (A) Workflow for isolating single compounds from plant material. In the bioassay-guided fractionation box, the vertical arrows indicate examples of chromatographic methods employed to obtain further fractions of a sample. For example, F1-F8 are example names of fractions obtained from the flash chromatography of the ethyl acetate partition of the crude extract. (B) Workflow for the identification of a previously undiscovered compound. (C) Workflow for the identification of a previously discovered compound.

Extraction Techniques

Maceration and decoction

Maceration is a simple and widely used extraction technique in which pulverized biomass is left to soak in a solvent in a closed container at ambient temperature (167). Stirring may be incorporated to speed up the extraction process. Macerations are typically run for at least three days (238). Eventually, the concentration of compounds in the solvent reach equilibrium with the concentration of compounds in the biomass and the extraction effectively stops (167). Maceration is usually followed by filtration, where the solvent containing the extracted compounds is completely separated from the extracted biomass (marc). In cases where the pulverized biomass is very fine and easily clogs up filter paper, centrifugation is performed beforehand to force the biomass to the bottom of the container prior to decanting for filtration. Often, a maceration is followed up by a second or more macerations, where all residual biomass is returned to its container and fresh solvent is added. Macerations are often used in traditional medicinal practices for chemical extraction, as are decoctions, where the biomass of interest is immersed in boiling water throughout the boiling process (239). Decoctions are usually performed for 15-20 minutes, although different types of decoctions can run for much longer (239; 240). An infusion is different from a decoction, where boiling solvent, also usually water, is poured onto the biomass. For the purposes of analyzing plants used in traditional medicine, the traditional extraction technique is often replicated so as to most accurately assess the traditional preparations under study.

Reflux, Soxhlet extraction, and percolation

Reflux extraction is a continuous solvent extraction usually performed in a round bottomed flask or boiling flask containing both the extracting solvent and the material undergoing extraction (7). It utilizes elevated, controlled temperatures at ambient pressure to increase extraction efficiency. As such, reflux is a heated extraction technique, and thermolabile components are at risk of degradation. The elevated temperatures result in reflux and gradual evaporation of the extracting solvent; as such, the round bottomed flask neck is connected to a condenser that preserves the volume of extracting solvent in the system. Common solvents for natural products reflux extractions include: ethanol, methanol, and ethyl acetate; eight hours is a common extraction time.

Soxhlet extraction is also a continuous solvent extraction, but the extracting solvent and material are placed in separate compartments (221). The extracting solvent is present in a round flask at the base and is heated to a boil. The Soxhlet apparatus is placed into the mouth of the flask and allows the vapors of the solvent to be condensed by a condenser above and the now cold solvent to drip into the thimble, where the material is stored. Drops of solvent gradually fill the thimble until it automatically siphons back down to the round flask, carrying extracted compounds with it. This way, as with reflux extraction, the total volume of extracting solvent is preserved. Unlike reflux extraction, Soxhlet is a cold extraction technique because it is the condensed solvent that contacts the material. After siphoning, however, the extract is transferred into the solvent being heated, which may lead to degradation of thermolabile components. For more reading on Soxhlet, evolutions thereof, and applications, a review has been written on the topic (241). Commonly, extraction time is determined by the number of cycles (fill/siphon) completed per hour, and 4-6 cycles per hour are often observed. A total of 72 cycles is often used as a benchmark, though this can be shortened, especially if it is a fraction of a crude extract that is being extracted.

A similar technique to the reflux and Soxhlet extractions is percolation, which is performed using a percolator, an apparatus similar to a separatory funnel (242). The material to be extracted sits above the drain valve, sometimes packed in between filters or sometimes isolated from the valve by a cotton plug. The material is first soaked with extraction solvent, and then additional solvent is poured so as to allow the extract to percolate drop-wise through the drain valve (221). Successive percolations can be performed for exhaustive extraction. The main drawback of a percolation extraction is high consumption of solvent and time due to lack of agitation and dependence on gravity for flow. In order to reduce the overall solvent consumption, the extract can be reused in subsequent percolations, rather than fresh solvent. In order to have a successful percolation, the particle size of the ground material must be coarser than material used in other extraction techniques.

Ultrasound-assisted extraction

Ultrasound-assisted extraction (UAE) is an extraction technique where, typically in a maceration-type setup, ultrasound waves are used to assist in the extraction process (243). The employment of ultrasound reduces the extraction time to minutes, reduces the volume of solvent needed, and consumes less energy as compared to other extraction techniques. Commonly used UAE systems include: Erlenmeyer flask in an ultrasound bath, an ultrasound reactor with stirring, and use of an ultrasound probe. For the extraction of chemicals from plant material, the ultrasound bath is preferred, though high power ultrasonic probes are preferred for most other applications. In both systems, transducers serve as the source of ultrasound waves. A number of mechanisms have been identified as aiding in the effectiveness of ultrasound to increase extraction efficiency: fragmentation, erosion,

sonocapillary effect, sonoporation, local shear stress and destruction-detexturation of plant structures. These mechanisms, as well as parameters that affect the extraction process, have been thoroughly discussed in a recent review of the field (243).

Essential oil extraction

An essential oil is a concentrated hydrophobic liquid obtained from a plant that contains the volatile aroma compounds (e.g. terpenoids) that yield its characteristic fragrance. The most common method of essential oil extraction is steam distillation, where steam from boiling water passes through the plant material of interest, releases its essential oil, carries it through a condenser, after which the water and oil deposit and form two layers that can be separated (244). Hydro-distillation is also common and follows the same principle, except that the plant material is placed in the boiling water. Other methods of essential oil extraction are discussed in a number of review articles (244; 245). Of note, enfleurage, specifically the hot enfleurage, is considered the oldest known procedure for extracting essential oils. In this technique, solid odorless fats are heated and stirred with plant material, with spent plant material removed and fresh material added repeatedly until the fat is satisfactorily saturated with fragrance. In the cold enfleurage, plant material is placed on solid, odorless fat in a chassis, and diffusion of essential oils into the fat is allowed to take place over the course of 1-3 days. Fresh plant material is repetitively replenished until saturation is achieved.

Supercritical fluid extraction

Supercritical fluid extraction (SFE) is a chemical extraction process in which the extracting solvent is a supercritical fluid (SCF) (246). An SCF is any substance at a temperature and pressure above its critical point. As a result, an SCF has no distinct liquid or gas phase but is rather in a state between these two extremes, able to both effuse through solids (like a gas) and dissolve compounds (like a liquid). CO_2 is the most widely used SCF for extraction, usually employed for large-scale decaffeination of coffee beans (247). A dedicated instrument is required to perform SFE. The instrument first withdraws liquid CO_2 from a CO_2 tank, heats and pressurizes it beyond the critical temperature (31 °C) and pressure (74 bar), and then either flows the supercritical CO_2 through the biomass to be extracted or fills a vessel containing the biomass for a static extraction. After a predetermined contact period, the instrument separates the extract from the now gaseous CO_2, condenses the gas back to its liquid form, and returns it to the storage tank. Alternatively, the used CO_2 can be vented, leaving the extract behind in a collection vessel.

There are some limitations to SFE. CO_2 is a poor solvent for polar molecules due to its hydrophobicity. This can be somewhat circumvented by pumping co-solvents such as methanol through the biomass along with the supercritical CO_2, thus increasing the range of compounds extracted. On the other hand, this limitation gives SFE a niche in the extraction and analysis of hydrophobic compounds such as essential oils, with several reviews written on the topic (248; 249). Another limitation is cost, which primarily arises from the need to pressurize the CO_2. SFE is often used when extraction selectivity and speed are very important. Because different co-solvents can be used and the properties of an SCF can be adjusted by changing the temperature and pressure, selective extractions can be performed. For instance, it was found that by varying temperature, pressure, and co-solvents in an extraction of *Plantago major*, selective enrichment of triterpenic acids, α-LNA, and oleanolic

and ursolic acids could be achieved (250). Additionally, an SFE can be completed in relatively short time due to the enhanced diffusion properties of SCFs as compared to liquids. Another advantage of utilizing SCFs is that they largely circumvent oxidizing and thermally degrading extracted compounds. They are also less costly to dispose of (e.g. CO_2 can be released into the air) and are generally non-toxic, contaminant-free, and inexpensive. A commonly cited advantage of SFE its environmental friendliness. However, in applications that require the full range of polar compounds to be extracted, substantial amount of modifier such as 30% methanol must be used, negating this benefit (242).

Accelerated solvent extraction

Accelerated solvent extraction (ASE) is a fully automated rapid extraction technique that enjoys widespread use due to rapid extraction times requiring little solvent. The technique was developed by Dionex Corporation and introduced in 1995, and they remain the sole manufacturer of ASE equipment (251). It employs common solvents at elevated temperature and pressure, which increases extraction efficiency. Because the temperatures used are usually above the boiling point of the solvent, the increased pressure (1,000-2,000 psi) functions to maintain the liquid state. Commonly used organic solvents include *n*-hexane, dichloromethane, acetone, and methanol. ASE is capable of extraction for sample sizes of 100 grams or less in minutes while consuming very small volumes of solvent. As a result, the cost per sample tends to be lower than that of other extraction techniques. A main advantage of ASE is that it aims to maximize the extraction of compounds present at low concentrations in the matrix, and it generally is an exhaustive extraction technique. A disadvantage is the increased likelihood of thermal degradation of susceptible compounds. While most ASE

extractions utilize a temperature between 75–125°C, 100°C is the most commonly setting chosen. Temperature is the dominant factor in ASE's exhaustive extraction, with selectivity tunable by lowering extracting temperature and choosing an appropriate solvent. ASE is increasingly used in the extraction of contaminants in foods for analysis, with a review having been written on the topic, giving a deeper overview of the technique (252).

Microwave-Assisted Extraction

Microwave-Assisted Extraction (MAE) is a rapid extraction technique in which solvent extraction is supported by heating with microwaves (253). As in ASE, the heating yields the benefit of increased extraction efficiency. This brings the advantage of lowering volume of solvent and cost, but also the limitation of thermal degradation of susceptible compounds. MAE can be performed in ways as simple as inserting a maceration flask into a microwave oven to ways as complex as utilizing a dedicated instrument with a variety of controls and vessel options. Many different types of MAE instruments have been developed. For high-throughput sample preparation, for example, an instrument may enclose numerous maceration capsules in a microwave box for heating. MAE can also be used to assist reflux and Soxhlet extractions by physically placing the biomass-containing piece of glassware in a special-made microwave unit (254; 255). There are several examples of the literature of natural products having been extracted more efficiently from a biomass of interest via MAE, such as luteolin and apigenin from tree peony pod and fucoidan from marine algae (256; 257).

Extraction efficiencies

In order to provide insight into the relative extraction efficiencies of some of the most popular extraction methods, a few examples from the literature are given where extraction techniques have been optimized. Interestingly, most studies of comparative extraction efficiencies study the extraction of pollutants rather than natural products, though conclusions may be drawn from these studies. Here, Soxhlet extraction has been considered as the reference. ASE and Soxhlet extraction have been found to extract volatile and phenolic compounds with higher efficiency than SFE from mint (Lamiaceae) species (258). Soxhlet was also found to achieve the higher extraction yield of terpenoids and sterols from tobacco than ASE, though the latter was faster and used less solvent (259). However, for the extraction of polycyclic aromatic hydrocarbons and organochlorine pesticides from soils, Soxhlet and MAE were found to have similar efficiencies, though ASE proved more efficient than the two, and both MAE and ASE consumed less solvent and time (260). In a study on the extraction of twelve polychlorinated biphenyls (PCBs) from algae samples, Soxhlet and SFE were found to have same extraction efficiencies for most PCBs, though SFE had the advantage of leading to the detection all PCBs at lower concentrations and reducing extraction time and solvent consumption (261). In a study on the extraction of N-nitrosamines and aromatic amines from various soil matrices, MAE was found to be superior to Soxhlet while also requiring just 3 minutes for extraction (262). It is the opinion of the authors based on the literature and experience that Soxhlet is often capable of extraction efficiencies similar to ASE and MAE. However, other extraction methodologies are often chosen for increased throughput, reduced solvent usage, or available processing time. A comparison of other attributes of extractions techniques is summarized in **Table A2.1**. The following section will

discuss chromatographic techniques, and a comparison of their attributes is summarized in **Table A2.2**.

Table A2.1. Comparison of attributes of different extraction methods.

	Maceration	Decoction	Infusion	Reflux	Soxhlet	Percolation	UAE	SFE	ASE	MAE
Often takes < 1 hour		✓	✓				✓	✓	✓	✓
Hot extraction		✓	✓	✓					✓	✓
Requires little solvent		✓	✓	✓	✓		✓	✓	✓	✓
Limited risk of compound degradation	✓					✓	✓	✓		
Cold extraction					✓					
Exhaustive in most cases	✓			✓	✓		✓		✓	✓
Requires instrumentation								✓	✓	✓

Table A2.2. Comparison of attributes of different chromatographic methods.

	Flash	HPLC	GC	SFC
Can be analytical or preparative		✓	✓	✓
More amenable to larger sample sizes	✓	✓		
More amenable to compound isolation	✓	✓	✓	✓
Variable separation chemistries	✓	✓		✓

Chromatographic techniques

Flash chromatography

Flash chromatography is a type of preparative (as opposed to analytical) liquid chromatography used for the separation of organic compounds, which is widely used for natural product extract separation. While flash chromatography began as a low-pressure technique, now vacuum pressure or, more often, pumps are employed to achieve medium pressures for faster flow rates and quicker separation (263). Numerous types of columns (and hence separation methods) exist. Although columns can be packed in the laboratory, one of the key advantages to flash chromatography is that columns can be purchased as pre-packed, one-time use columns. One of the most commonly used columns is packed with a silica adsorbent with a particle size usually between 40-60 μm (264). Particle shapes are often irregular, and the particle size distribution in any particular column tends to be relatively wide.

The smaller the silica particle size, the more tightly packed a column is, the more backpressure builds in response to a given flow rate of a mobile phase. As compared to high-performance liquid chromatography (HPLC), flash chromatography uses larger particle sizes and thus generates lower backpressures than HPLC. Flash chromatography is often performed on a flash instrument, which not only pumps the mobile phase but also detects column eluate, usually via a UV-Vis absorbance detector and sometimes with an evaporative light scattering detector (ELSD) and produces a chromatogram of the run. In addition to normal and reverse phase columns, amine, cyano, diol, ion exchange, and many more types of columns are available. **Fig. A2.2A** shows examples of different flash columns. Flash

chromatography has been used extensively as a step in bioassay-guided fractionation and to isolate single compounds (8; 265-268). Given the importance of flash chromatography as a

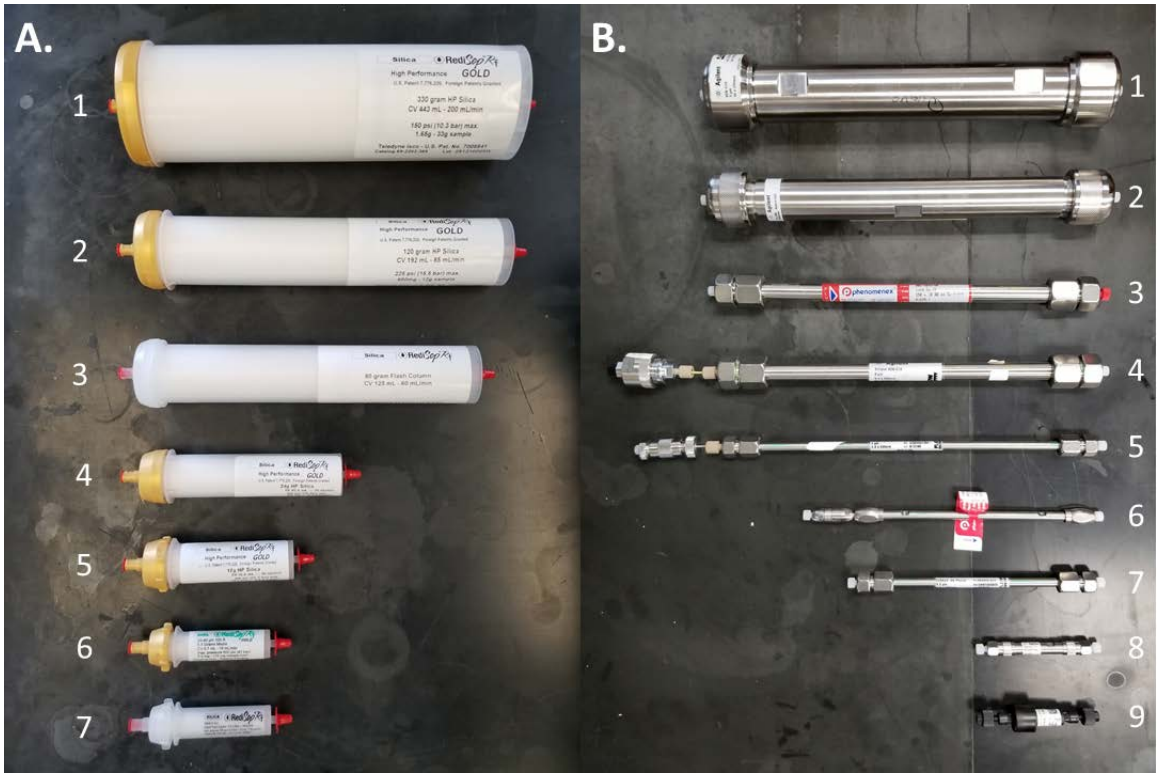

Fig. A2.2. Examples of column employed for flash chromatography and HPLC. (A) Commercially-available Teledyne Isco flash columns arranged from high to low (1-7) loading capacities ranging from 33 g to 5.5 mg. Most of the columns are silica columns; column 6 is a diol column. (B) HPLC columns arranged from large to small (1-9) sizes ranging from 30 x 250 mm to 6.4 x 30 mm. Columns 1 and 2 are preparative columns, 3 and 4 are semi-preparative, and the rest are analytical. Columns 4 and 5 are fitted with compatible guard columns. Most of the columns are C-18 columns, and particle sizes range from 2.6-5 µm. Columns 3 is a C-5 column, while columns 7 and 9 phenyl columns.

separation technique, efforts have been made to construct flash apparatuses with inexpensive setup costs (269).

High-performance liquid chromatography (HPLC)

HPLC is a type of liquid chromatography that can be used for both analytical and preparative purposes. Analytical HPLC and larger scale preparative HPLC each require separate, dedicated instruments, although hybrid systems are available, most commonly for analytical and semi-preparative HPLC. As compared to flash chromatography, HPLC columns contain silica with smaller particle sizes ranging from 2 μm to 50 μm (264). Additionally, particles are spherical in shape, and in any given column the particle size distribution is narrow. Particle size plays a role in resolution. Consider the fundamental resolution equation

$$R = \frac{\sqrt{N}}{4} \times \frac{\alpha - 1}{\alpha} \times \frac{K'}{1+K}$$

where N = efficiency, α = efficiency, and K = retention capacity. Since separation efficiency increases with decreased particle size, HPLC has the advantage of higher efficiency as compared to flash chromatography, allowing for higher resolutions to be reached. This concept is modeled by the theoretical plate model of chromatography, which supposes that a chromatographic column consists of a large number of imaginary separate layers called theoretical plates (N). As such, decreased particle size results in decreased height equivalent to a theoretical plate; thus, more theoretical plates are present in a given column length, increasing separation efficiency.

Modern HPLC instruments nearly always include a UV/Vis or a photodiode array (PDA) detector as a spectroscopic component for the characterization of column eluate. For natural product extracts, analytical HPLC is used specifically for chemical characterization, where

chromatograms are compared for different runs, be they same-extract batches, different extracts, chemical standards, etc. This function utilizes small amounts of extract or standards; therefore, column eluate is usually not collected because it amounts to very little material. In preparative HPLC, on the other hand, column eluate is collected because the purpose of the separation is the production of large amounts of extract fractions. Therefore, column length and especially diameter for preparative HPLC are larger than those for analytical HPLC (typically 2.1–4.6 mm diameter, 30–250 mm length), as these attributes yield higher column throughput and capacity. Column particle sizes are often slightly larger than those of analytical HPLC columns, where resolution is more highly emphasized. Beyond these factors, several differences between analytical and preparative HPLC result in the need for separate instrumentation for each. Chief among these differences is the capacity to accommodate higher flow rates in preparative HPLC while maintaining an acceptable backpressure that will not damage the instrument of the chromatographic column.

It is possible to use an analytical HPLC instrument for fraction production; this is often called semi-preparative HPLC. This usually calls for a larger analytical column – still much smaller than preparative columns – and many more runs are required as compared to preparative HPLC to produce a given amount of a fraction. Additionally, an even higher resolution form of analytical HPLC is UPLC (ultra-performance liquid chromatography). UPLC is chiefly characterized by even smaller particles sizes (sub 2 um), resulting in a higher theoretical plate count and thus increased separation efficiency. Because of this, UPLC columns sizes are often shorter to reduce run times, and UPLC instruments require the capacity to accommodate even higher backpressures. Numerous types of columns exist for all HPLC instruments. In addition to normal phase and reverse phase columns, there are size-exclusion, ion-exchange, chiral, and bioaffinity columns, among many others. **Fig. A2.2B** shows

examples of different HPLC columns. Columns may be fitted with a guard column on the inlet end to protect them from particulate matter in a sample by trapping it in the sacrificial guard column. Besides the column, the schematic of a HPLC instrument usually consists of a degasser, sampler, pumps, and a detector, usually a UV/Vis or a photodiode array (PDA) detector.

There are established methods for the separation of compounds for botanicals and herbs of commerce. Refer to pharmacopoeia of the United States (270), Europe (271), and China (272) for methods on specific materials.

Gas chromatography (GC)

GC is a group of analytical separation techniques used to separate volatile compounds in the gas phase (273). While the success of GC has largely been associated with analytical purposes, GC can be successfully used for preparative purposes as well (274). Unlike liquid chromatography where the sample, dissolved in liquid, is pushed by a liquid mobile phase through a packed column, in GC the sample, also dissolved in liquid, is vaporized and pushed by an inert gas mobile phase through a heated column, usually hollow. Separation occurs only due to the interaction of the sample components with the coating inside the hollow column (the stationary phase). Because the mobile phase is inert, separation is not due to differential chemical interactions with the mobile phase (none occur). The stationary phase can be either a liquid on an inert support (gas-liquid chromatography) or, more commonly, a solid adsorbent (gas-solid chromatography). A very typical GC column is a fused-silica capilllary of varying length from 5 to 100 m, in which the inner surface of a silica capillary is coated with one of several polymer stationary phases and the outside of the capillary is coated

with a polyamide polymer to add strength. A review of many of the types of GC columns describes them in detail (275). Usually, non-polar samples are analyzed by GC, interacting with a similar stationary phase to achieve sufficient separation. As such, in the realm of natural products, GC is most adept to separation of components of non-polar, volatile samples such as essential oils.

The schematic of a GC instrument begins with a source of carrier gas connected to a flow controller (273). The most common carrier gases are helium, nitrogen, argon, and hydrogen, but the exact gas to use is usually determined by the detector being employed. Carrier gas then flows to the column inlet (or injector), which provides the means to introduce a sample into a continuous flow of carrier gas. The inlet is a piece of hardware attached to the column head. The most common inlet type is an S/SL (split/splitless) injector, where a small, heated chamber facilitates volatilization of the sample solution. Once the sample is swept by the carrier gas, it flows through a column heated by an oven, after which the sample finally hits a detector. The flame ionization detector (FID) and the thermal conductivity detector (TCD) are the most typically employed detectors. Both can accommodate a wide range of sample concentrations and are sensitive to a wide range of components. Other detectors have a shorter range of usability but are used when dealing with specific types of substances.

Supercritical fluid chromatography

Supercritical fluid chromatography (SFC) is very similar to LC, where the defining feature is that the mobile phase is a supercritical fluid, usually CO_2. The instrumentation is nearly identical to that of LC, and there are both analytical and preparative instruments. The pumping system consists of two pumps: one delivers supercritical CO_2, and the other delivers

a co-solvent, such as a simple alcohol, acetonitrile, chloroform, or ethyl acetate. The co-solvent and CO_2 are homogenized by a static mixer, and the mobile phase is delivered to the autosampler, equipped with an injection value for delivery to the front of the chromatographic column. The columns are present in an oven to maintain a temperature of above 40° C for supercritical conditions to be achieved with CO_2. Column eluate then reaches the detector. Until this point, the instrumentation is almost identical to that of liquid chromatography. An additional component is the automated backpressure regulator, which provides a control parameter not found in LC – pressure. In terms of operation, SFC is as simple and robust as LC, and fraction collecting is even easier due to the evaporation of the CO_2 component of the mobile phase. For natural products, supercritical fluid chromatography is mainly utilized for the separation of non-polar compounds such as carotenoids, fatty acids, and terpenes, though it is has also been successfully used with more polar natural products (276-279).

Prefractionation

Of great importance, flash chromatography and HPLC are often employed in the pre-fractionation of crude extracts so as to remove chemicals unlikely to be pharmacologically active prior to screening (165; 166; 280-289). Pre-fractionation prior to high throughput screening (HTS) results in higher hit rates, such as in screening campaigns that revealed pharmacological activity of fractions where the crude extracts were previously identified as inactive (165; 166). A review has been written with an expanded discussion on this topic and the place of natural products in drug discovery (159). Pre-fractionation is also used to “clean up” a fraction or extract so as to remove compounds that may bind to a stationary phase to be

used for subsequent chromatographic separation (290). In addition to chromatographic methods of pre-fractionation, a manual method of liquid-liquid partitioning is commonly employed prior to flash chromatography or HPLC. The extract is suspended in a solvent (e.g., water) and successively partitioned against solvents of differing polarity (e.g., hexanes, ethyl acetate, n-butanol) using a separatory funnel apparatus to create two distinct layers of solvent and extract constituents at each step. The advantage of this method is avoidance of loss of compounds to the column matrix, but a disadvantage is the manual and time-consuming nature of the technique.

Solid phase extraction

Solid phase extraction (SPE) is a sample preparation technique where compounds in a liquid mixture are separated from each other based on chemical and physical characteristics. The most common SPE format consists of a syringe cartridge that contains 50 mg to 20 g of stationary phase (291). After pouring the sample solution into the cartridge, a plunger or vacuum can be used to push it through the stationary phase. Any type of stationary phase can be used, except those used for exclusion chromatography. As such, SPE allows for rapid, simple, and reproducible analyte purification. While liquid-liquid partitioning can be used for similar purposes, it is more time consuming and emulsions may form between different liquid phases. SPE is also often employed for analyte concentration. Very commonly, a stationary phase is selected such that it retains the analytes of interest; subsequently, the cartridge is rinsed with a small volume of a strong solvent to elute the analytes (292). Opposite to this retentive mode, SPE can be utilized in non-retentive mode, where it is the desired solutes that pass through the stationary phase (291). When SPE is used to prepare a sample prior to

HPLC, the need for a guard column may be negated (290). SPE can also serve as a concentration step for compounds which are retained; a relatively large volume containing a small amount of the analytes of interest can be loaded onto the column. Then the analytes are eluted with a small volume of very strong solvent, thus increasing their concentration for analysis without the time required to dry down the initial extraction solvents.

Spectroscopic Techniques

Mass spectrometry

Mass spectrometry (MS) is an analytical technique for determining the mass of individual compounds that comprise a given sample. This is achieved through the ionization of chemical species and their sorting based on their mass-to-charge ratio (*m/z*). Solids, liquids, or gasses may be analyzed by mass spectrometery. There are three main components of a mass spectrometer: ion source, mass analyzer, and detector. The ion source ionizes the chemical species present in the sample. For gaseous samples, the most common ionization techniques are electron ionization and chemical ionization, whereas for liquid samples, the most common are electrospray ionization (ESI) and atmospheric-pressure chemical ionization (APCI). For solid samples and some proteins, matrix-assisted laser desorption/ionization (MALDI) is employed. In ESI, a high voltage is applied to a liquid being sprayed in order to create an aerosol of ions, whereas in APCI the nebulized effluent passes over a coronal discharge needle and as the liquid evaporates due to elevated temperature the remaining compounds acquire a charge. On the other hand, there is an array of ambient ionization techniques, where ions are produced outside of the mass spectrometer in ambient conditions from samples that require little to no pretreatment (293). Since the development of the first reported technique, desorption electrospray ionization (DESI), dozens more have been developed (294).

After ionization, ions are transported by magnetic or electric fields to the mass analyzer, which separates ions based on their *m/z*. The time-of-flight (TOF) analyzer is a mass analyzer that uses an electric field to accelerate ions toward a detector, measuring the time they take to reach it. Velocities of the ions depend solely on their masses due to identical charge, which

tends to make all kinetic energies constant. As such, ions with lower masses will travel faster and reach the detector sooner. Quadrupole mass analyzers utilize a quadrupole field created between 4 parallel rods. Oscillating electrical fields produced by the rods stabilize or perturb the paths of ions passing such that, at any time, only the ions in a certain range of *m/z* are passed through. The quadrupole ion trap is very similar, except that the ions are trapped and sequentially ejected toward the detector. The state-of-the-art of mass analyzers is the Orbitrap, where ions are electrostatically trapped in an orbit around a central, spindle-shaped electrode such that they also oscillate the electrode's long axis. Through detector plates, the instrument records image currents generated by the oscillations, the frequencies of which depend on the *m/z* values of the ions. Fourier transformation is used to translate the image currents to mass spectra.

Imaging mass spectrometry (IMS) is a powerful method for the analysis of chemicals in a biological sample of interest. IMS was first popularized by the MALDI ionization method (295) and it can be used on a tissue section, bacterial colony, or even a whole organism. The sample is mounted on a conductive support, a thin layer of matrix is applied, and the sample is positioned on a stage in a vacuum (296). The surface of the sample is scanned by a laser, ionizing compounds, and then a 2D image of the sample is constructed with mass data. 3D images can also be constructed using cross-sections of samples. MALDI is the most commonly used ionization method for imaging, and it has the advantage of allowing for the detection of molecules in a wide *m/z* range. What may be the key shortcomings of using MALDI in natural product research is interference by low mass-to-charge molecules present in the MALDI matrix as well as reproducibility, contingent on the quality of the sample (297). Ambient ionization methods such as DESI circumvent these shortcomings due to the ability to ionize samples under ambient conditions and the lack of sample preparation (296).

Tandem mass spectrometry (MS/MS) is an important analytical tool in the field of natural products research. After a first stage of MS where, as described above, ions are formed and separated by their *m/z* ratio, a second stage of MS is performed. In this second stage, ions of a certain *m/z* are fragmented. Each molecule of an individual compound always fragments into a characteristic pattern that depends on the fragmentation technique employed, allowing mass spectra to be used as "fingerprints" for identifying compounds. Indeed, functional groups such as alkyl chains may be structurally elucidated based on fragmentation of the group specific to its chemical characteristics and the fragmentation technique. Throughout the 1960s to 1980s hundreds of proposed structures were determined for natural products, many identified due in part to fragmentation studies (298). MS/MS is also the backbone of molecular networking, an informatics approach used for both dereplication and identification of structural analogs (299-301). Through this approach, all MS/MS data in an experiment is mapped according to mass spectral structural space, resulting in the clustering of molecular families with related MS/MS spectra.

Nuclear Magnetic Resonance spectroscopy

Nuclear Magnetic Resonance (NMR) spectroscopy, or simply NMR, is a spectroscopic technique for observing local magnetic fields around atomic nuclei. Because these fields are highly unique to individual atoms in any given compound, NMR is primarily employed for the elucidation of chemical structures in natural products research. Over the past several decades, improvements to NMR hardware and methodology have reduced the amount of sample required for analysis from tens of milligrams to often under 1 mg. A NMR experiment operates by first applying a constant magnetic field (B_0) to the sample such that

the magnetic nuclear spins align with B_0 either with the field (low-energy state) or 180° against the field (high-energy state). Because resolution depends directly on magnetic field strength, modern NMR spectrometers are fitted with a very powerful and large liquid helium-cooled superconducting magnet. Second, radio frequency (RF) pulses are used to perturb the alignment in order to obtain a nuclear magnetic resonance response, also called a free induction decay (FID). Following the pulse, the population nuclei in the sample are excited and flip orientations. This flipping of energy states produces a very weak voltage, which is detectable in sensitive radio receivers surrounding the sample tube. This signal is then digitized and Fourier transformed to yield a frequency spectrum of the NMR signal, or the NMR spectrum.

This nuclear magnetic resonance phenomenon is commonly used to study ^{1}H and ^{13}C atoms in a compound in order to determine each of their environments and subsequently elucidate the compound's structure. These isotopes, respectively present in 99.98% and 1.1% abundance, are studied because they exhibit nuclear spin and are thus detectable by NMR. The general workflow for determining the structure of a natural product often begins by obtaining a proton (^{1}H) spectrum and carbon-13 (^{13}C) spectrum. For organic compounds, the ^{1}H NMR spectrum is characterized by peaks representing at least one proton each, each having a unique chemical shift in the range +14 to -4 ppm, indicating local electronegativity. Peaks containing multiple peaks represent the spin-spin coupling between protons, and the integration curve for each peak relative to the others reflects the number of protons represented by that peak. The ^{13}C spectrum is analogous to ^{1}H spectrum in that it allows the identification of carbon atoms, though ^{13}C chemical shifts fall along a much larger range than for ^{1}H. This 1D data is then combined with additional data from 2D experiments, obtained from spectra such as the ^{1}H-^{1}H correlation (COSY) spectrum and the one-bond ^{13}C-^{1}H

correlation (e.g. HMQC) spectrum, to determine the structures of fragments of a compound. These fragments are then tied together using information from the long-range ^{13}C-^{1}H correlation (HMBC) spectrum. Many different pulse sequences for 2D NMR have been developed to obtain various correlations. It is necessary to combine a variety of NMR methods with calculations of the energies of different conformations, and techniques for doing so have been thoroughly reviewed (229). Here, we give an overview of the most commonly employed 2D NMR techniques.

COSY (Correlation Spectroscopy) provides correlation data for all coupled protons (^{1}H-^{1}H correlation). This data gives unequivocal proof of proton assignments. DEPT (Distortionless Enhancement of Polarization Transfer) determines the number of hydrogen atoms bonded to each carbon in the molecule, and thus differentiates between primary, secondary and tertiary carbon atoms. HETCOR (Heteronuclear Correlation spectroscopy) reveals all coupling of protons and attached carbons (^{1}H-^{13}C correlation), complementing DEPT, but is less frequently used. HMQC (Heteronuclear Multiple Quantum Coherence) gives the same results as HETCOR, but is much more efficient in terms of sensitivity and speed and has almost completely replaced the technique. HMBC (Heteronuclear Multiple Bond Correlation) allows long-range correlation of protons and attached carbons (^{1}H-^{13}C correlation) over 2-3 bonds. It is important to note that all the aforementioned 2D techniques examine through-bond correlations. NOESY (Nuclear Overhauser Effect Spectroscopy) is unique in that, instead of determining through-bond relationships, the technique determines through-space NOE relationships. The NOE is the transfer of energy from one nucleus to another (usually protons) when the first nucleus relaxes from an excited nuclear spin state to its ground nuclear spin state. The NOESY spectrum reveals which protons are close enough to each

other to transfer energy this way. NOE is not observed beyond roughly 5 Angstroms, and is usually observed within 3 Angstroms.

In addition to NMR's utility in the determination of chemical structures, it can also be employed for spectral fingerprinting of complex mixtures, such as a natural product extract or fraction. Due to the NMR's inherent reproducibility the instrument can provide rapid analysis of an extract. This data can be prepared to a previously prepared data set to determine if the material is the same as other batches or lots of the same material. It can also be employed to determine if a sample is indeed authentic or adulterated. The limitation of these analyses is based on the diversity and depth of the samples used for the training set to create the model of what is an "authentic sample". Nevertheless, given a robust enough set of authentic samples NMR fingerprinting is an extremely powerful tool for determining batch-to-batch consistency or adulteration of raw materials. Several reviews have discussed the details of these techniques (302; 303).

Hyphenated techniques

When two or more different analytical techniques are coupled via a proper interface, a hyphenated technique has been set (237). Most commonly, chromatographic techniques are coupled to spectroscopic techniques, with the benefit of rapid identification of natural products directly from plant and marine extracts or fractions without the necessity of isolation. For example, HPLC is often coupled to MS to make HPLC-MS. In this case, the compounds that comprise a given sample are separated over time by HPLC and then introduced into an MS, yielding mass data of the HPLC eluate over time. This way, separation and detection are performed via one technique. The most common separation

techniques that see hyphenated use are HPLC and GC, whereas the most common spectroscopy techniques are MS and NMR. UV detection is built into most automated chromatographic techniques and is not considered a standalone spectroscopic technique here. The ability to rapidly identify compounds allows for dereplication of natural products, metabolomics studies, chemotaxonomic studies, chemical fingerprinting, quality control of extracts, and many other studies. We will discuss dereplication here and metabolomics in the next section.

Dereplication is the process of identifying compounds for which the structure is already known (304). It is an integral part of natural products discovery, as it ensures that time and resources are not wasted toward elucidating structures of compounds that are already known. Most commonly, LC-MS is utilized to analyze crude extracts and fractions thereof to identify the masses of all constituents. These mass values are then screened against databases in order to identify putative chemical formulae and structures for the compounds. In bioassay-guided fraction studies, bioactive fractions are analyzed as such to determine whether active fractions contain previously-identified compounds with the known therapeutic activity of interest. Some of the most commonly consulted databases include Scifinder (305), Dictionary of Natural Products (306), NAPRALERT (307), Global Natural Products Social Molecular Network (308), and MarinLit (309). In microbial dereplication specifically, it is highly desirable to identify microbial strains capable of producing novel chemistries. To this extent, LC-MS data is often analyzed by principle component analysis or other multi-variate methods to identify strains that synthesize molecules most different from where the rest of the strains cluster. There has also been interest in the field of natural product peptides to develop informatics tools to predict fragmentation data of known structures. This knowledge would

help find matches with experimental fragmentation data, further aiding in dereplication (310-313).

While LC-MS enjoys an important role in natural products discovery, LC-NMR has proved less useful (229). Whereas MS is capable of detecting the masses of LC eluates almost instantaneously during the course of continuous flow, NMR is capable of no more than obtaining ^{1}H spectra, which takes several seconds. Additionally, LC-NMR requires either the use of costly deuterated solvents or the use of solvent peak suppression, which could result in loss of sample signals. To circumvent the first limitation, either (i) a stopped flow mode is employed where a valve stops elution when analyte reaches the flow cell volume of the rf coil, or (ii) without interrupting the chromatographic run, a loop-storage mode is employed, where fractions are stored in individual capillary loops for later NMR analysis (314). In both cases, analyte can be subjected to NMR longer to achieve adequate data acquisition times for less abundant material and for more time consuming sequences such as ^{13}C NMR. To further improve NMR detection after LC, fractions can be prepared for NMR by solid phase extraction (SPE), concentrating them into an appropriate deuterated solvent prior to analysis. Indeed, numerous laboratories have had success with automated LC-SPE-NMR for the identification of natural products (315; 316). MS can be coupled to this hyphenated technique via a splitter that performs a typically 95:5 split of the flow to NMR versus MS (317).

Metabolomics

Recent advances in computing power and analytical instrumentation has allowed previously unthinkable analyses to be performed. These advances, combined with techniques developed from genomics, have allowed the use of larger data sets to produce proteomics and

metabolomics analyses. The term proteomics, as well as proteome, was coined in 1995 (318) and can be narrowly defined as analyzing the expressed levels of proteins in a cell, thus providing insight into the current physiological state. From proteomics it was a short transition to the transcriptome, proteome, and finally analyzing the metabolome, the small molecules and metabolic products produced by an organism. Metabolomics in its most general definition involves completely analyzing all the known and/or unknown metabolites in a given biological sample (319).

Metabolomic analysis involves three major parts: sample preparation, data acquisition, and data analysis or chemometrics. The data acquisition can make use of several analytical instruments; NMR, GC-MS, or LC-MS to perform a targeted or non-targeted analysis. The preferred instrument in MS-based metabolomics is a high accuracy MS such as TOF, FT, or Orbitrap. Metabolomics analyses can be grouped based on approach: targeted and untargeted. In a targeted metabolomics study, the levels of a known set of compounds are quantified. The study can be quantitative or semi-quantitative by using appropriate chemical standards in the study design (320). One of the advantages of a targeted study is that since the compounds of interest are defined initially, the sample preparation and analytical methodologies can be optimized for those compounds, thus potentially reducing signal interference from other compounds. An untargeted metabolomics study is the analysis of all the measurable compounds in a sample, both the chemical knowns and unknowns (320). Due to the nature of the study, careful sample preparations must be followed with a focus on minimizing any compound loss, degradation, or unintentionally enriching one group of compounds. The analytical method used to generate the metabolomics data must be broad spectrum and may require using multiple separations in tandem, such as HILIC and RP-C18 LC-MS methods. An untargeted study may generate a large amount of data and therefore is best analyzed with

a one of several chemometric data platforms such as MetaboAnalyst (321), XCMS (322), or others (323).

For many ethnobotanically related questions, an untargeted metabolomic analysis is the preferred study design. Again, sample preparation must be carefully designed and all samples processed using the same methods. The method of sample preparation needs to consider both the location and time the plant material is harvested, as well as if the plant tissue will be processed fresh, frozen or dried. The tissue is usually ground or homogenized to increase the extraction efficiency, and care must be taken to avoid sample cross contamination such as from the grinding equipment itself. The extraction of the plant material can be accomplished using various methods and solvents, many of which are discussed previously in this chapter. For metabolomics studies, a mid-polar solvent such as aqueous methanol or aqueous ethanol is commonly used. Depending on the extraction method, the crude extract can be directly analyzed, or it may need to be concentrated and prepared at a set concentration prior to the analysis. A 2009 review examined the aspects of plant sample preparation in detail (324). The data acquisition portion of the analysis will depend on what instrumentation is available. A high accuracy LC-MS system is recommended; however, direct MS infusion of the sample is also possible (325). The combination of HPLC and MS will provide an advantage of two dimensions of separation for the sample: the LC chromatographic separation as well as resolution in the mass domain. This allows for shorter chromatographic methods using smaller columns such as a 2.1 x 50 mm. Efforts should be made to develop a chromatographic system that resolves a wide range of compounds and is rapid. A 2017 review addresses the use of LC mobile phases and mobile phase additives to maximize ionization for plant metabolomics (326). Since the chemicals of interest are not known in an

untargeted metabolomics method, maximizing the number of chemicals that ionize for MS analysis is very important.

Once the data has been collected, it must be analyzed to identify individual features (327). For LC-MS data, a feature is an ion with a unique *m/z* and retention time. Every detected metabolite will have at least one and often several features. As part of the data analysis, a pre-processing step should be incorporated in order to determine the method's noise floor and filter out "known unknowns" and identified contaminants. The remaining features may need to be filtered further, normalized, and scaled in order to yield the most information from the analytical analysis (328; 329). Once the features are processed, they can be visualized and interpreted using a variety of algorithms and data visualization techniques, depending on the type of study being undertaken. One common method of analyzing the data is to use principle component analysis (PCA) (330).

Additionally, high-resolution mass spectral data can be used to dereplicate known compounds. One approach that has yielded success is searching chemical databases that can be filtered by botanical genus or species for compounds with exact masses corresponding to the experimental ions and comparing empirical formulas and fragmentation patterns (8). The Dictionary of Natural Products and Scifinder are both useful for this type of screening.

Final Considerations

In this chapter we have summarized the chemistry workflow for an ethnobotanical approach to natural product isolation and drug discovery. This workflow begins with the plant collection itself, and is followed by plant material processing, extraction, chromatography, and spectroscopic analysis. The processing of plant material and their extraction essentially

determines the portion of the chemical library contained in the plant that will be examined by all future studies. The chromatography of these extracts, especially when done in a bioassay-guided fraction framework, is perhaps the most time-consuming part of the workflow. Indeed, all fractions generated must be handled and stored with care. Although often only one fraction out of a set is proceeded with for further chromatographic separation, particularly in drug discovery, sister fractions should be preserved for potential future studies, including for studies of the originally-pursued bioactivity. For example, it may very well be that a less active fraction, upon further fractionation, proves to be a source of highly bioactive compounds. To the extent that numerous fractions are generated through such studies, it is of the utmost importance to practice good note keeping and to maintain an updated database. This way, the origin and method of production of every fraction is known. If the same fractions are made on separate occasions or by different scientists, their identity can be compared to those of previous batches via spectroscopic methods such as analytical HPLC, ensuring reproducibility. With advances in spectroscopic technology in the past decade, now only very small quantities of fractions and single compounds are required for chemical analyses. The nature of ethnobotanical drug discovery is highly interdisciplinary, and collaborations are highly favored for combining areas of expertise of different laboratories, including botany, phytochemistry, *in vitro* and *in vivo* biological assays, and drug screening.

APPENDIX III

Targeting Virulence in *Staphylococcus aureus* by Chemical Inhibition of the Accessory Gene Regulator System *In Vivo*

This has been published in *mSphere* (2018) 3(1): e00500-17. PMCID: PMC5770542

Salam, A. M.; Quave, C. L., Targeting virulence in *Staphylococcus aureus* by chemical inhibition of the accessory gene regulator system *in vivo*. *mSphere* **2018,** *3* (1).

Targeting virulence in *Staphylococcus aureus* by chemical inhibition of the accessory gene regulator system *in vivo*

Akram Salam[a], Cassandra L. Quave[b,c,d*]

[a]Program in Molecular and Systems Pharmacology, Laney Graduate School, Emory University, Atlanta, Georgia, USA

[b]Center for the Study of Human Health, Emory University, 550 Asbury Circle, Candler Library 107E, Atlanta, Georgia, USA

[c]Department of Dermatology, Emory University School of Medicine, 615 Michael St., Rm 105L Whitehead Bldg., Atlanta, GA, USA

[d]Antibiotic Resistance Center, Emory University, Atlanta, GA, USA

*****Address correspondence to Cassandra Quave, cquave@emory.edu

Keywords: quorum sensing, virulence, therapeutics, antimicrobial, *Staphylococcus aureus*

Abstract

Methicillin-resistant Staphylococcus aureus (MRSA) presents one of the most serious health concerns worldwide. The WHO labeled it as a “high priority” pathogen in 2017, also citing the more recently-emerged vancomycin-intermediate and resistant strains. With the spread of antibiotic resistance due in large part to the selective pressure exerted by conventional antibiotics, the use of anti-virulence strategies has been recurrently proposed as a promising therapeutic approach. In MRSA, virulence is chiefly controlled by quorum sensing (QS); inhibitors of QS are called quorum quenchers (QQ). In *S. aureus*, the majority of QS components are coded for by the accessory gene regulator (Agr) system. Although much work has been done to develop QQs against MRSA, only a few studies have progressed to *in vivo* models. Those studies include both prophylactic and curative models of infection as well as combination treatments with antibiotic. Across the board, high efficacy is seen at attenuating MRSA virulence and pathogenicity, with some studies also showing effects such as synergy with antibiotics and antibiotic re-sensitization. This minireview aims to summarize and derive conclusions from the literature on the *in vivo* efficacy of QQ agents in MRSA infection models. *In vitro* data is also summarized to provide sufficient background on the hits discussed. On the whole, the reported *in vivo* effects of the reviewed QQs against MRSA represent positive progress at this early stage in drug development. Follow-up studies will be needed to propel the field forward that thoroughly examine *in vitro* and *in vivo* activity and pursue lead optimization.

Introduction

The alarming rise of antibiotic resistance presents significant challenges to human health on a global scale (331). MRSA, particularly community-associated (CA-MRSA) strains such as USA300, presents a unique threat due to its hypervirulent nature (332). While *S. aureus* causes an array of diseases such as infective endocarditis, osteoarticular infections, prosthetic device infections, bacteremia, and pneumonia, approximately 90% of *S. aureus* infections are skin and soft tissue infections (SSTIs) (333; 334). For the treatment of MRSA infections, physicians are now turning more than ever to antibiotics of last resort. What is more, resistance to even these antibiotics, like linezolid, has begun spreading (188-190). A major contributor to this phenomenon is that conventional antibiotics target cellular processes necessary for bacterial survival (335). As such, great selective pressure is exerted on bacterial populations, which divide and mutate rapidly, to genetically develop resistance (12; 191). A different type of target in *S. aureus*, namely quorum sensing (QS), shows promise for circumventing this shortcoming (123; 192).

QS is a system by which many bacterial species monitor their local population density via secretion and detection of small autoinducer molecules in order to modulate gene expression (18; 26). All QS systems possess three common mechanisms: autoinducer production, accumulation, and detection. The three most thoroughly studied QS systems are based on the following autoinducers: the acylated homoserine lactones utilized by Gram-negative bacteria (also called autoinducer-1), the peptide signals used by Gram-positive bacteria, and autoinducer-2, which is utilized by both (176). Additional QS signaling molecules include autoinducer-3, the *Pseudomonas* quinolone signal (PQS), and the diffusible signal factor (DSF). QS has been established as a mediator of virulence through which bacteria regulate

genes involved in host invasion, immune evasion, and dissemination. Interest in quorum sensing inhibition as an anti-virulence strategy against a variety of human pathogens has increased greatly over the past decade (42). In the case of *S. aureus*, the field continues to expand.

The Agr system as an emerging target for drug development in virulent *S. aureus* infection

In *S. aureus*, the majority of QS components are encoded by the accessory gene regulator (Agr) system, which regulates most temporally expressed *S. aureus* virulence factors (**Fig. A3.1**) (26; 336). When the concentration of *S. aureus'* secreted autoinducer peptide (AIP) reaches a critical threshold value as the result of increased bacterial population density, the majority of virulence response systems are triggered. This includes production of virulence factors and mechanisms of antibiotic resistance (e.g. upregulated efflux pump) (17; 172; 174; 337-339). The *agr* chromosomal locus encodes two transcripts, RNAII and RNAIII, which are divergently transcribed from the P2 and P3 promoters, respectively (340). The RNAII segment of *agr* is an operon of four genes, *agrBDCA*, which encode all the main components of QS (26; 336). AgrB is an integral membrane endopeptidase that converts the precursor AIP peptide, AgrD, to mature AIP and exports it (336; 341). AIP is recognized by the membrane-bound receptor histidine kinase AgrC, which subsequently phosphorylates AgrA in the cytosol (342). AgrA is a member of a family of conserved response regulators with CheY-like receiver domains; upon phosphorylation it binds to P2 and P3, upregulating *agr* transcription of RNAII and III (62). Additionally, AgrA directly induces expression of several phenol-soluble modulins (PSMs). The RNAIII segment of *agr* codes for a regulatory,

small RNA molecule that acts as the primary effector of the quorum sensing system by up-regulating virulence factor expression and down-regulating cell surface protein expression (19; 20). The RNAIII transcript also contains the 26 amino acid δ-toxin gene (*hld*). Four allelic groups of *agr* have been identified within *S. aureus*, categorized as *agr* I-IV (21).

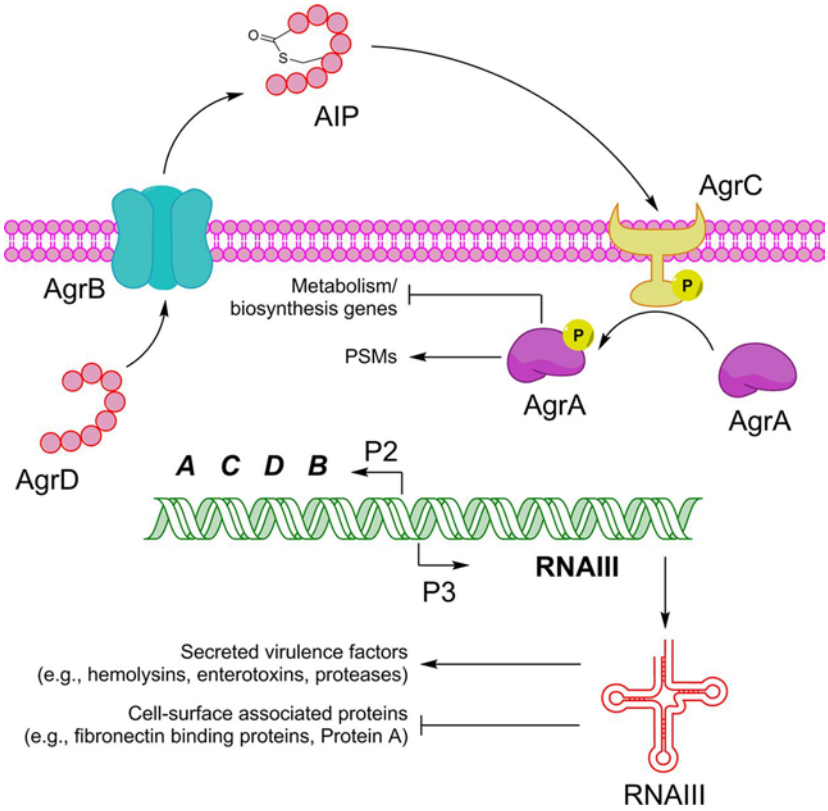

Fig. A3.1. Schematic of the *S. aureus* accessory gene regulatory (Agr) system.

Inhibiting QS would constrain the *S. aureus'* ability kill host cells, evade host immunity, and disseminate. Indeed, it is through the production of QS-regulated toxins such as δ-toxin, Panton-Valentine leukocidin, and staphylococcal enterotoxin C that the pathogen achieves these feats (24; 343-346). Additionally, targeting *S. aureus* QS, and thus virulence, rather than survival has been proposed to exert less selective pressure for the development of resistance than conventional antibiotics (175; 192; 193). This may indeed be the case, with numerous QS inhibitors, or quorum quenchers (QQs), demonstrating a markedly diminished ability to give rise to resistance relative to conventional antibiotics in preliminary studies (8; 73). Moved by this promising strategy, much research has been devoted to QQ discovery against MRSA, yielding a wealth of *in vitro* data and an increasing number of QQ agents tested *in vivo*. Herein we review the current status of the field by examining reports on *in vivo* testing of QQs as an anti-virulence strategy against MRSA.

Synthetic Quorum Quenchers

The synthetic quorum quenchers discussed here are small molecules and antisense nucleic acids. All were discovered via varying approaches including combinatorial chemistry, high-throughput screening, and software prediction.

Biaryl hydroketones

Biaryl hydroxyketones have been identified that target the response regulator AgrA by disrupting the AgrA-P3 interaction and, consequently, virulence factor production (347). In a

follow-up study involving a combinatorial library synthesized based on the most efficacious biaryl hydroxyketone, compound F12 demonstrated 98% inhibition of rabbit erythrocyte hemolysis *in vitro* by MRSA (USA300 strain) at 1 µg/mL (348). In their latest work, Kuo et al. examined the *in vivo* efficacy of F12 as well as F1 and F19 (**Fig. A3.2A**), two other compounds that displayed similarly high bioactivity (74). They utilized a murine wound infection model and a *Galleria mellonella* insect larva model of infection. The infecting strain used in both cases was a USA300 clinical isolate from a patient from Metro Health Medical Center, Cleveland, Ohio.

The three compounds were first shown to exhibit no toxicity up to 200 µM in a lactate dehydrogenase assay of the murine macrophage cell line J774.2. In the murine wound infection model, a dorsal excisional wound created with a punch biopsy tool was inoculated with 1×10^7 CFU of aUSA300 strain. Topical application of F12 twice a day at 20 mg/kg for 8 days performed comparably to F1 and promoted modest wound healing relative to vehicle throughout the treatment duration. In uninfected wounds, treatment offered no healing advantage. Bacterial burden, assessed 1 day after administration of the final treatment dose, was found to be statistically similar in all treatment groups.

In a *Galleria mellonella* larva model of MRSA infection, 2×10^7 CFU of a USA300 strain was administered to establish infection along with a 20 mg/kg dose of F1, F12, or F19 as treatment. The treatment was repeated every 6 h over the course of up to 84 h. Administration of F12 increased survival from 12 h in untreated controls to 42 h, being outperformed by F1 (60 h) and F19 (66 h). Combination therapy of each of the biaryl hydroxyketones with the β-lactam antibiotics cephalothin or naphcillin, to both of which USA300 is resistant in monotherapy, further increased survival. This result indicates a synergism between the QQ

compounds and the antibiotics. F19 was found to offer the greatest survival advantage, up to 84 h, with each antibiotic. Finally, combination of 1 μg/mL F1, F12, or F19 reduced the MIC

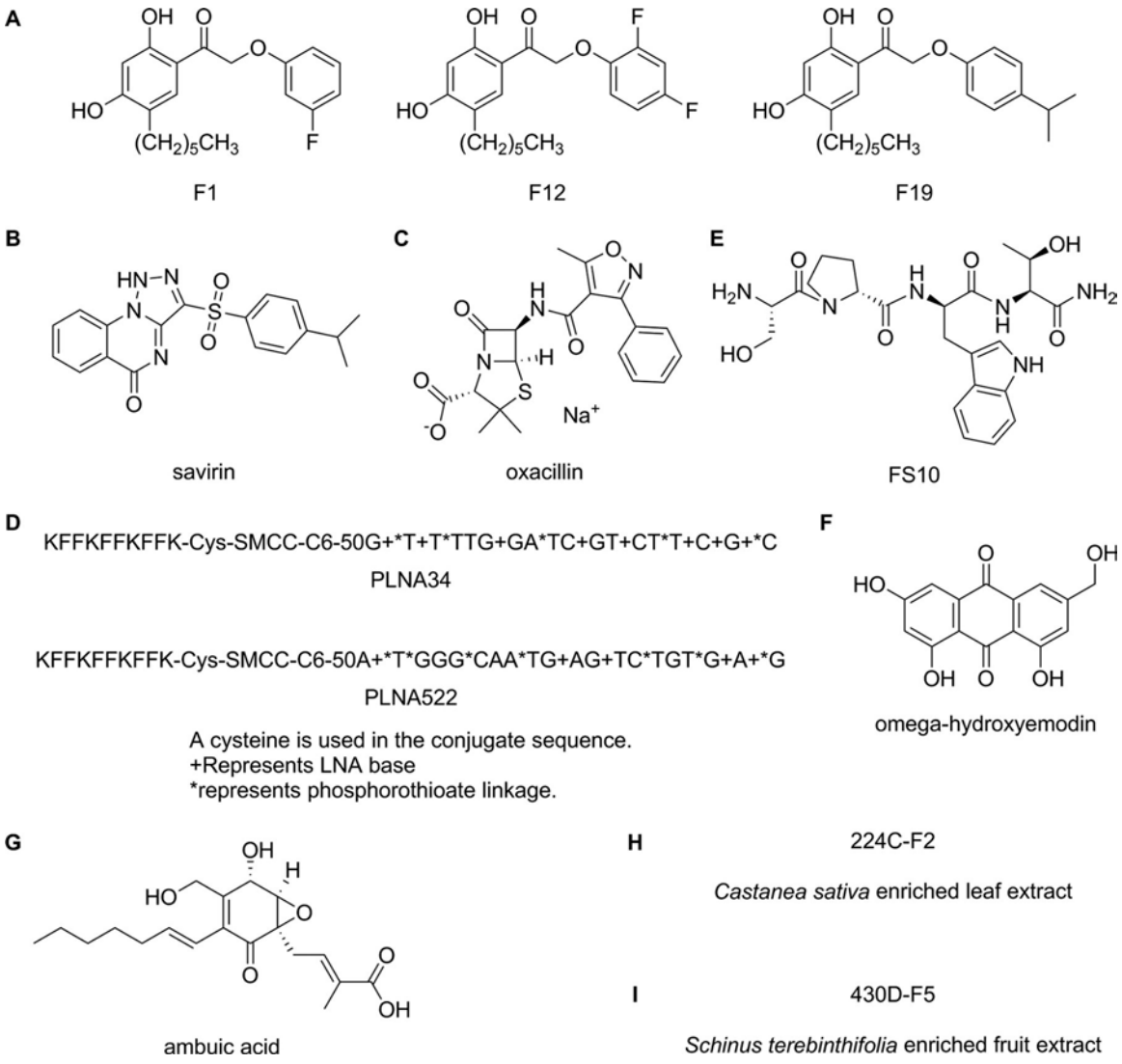

Fig. A3.2. Quorum quenching compounds tested *in vivo* for inhibition of MRSA virulence. (A) Biaryl hydroxyketones F1, F12, and F19, (B) savirin, (C) oxacillin, (D) peptide-conjugated locked nucleic acids, (E) tetrapeptide RIP derivative FS10, (F) ω-hydroxyemodin, (G) ambuic acid, (H) enriched *Castanea sativa* leaf extract 224C-F2, (I) enriched *Schinus terebinthifolia* fruit extract 430D-F5.

of nafcillin and cephalothin from 60 and 40 µg/mL to 1 µg/mL, the level of current MRSA antibiotic treatments.

Savirin

Savirin is a small molecule with QQ activity identified via high throughput screening by Sully et al (**Fig. A3.2B**) (73). The screen tested for inhibition of fluorescence in a *S. aureus* reporter strain of AIP-induced *agr*::P3 activation. Savirin, in turn, also exhibited minimal effects on exponential phase growth in dose-response experiments. Sully et al. showed that savirin inhibited *agr*::P3 activation in all *agr* allelic types of *S. aureus* and that it also inhibited RNAIII production and *agr*-dependent stationary phase growth. Favorably, the latter effects were not exerted in *S. epidermidis*, an important skin commensal in host defense (349). Due to this selectivity over *S. epidermidis*, AgrA was pursued as savirin's likely molecular target rather than AgrC, where the two residues that are critical for *agr* activation are conserved between the species (350). $AgrA_C$ (AgrA C-terminal DNA-binding domain) was confirmed as the target via *in silico* docking, electrophoretic mobility shift, and an *agr*::P3 *lux* reporter strain with constitutively-produced AgrA. They then showed that this resulted in inhibition of *agr*-specific transcription regulation of major SSTI virulence factors. This was shown via microarray analysis, qRT-PCR, and direct measurements of virulence factor function.

The group studied an airpouch skin infection model using *Nox2*$^{-/-}$ mice, which allowed for maximal *S. aureus agr* expression. A load of 4×10^7 CFU of USA300 *agr* type I MRSA strain (LAC, Los Angeles Clone) expressing a fluorescent reporter of *agr*::P3 activation (AH1677) was subcutaneously co-administered to the mice with 10 µg savirin (351). Savirin treatment

led to a marked reduction in *agr*::P3 activation in bacteria. Additionally, 24 h after infection, weight loss due to infection (a measure of morbidity) was greatly attenuated, as was bacterial burden in the pouch and in the systemic circulation. In mice infected with LAC Δ*agr*, 10 µg savirin had no effect on weight loss or bacterial burden, indicating that savirin selectively inhibits *agr* activation.

Sully et al. also evaluated savirin in a model of *agr*-dependent dermonecrotic skin infection in SKH1 hairless immunocompetent mice (352; 353). A bacterial load of 4×10^7 CFU of LAC was co-administered with 5 µg savirin. Throughout the course of the 7-day treatment, abscess and ulcer areas were severely diminished relative to vehicle control. On day 3, bacterial load in the treated and control mice were the same, indicating that savirin treatment did not affect bacterial viability at this time point. On day 7, a decrease in bacterial population of approximately 2 log units was observed in both the abscesses and systemic circulation (as observed from the spleen). This was attributed, at least in part, to macrophages, which they showed more effectively killed LAC *in vitro* after savirin treatment. The bacterial clearance observed was similar to the phenotype of the *agr* deletion mutant without treatment. Another treatment with administration of 10 µg savirin delayed to 24 h and 48 h post initiation of infection lead to a reduced reduction of ulcer area in the initial days of infection. Abscess area throughout treatment and ulcer area in the later days of infection did not change significantly relative to vehicle. Finally, they showed that exposing LAC to 5 µg doses of savirin in *in vivo* serial passaging through the skin of 10 individual mice did not lead to development of tolerance to savirin inhibition of *agr* function.

Oxacillin

Waters et al. discovered and explored the ability of oxacillin (OXA), to which MRSA is resistant, to attenuate MRSA virulence when administered at sub-growth inhibitory concentrations (**Fig. A3.2C**) (354). They rationalized that such dosing would increase MRSA methicillin resistance and subsequently downregulate the Agr system and virulence.

The group established sepsis in CD1 female mice via tail vain injection of 5×10^6 CFU of a USA300 strain. The mice were sorted into groups of five, and the infection was given 9 hours to establish before OXA was administered. One group of mice was treated with 75 mg/kg doses of OXA while another was treated with 7.5 mg/kg, both twice a day. Infection was allowed to proceed for 28 hours or one week. On day 7, OXA treatment at both the low and high doses had resulted in significant reduction of bacterial burden, with kidney CFU reduced by 4 log units and blood CFU cleared completely (as observed from spleen). Additionally, while 8/10 untreated mice developed kidney abscesses, only 4/10 of the low-dose OXA and none of the high-dose OXA mice had visible kidney abscesses.

In a pneumonia model of MRSA infection, in which mice were intranasally infected with 2-3×10^8 CFU of a USA300 strain, the same treatments demonstrated positive results when given starting 3.5 h post infection. Seven-day survival increased from 20% in the untreated group to 60% in both treatment groups. Additionally, the blood levels of the USA300 strain in the treated mice were 3 log units less than control. To confirm OXA-mediated attenuation of virulence, they showed that OXA exposure represses cytotoxicity of USA300 culture supernatants on neutrophils. Transcriptome analysis further revealed how OXA may be attenuating virulence via modulation of gene expression. For example, repression of *agr* and activation of *rot* (repressor of toxins) were observed.

Peptide-conjugated locked nucleic acids

Da et al. took an antisense oligonucleotide approach to inhibiting the Agr system, choosing to target AgrA due to its being relatively conserved in all four *agr* allelic groups (71). Their oligonucleotide of choice was LNA, or locked nucleic acid, a modified RNA nucleotide where the ribose moiety is modified with an extra bridge connecting the 2' oxygen and 4' carbon. Two antisense LNAs were synthesized and covalently conjugated with cell penetrating peptide (KFF)3K, resulting in two peptide-conjugated locked nucleic acids (PLNAs): PLNA34 and PLNA522 (**Fig. A3.2D**). Both were shown to have no growth inhibitory effect on LAC up to 40 μM. qRT-PCR showed that both PLNA34 and PLNA522 decreased *agrA* transcription at 12.5 μM, with PLNA34 producing the greater effect. Similar levels of decreased transcription were consequently observed for RNAIII. PLNA34 treatment was shown to suppress the expression of several *agr*-regulated toxin genes: *psm-α*, *psm-β*, *hla*, and *pvl*. Additionally, culture filtrates from PLNA34-treated cells had decreased hemolytic activity. They also exhibited a significantly reduced ability to lyse human neutrophils and induce chemotaxis in them. In C57BL/6J mice, 40 μM PLNA34 dosed with subcutaneous injection of LAC resulted in the formation of smaller abscesses and abrogated the development of epidermal necrosis, ulceration, and dermal necrosis. These protective effects were accompanied on day 6 by a decrease in bacterial population of more than four orders of magnitude.

Peptide quorum quenchers

The one peptide quorum quencher discussed here is a derivative of RNAIII inhibiting peptide (RIP). RIP is endogenously produced by *S. aureus* and functions to inhibit quorum sensing.

RNAIII inhibiting peptide (RIP) derivative

Simonetti et al. aimed to evaluate the *in vivo* efficacy of the combined administration of the tetrapeptide RIP derivative FS10 (**Fig. A3.2E**) and tigecycline in a mouse abscess model of MRSA infection (69). The MSSA strain ATCC 29213 and the MRSA strain ATCC 43300 were used throughout the study. Both strains showed susceptibility to tigecycline, which exhibited MICs of 0.12 and 0.25 µg/mL for the MSSA and MRSA, respectively. FS10, on the other hand, did not demonstrate growth inhibition at doses as high as 256 µg/mL. In terms of hemolytic activity, FS10 was highly ineffective at permeabilizing erythrocytes, causing <8% cellular disruption at high dose.

In the mouse wound infection model, infected BALB/c mice received treatment 24 h post-infection with either FS10 alone, tigecycline alone, or a combination. Tigecycline was given via intra-peritoneal administration daily for 7 days at 7 mg/kg while 20 µg FS10 was administered via wound dressing every 2 days. At day 8 post-wounding, comparable trends were observed in both MSSA and MRSA infections. As for the MRSA infections, the mean bacterial count in untreated controls was $4.5\times10^{9} \pm 1.4\times10^{9}$ CFU/g of infected skin, which is significantly higher than the counts recovered from the treatment groups. FS10 alone had a slight growth inhibitory effect, reducing bacterial count to $3.7\times10^{8} \pm 1.6\times10^{8}$ CFU/g. Tigecycline alone had a strong effect, bringing the count down to $6.4\times10^{5} \pm 1.7\times10^{5}$ CFU/g. The combination treatment led to the strongest growth inhibitory effect, reducing bacterial count to $4.6\times10^{3} \pm 1.3\times10^{3}$ CFU/g.

Finally, histological evaluation of the excised MRSA-infected tissues was done in order to assess the biological impact of different treatments on three wound healing parameters: epithelialization, granulation tissue, and collagen organization. A scoring system of 0-4 was utilized, with 0 being extensively disturbed and 4 being normal. Tigecycline treatment and FS10 treatment both resulted in similar healing scores in the range of moderate healing across the three parameters (all scores between 2.80 and 3.00). The combination treatment, however, resulted in scores closer to that of the untreated control, all in the range of marked healing (scores between 3.20 and 3.50).

Natural Product Quorum Quenchers

Of the four natural product quorum quenchers discussed here, two are small molecules isolated from fungi while the other two are enriched plant extracts.

ω-hydroxyemodin

The group that reported on the synthetic small molecule savirin had previously pursued natural product QQs, identifying a number of polyhydroxyanthraquinones from the fungus *Penicillium restrictum* (154). A compound named ω-hydroxyemodin (OHM) (**Fig. A3.2F**) demonstrated the most potent inhibition of *agr* signaling in LAC and was therefore chosen for further study (72).

Daly et al. first showed that OHM inhibits expression of all four *agr* types at concentrations that are not cytotoxic to LAC or to human alveolar (A549), kidney (HEK293), and hepatocyte cell lines. They demonstrated this using strains expressing yellow fluorescent

protein (YFP) under the control of the *agr*::P3 promoter. After ruling out AgrC as the target of OHM using an *agr* I isolate expressing constitutively active AgrC (R238H), they tested whether OHM inhibits *agr* function by targeting AgrA binding to promoter DNA (355). They found that OHM demonstrated a dose-dependent inhibition of $AgrA_C$ binding to *agr* promoter DNA via: molecular docking, an electrophoretic mobility shift assay, a bead-based assay of DNA-transcription factor binding, and surface plasmon resonance. OHM was found to also inhibit *agr* I expression in *S. epidermidis*, likely because the OHM binding site on $AgrA_C$ is conserved between the species.

OHM was then assessed *in vivo* in a mouse model of MRSA skin infection (356). A load of 5×10^7 to 7×10^7 CFU of LAC was subcutaneously injected into mice with 5 µg OHM. By day 3, treated mice had abscess and ulcer areas less than half the size of control, abscess bacterial burden reduced by half a log unit, and markedly reduced weight loss. By day 7, bacterial burden was reduced by 1.5 log units. In the mice infected with LACΔ*agr*, no differences were observed between the OHM- and vehicle-treated mice. These results demonstrate that OHM specifically disrupts *agr* signaling with no direct effects on the host. Bacterial clearance suggested an increased capacity of host immunity to combat infection in the absence of *agr* signaling and subsequent toxin production. Indeed, OHM treatment of LAC, but not LACΔ*agr*, was found to increase *in vitro* bacterial clearance by both mouse macrophages and human polymorphonuclear leukocytes (PMNs). Additionally, treatment was found to approximately double PMN viability in a 2 h incubation with LAC but not LACΔ*agr* supernatant, as indicated by LDH release.

Ambuic acid

Todd et al. explored the antivirulence potential of the fungal metabolite ambuic acid (**Fig. A3.2G**), rationalizing that it targets AgrB and thus AIP synthesis in *S. aureus* (183). They developed a USA300 strain with the *agr* locus deleted and the *agrBD* genes of the *agr* I type integrated at a phage attachment site, the genes under the regulation of the *sarA* P1 promoter. This mutant strain, therefore, not only produces AIP constitutively, but would only see an inhibition of AIP production due to perturbations specific to signal biosynthesis. Mass spectrometric measurements were performed to quantify the AIP production of the wild-type and mutant strain upon treatment with ambuic acid and AIP-II, a known AgrC antagonist. Supporting ambuic acid's role as an AIP synthesis inhibitor, AIP-II treatment resulted in inhibition of AIP production in the wild-type strain only, as expected, while ambuic acid treatment itself caused inhibition in both strains. Furthermore, ambuic acid treatment was found via Western blot to inhibit MRSA production of α-toxin in a dose-dependent manner and was found via quantitative real-time PCR to inhibit RNAIII production, consistent with a repression of the Agr quorum sensing system.

A murine mouse model of MRSA skin infection was pursued to evaluate ambuic acid activity *in vivo*. Male BALB/c mice received 50 µL intradermal injections into the abdominal skin of inoculum suspensions containing 1×10^8 CFU of LAC and either DMSO or 5, 25, or 50 µg ambuic acid dissolved in DMSO. Over the course of the 14-day experiment, the single 25 µg prophylactic dose of ambuic acid was found to almost completely abrogate skin ulcer formation while the 5 µg dose roughly halved the lesion size. Additionally, ambuic acid treatment caused significantly less infection-induced morbidity in the mice than vehicle treatment, as assessed by weight loss. Infection by a LAC strain containing an *agr*-driven *lux* reporter revealed real-time suppression of *agr* activity *in vivo* by 5 µg ambuic acid over the course of a 5 h period post-challenge.

To confirm whether ambuic acid could potentially broadly target virulence for multiple Gram-positive pathogens, Todd et al. compared 50% inhibitory concentration (IC_{50}) values for AIP synthesis inhibition in: *Staphylococcus aureus* (*agr I, II, III*), *Staphylococcus epidermidis* (*agr I, II, III*), *Staphylococcus lugdunensis* (*agr I*), *Staphylococcus saprophyticus*, *Listeria monocytogenes*, and *Enterococcus faecalis*. Ambuic acid demonstrated IC_{50} values of < 25 μM in 8 of the 11 strains.

Castanea sativa leaf extract

Quave et al. reported on an enriched extract of *Castanea sativa* leaves, 224C-F2 (**Fig. A3.2H**), which demonstrated non-bactericidal QQ activity against LAC (8; 41). 224C-F2 exhibited inhibition of *agr* expression in all *agr* types with IC_{50} values from 1.56–25 μg/mL. No effects on growth were observed at up to 100 μg/mL. QQ activity was confirmed by the ability of 224C-F2 doses as low as 0.25 μg/mL to significantly reduce δ-toxin production of the strain NRS385, a heavy exotoxin producer, as determined by HPLC. Additionally, doses as low as 6.25 μg/mL significantly reduced red blood cell lysis by LAC supernatants. 224C-F2 demonstrated lack of cytotoxicity *in vitro* to human keratinocytes, a panel of skin commensals, and murine skin. After 15 days of serial passaging in NRS385, 224C-F2 consistently reduced δ-toxin production, indicating no development of resistance. 224C-F2 was then tested in an *in vivo* prophylactic model of MRSA infection.

A load of 1×10^8 CFU of LAC (AH1263) or its *agr* deletion mutant (AH1292) with either 224C-F2 (5 μg or 50 μg) or DMSO were injected intradermally into abdominal skin of female C5Bl/6 mice. Not only did 224C-F2 decrease infection-induced ulcer area in a dose-dependent manner, but it significantly attenuated infection-induced morbidity relative to

vehicle (as assessed by weight loss). Specifically, a 5 μg dose reduced peak abscess area to 1/3, while 50 μg almost completely prevented abscess formation throughout the 14-day experiment. Finally, mice receiving treatment only did not display signs of dermal irritation or clinical illness.

Schinus terebinthifolia berry extract

Muhs et al. reported on an enriched *Schinus terebinthifolia* extract, 430D-F5 (**Fig. A3.2I**), with non-bactericidal QQ activity against all four MRSA (USA300) *agr* allelic groups (265). IC_{50} values for inhibition of *agr* expression in the reporter strain assay were 2, 4, 4, and 32 μg/mL for *agr* I-IV, respectively. Importantly, no inhibition of growth was observed upon dosing with 64 μg/mL or less. 430D-F5 treatment caused significant, dose-dependent reduction in: δ-toxin production in several *S. aureus* strains, α-toxin production in LAC, and LAC supernatant hemolytic activity *in vitro*. In assessing extract cytotoxicity, fluorescence microscopy and LDH release showed that treatment protected HaCaTs from damage by NRS385 supernatants at concentrations as low as 8 μg/mL. Additionally, 430D-F5 exhibited limited potential for perturbing the skin microbiome, indicated by the high growth inhibitory concentrations observed against a panel of common skin commensals. Intradermal treatment of mouse skin showed no deleterious effects.

In a prophylactic mouse model of MRSA skin infection, a single 50 μg dose of 430D-F5 administered with 1×10^8 CFU of LAC almost completely attenuated skin ulcer formation. Treated animals also displayed significantly less morbidity relative to vehicle, as assessed by weight loss. A MRSA *agr* P3-lux reporter confirmed that *agr* expression, and thus QS, was inhibited by the treatment.

Conclusions

All studies utilized a mouse model of skin infection where the duration of treatment was at least about one week. Of the studies that determined bacterial count at the site of infection over time, most reported that the count was unaffected or little-effected by around day 3 and then extensively reduced by around day 7. To address why this reduction might occur, the savirin and OHM studies presented evidence for both hits indicating that the reduction may be due at least in part to an increased capacity of the immune system to clear the infection. Related to this, while the AgrA-targeting F12 biaryl hydroketone greatly extended survival in a *Galleria mellonella* larva model of infection, in mice it yielded modest wound healing and was the only QQ hit covered in this review reported to cause no reduction of bacterial counts in mice. Such outcomes highlight the importance of tracking *agr* expression *in vivo* in a given infection model in order to confirm whether therapeutic effects coincide with real-time inhibition of *agr* expression. Another interesting outcome is that even though both savirin and OHM target $AgrA_C$, which is highly conserved between *S. aureus* and not *S. epidermidis*, only the former acts selectively against *S. aureus*. The binding sites of both QQ hits have been described via molecular docking. Savirin was docked at Tyr229, which in *S. epidermidis* is a Phe; OHM was docked near Arg218, a residue strictly conserved across Staphylococcal species (357; 358). AgrB is yet another QS component successfully targeted by a QQ hit. Because of this and its conservation across many Gram-positive bacterial pathogens, AgrB represents an attractive target for targeted drug discovery efforts (359).

The contribution of the Agr sysrem to MRSA skin infections is firmly established in the literature, whereas its role in other types of infection has received somewhat less attention.

This, as well as the fact that the majority of MRSA cases are infections of the skin, contributes to the focus on QQ testing on *in vivo* models of skin infection. The question of whether QQ represents an effective therapeutic strategy for other infections must continue to be explored. In particular, some focus should be dedicated toward the actual QQ treatment of various MRSA *in vivo* infection models. For instance, the current literature demonstrates that *agr* dysfunction is associated with MRSA bacteremia (360-364). Some studies suggest that the incidence of *agr* dysfunction in bacteremia is somehow beneficial, perhaps sustained by a need for cooperation between agr^+ cells and agr^- cheaters in a systemic infection (365-367). Such studies call into questions the potential efficacy of QQ in bacteremia. On the other hand, it may be that QQ treatment induces large-scale shutdown of QS in the agr^+ segment of a bacteremia population, tipping the effective balance of agr^+ and agr^- cells in the population. Such an outcome, which could perturb the ability of MRSA cells to cooperate effectively to sustain pathogenicity, cannot be ruled out by available studies. *In vivo* exploration of bacteremia and other forms of MRSA infection represents a powerful strategy for unraveling such uncertainties.

As MRSA QQs are emerging that demonstrate strong potential for drug development, the field will inevitably see exciting studies that explore the hits more in depth. While a priority is to explore curative QQ strategies against MRSA infection, the current progress on prophylaxis cannot be underestimated. For instance, MEDI4893 is a human anti-α-toxin monoclonal antibody developed by MedImmune that is currently in phase II clinical trials against *S. aureus* α-toxin in mechanically ventilated adult subjects for prophylactic use (368). While the success of MEDI4893 provides further validation of therapeutic use of targeting toxins, Agr-targeting QQs stand to target an entire repertoire of toxins and virulence mechanisms. Mechanistic studies will prove important as they will demonstrate whether

different QQs affect virulence differently, providing valuable information for future drug development. There is much room and need for lead optimization in the discovery QQs with improved bioactivity and pharmacokinetic properties such as serum half-lives that allow for less frequent dosing. For instance, one strategy to optimize peptides is N-methylation, which has been shown to both restrict conformational flexibility, potentially increasing binding affinity to the target, and to yield resistance to hydrolysis by peptidases in the gut wall, allowing for improved oral bioavailability (369). QQ effects on commensals, especially growth inhibition, represent a key consideration for avoiding microbiome disruption and development of resistance mechanisms that could then be transferred to different bacterial species. Other side effects such as increased biofilm production, which has been associated with *agr*-dysfunction, must also be considered. For instance, Quave et al. determined that 224C-F2 did not promote biofilm production and that this was likely due to its moderate biofilm-inhibiting activity (8). A QQ that exhibits no such activity may be helped *in vivo* with concurrent administration of a biofilm inhibitor. Moving forward, although *agr* I strains of *S. aureus* predominate in human disease, QQs that are further in drug development should be tested in *in vivo* models of infection by strains besides LAC(334). Many other strains such as MW2 (*agr* III) exhibit high virulence and are of great concern in the clinic.

A promising outlook is portrayed by the current literature on the *in vivo* efficacy of QQs for inhibiting MRSA virulence and pathogenicity. This is highlighted by the fact that, at this early stage in drug discovery, very favorable responses in animal infection models have been achieved. Additionally, outcomes of great therapeutic interest have been reported, such as the sensitization to obsolete antibiotics with the biaryl hydroketones and synergism with RIP derivative-antibiotic combination treatment. These preliminary data, however, must not be overanalyzed. For example, being at such an early stage in drug development, the QQ hits

covered herein likely have off-target effects yet to be explored. As with all other anti-infectives, resistance to QQs is likely to develop. Therefore, studies must be undertaken to elucidate potential rates of resistance. For most of the QQ hits discussed, resistance frequency studies have not yet been performed in which the bacteria are collected from treated animals and tested for return of virulence in the presence QQ. Given that these are not antibacterial agents but antivirulence agents, the development and spread of resistance may be relatively slow in theory. Resistance may be further slowed down by utilizing QQs as adjuvants to conventional antibiotics. Indeed, the study of synergism and resistance development in antibiotic-QQ combination therapy represents one of the most important and logical steps toward bringing QQs to the clinic.

Conflict of Interest

CQ is a named inventor on two patent applications concerning the technology presented in this paper. The authors declare that any competing interests do not alter their adherence to all *mBio* policies.

Author Contributions

AS wrote the manuscript; CQ provided guidance and revisions.

Funding

This work was supported by grants from the NIH (R01 AT007052 [CQ] and T32 GM008602 [AS]). The content is solely the responsibility of the authors and does not necessarily reflect the official views of the NIH. The funding agency had no role in study design, data collection and analysis, decision to publish, or preparation of the manuscript.

APPENDIX IV

Ethnobotany in Antibiotic Drug Discovery: Emerging Trends

This is an excerpt written by me for a manuscript published in *Chemical Reviews*:

Porras, G.; Chassagne, F.; Lyles, J. T.; Marquez, L.; Dettweiler, M.; Salam, A. M.; Samarakoon, T.; Shabih, S.; Farrokhi, D. R.; Quave, C. L., Ethnobotany and the Role of Plant Natural Products in Antibiotic Drug Discovery. *Chemical Reviews* **2020**. https://doi.org/10.1021/acs.chemrev.0c00922 PMID: 33164487

Emerging Trends in Antibacterial Drug Discovery From Plants

The crisis of antibiotic resistance necessitates creative and innovative approaches, from chemical identification and analysis to assessment of bioactivity. In the area of natural product drug discovery, much progress is being made in the generation and analysis of large chemical datasets. In parallel, our understanding of antibacterial activity is being broadened by assays for bacterial virulence inhibition and the study of synergy and other interactions between plant compounds. Together, these increasingly sophisticated chemical and pharmacological approaches are beginning to open up the complexities of ethnobotanical antimicrobials to useful scientific investigation. Perhaps more than any other space in drug development, antibiotic development is in dire need of innovation in order to reinvigorate a waning pipeline. Small molecules remain the primary focus of drug discovery for antibiotics. While it is very important to consider innovations beyond this realm, such as bacteriophage therapy and fecal microbiota transplant, we focus on innovations connected to small molecule discovery and development.

Ethnobotany is uniquely positioned to fill in a portion of the preclinical antibiotic innovation gap thanks to both: (1) its utilization of established traditional medicinal knowledge to hone in on promising plants and to (2) the unique and promising region of the biologically relevant chemical space occupied by plant natural products. At the same time, it must be noted that most studies cited in this review tend to use similar experimental approaches depending on whether extracts or purified compounds are under investigation. These approaches include classical bioassay-guided fractionation and structure elucidation by NMR after compound isolation and purification. In this section, we outline a number of emerging trends in drug discovery that are particularly well-suited for adoption into ethnobotanical antibiotic drug

discovery. As the technological capacity of laboratories across the world grows, many of these trends will be adopted extensively and contribute to a streamlining of laboratory workflow.

Chemical Innovations

Plant natural products occupy a vast and largely untapped portion of the biologically relevant chemical space. Many chemical innovations for drug discovery can be applied specifically to ethnobotanical drug discovery of antibiotics in order to advance the field.

Machine Learning

Machine learning (ML), a subset of artificial intelligence (AI), can be used to streamline decision-making by utilizing abundant, high quality data to answer well-specified questions (370). Very recently, ML has been successfully utilized for the identification of a structurally divergent antibiotic lead, halicin, which has demonstrated potent broad-spectrum antibiotic activity *in vitro* and in mouse models of infection. The investigators first trained a directed-message passing deep neural network model on a group of 2,335 compounds binarized as hit or non-hit for *E. coli* growth inhibition. In this model, "messages" are passed along bonds with information on neighboring atoms and bonds multiple times to create higher-level bond messages which together combine into a single continuous vector representing the whole molecule. As such, the model associates structural characteristics with bioactivity in order to predict probabilities of new compounds of exerting growth inhibitory activity against *E. coli*. The investigators used the *in silico* model to screen >107 million compounds across a number

of discrete chemical libraries. Of the top hits, 99 were obtained and screened *in vitro* by the investigators, whose workflow ultimately yielded halicin (371).

In the breakthrough example above, ML was utilized in the drug screening stage to identify a small group of compounds with a very high probability of possessing antibiotic activity against *E. coli*. ML can in fact be applied at all stages of drug discovery and can be based on any of a wide variety of data such as images, text, chemical structures, spectroscopic data and omics data (370). AI has only in the last few years begun to see practical application in drug discovery, much of this progress being due to advances in ML algorithms such as deep learning, which was utilized in the study above (371). The hope in the pharmaceutical industry is that the application of ML will increase drug development success rates and lower costs and it is being utilized by most large biopharma companies (370; 372). Indeed, as of February 2020, 43 biopharma companies have made collaborations with one or multiple AI companies to power drug discovery efforts (373).

Academic research labs are also increasingly applying ML to drug discovery efforts, with several studies having been done on plant natural products specifically. A recent study reported the success of a deep recurrent neural network model in *de novo* molecule generation of new chemical entities that modulate the retinoid X receptor (RXR) (374). This deep learning model was trained on the SMILES strings of a set 541,555 bioactive molecules from ChEMBL; by transfer learning, this model could generate new molecular structures based on template compounds. The investigators selected six known plant natural product RXR ligands and of the 1,000 SMILES strings generated, 201 were predicted as RXR agonists by self-organizing map-based prediction of drug equivalence relationships (SPiDER) target prediction software (375). Four compounds were chosen for synthesis and characterization *in vitro* for modulatory activity on the three RXR subtypes. Of the four, one

demonstrated full agonistic activity on RXRα and RXRβ with low micromolar EC_{50} values. This early success as well as the success of halicin should not, however, draw attention away from the progress yet to be made with ML. A recent review paper, for example, recommends the use of AI to correlate natural product 2D structure with biological function (376). The ability to predict biological function of a natural product would greatly streamline bioassay-guided fractionation efforts, but as of now only a foundation has been laid for the pursuit of this goal. Furthermore, not all AI approaches have enjoyed market success. For example, due to poor financial returns IBM is stopping development and sales of its AI technology Watson for Drug Discovery, though Pfizer continues to use it for hypothesis generation (77).

ML will occupy a growing role in plant natural products antibiotic development as it possesses the potential to aid the emerging trends below in answering important questions. For a more in-depth discussion of how ML can be applied to drug discovery and development, refer to the review by Vamathevan et al (370).

Molecular Networking and Dereplication

Since its introduction in 2012, molecular networking (MN) has emerged as revolutionary tool in natural product isolation, streamlining the process immensely (169). This dereplication technique allows for rapid identification of compounds in complex mixtures by visualizing and organizing tandem MS/MS data sets and annotating them based on data sets of known compounds. As such, MN-based dereplication relies on the quality and availability of MS/MS data, for which the world's largest repository and data analysis tool is Global Natural Products Social Molecular Networking (GNPS) (168; 231). Two ways to improve dereplication when relevant MS/MS data is unavailable are via in-house experimental

MS/MS data and via *in silico* MS/MS data (169). The idea behind the former is that, using natural product samples enriched for a particular chemical class generated in one's own lab, one can generate an MS/MS database on which a new dataset can be annotated for the identification of chemicals of that class and their derivatives. This strategy was pioneered by Fox Ramos et al. and was used to isolate three new and three known monoterpene indole alkaloids from the bark of *Geissospermum laeve* (Vell.) Miers (Apocynacaeae) as well as dereplicate five known compounds previously undescribed in the genus (377). As for using *in silico* MS/MS data, the goal is to generate new databases to annotate on by using ML to generate MS/MS data of known compounds that lack experimental MS/MS data. The first *in silico* databases (ISDBs) were created by Allard et al. by using the ML-based tool CFM-ID v. 1.10 to generate MS/MS data for >220,000 compounds in the Dictionary of Natural Products and >170,000 compounds in the Universal Natural Products Database (75; 76; 306; 378; 379). A number of studies have since used these ISDBs for successful targeted plant natural product isolations (230; 380).

MN allows other layers of information besides MS/MS to be mapped over networks, including analytical, taxonomical and biological details and this has been increasingly leveraged to inform natural product prioritization (381-383). For example, one investigation by Olivon et al. used MN embedding both bioactivity and taxonomic data to identify potentially bioactive scaffolds from 292 Euphorbiaceae extracts from New Caledonia (382). The collection was screened against the oncogenic Wnt signaling pathway and chikungunya virus (CHIKV) replication. Crude extract activity levels in each assay (for example, 0 to 5 µg/mL IC_{50}) were assigned a unique color tag and applied to the MN; as such, clusters of potentially bioactive metabolites became easily visualized. To better narrow down potential bioactive candidates and exclude ubiquitous compounds, extracts' genus/species and plant

part were also assigned a unique color tag which was applied to the MN. This way, four bioactive clusters related to the leaves of *Bocquillonia nervosa* Airy Shaw (Euphorbiaceae) were identified as being associated with high efficacy in both bioassays. Ultimately, the investigators' workflow led to the isolation of a daphnane diterpene orthoester and four 12-deoxyphorbols with potent bioactivities. For an expanded discussion on natural product MN strategies and natural product prioritization, refer to reviews by Fox Ramos et al. and Wolfender et al (169; 384).

A tool of great interest that works well with dereplication protocols is the droplet probe, which enables the *in situ* analysis of metabolites from a biological sample (385). The droplet probe works by depositing a solvent droplet on a sample such as a leaf; this droplet extracts the metabolites from the area it covers and the microextract is injected into LC-MS. There are, in fact, many iterations of mass spectrometry imaging (MSI) that allow for such *in situ* analyses, such as DESI-MSI (desorption electrospray ionization), MALDI-MS (matrix assisted laser desorption ionization) and LAESI-MS (laser ablation electrospray ionization) (154; 386-388). The droplet probe distinguishes itself in that it uses chromatography while the others do not, requires no sample preparation (as does LAESI), can sample any surface and does not damage the sample. Additionally, the droplet probe can perform repeated sampling to concentrate microextractions by retaining a droplet on the top of the syringe. It does, however, lack the ability to take spatial measurements at high resolution due to the droplet size and so the other three techniques are superior at imaging. The droplet probe has been used to rapidly identify and differentiate acetogenin analogues and even isomers from the various organs of *Asimina triloba* (L.) Dunal (Annonaceae) through coupling to UPLC-PDA-HRMS/MS (389). In a later study also by the Oberlies group, the investigators successfully identified cytotoxic prenylated xanthones from an herbarium voucher specimen

of *Garcinia mangostana* (Clusiaceae) without damaging the specimen (390). Although MS/MS data acquired from droplet probe experiments have yet to be used for prioritization of natural product isolation via MN, the possibility now exists of doing so without performing bulk extractions.

Although molecular networking is typically thought of as utilizing MS data, NMR spectroscopy is the other major analytical platform that yields highly specific fingerprints for a given compound (391). A new tool has been developed for molecular networking with NMR data called Metabolomics And Dereplication By Two-dimensional Experiments (MADByTE) (77). MADByTE utilizes HSQC and TOCSY data to construct spin systems of a compound. Spin systems represent particular fragments of a compound; while MS/MS fragments also represent fragments, the two concepts are different. The spin systems are treated as features and a sample is a collection of its features. If a compound is present in two samples, those samples will share features that correspond to it. From spin system features, MADByTE can generate a number of association networks and then output them as a graphML file for use in Cytoscape or Gephi. MADByTE is also capable of mapping bioactivity metadata over networks to visualize bioactivity profiles for sample prioritization. For MN, MADByTE does not use a centralized database of NMR spectra; rather, investigators can query against in-house experimental data (392). Other functions are currently being developed, including integration of MS data and the utilization of *in silco* databases for tentative structure elucidation (77).

Metabolite Generation

The ability to efficiently produce desired natural products is of great importance to drug discovery. Typically, such production is done in bioreactors by reconstituting biosynthetic machinery in species such as *Escherichia coli* and *Saccharomyces cerevisiae.* A challenge in this process, however, is that many biosynthetic pathways are not fully characterized. Genome mining is a strategy by which biosynthetic pathways are computationally predicted and prioritized for further studies such as natural product isolation (393). A number of bioinformatics tools exist for the identification of natural product biosynthetic pathways from sequenced DNA (394). Two examples are AntiSMASH (395), a comprehensive pipeline used for bacterial and fungal genomes and plantiSMASH (396), an antiSMASH derivative that includes plant-specific cluster detection rules, co-expression analysis and comparative genomic analysis. It is worth expanding on the latter two analyses. Co-expression analysis uses genes of known biosynthetic enzymes as bait and ranks other genes by correlation coefficient to the bait to identify candidate genes of biosynthetic enzymes. Rajniak et al. successfully used a combination of untargeted metabolomics and co-expression analysis to identify 4-hydroxyindole-3carbonyl nitrile (4-OH-ICN), a previously unknown *Arabidopsis thaliana* (L.) Heynh. (Brassicaceae) cyanogenic metabolite and elucidate its biosynthesis by using the *CYP82C2* gene as bait (397). Comparative genomic analysis, on the other hand, uses phylogenetic profiling to find co-occurrence across genomes. CLIME (clustering by inferred models of evolution) is an algorithm that performs this analysis and it has been used to predict new members of a number of biosynthetic pathway based on shared inferred ancestry (398).

While missing enzyme identification can be performed within the native species, similar enzymes in other organisms can be found via genome mining to construct an artificial pathway. Biosynthetic enzyme discovery studies often utilize genomic databases such as the

Kyoto Encyclopedia of Genes and Genomes (KEGG) and the Medicinal Plant Genome Project, as well as transcriptomic databases such as the 1000 Plants (1KP) project (399-401). Luo et al. used the Medicinal Plant Genomics Resource, among other tools, to select six *Cannabis* (Cannabaceae) enzymes with potential geranylpyrophosphate:olivetolate geranyltransferase (GOT) activity, necessary for the biosynthesis of a precursor to a number of cannabinoids. Ultimately, the investigators constructed the complete biosynthesis of several major cannabinoids from galactose in *S. cerevisiae* (402; 403). For a thorough discussion on computational tools for discovering and engineering natural product biosynthetic pathways, refer to the review by Ren et al (394).

The ability to generate derivatives of natural products has also been an emerging trend in the field of plant natural products. After identifying and engineering a suitable host organism and planning and engineering a metabolic pathway, many routes are possible to generating novel natural products; these steps are elaborated on in a review by Cravens et al (404). Unnatural substrates can be fed to engineered microorganisms when the relevant biosynthetic enzymes are able to accommodate these structures for reactions (405-407). Additionally, biosynthetic enzymes can be replaced, added, or removed from a pathway to alter metabolite production (408-410). Finally, novel enzymes can be incorporated into a biosynthetic pathway, with protein engineering likely needed to facilitate substrate accommodation (411-413). While few studies have actually performed these feats, advancements in metabolic and protein engineering, discussed in dedicated review papers, will greatly enable the further pursuit of these strategies (404; 414-417). Though no FDA-approved natural products have yet been generated by engineered biosynthetic pathways, this approach is promising for ethnobotanical antibiotic discovery. Engineered biosynthetic pathways can probe natural product derivatives

in a manner different from that of synthetic chemistry, potentially lending it access to a unique portion of the biologically relevant chemical space.

Another system that can be thought of as a bioreactor for producing desired plant natural products are plants themselves. Cyber-agriculture is the growth of plants in contained environments under artificial climate control (418). It has been developed to address challenges in agriculture, including optimizing the flavor and nutrient content of edible plants and reducing waste and costs. A recent proof-of-principle study has shown that by combining cyber-agriculture with metabolomics phenotyping, or chemotyping and predictive ML, the flavor profile of common sweet basil (*Ocimum basilicum* var "Sweet", Lamiaceae) could be optimized (419). Johnson et al. grew basil plants in a Food Server, which is a large, multi-tray, multi-rack hydroponic configuration of the Food Computer the size of a shipping crate. By experimenting with different growth conditions, or climate recipes, a condition was identified in which the production of volatile flavor-active compounds was increased. Possible future uses for cyber-agriculture include experimentation on different plants and the analysis of different conditions such as stressors to modulate the production of compounds of interest. This strategy will use ML to determine optimal recipes to contribute to the emerging field of ethnophytotechnology (420).

Endophytic Fungi

The ability of endophytes to alter and contribute to their host plant's chemistry is well known, though the intricacies of this phenomenon remained poorly understood until recently (53). Endophytes are endosymbiotic microorganisms that reside in internal plant tissues beneath the epidermal cell layer without causing disease (421; 422). They have been shown to

enhance host drought tolerance, growth, nutrient gain and resilience to stressors and pests (423; 424). Because of the chemistry they confer to plants, endophytes, mainly fungal and bacterial, have long been of great interest to drug discovery (425; 426). Some fungal endophytes have even been shown to produce the same bioactive compounds as their hosts, which called more into question the extent to which plants alone are the sources of some botanical compounds (427-429). Other studies have demonstrated that the presence of endophytes in plants does in fact alter the *in vitro* bioactivity of their extracts (430; 431). More recent ecological studies have explored in greater depth the ways in which endophytes interact with plants and play roles in their physiology. Khare et al. discuss endophytism and the latest insights in the field (432). While much progress has been made in understanding the biology endophytes, Khare et al. call for the exploration of the vast majority of endophytes that remain untouched, deduction of the biochemistry and physiology of endophytes up to genomic and metabolomics levels and the creation of a database for endophytic microorganisms and their metabolites (432).

A recent review by Martiez-Klimova et al. covers antimicrobials isolated from endophytes between 2006-2016 (433). Indeed, endophytes have evolved mechanisms to compete with other microbes inside plants and as such represent promising sources of antimicrobial compounds. Recent studies have capitalized on progress in the field and have discovered antibiotic compounds from endophytes. For example, Ibrahim et al. describe their collections from wild and highbush blueberry plants of the novel endophytic fungus *Xylaria ellisii*, the genus of which is unique in its diverse production of secondary metabolites (434). By dereplicating extracts against the Dictionary of Natural Products, Antibase and NORINE and performing a comparative analysis against known fungal metabolites, 11 previously reported compounds were identified. Following this, eight new proline-containing cyclic

nonribosomal pentapeptides were identified named ellisiiamides A–H; ellisiiamide A was active against *E. coli* (MIC = 100 µg/mL), a first report for this scaffold. Further investigation of plant endophytes, and especially those plants identified through the ethnobotanical approach as being used in traditional medicine for infections, holds great potential for future antibiotic discovery.

Structure Elucidation

The field of anisotropic NMR has recently seen significant advancements that greatly improve its accessibility to natural product chemists. Residual dipolar couplings (RDCs) and residual chemical shift anisotropies (RCSAs) are examples of anisotropic NMR data, the former reporting the relative angles between internuclear vectors, usually C–H bonds and the latter reporting the relative orientations of carbon chemical shift tensors (435-440). As such, these two anisotropic techniques complement each other and are particularly useful for structure elucidation in proton-deficient organic molecules. They have been used to unequivocally determine the 3D configurations several complex natural products, the structures of which having previously been questioned (441). To obtain anisotropic NMR data, an anisotropic sample environment is needed and this can be achieved by an alignment medium such as compressed or stretched polymeric gels. An anisotropic environment precludes fully random molecular rotation, which renders dipolar coupling (DC) and chemical shift anisotropy (CSA) unobservable; consequently, residual DC and CSA are observable. RDCs and RCSAs are measurable by eliminating the isotopic contribution to the interactions via a control under an alternative alignment. In a recent publication, Liu et al. describe the 2-3 day synthesis of two such gels and the sample setup as well as the 0.5-4 day

experiments (442). Their results make the utilization of anisotropic NMR more accessible than ever to non-experts and hence more available for addressing complex structural assignment questions. Anisotropic NMR data can especially be used to aid in the structure elucidation of complex natural products by Computer-Assisted Structure Elucidation (CASE), which has less success determining the structures of proton-poor compounds. CASE programs reduce the rate of error in natural product structure elucidation by generating all possible structures that agree with the input data, usually 2D COSY and HMBC data and ranking them by probability (443). In the case that a CASE program generates multiple probable structures, further experimentation is done to select between the alternatives (444). To read about new developments in CASE methodology and future directions in the field, refer to the recent review by Burns et al (445). Most CASE programs do not solve for absolute configuration, but only for planar structures. As mentioned above, by combining RDC and RCSA data 3D structures can be unequivocally determined for complex natural products (441). To make use of these anisotropic NMR data, computational chemistry methods such as density functional theory (DFT) are used to generate 3D conformers based on probable 2D constitutions and 3D configurations. This strategy has already been implemented by the development of StereoFitter by Mestrelab, the first to our knowledge to take advantage of anisotropic NMR data to introduce 3D conformational and configurational analysis into CASE (446). Currently, StereoFitter accepts RDC, Nuclear Overhauser Effect (NOE), J-coupling and chemical shift data to calculate 3D structure. Structure elucidation is often the rate limiting step in natural products research (447). The ability to rapidly determine the 3D structure of a compound computationally based on NMR data promises to further streamline natural product drug discovery efforts.

A key emerging trend in structure elucidation is the continuation of the NMR Raw Data Initiative, begun in 2016, which aims to address the urgent need for public availability of raw NMR data (448). For further discussion on this need, the layers of rationale behind it and action items for implementation, refer to the recent review by McAlpine et al (449). In brief, raw NMR data is necessary for: structure revisions, impurity detection and quantification, dereplication, enabling new methodologies such as the new analysis of published data by optimal processing of the free induction decay (FID), assigning signals from other nuclei such as ^{19}F, building data repositories for purposes such as dereplication (via MADByTE, for example) and clinical applications such as magnetic resonance spectroscopy (MRS). While McAlpine et al (449) outline a number of action items, the ultimate action item is the creation of a global and unified repository for raw NMR data.

Another emerging trend is the increased use of the cryo-electron microscopy (cryo-EM) technique microcrystal electron diffraction (microED), which has proven to be of astounding utility for the structure elucidation of small molecules, including natural products (450). With microED, the structure of a small molecule in nanocrystal form on an EM grid can be solved. A nanocrystal is a crystal thousands of times smaller and much easier to produce than the crystals X-ray diffraction requires, and nanocrystals often spontaneously occur in simple powders. Two breakthrough studies published back-to-back in late 2018 demonstrate that microED can in minutes obtain structures with atomic resolution, in many cases better than 1 Å, from pure powder samples, pure rotary evaporated samples and even heterogeneous mixtures by selecting single crystals off the EM grid (451; 452).

References

1. Bruhn JG, Helmstedt B. 1981. Ethnopharmacology: objectives, principles and perspectives. *Natural products as medicinal agents*
2. Cox PA, Balick MJ. 1994. The ethnobotanical approach to drug discovery. *Sci. Am.* 270:82-7
3. Capasso L. 1998. 5300 years ago, the Ice Man used natural laxatives and antibiotics. *The Lancet* 352:1864
4. Schultes RE, Reis Sv. 1995. *Ethnobotany: evolution of a discipline*. Portland: Dioscorides Press
5. Organization WH. 2013. WHO traditional medicine strategy: 2014-2023, Geneva
6. Schultes RE. 1984. Fifteen years of study of psychoactive snuffs of South America: 1967-1982--a review. *Journal of ethnopharmacology* 11:17-32
7. Sarker SD, Latif Z, Gray AI. 2006. *Natural Products Isolation*. Totowa, New Jersey: Humana Press
8. Quave CL, Lyles JT, Kavanaugh JS, Nelson K, Parlet CP, et al. 2015. *Castanea sativa* (European Chestnut) leaf extracts rich in ursene and oleanene derivatives block *Staphylococcus aureus* virulence and pathogenesis without detectable resistance. *PLoS One* 10:e0136486
9. Davies J, Davies D. 2010. Origins and evolution of antibiotic resistance. *Microbiology and molecular biology reviews : MMBR* 74:417-33
10. Dickey SW, Cheung GYC, Otto M. 2017. Different drugs for bad bugs: antivirulence strategies in the age of antibiotic resistance. *Nature reviews. Drug discovery* 16:457
11. Mulligan MJ, Cobbs CG. 1989. Bacteriostatic versus bactericidal activity. *Infectious disease clinics of North America* 3:389-98
12. CDC. 2013. Antibiotic resistance threats in the United States, Atlanta, GA
13. 2014. *WHO's first global report on antibiotic resistance reveals serious, worldwide threat to public health*. http://www.who.int/mediacentre/news/releases/2014/amr-report/en/
14. CDC. 2019. Antibiotic Resistance Threats in the United States, Atlanta, GA
15. WHO. 2017. WHO publishes list of bacteria for which new antibiotics are urgently needed. Geneva
16. Salam AM, Quave CL. 2018. Targeting virulence in *Staphylococcus aureus* by chemical inhibition of the accessory gene regulator system *in vivo*. *mSphere* 3
17. Recsei P, Kreiswirth B, O'Reilly M, Schlievert P, Gruss A, Novick RP. 1986. Regulation of exoprotein gene expression in *Staphylococcus aureus* by agar. *Molecular & general genetics : MGG* 202:58-61
18. Khan BA, Yeh AJ, Cheung GY, Otto M. 2015. Investigational therapies targeting quorum-sensing for the treatment of *Staphylococcus aureus* infections. *Expert opinion on investigational drugs* 24:689-704
19. Novick RP, Ross HF, Projan SJ, Kornblum J, Kreiswirth B, Moghazeh S. 1993. Synthesis of staphylococcal virulence factors is controlled by a regulatory RNA molecule. *The EMBO journal* 12:3967-75
20. Abdelnour A, Arvidson S, Bremell T, Ryden C, Tarkowski A. 1993. The accessory gene regulator (agr) controls *Staphylococcus aureus* virulence in a murine arthritis model. *Infection and Immunity* 61:3879-85
21. Robinson DA, Monk AB, Cooper JE, Feil EJ, Enright MC. 2005. Evolutionary genetics of the accessory gene regulator (agr) locus in *Staphylococcus aureus*. *Journal of Bacteriology* 187:8312-21
22. Spaan AN, Surewaard BG, Nijland R, van Strijp JA. 2013. Neutrophils versus Staphylococcus aureus: a biological tug of war. *Annual review of microbiology* 67:629-50

23. Foster TJ, Geoghegan JA, Ganesh VK, Hook M. 2014. Adhesion, invasion and evasion: the many functions of the surface proteins of Staphylococcus aureus. *Nature reviews. Microbiology* 12:49-62
24. Otto M. 2014. *Staphylococcus aureus* toxins. *Current Opinion in Microbiology* 17:32-7
25. Tsuji BT, Rybak MJ, Cheung CM, Amjad M, Kaatz GW. 2007. Community- and health care-associated methicillin-resistant Staphylococcus aureus: a comparison of molecular epidemiology and antimicrobial activities of various agents. *Diagnostic microbiology and infectious disease* 58:41-7
26. Novick RP. 2003. Autoinduction and signal transduction in the regulation of staphylococcal virulence. *Molecular microbiology* 48:1429-49
27. Rooijakkers SH, van Kessel KP, van Strijp JA. 2005. Staphylococcal innate immune evasion. *Trends in microbiology* 13:596-601
28. Lowy FD. 1998. Staphylococcus aureus infections. *The New England journal of medicine* 339:520-32
29. Daum RS. 2007. Clinical practice. Skin and soft-tissue infections caused by methicillin-resistant Staphylococcus aureus. *The New England journal of medicine* 357:380-90
30. Hersh AL, Chambers HF, Maselli JH, Gonzales R. 2008. National trends in ambulatory visits and antibiotic prescribing for skin and soft-tissue infections. *Archives of internal medicine* 168:1585-91
31. Mayville P, Ji G, Beavis R, Yang H, Goger M, et al. 1999. Structure-activity analysis of synthetic autoinducing thiolactone peptides from Staphylococcus aureus responsible for virulence. *Proc Natl Acad Sci U S A* 96:1218-23
32. Schwan WR, Langhorne MH, Ritchie HD, Stover CK. 2003. Loss of hemolysin expression in Staphylococcus aureus agr mutants correlates with selective survival during mixed infections in murine abscesses and wounds. *FEMS immunology and medical microbiology* 38:23-8
33. Park J, Jagasia R, Kaufmann GF, Mathison JC, Ruiz DI, et al. 2007. Infection control by antibody disruption of bacterial quorum sensing signaling. *Chem Biol* 14:1119-27
34. Wright JS, 3rd, Jin R, Novick RP. 2005. Transient interference with staphylococcal quorum sensing blocks abscess formation. *Proceedings of the National Academy of Sciences of the United States of America* 102:1691-6
35. Stryjewski ME, Chambers HF. 2008. Skin and soft-tissue infections caused by community-acquired methicillin-resistant Staphylococcus aureus. *Clinical Infectious Diseases* 46 Suppl 5:S368-77
36. Wright JD, Holland KT. 2003. The effect of cell density and specific growth rate on accessory gene regulator and toxic shock syndrome toxin-1 gene expression in Staphylococcus aureus. *FEMS microbiology letters* 218:377-83
37. Kennedy AD, Bubeck Wardenburg J, Gardner DJ, Long D, Whitney AR, et al. 2010. Targeting of alpha-hemolysin by active or passive immunization decreases severity of USA300 skin infection in a mouse model. *The Journal of infectious diseases* 202:1050-8
38. Quave CL, Plano LR, Pantuso T, Bennett BC. 2008. Effects of extracts from Italian medicinal plants on planktonic growth, biofilm formation and adherence of methicillin-resistant *Staphylococcus aureus*. *J. Ethnopharmacol.* 118:418-28
39. Quave CL, Pieroni A, Bennett BC. 2008. Dermatological remedies in the traditional pharmacopoeia of Vulture-Alto Bradano, inland southern Italy. *J Ethnobiol Ethnomed* 4:5
40. Tartaglia B. 2003. *Medicina Popolare*. Aquilonia, AV: Museo etnografico di Aquilonia. 343 pp.
41. Quave CL, Plano LR, Bennett BC. 2011. Quorum sensing inhibitors of *Staphylococcus aureus* from Italian medicinal plants. *Planta Med.* 77:188-95

42. Whiteley M, Diggle SP, Greenberg EP. 2017. Progress in and promise of bacterial quorum sensing research. *Nature* 551:313-20
43. Pieroni A, Quave CL, Villanelli ML, Mangino P, Sabbatini G, et al. 2004. Ethnopharmacognostic survey on the natural ingredients used in folk cosmetics, cosmeceuticals and remedies for healing skin diseases in the inland Marches, Central-Eastern Italy. *J. Ethnopharmacol.* 91:331-44
44. Jenul C, Horswill AR. 2018. Regulation of *Staphylococcus aureus* virulence. *Microbiol. Spectr.* 6
45. Sully EK, Malachowa N, Elmore BO, Alexander SM, Femling JK, et al. 2014. Selective chemical inhibition of *agr* quorum sensing in *Staphylococcus aureus* promotes host defense with minimal impact on resistance. *PLoS Pathog.* 10:e1004174
46. Daly SM, Elmore BO, Kavanaugh JS, Triplett KD, Figueroa M, et al. 2015. ω-Hydroxyemodin limits *Staphylococcus aureus* quorum sensing-mediated pathogenesis and inflammation. *Antimicrob. Agents Chemother.* 59:2223-35
47. Salam A, Quave C. 2018. Opportunities for plant natural products in infection control. *Current Opinion in Microbiology* 45:189-94
48. Caesar LK, Cech NB. 2019. Synergy and antagonism in natural product extracts: when 1 + 1 does not equal 2. *Nat. Prod. Rep.* 36:869-88
49. Dettweiler M, Marquez L, Bao M, Quave CL. 2020. Quantifying synergy in the bioassay-guided fractionation of natural product extracts. *PLoS One* 15:e0235723
50. Elfawal MA, Towler MJ, Reich NG, Golenbock D, Weathers PJ, Rich SM. 2012. Dried whole plant *Artemisia annua* as an antimalarial therapy. *PloS one* 7:e52746
51. Elfawal MA, Towler MJ, Reich NG, Weathers PJ, Rich SM. 2015. Dried whole-plant *Artemisia annua* slows evolution of malaria drug resistance and overcomes resistance to artemisinin. *Proceedings of the National Academy of Sciences of the United States of America* 112:821-6
52. Junio HA, Sy-Cordero AA, Ettefagh KA, Burns JT, Micko KT, et al. 2011. Synergy-directed fractionation of botanical medicines: a case study with goldenseal (*Hydrastis canadensis*). *Journal of natural products* 74:1621-9
53. Egan JM, Kaur A, Raja HA, Kellogg JJ, Oberlies NH, Cech NB. 2016. Antimicrobial fungal endophytes from the botanical medicine goldenseal (Hydrastis canadensis). *Phytochemistry letters* 17:219-25
54. Salam A, Lyles J, Quave C. 2019. Methods in the Extraction and Chemical Analysis of Medicinal Plants. In *Methods and Techniques in Ethnobiology and Ethnoecology*, ed. UP Albuquerque, RFPd Lucena, LVFCd Cunha, RRN Alves:257-83. New York, NY: Springer. Number of 257-83 pp.
55. Chambers HF, Deleo FR. 2009. Waves of resistance: *Staphylococcus aureus* in the antibiotic era. *Nat. Rev. Microbiol.* 7:629-41
56. Lowy FD. 1998. *Staphylococcus aureus* infections. *N. Engl. J. Med.* 339:520-32
57. Tong SY, Davis JS, Eichenberger E, Holland TL, Fowler VG, Jr. 2015. *Staphylococcus aureus* infections: epidemiology, pathophysiology, clinical manifestations, and management. *Clin Microbiol Rev* 28:603-61
58. Thomer L, Schneewind O, Missiakas D. 2016. Pathogenesis of *Staphylococcus aureus* bloodstream infections. *Annu Rev Pathol* 11:343-64
59. Dayan GH, Mohamed N, Scully IL, Cooper D, Begier E, et al. 2016. *Staphylococcus aureus*: the current state of disease, pathophysiology and strategies for prevention. *Expert Rev. Vaccines* 15:1373-92
60. Novick RP, Geisinger E. 2008. Quorum sensing in staphylococci. *Annu. Rev. Genet.* 42:541-64

61. Bronesky D, Wu Z, Marzi S, Walter P, Geissmann T, et al. 2016. *Staphylococcus aureus* RNAIII and its regulon link quorum sensing, stress responses, metabolic adaptation, and regulation of virulence gene expression. *Annu. Rev. Microbiol.* 70:299-316
62. Koenig RL, Ray JL, Maleki SJ, Smeltzer MS, Hurlburt BK. 2004. *Staphylococcus aureus* AgrA binding to the RNAIII-*agr* regulatory region. *Journal of bacteriology* 186:7549-55
63. Ji G, Beavis R, Novick RP. 1997. Bacterial interference caused by autoinducing peptide variants. *Science* 276:2027-30
64. Quave CL, Horswill AR. 2014. Flipping the switch: tools for detecting small molecule inhibitors of staphylococcal virulence. *Front. Microbiol.* 5
65. Cirioni O, Mocchegiani F, Cacciatore I, Vecchiet J, Silvestri C, et al. 2013. Quorum sensing inhibitor FS3-coated vascular graft enhances daptomycin efficacy in a rat model of staphylococcal infection. *Peptides* 40:77-81
66. Brackman G, Cos P, Maes L, Nelis HJ, Coenye T. 2011. Quorum sensing inhibitors increase the susceptibility of bacterial biofilms to antibiotics in vitro and in vivo. *Antimicrobial agents and chemotherapy* 55:2655-61
67. Chifiriuc MC, Bleotu C, Ditu LM, Smarandache D, Sasarman E, et al. 2009. In vivo experimental model for the study of the influence of subinhibitory concentrations of phenyllactic acid on Staphylococcus aureus pathogenicity. *Roumanian archives of microbiology and immunology* 68:34-7
68. Zhu H, Kumar A, Ozkan J, Bandara R, Ding A, et al. 2008. Fimbrolide-coated antimicrobial lenses: their in vitro and in vivo effects. *Optometry and vision science : official publication of the American Academy of Optometry* 85:292-300
69. Simonetti O, Cirioni O, Cacciatore I, Baldassarre L, Orlando F, et al. 2016. Efficacy of the quorum sensing inhibitor FS10 alone and in combination with tigecycline in an animal model of staphylococcal infected wound. *PloS one* 11:e0151956
70. Bhattacharyya S, Agrawal A, Knabe C, Ducheyne P. 2014. Sol-gel silica controlled release thin films for the inhibition of methicillin-resistant Staphylococcus aureus. *Biomaterials* 35:509-17
71. Da F, Yao L, Su Z, Hou Z, Li Z, et al. 2016. Antisense locked nucleic acids targeting agrA inhibit quorum sensing and pathogenesis of community-associated methicillin-resistant *Staphylococcus aureus*. *Journal of applied microbiology*
72. Daly SM, Elmore BO, Kavanaugh JS, Triplett KD, Figueroa M, et al. 2015. omega-Hydroxyemodin limits *Staphylococcus aureus* quorum sensing-mediated pathogenesis and inflammation. *Antimicrobial agents and chemotherapy* 59:2223-35
73. Sully EK, Malachowa N, Elmore BO, Alexander SM, Femling JK, et al. 2014. Selective chemical inhibition of agr quorum sensing in *Staphylococcus aureus* promotes host defense with minimal impact on resistance. *PLoS pathogens* 10:e1004174
74. Kuo D, Yu G, Hoch W, Gabay D, Long L, et al. 2015. Novel quorum-quenching agents promote methicillin-resistant *Staphylococcus aureus* (MRSA) wound healing and sensitize MRSA to beta-lactam antibiotics. *Antimicrobial agents and chemotherapy* 59:1512-8
75. Allard PM, Peresse T, Bisson J, Gindro K, Marcourt L, et al. 2016. Integration of molecular networking and in-silico MS/MS fragmentation for natural products dereplication. *Analytical chemistry* 88:3317-23
76. Zani CL, Carroll AR. 2017. Database for Rapid Dereplication of Known Natural Products Using Data from MS and Fast NMR Experiments. *J Nat Prod* 80:1758-66
77. Egan J, Linington R. 2019. *Reinforcing Bioactivity Directed Discovery Using MADByTE (Metabolomics And Dereplication By Two-dimensional Experiments)*.

78. Mustafa B, Hajdari A, Krasniqi F, Hoxha E, Ademi H, et al. 2012. Medical ethnobotany of the Albanian Alps in Kosovo. *J. Ethnobiol. Ethnomed.* 8:6
79. Wall J, Aksoy E, Köse N, Okan T, Köse c. 2018. What women know that men do not about chestnut trees in Turkey: A method of hearing muted knowledge. *Journal of Ethnobiology* 38:138-54
80. Kosňovská J. 2013. The origin, archaeobotany and ethnobotany of Sweet Chestnut (*Castanea sativa* Miller) in the Czech Republic. *Interdiscip. Archaeol.* 2:163–76
81. Kirchdoerfer RN, Garner AL, Flack CE, Mee JM, Horswill AR, et al. 2011. Structural basis for ligand recognition and discrimination of a quorum-quenching antibody. *J. Biol. Chem.* 286:17351-8
82. Lacroix D, Prado S, Deville A, Krief S, Dumontet V, et al. 2009. Hydroperoxy-cycloartane triterpenoids from the leaves of *Markhamia lutea*, a plant ingested by wild chimpanzees. *Phytochemistry* 70:1239-45
83. Banskota AH, Tezuka Y, Tran KQ, Tanaka K, Saiki I, Kadota S. 2000. Thirteen novel cycloartane-type triterpenes from *Combretum quadrangulare*. *J. Nat. Prod.* 63:57-64
84. Cabrera G, Gallo M, M. Seldes A. 1996. Cycloartane derivatives from *Tillandsia usneoides*. *J. Nat. Prod.* 59:343-7
85. Kato T, Frei B, Heinrich M, Sticher O. 1996. Antibacterial hydroperoxysterols from *Xanthosoma robustum*. *Phytochemistry* 41:1191-5
86. Luo HF, Li Q, Yu S, Badger TM, Fang N. 2005. Cytotoxic hydroxylated triterpene alcohol ferulates from rice bran. *J. Nat. Prod.* 68:94-7
87. Sheu J-H, Huang S-Y, Duh C-Y. 1996. Cytotoxic oxygenated desmosterols of the red alga *Galaxaura marginata*. *J. Nat. Prod.* 59:23-6
88. Cabrera GM, Seldes AM. 1995. Hydroperoxycycloartanes from *Tillandsia recurvata*. *J. Nat. Prod.* 58:1920-4
89. Wasserman HH, Ives JL. 1981. Singlet oxygen in organic synthesis. *Tetrahedron* 37:1825-52
90. Nickon A, Bagli JF. 1961. Reactivity and geometry in allylic systems. I. Stereochemistry of photosensitized oxygenation of monoölefins. *J. Am. Chem. Soc.* 83:1498-508
91. Prein M, Adam W. 1996. The Schenck Ene Reaction: diastereoselective oxyfunctionalization with singlet oxygen in synthetic applications. *Angew. Chem. Int. Ed. Engl.* 35:477-94
92. Clennan EL. 2000. New mechanistic and synthetic aspects of singlet oxygen chemistry. *Tetrahedron* 56:9151-79
93. Matsushita S, Terao J. 1980. Singlet oxygen-initiated photooxidation of unsaturated fatty acid esters and inhibitory effects of tocopherols and β-carotene. In *Autoxidation in Food and Biological Systems*, ed. S M.G., K M. Boston, MA: Springer. Number of.
94. Yamauchi R, Kojima M, Isogai M, Kato K, Ueno Y. 1982. Chlorophyll-sensitized photooxidation products of spinach galactolipids. *Agric. Biol. Chem.* 46:2815-20
95. Kenney RL, Fisher GS. 1959. Photosensitized oxidation of myrcene. *J. Am. Chem. Soc.* 81:4288-91
96. Popova MP, Chinou IB, Marekov IN, Bankova VS. 2009. Terpenes with antimicrobial activity from *Cretan propolis*. *Phytochemistry* 70:1262-71
97. Ruekberg B. 2020. A Closer Examination of the Mechanism of the Hydrogen Peroxide Iodine-Clock Reaction with Respect to the Role of Hypoiodite Species. *Journal of Chemical Education* 97:1688-93
98. Schenck GO. 1948. Zur Theorie der photosensibilisierten Reaktion mit molekularem Sauerstoff. *Naturwissenschaften* 35:28-9

99. Schenck GO, Neumüller O-A. 1958. Zur photosensibilisierten Autoxydation der Steroide. Synthese tertiärer Steroid-hydroperoxyde, insbesondere des: Δ6-Allopregnen-3β-ol-20-on-5α-hydroperoxyds. *Justus Liebigs Ann Chem* 618:194-201
100. Fourrey JL, Rondest J, Polonsky J. 1970. Sur quelques oxydations de type biogénétique. *Tetrahedron* 26:3839-47
101. Krieg M, Whitten DG. 1984. Self-sensitized photooxidation of protoporphyrin IX and related free-base porphyrins in natural and model membrane systems. Evidence for novel photooxidation pathways involving amino acids. *J Am Chem Soc* 106:2477-9
102. Boskou D. 2011. Olive Oil. In *Vegetable Oils in Food Technology*, ed. FD Gunstone:243-71. Number of 243-71 pp.
103. Huang SC, Hung CF, Wu WB, Chen BH. 2008. Determination of chlorophylls and their derivatives in *Gynostemma pentaphyllum* Makino by liquid chromatography–mass spectrometry. *J Pharm Biomed Anal* 48:105-12
104. Gauthier-Jaques A, Bortlik K, Hau J, Fay LB. 2001. Improved method to track chlorophyll degradation. *J Agric Food Chem* 49:1117-22
105. Zvezdanović J, Petrovic S, Marković D, AndjelkoviĆ T, AndjelkoviĆ D. 2014. Electrospray ionization mass spectrometry combined with ultra high performance liquid chromatography in the analysis of in vitro formation of chlorophyll complexes with copper and zinc. *J Serb Chem Soc* 79
106. WHO. 2003. World Health Organization guidelines on good agricultural and collection practices (GACP) for medicinal plants, Geneva, Switzerland
107. 2019. *SERNEC Data Portal*. http//:sernecportal.org/portal/index.php
108. Pignatti S. 2002. *Flora d'Italia*. Bologna, Italy: Edizioni Edagricole
109. Caputo M, Lyles JT, Salazar MS, Quave CL. 2020. LEGO MINDSTORMS Fraction Collector: A low-cost tool for a preparative high-performance liquid chromatography system. *Anal. Chem.* 92:1687-90
110. WHO. 2020. *Public Health Importance of Antimicrobial Resistance*. https://www.who.int/drugresistance/AMR_Importance/en/
111. Rello J, Parisella FR, Perez A. 2019. Alternatives to antibiotics in an era of difficult-to-treat resistance: new insights. *Expert Rev. Clin. Pharmacol.* 12:635-42
112. Tyers M, Wright GD. 2019. Drug combinations: a strategy to extend the life of antibiotics in the 21st century. *Nat. Rev. Microbiol.* 17:141-55
113. Alford MA, Pletzer D, Hancock REW. 2019. Dismantling the bacterial virulence program. *Microb. Biotechnol.* 12:409-13
114. Fleitas Martínez O, Cardoso MH, Ribeiro SM, Franco OL. 2019. Recent advances in anti-virulence therapeutic strategies with a focus on dismantling bacterial membrane microdomains, toxin neutralization, quorum-sensing interference and biofilm inhibition. *Front. Cell Infect. Microbiol.* 9:74
115. Wu S-C, Liu F, Zhu K, Shen J-Z. 2019. Natural products that target virulence factors in antibiotic-resistant *Staphylococcus aureus*. *J. Agric. Food Chem.* 67:13195-211
116. Tan L, Li SR, Jiang B, Hu XM, Li S. 2018. Therapeutic targeting of the *Staphylococcus aureus* accessory gene regulator (*agr*) system. *Front. Microbiol.* 9:55
117. Salam A, Quave C. 2018. Targeting virulence in *Staphylococcus aureus* by chemical inhibition of the accessory gene regulator system *in vivo*. *mSphere* 3:e00500-17
118. O'Riordan K, Lee JC. 2004. *Staphylococcus aureus* capsular polysaccharides. *Clin. Microbiol. Rev.* 17:218-34

119. Foster TJ, Geoghegan JA, Ganesh VK, Höök M. 2014. Adhesion, invasion and evasion: the many functions of the surface proteins of *Staphylococcus aureus*. *Nat. Rev. Microbiol.* 12:49-62
120. Lin Y-C, Peterson ML. 2010. New insights into the prevention of staphylococcal infections and toxic shock syndrome. *Expert Rev. Clin. Pharmacol.* 3:753-67
121. Otto M. 2014. *Staphylococcus aureus* toxins. *Curr. Opin. Microbiol.* 17:32-7
122. Fraser J, Arcus V, Kong P, Baker E, Proft T. 2000. Superantigens – powerful modifiers of the immune system. *Mol. Med. Today* 6:125-32
123. Quave CL, Horswill AR. 2014. Flipping the switch: tools for detecting small molecule inhibitors of staphylococcal virulence. *Frontiers in microbiology* 5:706
124. Boles BR, Thoendel M, Roth AJ, Horswill AR. 2010. Identification of genes involved in polysaccharide-independent *Staphylococcus aureus* biofilm formation. *PLoS One* 5:e10146
125. Olson ME, Nygaard TK, Ackermann L, Watkins RL, Zurek OW, et al. 2013. Staphylococcus aureus nuclease is an SaeRS-dependent virulence factor. *Infect. Immun.* 81:1316-24
126. McDougal LK, Steward CD, Killgore GE, Chaitram JM, McAllister SK, Tenover FC. 2003. Pulsed-Field Gel Electrophoresis Typing of Oxacillin-Resistant Staphylococcus aureus Isolates from the United States: Establishing a National Database. *Journal of Clinical Microbiology* 41:5113-20
127. Beenken KE, Blevins JS, Smeltzer MS. 2003. Mutation of sarA in *Staphylococcus aureus* limits biofilm formation. *Infection and immunity* 71:4206-11
128. Peschel A, Otto M. 2013. Phenol-soluble modulins and staphylococcal infection. *Nat. Rev. Microbiol.* 11:667-73
129. Otto M. 2014. Phenol-soluble modulins. *Zentralbl. Bakteriol.* 304:164-9
130. Dinges MM, Orwin PM, Schlievert PM. 2000. Exotoxins of *Staphylococcus aureus*. *Clin. Microbiol. Rev.* 13:16-34
131. Yao Y, Sturdevant DE, Otto M. 2005. Genomewide analysis of gene expression in *Staphylococcus epidermidis* biofilms: Insights into the pathophysiology of *S. epidermidis* biofilms and the role of phenol-soluble modulins in formation of biofilms. *J. Infect. Dis.* 191:289-98
132. Dunman PM, Murphy E, Haney S, Palacios D, Tucker-Kellogg G, et al. 2001. Transcription profiling-based identification of *Staphylococcus aureus* genes regulated by the *agr* and/or sarA loci. *J. Bacteriol.* 183:7341-53
133. Queck SY, Jameson-Lee M, Villaruz AE, Bach T-HL, Khan BA, et al. 2008. RNAIII-independent target gene control by the *agr* quorum-sensing system: insight into the evolution of virulence regulation in *Staphylococcus aureus*. *Mol. Cell* 32:150-8
134. Periasamy S, Joo H-S, Duong AC, Bach T-HL, Tan VY, et al. 2012. How *Staphylococcus aureus* biofilms develop their characteristic structure. *Proc. Natl. Acad. Sci. U. S. A.* 109:1281-6
135. Vuong C, Kocianova S, Yao Y, Carmody AB, Otto M. 2004. Increased colonization of indwelling medical devices by quorum-sensing mutants of *Staphylococcus epidermidis in vivo*. *J. Infect. Dis.* 190:1498-505
136. Muhs A, Lyles JT, Parlet CP, Nelson K, Kavanaugh JS, et al. 2017. Virulence inhibitors from Brazilian Peppertree block quorum sensing and abate dermonecrosis in skin infection models. *Sci. Rep.* 7:42275
137. Dinda B, Debnath S, Mohanta BC, Harigaya Y. 2010. Naturally occurring triterpenoid saponins. *Chem. Biodivers.* 7:2327-580
138. Vil VA, Terent'ev AO, Savidov N, Gloriozova TA, Poroikov VV, et al. 2019. Hydroperoxy steroids and triterpenoids derived from plant and fungi: Origin, structures and biological activities. *J. Steroid Biochem. Mol. Biol.* 190:76-87

139. Tang H, Porras G, Brown MM, Chassagne F, Lyles JT, et al. 2020. Triterpenoid acids isolated from *Schinus terebinthifolia* fruits reduce *Staphylococcus aureus* virulence and abate dermonecrosis. *Sci. Rep.* 10:8046
140. Parlet CP, Kavanaugh JS, Crosby HA, Raja HA, El-Elimat T, et al. 2019. Apicidin attenuates MRSA virulence through quorum-sensing inhibition and enhanced host defense. *Cell Rep.* 27:187-98.e6
141. Todd DA, Parlet CP, Crosby HA, Malone CL, Heilmann KP, et al. 2017. Signal biosynthesis inhibition with ambuic acid as a strategy to target antibiotic-resistant infections. *Antimicrob. Agents Chemother.* 61:e00263-17
142. Dengler V, Meier PS, Heusser R, Berger-Bächi B, McCallum N. 2011. Induction kinetics of the *Staphylococcus aureus* cell wall stress stimulon in response to different cell wall active antibiotics. *BMC Microbiol.* 11:16
143. Attia AS, Benson MA, Stauff DL, Torres VJ, Skaar EP. 2010. Membrane damage elicits an immunomodulatory program in *Staphylococcus aureus*. *PLoS Pathog.* 6:e1000802
144. Hershkovits AS, Pozdnyakov I, Meir O, Mor A. 2019. Sub-inhibitory membrane damage undermines *Staphylococcus aureus* virulence. *Biochim. Biophys. Acta Biomembr.* 1861:1172-9
145. Waters EM, Rudkin JK, Coughlan S, Clair GC, Adkins JN, et al. 2016. Redeploying β-lactam antibiotics as a novel antivirulence strategy for the treatment of methicillin-resistant *Staphylococcus aureus* infections. *J. Infect. Dis.* 215:80-7
146. Rodrigues T, Reker D, Schneider P, Schneider G. 2016. Counting on natural products for drug design. *Nat. Chem.* 8:531-41
147. Morrison KC, Hergenrother PJ. 2014. Natural products as starting points for the synthesis of complex and diverse compounds. *Nat. Prod. Rep.* 31:6-14
148. Hamel PB, Chiltoskey MU. 1975. *Cherokee Plants and Their Uses -- A 400 Year History*. Sylva, NC: Herald Publishing Co. 29 pp.
149. Taylor LA. 1940. *Plants Used As Curatives by Certain Southeastern Tribes*. pp 16. Cambridge, MA: Botanical Museum of Harvard University
150. Tantaquidgeon G. 1972. *Folk Medicine of the Delaware and Related Algonkian Indians*. pp 128. Harrisburg, PA: Pennsylvania Historical Commission Anthropological Papers #3
151. Tantaquidgeon G. 1928. Mohegan Medicinal Practices, Weather-Lore and Superstitions. In *Forty-third Annual Report of the Bureau of American Ethnology*:265. Number of 265 pp.
152. Gillaspy AF, Hickmon SG, Skinner RA, Thomas JR, Nelson CL, Smeltzer MS. 1995. Role of the accessory gene regulator (agr) in pathogenesis of staphylococcal osteomyelitis. *Infect. Immun.* 63:3373-80
153. M100. 2019. *Performance Standards for Antimicrobial Susceptibility Testing*. Clinical and Laboratory Standards Institute
154. Figueroa M, Jarmusch AK, Raja HA, El-Elimat T, Kavanaugh JS, et al. 2014. Polyhydroxyanthraquinones as quorum sensing inhibitors from the guttates of *Penicillium restrictum* and their analysis by desorption electrospray ionization mass spectrometry. *J. Nat. Prod.* 77:1351-8
155. Quave CL, Horswill AR. 2018. Identification of Staphylococcal Quorum Sensing Inhibitors by Quantification of õ-Hemolysin with High Performance Liquid Chromatography. In *Quorum Sensing: Methods and Protocols*, ed. L Leoni, G Rampioni:363-70. New York, NY: Springer New York. Number of 363-70 pp.
156. Atanasov AG, Waltenberger B, Pferschy-Wenzig EM, Linder T, Wawrosch C, et al. 2015. Discovery and resupply of pharmacologically active plant-derived natural products: A review. *Biotechnology advances* 33:1582-614

157. Newman DJ, Cragg GM. 2020. Natural Products as Sources of New Drugs over the Nearly Four Decades from 01/1981 to 09/2019. *Journal of natural products* 83:770-803
158. Lewis WH, Elvin-Lewis MP. 2003. *Medical botany: plants affecting human health*. John Wiley & Sons
159. Harvey AL, Edrada-Ebel R, Quinn RJ. 2015. The re-emergence of natural products for drug discovery in the genomics era. *Nature reviews. Drug discovery* 14:111-29
160. Shen B. 2015. A new golden age of natural products drug discovery. *Cell* 163:1297-300
161. Szychowski J, Truchon JF, Bennani YL. 2014. Natural products in medicine: transformational outcome of synthetic chemistry. *Journal of medicinal chemistry* 57:9292-308
162. Maier ME. 2015. Design and synthesis of analogues of natural products. *Organic & biomolecular chemistry* 13:5302-43
163. Henrich CJ, Beutler JA. 2013. Matching the power of high throughput screening to the chemical diversity of natural products. *Nat Prod Rep* 30:1284-98
164. Wilson BAP, Thornburg CC, Henrich CJ, Grkovic T, O'Keefe BR. 2020. Creating and screening natural product libraries. *Natural Product Reports* 37:893-918
165. Wagenaar MM. 2008. Pre-fractionated microbial samples--the second generation natural products library at Wyeth. *Molecules (Basel, Switzerland)* 13:1406-26
166. Appleton DR, Buss AD, Butler MS. 2007. A simple method for high-throughput extract prefractionation for biological screening. *CHIMIA* 61:327-31
167. Sarker SD, Nahar L. 2012. An introduction to natural products isolation. *Methods in molecular biology (Clifton, N.J.)* 864:1-25
168. Quinn RA, Nothias LF, Vining O, Meehan M, Esquenazi E, Dorrestein PC. 2017. Molecular Networking As a Drug Discovery, Drug Metabolism, and Precision Medicine Strategy. *Trends Pharmacol Sci* 38:143-54
169. Fox Ramos AE, Evanno L, Poupon E, Champy P, Beniddir MA. 2019. Natural products targeting strategies involving molecular networking: different manners, one goal. *Natural product reports* 36:960-80
170. Rossiter SE, Fletcher MH, Wuest WM. 2017. Natural products as platforms to overcome antibiotic resistance. *Chemical reviews* 117:12415-74
171. UN. 2011. *United Nations Convention on Biological Diversity: Nagoya Protocol*. Montreal: Secretariat of the Convention on Biological Diversity
172. Yarwood JM. 2003. Quorum sensing in *Staphylococcus* infections. *J Clin Invest* 112:1620-5
173. Yang G, Cheng H, Liu C, Xue Y, Gao Y, et al. 2003. Inhibition of Staphylococcus aureus pathogenesis in vitro and in vivo by RAP-binding peptides. *Peptides* 24:1823-8
174. Reuter K, Steinbach A, Helms V. 2016. Interfering with bacterial quorum sensing. *Perspectives in medicinal chemistry* 8:1-15
175. Clatworthy AE, Pierson E, Hung DT. 2007. Targeting virulence: a new paradigm for antimicrobial therapy. *Nature chemical biology* 3:541-8
176. LaSarre B, Federle MJ. 2013. Exploiting quorum sensing to confuse bacterial pathogens. *Microbiology and molecular biology reviews : MMBR* 77:73-111
177. Yang NJ, Hinner MJ. 2015. Getting Across the Cell Membrane: An Overview for Small Molecules, Peptides, and Proteins. In *Site-Specific Protein Labeling: Methods and Protocols*, ed. A Gautier, MJ Hinner:29-53. New York, NY: Springer New York. Number of 29-53 pp.
178. Zhou Y, Joubran C, Miller-Vedam L, Isabella V, Nayar A, et al. 2015. Thinking Outside the "Bug": A Unique Assay To Measure Intracellular Drug Penetration in Gram-Negative Bacteria. *Analytical Chemistry* 87:3579-84

179. Bhat J, Narayan A, Venkatraman J, Chatterji M. 2013. LC–MS based assay to measure intracellular compound levels in Mycobacterium smegmatis: Linking compound levels to cellular potency. *Journal of Microbiological Methods* 94:152-8
180. Srivastava SK, Rajasree K, Fasim A, Arakere G, Gopal B. 2014. Influence of the AgrC-AgrA complex on the response time of Staphylococcus aureus quorum sensing. *Journal of Bacteriology* 196:2876-88
181. Kavanaugh JS, Thoendel M, Horswill AR. 2007. A role for type I signal peptidase in Staphylococcus aureus quorum sensing. *Molecular microbiology* 65:780-98
182. Junio HA, Todd DA, Ettefagh KA, Ehrmann BM, Kavanaugh JS, et al. 2013. Quantitative analysis of autoinducing peptide I (AIP-I) from Staphylococcus aureus cultures using ultrahigh performance liquid chromatography-high resolving power mass spectrometry. *Journal of chromatography. B, Analytical technologies in the biomedical and life sciences* 930:7-12
183. Todd DA, Parlet CP, Crosby HA, Malone CL, Heilmann KP, et al. 2017. Signal biosynthesis inhibition with ambuic acid as a strategy to target antibiotic-resistant infections. *Antimicrobial agents and chemotherapy* 61
184. White MJ, Boyd JM, Horswill AR, Nauseef WM. 2014. Phosphatidylinositol-Specific Phospholipase C Contributes to Survival of Staphylococcus aureus USA300 in Human Blood and Neutrophils. *Infection and Immunity* 82:1559-71
185. Dettweiler M, Melander RJ, Porras G, Risener C, Marquez L, et al. 2020. A Clerodane Diterpene from Callicarpa americana Resensitizes Methicillin-Resistant Staphylococcus aureus to β-Lactam Antibiotics. *ACS Infectious Diseases* 6:1667-73
186. Rand KH, Houck HJ, Brown P, Bennett D. 1993. Reproducibility of the microdilution checkerboard method for antibiotic synergy. *Antimicrob Agents Chemother* 37:613-5
187. Smith RA, M'Ikanatha N M, Read AF. 2015. Antibiotic resistance: a primer and call to action. *Health communication* 30:309-14
188. Mandal SM, Ghosh AK, Pati BR. 2015. Dissemination of antibiotic resistance in methicillin-resistant *Staphylococcus aureus* and vancomycin-resistant *S aureus* strains isolated from hospital effluents. *American journal of infection control* 43:e87-8
189. Morales G, Picazo JJ, Baos E, Candel FJ, Arribi A, et al. 2010. Resistance to linezolid is mediated by the *cfr* gene in the first report of an outbreak of linezolid-resistant *Staphylococcus aureus*. *Clinical Infectious Diseases* 50:821-5
190. Gu B, Kelesidis T, Tsiodras S, Hindler J, Humphries RM. 2013. The emerging problem of linezolid-resistant *Staphylococcus*. *The Journal of antimicrobial chemotherapy* 68:4-11
191. Woodin KA, Morrison SH. 1994. Antibiotics: mechanisms of action. *Pediatrics in review / American Academy of Pediatrics* 15:440-7
192. Silva LN, Zimmer KR, Macedo AJ, Trentin DS. 2016. Plant Natural Products Targeting Bacterial Virulence Factors. *Chemical reviews* 116:9162-236
193. Scutera S, Zucca M, Savoia D. 2014. Novel approaches for the design and discovery of quorum-sensing inhibitors. *Expert opinion on drug discovery* 9:353-66
194. Vadekeetil A, Alexandar V, Chhibber S, Harjai K. 2016. Adjuvant effect of cranberry proanthocyanidin active fraction on antivirulent property of ciprofloxacin against Pseudomonas aeruginosa. *Microbial pathogenesis* 90:98-103
195. Deng Y, Lim A, Lee J, Chen S, An S, et al. 2014. Diffusible signal factor (DSF) quorum sensing signal and structurally related molecules enhance the antimicrobial efficacy of antibiotics against some bacterial pathogens. *BMC microbiology* 14:51

196. Jabra-Rizk MA, Meiller TF, James CE, Shirtliff ME. 2006. Effect of farnesol on Staphylococcus aureus biofilm formation and antimicrobial susceptibility. *Antimicrobial agents and chemotherapy* 50:1463-9
197. van der Meer JW, Fears R, Davies SC, ter Meulen V. 2014. Antimicrobial innovation: combining commitment, creativity and coherence. *Nature reviews. Drug discovery* 13:709-10
198. Thabit AK, Crandon JL, Nicolau DP. 2015. Antimicrobial resistance: impact on clinical and economic outcomes and the need for new antimicrobials. *Expert opinion on pharmacotherapy* 16:159-77
199. Pieren M, Tigges M. 2012. Adjuvant strategies for potentiation of antibiotics to overcome antimicrobial resistance. *Current opinion in pharmacology* 12:551-5
200. Wright GD. 2016. Antibiotic adjuvants: Rescuing antibiotics from resistance. *Trends in microbiology* 24:862-71
201. Johnson BK, Abramovitch RB. 2017. Small molecules that sabotage bacterial virulence. *Trends in pharmacological sciences* 38:339-62
202. DeCorte BL. 2016. Underexplored opportunities for natural products in drug discovery. *Journal of medicinal chemistry* 59:9295-304
203. Wetzel S, Bon RS, Kumar K, Waldmann H. 2011. Biology-oriented synthesis. *Angewandte Chemie (International ed. in English)* 50:10800-26
204. Kellenberger E, Hofmann A, Quinn RJ. 2011. Similar interactions of natural products with biosynthetic enzymes and therapeutic targets could explain why nature produces such a large proportion of existing drugs. *Nat Prod Rep* 28:1483-92
205. Quinn RJ, Carroll AR, Pham NB, Baron P, Palframan ME, et al. 2008. Developing a drug-like natural product library. *Journal of natural products* 71:464-8
206. Morrison KC, Hergenrother PJ. 2014. Natural products as starting points for the synthesis of complex and diverse compounds. *Nat Prod Rep* 31:6-14
207. Wright GD. 2017. Opportunities for natural products in 21(st) century antibiotic discovery. *Nat Prod Rep* 34:694-701
208. Rahman MM, Shiu WKP, Gibbons S, Malkinson JP. 2018. Total synthesis of acylphloroglucinols and their antibacterial activities against clinical isolates of multi-drug resistant (MDR) and methicillin-resistant strains of *Staphylococcus aureus*. *European journal of medicinal chemistry* 155:255-62
209. Song M, Teng Z, Li M, Niu X, Wang J, Deng X. 2017. Epigallocatechin gallate inhibits *Streptococcus pneumoniae* virulence by simultaneously targeting pneumolysin and sortase A. *Journal of cellular and molecular medicine* 21:2586-98
210. Brackman G, Garcia-Fernandez MJ, Lenoir J, De Meyer L, Remon JP, et al. 2016. Dressings loaded with cyclodextrin-hamamelitannin complexes increase *Staphylococcus aureus* susceptibility toward antibiotics both in single as well as in mixed biofilm communities. *Macromolecular bioscience* 16:859-69
211. Vermote A, Brackman G, Risseeuw MDP, Coenye T, Van Calenbergh S. 2017. Novel hamamelitannin analogues for the treatment of biofilm related MRSA infections-A scaffold hopping approach. *European journal of medicinal chemistry* 127:757-70
212. Vivanco JM, Bais HP, Stermitz FR, Thelen G, Callaway R. 2004. Biogeographical variation in community response to root allelochemistry: Novel weapons and exotic invasion. *Ecol Lett* 7:285-92
213. Enquist PA, Gylfe A, Hagglund U, Lindstrom P, Norberg-Scherman H, et al. 2012. Derivatives of 8-hydroxyquinoline--antibacterial agents that target intra- and extracellular Gram-negative pathogens. *Bioorganic & medicinal chemistry letters* 22:3550-3

214. Anantharajah A, Faure E, Buyck JM, Sundin C, Lindmark T, et al. 2016. Inhibition of the injectisome and flagellar type III secretion systems by INP1855 impairs *Pseudomonas aeruginosa* pathogenicity and inflammasome activation. *J Infect Dis Med* 214:1105-16
215. Jarvis C, Han Z, Kalas V, Klein R, Pinkner JS, et al. 2016. Antivirulence isoquinolone mannosides: Optimization of the biaryl aglycone for FimH lectin binding affinity and efficacy in the treatment of chronic UTI. *ChemMedChem* 11:367-73
216. Cushnie TP, Cushnie B, Lamb AJ. 2014. Alkaloids: an overview of their antibacterial, antibiotic-enhancing and antivirulence activities. *International journal of antimicrobial agents* 44:377-86
217. Nait Chabane Y, Mlouka MB, Alexandre S, Nicol M, Marti S, et al. 2014. Virstatin inhibits biofilm formation and motility of *Acinetobacter baumannii*. *BMC microbiology* 14:62
218. Willis KJ, ed. 2017. *State of the World's Plants Report*. London, England: Royal Botanic Gardens, Kew.
219. Tu Y. 2011. The discovery of artemisinin (qinghaosu) and gifts from Chinese medicine. *Nature medicine* 17:1217-20
220. de la Parra J, Quave CL. 2017. Ethnophytotechnology: Harnessing the power of ethnobotany with biotechnology. *Trends in biotechnology* 35:802-6
221. Seidel V. 2012. Initial and bulk extraction of natural products isolation. *Methods in molecular biology (Clifton, N.J.)* 864:27-41
222. Patwardhan B, Mashelkar RA. 2009. Traditional medicine-inspired approaches to drug discovery: can Ayurveda show the way forward? *Drug discovery today* 14:804-11
223. Wagner H, Ulrich-Merzenich G. 2009. Synergy research: approaching a new generation of phytopharmaceuticals. *Phytomedicine : international journal of phytotherapy and phytopharmacology* 16:97-110
224. FDA. 2016. Guidance for Industry: Botanical Drug Products. ed. CfDEa Research: US Department of Health and Human Services, Food and Drug Administration
225. Allard PM, Genta-Jouve G, Wolfender JL. 2017. Deep metabolome annotation in natural products research: towards a virtuous cycle in metabolite identification. *Current opinion in chemical biology* 36:40-9
226. Ngo LT, Okogun JI, Folk WR. 2013. 21st Century natural product research and drug development and traditional medicines. *Nat Prod Rep* 30:584-92
227. Seger C, Sturm S, Stuppner H. 2013. Mass spectrometry and NMR spectroscopy: modern high-end detectors for high resolution separation techniques--state of the art in natural product HPLC-MS, HPLC-NMR, and CE-MS hyphenations. *Nat Prod Rep* 30:970-87
228. Rathahao-Paris E, Alves S, Junot C, Tabet J-C. 2015. High resolution mass spectrometry for structural identification of metabolites in metabolomics. *Metabolomics* 12:10
229. Breton RC, Reynolds WF. 2013. Using NMR to identify and characterize natural products. *Nat Prod Rep* 30:501-24
230. Klein-Junior LC, Cretton S, Allard PM, Genta-Jouve G, Passos CS, et al. 2017. Targeted isolation of monoterpene indole alkaloids from *Palicourea sessilis*. *Journal of natural products* 80:3032-7
231. Wang M, Carver JJ, Phelan VV, Sanchez LM, Garg N, et al. 2016. Sharing and community curation of mass spectrometry data with Global Natural Products Social Molecular Networking. *Nature biotechnology* 34:828-37
232. Kenny CR, Furey A, Lucey B. 2015. A post-antibiotic era looms: can plant natural product research fill the void? *British journal of biomedical science* 72:191-200
233. Cragg GM, Newman DJ. 2013. Natural products: a continuing source of novel drug leads. *Biochimica et biophysica acta* 1830:3670-95

234. WHO. 2003. *WHO Guidelines on Good Agricultural and Collection Practices (GACP) for Medicinal Plants*. http://apps.who.int/medicinedocs/en/d/Js4928e/
235. Bijttebier S, Van der Auwera A, Foubert K, Voorspoels S, Pieters L, Apers S. 2016. Bridging the gap between comprehensive extraction protocols in plant metabolomics studies and method validation. *Anal Chim Acta* 935:136-50
236. Sturm S, Seger C. 2012. Liquid chromatography-nuclear magnetic resonance coupling as alternative to liquid chromatography-mass spectrometry hyphenations: curious option or powerful and complementary routine tool? *J Chromatogr A* 1259:50-61
237. Sarker SD, Nahar L. 2012. Hyphenated techniques and their applications in natural products analysis. *Methods in Molecular Biology* 864:301-40
238. Handra SS, Khanuja SPS, Longo G, Rakesh DD. 2008. *Extraction technologies for medicinal and aromatic plants*. Trieste, Italy: United Nations Industrial Development Organization and the International Centre for Science and High Technology
239. Jones WP, Kinghorn AD. 2012. Extraction of plant secondary metabolites. *Methods in Molecular Biology* 864:341-66
240. Nafiu MO, Hamid AA, Muritala HF, Adeyemi SB. 2017. Preparation, Standardization, and Quality Control of Medicinal Plants in Africa. In *Medicinal Spices and Vegetables from Africa*:171-204: Academic Press. Number of 171-204 pp.
241. Luque de Castro MD, Priego-Capote F. 2010. Soxhlet extraction: Past and present panacea. *J Chromatogr A* 1217:2383-9
242. McCloud TG. 2010. High throughput extraction of plant, marine and fungal specimens for preservation of biologically active molecules. *Molecules (Basel, Switzerland)* 15:4526-63
243. Chemat F, Rombaut N, Sicaire AG, Meullemiestre A, Fabiano-Tixier AS, Abert-Vian M. 2017. Ultrasound assisted extraction of food and natural products. Mechanisms, techniques, combinations, protocols and applications. A review. *Ultrasonics sonochemistry* 34:540-60
244. Tongnuanchan P, Benjakul S. 2014. Essential oils: extraction, bioactivities, and their uses for food preservation. *J Food Sci* 79:R1231-49
245. El Asbahani A, Miladi K, Badri W, Sala M, Ait Addi EH, et al. 2015. Essential oils: from extraction to encapsulation. *Int J Pharm* 483:220-43
246. Herrero M, Mendiola JA, Cifuentes A, Ibanez E. 2010. Supercritical fluid extraction: Recent advances and applications. *J Chromatogr A* 1217:2495-511
247. Capuzzo A, Maffei ME, Occhipinti A. 2013. Supercritical fluid extraction of plant flavors and fragrances. *Molecules (Basel, Switzerland)* 18:7194-238
248. Fornari T, Vicente G, Vazquez E, Garcia-Risco MR, Reglero G. 2012. Isolation of essential oil from different plants and herbs by supercritical fluid extraction. *J Chromatogr A* 1250:34-48
249. Pourmortazavi SM, Hajimirsadeghi SS. 2007. Supercritical fluid extraction in plant essential and volatile oil analysis. *J Chromatogr A* 1163:2-24
250. Stenholm A, Goransson U, Bohlin L. 2013. Bioassay-guided supercritical fluid extraction of cyclooxygenase-2 inhibiting substances in *Plantago major* L. *Phytochem Anal* 24:176-83
251. Mottaleb MA, Sarker SD. 2012. Accelerated solvent extraction for natural products isolation. *Methods in Molecular Biology* 864:75-87
252. Sun H, Ge X, Lv Y, Wang A. 2012. Application of accelerated solvent extraction in the analysis of organic contaminants, bioactive and nutritional compounds in food and feed. *J Chromatogr A* 1237:1-23
253. Chan CH, Yusoff R, Ngoh GC, Kung FW. 2011. Microwave-assisted extractions of active ingredients from plants. *J Chromatogr A* 1218:6213-25

254. Zhou T, Xiao X, Li G. 2012. Microwave accelerated selective Soxhlet extraction for the determination of organophosphorus and carbamate pesticides in ginseng with gas chromatography/mass spectrometry. *Analytical chemistry* 84:5816-22
255. Garcia-Ayuso LE, Sanchez M, Fernandez de Alba A, Luque de Castro MD. 1998. Focused microwave-assisted soxhlet: an advantageous tool for sample extraction. *Analytical chemistry* 70:2426-31
256. Wang H, Yang L, Zu Y, Zhao X. 2014. Microwave-assisted simultaneous extraction of luteolin and apigenin from tree peony pod and evaluation of its antioxidant activity. *Sci World J* 2014:506971
257. Mussatto SI. 2015. Microwave-assisted extraction of fucoidan from marine algae. *Methods in Molecular Biology* 1308:151-7
258. Rodriguez-Solana R, Salgado JM, Dominguez JM, Cortes-Dieguez S. 2015. Comparison of Soxhlet, accelerated solvent and supercritical fluid extraction techniques for volatile (GC-MS and GC/FID) and phenolic compounds (HPLC-ESI/MS/MS) from Lamiaceae species. *Phytochem Anal* 26:61-71
259. Shen J, Shao X. 2005. A comparison of accelerated solvent extraction, Soxhlet extraction, and ultrasonic-assisted extraction for analysis of terpenoids and sterols in tobacco. *Anal Bioanal Chem* 383:1003-8
260. Wang W, Meng B, Lu X, Liu Y, Tao S. 2007. Extraction of polycyclic aromatic hydrocarbons and organochlorine pesticides from soils: a comparison between Soxhlet extraction, microwave-assisted extraction and accelerated solvent extraction techniques. 602:211-22
261. Punin Crespo MO, Lage Yusty MA. 2005. Comparison of supercritical fluid extraction and Soxhlet extraction for the determination of PCBs in seaweed samples. *Chemosphere* 59:1407-13
262. Jurado-Sanchez B, Ballesteros E, Gallego M. 2013. Comparison of microwave assisted, ultrasonic assisted and Soxhlet extractions of N-nitrosamines and aromatic amines in sewage sludge, soils and sediments. *Sci Total Environ* 463-464:293-301
263. Stevens WC, Jr., Hill DC. 2009. General methods for flash chromatography using disposable columns. *Mol Divers* 13:247-52
264. Lloyd L, Ball S, Mapp K. 2010. *Is There Really a Difference Between Flash and HPLC for LC Purification?* http://www.chromatographyonline.com/there-really-difference-between-flash-and-hplc-lc-purification?id=&pageID=1&sk=&date=
265. Muhs A, Lyles JT, Parlet CP, Nelson K, Kavanaugh JS, et al. 2017. Virulence inhibitors from Brazilian Peppertree block quorum sensing and abate dermonecrosis in skin infection models. *Scientific reports* 7:42275
266. Moosmann B, Kneisel S, Wohlfarth A, Brecht V, Auwarter V. 2013. A fast and inexpensive procedure for the isolation of synthetic cannabinoids from 'Spice' products using a flash chromatography system. 405:3929-35
267. Liang ZK, Huang RG, Xie ZS, Xu XJ. 2015. Preparative isolation of paclitaxel and related taxanes from cell cultures of *Taxus chinensis* using reversed-phase flash chromatography. *Natural product research* 29:327-30
268. Hu JF, Garo E, Yoo HD, Cremin PA, Goering MG, et al. 2005. Cyclolignans from *Scyphocephalium ochocoa* via high-throughput natural product chemistry methods. *Phytochemistry* 66:1077-82
269. Jacobson BM. 1988. An inexpensive way to do flash chromatography. *J Chem Educ* 65:459
270. USP. 2018. *United States Pharmacopeia*. Rockville, Maryland: United States Pharmacopeial Convention

271. EPC. 2016. *European Pharmacopoeia*. Strasbourg, France: European Pharmacopoeia Commission
272. CPC. 2015. *Chinese Pharmacopoeia*. Chinese Pharmacopoeia Commission
273. Ozek T, Demirci F. 2012. Isolation of natural products by preparative gas chromatography. *Methods in Molecular Biology* 864:275-300
274. Zuo HL, Yang FQ, Huang WH, Xia ZN. 2013. Preparative gas chromatography and its applications. *J Chromatogr Sci* 51:704-15
275. Rahman MM, Abd El-Aty AM, Choi J-H, Shin H-C, Shin SC, Shim J-H. 2015. Basic overview on gas chromatography columns. In *Analytical Separation Science*: Wiley-VCH Verlag GmbH & Co. . Number of.
276. Jumaah F, Plaza M, Abrahamsson V, Turner C, Sandahl M. 2016. A fast and sensitive method for the separation of carotenoids using ultra-high performance supercritical fluid chromatography-mass spectrometry. 408:5883-94
277. Wada Y, Matsubara A, Uchikata T, Iwasaki Y, Morimoto S, et al. 2011. Metabolic profiling of beta-cryptoxanthin and its fatty acid esters by supercritical fluid chromatography coupled with triple quadrupole mass spectrometry. *J Sep Sci* 34:3546-52
278. Qiao X, An R, Huang Y, Ji S, Li L, et al. 2014. Separation of 25R/S-ergostane triterpenoids in the medicinal mushroom *Antrodia camphorata* using analytical supercritical-fluid chromatography. *J Chromatogr A* 1358:252-60
279. Hartmann A, Ganzera M. 2015. Supercritical fluid chromatography--Theoretical background and applications on natural products. *Planta medica* 81:1570-81
280. Eldridge GR, Vervoort HC, Lee CM, Cremin PA, Williams CT, et al. 2002. High-throughput method for the production and analysis of large natural product libraries for drug discovery. *Analytical chemistry* 74:3963-71
281. Hajji S, Beliveau J, Simon DZ, Salvador R, Aube C, Conti A. 1984. A rapid method for the prefractionation of essential oils. Application to the essential oil of Black Spruce [*Picea Mariana* (Mill.) BSP.]. *J Liq Chromatogr* 7:2671-7
282. Bugni TS, Harper MK, McCulloch MWB, Reppart J, Ireland CM. 2008. Fractionated marine invertebrate extract libraries for drug discovery. *Molecules (Basel, Switzerland)* 13:1372-83
283. Bindseil KU, Jakupovic J, Wolf D, Lavayre J, Leboul J, van der Pyl D. 2001. Pure compound libraries; a new perspective for natural product based drug discovery. *Drug discovery today* 6:840-7
284. Tu Y, Jeffries C, Ruan H, Nelson C, Smithson D, et al. 2010. Automated high-throughput system to fractionate plant natural products for drug discovery. *Journal of natural products* 73:751-4
285. Kato N, Takahashi S, Nogawa T, Saito T, Osada H. 2012. Construction of a microbial natural product library for chemical biology studies. *Curr Op Chem Biol* 16:101-8
286. Camp D, Davis RA, Campitelli M, Ebdon J, Quinn RJ. 2012. Drug-like properties: guiding principles for the design of natural product libraries. *Journal of natural products* 75:72-81
287. Ymele-Leki P, Cao S, Sharp J, Lambert KG, McAdam AJ, et al. 2012. A high-throughput screen identifies a new natural product with broad-spectrum antibacterial activity. *PloS one* 7:e31307
288. Hashimoto J, Watanabe T, Seki T, Karasawa S, Izumikawa M, et al. 2009. Novel in vitro protein fragment complementation assay applicable to high-throughput screening in a 1536-well format. *J Biomol Screen* 14:970-9
289. Wong KC, Hag Ali DM, Boey PL. 2012. Chemical constituents and antibacterial activity of Melastoma malabathricum L. *Natural product research* 26:609-18

290. Latif Z, Sarker SD. 2012. Isolation of natural products by preparative high performance liquid chromatography (prep-HPLC). *Methods in Molecular Biology* 864:255-74
291. Houssen WE, Jaspars M. 2012. Isolation of marine natural products. *Methods in Molecular Biology* 864:367-92
292. Nahar L, Sarker SD. 2012. Supercritical fluid extraction in natural products analyses. *Methods in Molecular Biology* 864:43-74
293. Ifa DR, Wu C, Ouyang Z, Cooks RG. 2010. Desorption electrospray ionization and other ambient ionization methods: current progress and preview. *Analyst* 135:669-81
294. Badu-Tawiah AK, Eberlin LS, Ouyang Z, Cooks RG. 2013. Chemical aspects of the extractive methods of ambient ionization mass spectrometry. *Annu Rev Phys Chem* 64:481-505
295. Caprioli RM, Farmer TB, Gile J. 1997. Molecular imaging of biological samples: localization of peptides and proteins using MALDI-TOF MS. *Analytical chemistry* 69:4751-60
296. Bouslimani A, Sanchez LM, Garg N, Dorrestein PC. 2014. Mass spectrometry of natural products: current, emerging and future technologies. *Natural Product Reports* 31:718-29
297. Esquenazi E, Yang YL, Watrous J, Gerwick WH, Dorrestein PC. 2009. Imaging mass spectrometry of natural products. *Natural Product Reports* 26:1521-34
298. Jarmusch AK, Cooks RG. 2014. Emerging capabilities of mass spectrometry for natural products. *Natural Product Reports* 31:730-8
299. Purves K, Macintyre L, Brennan D, Hreggviethsson GO, Kuttner E, et al. 2016. Using molecular networking for microbial secondary metabolite bioprospecting. *Metabolites* 6
300. Winnikoff JR, Glukhov E, Watrous J, Dorrestein PC, Gerwick WH. 2014. Quantitative molecular networking to profile marine cyanobacterial metabolomes. *J Antibiot (Tokyo)* 67:105-12
301. Duncan KR, Crusemann M, Lechner A, Sarkar A, Li J, et al. 2015. Molecular networking and pattern-based genome mining improves discovery of biosynthetic gene clusters and their products from *Salinispora* species. *Chem Biol* 22:460-71
302. de B. Harrington P, Wang X. 2017. Spectral representation of proton NMR spectroscopy for the pattern recognition of complex materials. *J Anal Test* 1:10
303. Markus MA, Ferrier J, Luchsinger SM, Yuk J, Cuerrier A, et al. 2014. Distinguishing *Vaccinium* species by chemical fingerprinting based on NMR spectra, validated with spectra collected in different laboratories. *Planta medica* 80:732-9
304. Lang G, Mayhudin NA, Mitova MI, Sun L, van der Sar S, et al. 2008. Evolving trends in the dereplication of natural product extracts: new methodology for rapid, small-scale investigation of natural product extracts. *Journal of natural products* 71:1595-9
305. ACS. 2018. *SciFinder*. scifinder.cas.org
306. DNP. 2017. *Dictionary of Natural Products*. http://dnp.chemnetbase.com
307. UIC. 2015. *NAPRALERT*. www.napralert.org
308. UCSD. 2018. *GNPS*. https://gnps.ucsd.edu/ProteoSAFe/static/gnps-splash.jsp
309. RSC. 2018. *Royal Society of Chemistry: MarinLit*. http://pubs.rsc.org/marinlit/
310. Ibrahim A, Yang L, Johnston C, Liu X, Ma B, Magarvey NA. 2012. Dereplicating nonribosomal peptides using an informatic search algorithm for natural products (iSNAP) discovery. *Proceedings of the National Academy of Sciences of the United States of America* 109:19196-201
311. Mohimani H, Liu WT, Mylne JS, Poth AG, Colgrave ML, et al. 2011. Cycloquest: identification of cyclopeptides via database search of their mass spectra against genome databases. *Journal of proteome research* 10:4505-12
312. Mohimani H, Yang YL, Liu WT, Hsieh PW, Dorrestein PC, Pevzner PA. 2011. Sequencing cyclic peptides by multistage mass spectrometry. *Proteomics* 11:3642-50

313. Ng J, Bandeira N, Liu WT, Ghassemian M, Simmons TL, et al. 2009. Dereplication and de novo sequencing of nonribosomal peptides. *Nat Methods* 6:596-9
314. Exarchou V, Krucker M, van Beek TA, Vervoort J, Gerothanassis IP, Albert K. 2005. LC-NMR coupling technology: recent advancements and applications in natural products analysis. *Magn Reson Chem* 43:681-7
315. Exarchou V, Godejohann M, van Beek TA, Gerothanassis IP, Vervoort J. 2003. LC-UV-solid-phase extraction-NMR-MS combined with a cryogenic flow probe and its application to the identification of compounds present in Greek oregano. *Analytical chemistry* 75:6288-94
316. Kenny O, Smyth TJ, Hewage CM, Brunton NP, McLoughlin P. 2014. 4-hydroxyphenylacetic acid derivatives of inositol from dandelion (*Taraxacum officinale*) root characterised using LC-SPE-NMR and LC-MS techniques. *Phytochemistry* 98:197-203
317. Gu WY, Li N, Leung EL, Zhou H, Yao XJ, et al. 2015. Rapid identification of new minor chemical constituents from Smilacis Glabrae Rhizoma by combined use of UHPLC-Q-TOF-MS, preparative HPLC and UHPLC-SPE-NMR-MS techniques. *Phytochem Anal* 26:428-35
318. Wasinger Valerie C, Cordwell Stuart J, Cerpa-Poljak A, Yan JX, Gooley AA, et al. 1995. Progress with gene-product mapping of the Mollicutes: Mycoplasma genitalium. *Electrophoresis* 16:1090-4
319. Griffiths WJ, Karu K, Hornshaw M, Woffendin G, Wang Y. 2007. Metabolomics and metabolite profiling: past heroes and future developments. *Eur J Mass Spectrom (Chichester)* 13:45-50
320. Roberts LD, Souza AL, Gerszten RE, Clish CB. 2012. Targeted Metabolomics. *Curr Protoc Mol Biol* CHAPTER:Unit30.2-Unit.2
321. Chong J, Soufan O, Li C, Caraus I, Li S, et al. 2018. MetaboAnalyst 4.0: towards more transparent and integrative metabolomics analysis. *Nucleic Acids Res*:gky310-gky
322. SRI. 2018. *The Scripps Research Institute: XCMS*. https://xcmsonline.scripps.edu
323. Roessner U, Dias DA, eds. 2013. *Metabolomics Tools for Natural Product Discovery*, Vols. 1055. Totowa, NJ: Humana Press.
324. Kim Hye K, Verpoorte R. 2009. Sample preparation for plant metabolomics. *Phytochem Anal* 21:4-13
325. Garcia-Flores M, Juarez-Colunga S, Garcia-Casarrubias A, Trachsel S, Winkler R, Tiessen A. 2015. Metabolic profiling of plant extracts using direct-injection electrospray ionization mass spectrometry allows for high-throughput phenotypic characterization according to genetic and environmental effects. *Journal of agricultural and food chemistry* 63:1042-52
326. Creydt M, Fischer M. 2017. Plant metabolomics: Maximizing metabolome coverage by optimizing mobile phase additives for nontargeted mass spectrometry in positive and negative electrospray ionization mode. *Analytical chemistry* 89:10474-86
327. Gorrochategui E, Jaumot J, Lacorte S, Tauler R. 2016. Data analysis strategies for targeted and untargeted LC-MS metabolomic studies: Overview and workflow. *Trends Analyt Chem* 82:425-42
328. van den Berg RA, Hoefsloot HC, Westerhuis JA, Smilde AK, van der Werf MJ. 2006. Centering, scaling, and transformations: improving the biological information content of metabolomics data. *BMC Genomics* 7:142
329. Xia J, Wishart DS. 2011. Web-based inference of biological patterns, functions and pathways from metabolomic data using MetaboAnalyst. *Nat Protoc* 6:743
330. Commisso M, Strazzer P, Toffali K, Stocchero M, Guzzo F. 2013. Untargeted metabolomics: an emerging approach to determine the composition of herbal products. *Computational and structural biotechnology journal* 4:e201301007

331. Marston HD, Dixon DM, Knisely JM, Palmore TN, Fauci AS. 2016. Antimicrobial Resistance. *Jama* 316:1193-204
332. Mediavilla JR, Chen L, Mathema B, Kreiswirth BN. 2012. Global epidemiology of community-associated methicillin resistant *Staphylococcus aureus* (CA-MRSA). *Current Opinion in Microbiology* 15:588-95
333. Tong SYC, Davis JS, Eichenberger E, Holland TL, Fowler VG. 2015. *Staphylococcus aureus* infections: epidemiology, pathophysiology, clinical manifestations, and management. *Clinical Microbiology Reviews* 28:603-61
334. Tong SYC, Chen LF, Fowler VG. 2012. Colonization, pathogenicity, host susceptibility and therapeutics for *Staphylococcus aureus*: What is the Clinical Relevance? *Seminars in Immunopathology* 34:185-200
335. Martinez JL. 2014. General principles of antibiotic resistance in bacteria. *Drug discovery today. Technologies* 11:33-9
336. Thoendel M, Horswill AR. 2013. Random mutagenesis and topology analysis of the autoinducing peptide piosynthesis proteins in *Staphylococcus aureus*. *Molecular microbiology* 87:318-37
337. Vuong C, Saenz HL, Gotz F, Otto M. 2000. Impact of the agr quorum-sensing system on adherence to polystyrene in *Staphylococcus aureus*. *J Infect Dis* 182:1688-93
338. Passador L, Cook JM, Gambello MJ, Rust L, Iglewski BH. 1993. Expression of *Pseudomonas aeruginosa* virulence genes requires cell-to-cell communication. *Science (New York, N.Y.)* 260:1127-30
339. Yao Y, Vuong C, Kocianova S, Villaruz AE, Lai Y, et al. 2006. Characterization of the *Staphylococcus epidermidis* accessory-gene regulator response: quorum-sensing regulation of resistance to human innate host defense. *J Infect Dis* 193:841-8
340. Manna AC, Bayer MG, Cheung AL. 1998. Transcriptional analysis of different promoters in the *sar* locus in *Staphylococcus aureus*. *Journal of Bacteriology* 180:3828-36
341. Zhang L, Lin J, Ji G. 2004. Membrane anchoring of the AgrD N-terminal amphipathic region is required for its processing to produce a quorum-sensing pheromone in *Staphylococcus aureus*. *The Journal of biological chemistry* 279:19448-56
342. Wang B, Zhao A, Novick R, Muir TW. 2014. Activation and inhibition of the receptor histidine kinase AgrC occurs through opposite helical transduction motions. *Molecular cell* 53:929-40
343. Queck SY, Jameson-Lee M, Villaruz AE, Bach TH, Khan BA, et al. 2008. RNAIII-independent target gene control by the agr quorum-sensing system: insight into the evolution of virulence regulation in *Staphylococcus aureus*. *Molecular cell* 32:150-8
344. Xia J, Gao J, Kokudo N, Hasegawa K, Tang W. 2013. Methicillin-resistant *Staphylococcus aureus* antibiotic resistance and virulence. *Bioscience trends* 7:113-21
345. Regassa LB, Couch JL, Betley MJ. 1991. Steady-state staphylococcal enterotoxin type C mRNA is affected by a product of the accessory gene regulator (*agr*) and by glucose. *Infection and Immunity* 59:955-62
346. Salgado-Pabon W, Breshears L, Spaulding AR, Merriman JA, Stach CS, et al. 2013. Superantigens are critical for *Staphylococcus aureus* infective endocarditis, sepsis, and acute kidney injury. *mBio* 4
347. Khodaverdian V, Pesho M, Truitt B, Bollinger L, Patel P, et al. 2013. Discovery of antivirulence agents against methicillin-resistant *Staphylococcus aureus*. *Antimicrobial agents and chemotherapy* 57:3645-52
348. Yu G, Kuo D, Shoham M, Viswanathan R. 2014. Combinatorial synthesis and *in vitro* evaluation of a biaryl hydroxyketone library as antivirulence agents against MRSA. *ACS combinatorial science* 16:85-91

349. Belkaid Y, Naik S. 2013. Compartmentalized and systemic control of tissue immunity by commensals. *Nature immunology* 14:646-53
350. George Cisar EA, Geisinger E, Muir TW, Novick RP. 2009. Symmetric signalling within asymmetric dimers of the *Staphylococcus aureus* receptor histidine kinase AgrC. *Molecular microbiology* 74:44-57
351. Hall PR, Elmore BO, Spang CH, Alexander SM, Manifold-Wheeler BC, et al. 2013. Nox2 modification of LDL is essential for optimal apolipoprotein B-mediated control of *agr* type III *Staphylococcus aureus* quorum-sensing. *PLoS pathogens* 9:e1003166
352. Cheung GY, Wang R, Khan BA, Sturdevant DE, Otto M. 2011. Role of the accessory gene regulator agr in community-associated methicillin-resistant *Staphylococcus aureus* pathogenesis. *Infection and Immunity* 79:1927-35
353. Voyich JM, Otto M, Mathema B, Braughton KR, Whitney AR, et al. 2006. Is Panton-Valentine leukocidin the major virulence determinant in community-associated methicillin-resistant *Staphylococcus aureus* disease? *J Infect Dis* 194:1761-70
354. Waters EM, Rudkin JK, Coughlan S, Clair GC, Adkins JN, et al. 2017. Redeploying beta-lactam antibiotics as a novel antivirulence strategy for the treatment of methicillin-tesistant *Staphylococcus aureus* infections. *J Infect Dis* 215:80-7
355. Geisinger E, Muir TW, Novick RP. 2009. *agr* receptor mutants reveal distinct modes of inhibition by staphylococcal autoinducing peptides. *Proceedings of the National Academy of Sciences of the United States of America* 106:1216-21
356. Malachowa N, Kobayashi SD, Braughton KR, DeLeo FR. 2013. Mouse model of *Staphylococcus aureus* skin infection. *Methods in molecular biology (Clifton, N.J.)* 1031:109-16
357. Sun F, Liang H, Kong X, Xie S, Cho H, et al. 2012. Quorum-sensing *agr* mediates bacterial oxidation response via an intramolecular disulfide redox switch in the response regulator AgrA. *Proceedings of the National Academy of Sciences of the United States of America* 109:9095-100
358. Nicod SS, Weinzierl RO, Burchell L, Escalera-Maurer A, James EH, Wigneshweraraj S. 2014. Systematic mutational analysis of the LytTR DNA binding domain of *Staphylococcus aureus* virulence gene transcription factor AgrA. *Nucleic Acids Res* 42:12523-36
359. Cech NB, Horswill AR. 2013. Small-molecule quorum quenchers to prevent *Staphylococcus aureus* infection. *Future microbiology* 8:1511-4
360. Fowler VG, Jr., Sakoulas G, McIntyre LM, Meka VG, Arbeit RD, et al. 2004. Persistent bacteremia due to methicillin-resistant *Staphylococcus aureus* infection is associated with *agr* dysfunction and low-level in vitro resistance to thrombin-induced platelet microbicidal protein. *J Infect Dis* 190:1140-9
361. Viedma E, Sanz F, Orellana MA, San Juan R, Aguado JM, et al. 2014. Relationship between *agr* dysfunction and reduced vancomycin susceptibility in methicillin-susceptible *Staphylococcus aureus* causing bacteraemia. *The Journal of antimicrobial chemotherapy* 69:51-8
362. Schweizer ML, Furuno JP, Sakoulas G, Johnson JK, Harris AD, et al. 2011. Increased mortality with accessory gene regulator (agr) dysfunction in *Staphylococcus aureus* among bacteremic patients. *Antimicrobial agents and chemotherapy* 55:1082-7
363. Harigaya Y, Ngo D, Lesse AJ, Huang V, Tsuji BT. 2011. Characterization of heterogeneous vancomycin-intermediate resistance, MIC and accessory gene regulator (agr) dysfunction among clinical bloodstream isolates of *Staphyloccocus aureus*. *BMC infectious diseases* 11:287

364. Painter KL, Krishna A, Wigneshweraraj S, Edwards AM. 2014. What role does the quorum-sensing accessory gene regulator system play during *Staphylococcus aureus* bacteremia? *Trends in microbiology* 22:676-85
365. Butterfield JM, Tsuji BT, Brown J, Ashley ED, Hardy D, et al. 2011. Predictors of *agr* dysfunction in methicillin-resistant *Staphylococcus aureus* (MRSA) isolates among patients with MRSA bloodstream infections. *Antimicrobial agents and chemotherapy* 55:5433-7
366. Pollitt EJ, West SA, Crusz SA, Burton-Chellew MN, Diggle SP. 2014. Cooperation, quorum sensing, and evolution of virulence in *Staphylococcus aureus*. *Infection and Immunity* 82:1045-51
367. Traber KE, Lee E, Benson S, Corrigan R, Cantera M, et al. 2008. agr function in clinical *Staphylococcus aureus* isolates. *Microbiology (Reading, England)* 154:2265-74
368. Diep BA, Hilliard JJ, Le VT, Tkaczyk C, Le HN, et al. 2017. Targeting alpha toxin to mitigate its lethal toxicity in ferret and rabbit models of *Staphylococcus aureus* necrotizing pneumonia. *Antimicrobial agents and chemotherapy* 61
369. Hilimire TA, Bennett RP, Stewart RA, Garcia-Miranda P, Blume A, et al. 2016. N-methylation as a strategy for enhancing the affinity and selectivity of RNA-binding peptides: application to the HIV-1 Frameshift-Stimulating RNA. *ACS chemical biology* 11:88-94
370. Vamathevan J, Clark D, Czodrowski P, Dunham I, Ferran E, et al. 2019. Applications of machine learning in drug discovery and development. *Nature reviews. Drug discovery* 18:463-77
371. Stokes JM, Yang K, Swanson K, Jin W, Cubillos-Ruiz A, et al. 2020. A Deep Learning Approach to Antibiotic Discovery. *Cell* 180:688-702.e13
372. Fleming N. 2018. How artificial intelligence is changing drug discovery. *Nature* 557:S55-s7
373. Smith S. 2020. 43 Pharma Companies Using Artificial Intelligence in Drug Discovery. In *BenchSci*
374. Merk D, Grisoni F, Friedrich L, Schneider G. 2018. Tuning artificial intelligence on the de novo design of natural-product-inspired retinoid X receptor modulators. *Communications Chemistry* 1:68
375. Reker D, Rodrigues T, Schneider P, Schneider G. 2014. Identifying the macromolecular targets of de novo-designed chemical entities through self-organizing map consensus. *Proceedings of the National Academy of Sciences* 111:4067-72
376. Liu M, Karuso P, Feng Y, Kellenberger E, Liu F, et al. 2019. Is it time for artificial intelligence to predict the function of natural products based on 2D-structure. *MedChemComm* 10:1667-77
377. Fox Ramos AE, Alcover C, Evanno L, Maciuk A, Litaudon M, et al. 2017. Revisiting Previously Investigated Plants: A Molecular Networking-Based Study of Geissospermum laeve. *Journal of Natural Products* 80:1007-14
378. Allen F, Pon A, Wilson M, Greiner R, Wishart D. 2014. CFM-ID: a web server for annotation, spectrum prediction and metabolite identification from tandem mass spectra. *Nucleic acids research* 42:W94-9
379. Gu J, Gui Y, Chen L, Yuan G, Lu HZ, Xu X. 2013. Use of natural products as chemical library for drug discovery and network pharmacology. *PLoS One* 8:e62839
380. Peresse T, Jezequel G, Allard PM, Pham VC, Huong DTM, et al. 2017. Cytotoxic Prenylated Stilbenes Isolated from Macaranga tanarius. *J Nat Prod* 80:2684-91
381. Naman CB, Rattan R, Nikoulina SE, Lee J, Miller BW, et al. 2017. Integrating Molecular Networking and Biological Assays To Target the Isolation of a Cytotoxic Cyclic Octapeptide, Samoamide A, from an American Samoan Marine Cyanobacterium. *Journal of Natural Products* 80:625-33

382. Olivon F, Allard PM, Koval A, Righi D, Genta-Jouve G, et al. 2017. Bioactive Natural Products Prioritization Using Massive Multi-informational Molecular Networks. *ACS chemical biology* 12:2644-51
383. Olivon F, Apel C, Retailleau P, Allard PM, Wolfender JL, et al. 2018. Searching for original natural products by molecular networking: detection, isolation and total synthesis of chloroaustralasines. *Organic Chemistry Frontiers* 5:2171-8
384. Wolfender J-L, Litaudon M, Touboul D, Queiroz EF. 2019. Innovative omics-based approaches for prioritisation and targeted isolation of natural products – new strategies for drug discovery. *Natural product reports* 36:855-68
385. Oberlies NH, Knowles SL, Amrine CSM, Kao D, Kertesz V, Raja HA. 2019. Droplet probe: coupling chromatography to the in situ evaluation of the chemistry of nature. *Natural product reports* 36:944-59
386. Wu C, Dill AL, Eberlin LS, Cooks RG, Ifa DR. 2013. Mass spectrometry imaging under ambient conditions. *Mass spectrometry reviews* 32:218-43
387. Huang MZ, Cheng SC, Cho YT, Shiea J. 2011. Ambient ionization mass spectrometry: a tutorial. *Analytica chimica acta* 702:1-15
388. Nemes P, Vertes A. 2007. Laser Ablation Electrospray Ionization for Atmospheric Pressure, in Vivo, and Imaging Mass Spectrometry. *Analytical Chemistry* 79:8098-106
389. Sica VP, El-Elimat T, Oberlies NH. 2016. In situ analysis of Asimina triloba (paw paw) plant tissues for acetogenins via the droplet-liquid microjunction-surface sampling probe coupled to UHPLC-PDA-HRMS/MS. *Analytical Methods* 8:6143-9
390. Kao D, Henkin JM, Soejarto DD, Kinghorn AD, Oberlies NH. 2018. Non-Destructive Chemical Analysis of a Garcinia mangostana L. (Mangosteen) Herbarium Voucher Specimen. *Phytochemistry letters* 28:124-9
391. Nagana Gowda GA, Raftery D. 2017. Recent Advances in NMR-Based Metabolomics. *Analytical Chemistry* 89:490-510
392. Egan JM, Santen Jv, Linington RG. 2020. *MADByTE NMR*. https://www.madbyte.org/
393. Smanski MJ, Zhou H, Claesen J, Shen B, Fischbach MA, Voigt CA. 2016. Synthetic biology to access and expand nature's chemical diversity. *Nature Reviews Microbiology* 14:135-49
394. Ren H, Shi C, Zhao H. 2020. Computational Tools for Discovering and Engineering Natural Product Biosynthetic Pathways. *iScience* 23:100795-
395. Medema MH, Blin K, Cimermancic P, de Jager V, Zakrzewski P, et al. 2011. antiSMASH: rapid identification, annotation and analysis of secondary metabolite biosynthesis gene clusters in bacterial and fungal genome sequences. *Nucleic acids research* 39:W339-W46
396. Kautsar SA, Suarez Duran HG, Blin K, Osbourn A, Medema MH. 2017. plantiSMASH: automated identification, annotation and expression analysis of plant biosynthetic gene clusters. *Nucleic acids research* 45:W55-W63
397. Rajniak J, Barco B, Clay NK, Sattely ES. 2015. A new cyanogenic metabolite in Arabidopsis required for inducible pathogen defence. *Nature* 525:376-9
398. Li Y, Calvo Sarah E, Gutman R, Liu Jun S, Mootha Vamsi K. 2014. Expansion of Biological Pathways Based on Evolutionary Inference. *Cell* 158:213-25
399. Kanehisa M, Goto S. 2000. KEGG: Kyoto Encyclopedia of Genes and Genomes. *Nucleic acids research* 28:27-30
400. Chen S, Xiang L, Guo X, Li Q. 2011. An introduction to the medicinal plant genome project. *Frontiers of Medicine* 5:178-84
401. Matasci N, Hung LH, Yan Z, Carpenter EJ, Wickett NJ, et al. 2014. Data access for the 1,000 Plants (1KP) project. *GigaScience* 3:17

402. Luo X, Reiter MA, d'Espaux L, Wong J, Denby CM, et al. 2019. Complete biosynthesis of cannabinoids and their unnatural analogues in yeast. *Nature* 567:123-6
403. Chappell J, DellaPenna D, O'Connor SE. *Medicinal Plant Genomics Resource*. http://medicinalplantgenomics.msu.edu/
404. Cravens A, Payne J, Smolke CD. 2019. Synthetic biology strategies for microbial biosynthesis of plant natural products. *Nature communications* 10:2142
405. Li Y, Li S, Thodey K, Trenchard I, Cravens A, Smolke CD. 2018. Complete biosynthesis of noscapine and halogenated alkaloids in yeast. *Proceedings of the National Academy of Sciences* 115:E3922-E31
406. Hawkins KM, Smolke CD. 2008. Production of benzylisoquinoline alkaloids in Saccharomyces cerevisiae. *Nature Chemical Biology* 4:564-73
407. Valliere MA, Korman TP, Woodall NB, Khitrov GA, Taylor RE, et al. 2019. A cell-free platform for the prenylation of natural products and application to cannabinoid production. *Nature communications* 10:565
408. Li Y, Smolke CD. 2016. Engineering biosynthesis of the anticancer alkaloid noscapine in yeast. *Nature communications* 7:12137
409. Beyraghdar Kashkooli A, van der Krol AR, Rabe P, Dickschat JS, Bouwmeester H. 2019. Substrate promiscuity of enzymes from the sesquiterpene biosynthetic pathways from Artemisia annua and Tanacetum parthenium allows for novel combinatorial sesquiterpene production. *Metabolic Engineering* 54:12-23
410. Sánchez C, Butovich IA, Braña AF, Rohr J, Méndez C, Salas JA. 2002. The Biosynthetic Gene Cluster for the Antitumor Rebeccamycin: Characterization and Generation of Indolocarbazole Derivatives. *Chemistry & Biology* 9:519-31
411. Fasan R, Chen MM, Crook NC, Arnold FH. 2007. Engineered alkane-hydroxylating cytochrome P450(BM3) exhibiting nativelike catalytic properties. *Angewandte Chemie (International ed. in English)* 46:8414-8
412. Payne JT, Poor CB, Lewis JC. 2015. Directed evolution of RebH for site-selective halogenation of large biologically active molecules. *Angewandte Chemie (International ed. in English)* 54:4226-30
413. Savile CK, Janey JM, Mundorff EC, Moore JC, Tam S, et al. 2010. Biocatalytic Asymmetric Synthesis of Chiral Amines from Ketones Applied to Sitagliptin Manufacture. *Science* 329:305-9
414. Skellam E. 2019. Strategies for Engineering Natural Product Biosynthesis in Fungi. *Trends Biotechnol* 37:416-27
415. Jeffryes JG, Seaver SMD, Faria JP, Henry CS. 2018. A pathway for every product? Tools to discover and design plant metabolism. *Plant science : an international journal of experimental plant biology* 273:61-70
416. Pyne ME, Narcross L, Martin VJJ. 2019. Engineering Plant Secondary Metabolism in Microbial Systems. *Plant physiology* 179:844-61
417. Lundy TA, Mori S, Thamban Chandrika N, Garneau-Tsodikova S. 2020. Characterization of a Unique Interrupted Adenylation Domain That Can Catalyze Three Reactions. *ACS chemical biology* 15:282-9
418. Harper C, Siller M. 2015. OpenAG: A Globally Distributed Network of Food Computing. *IEEE Pervasive Computing* 14:24-7
419. Johnson AJ, Meyerson E, de la Parra J, Savas TL, Miikkulainen R, Harper CB. 2019. Flavor-cyber-agriculture: Optimization of plant metabolites in an open-source control environment through surrogate modeling. *PLOS ONE* 14:e0213918

420. de la Parra J, Quave CL. 2017. Ethnophytotechnology: Harnessing the Power of Ethnobotany with Biotechnology. *Trends in Biotechnology* 35:802-6
421. Schulz B, Boyle C. 2006. What are Endophytes? In *Microbial Root Endophytes*, ed. BJE Schulz, CJC Boyle, TN Sieber:1-13. Berlin, Heidelberg: Springer Berlin Heidelberg. Number of 1-13 pp.
422. Bacon CW, White J. 2000. *Microbial endophytes*. CRC press
423. Bush LP, Wilkinson HH, Schardl CL. 1997. Bioprotective alkaloids of grass-fungal endophyte symbioses. *Plant physiology* 114:1
424. Nair DN, Padmavathy S. 2014. Impact of endophytic microorganisms on plants, environment and humans. *The Scientific World Journal* 2014
425. Strobel GA. 2003. Endophytes as sources of bioactive products. *Microbes and infection* 5:535-44
426. Suryanarayanan T, Thirunavukkarasu N, Govindarajulu M, Sasse F, Jansen R, Murali T. 2009. Fungal endophytes and bioprospecting. *Fungal biology reviews* 23:9-19
427. El-Elimat T, Raja HA, Graf TN, Faeth SH, Cech NB, Oberlies NH. 2014. Flavonolignans from Aspergillus iizukae, a fungal endophyte of milk thistle (Silybum marianum). *Journal of natural products* 77:193-9
428. Kusari S, Pandey SP, Spiteller M. 2013. Untapped mutualistic paradigms linking host plant and endophytic fungal production of similar bioactive secondary metabolites. *Phytochemistry* 91:81-7
429. Nisa H, Kamili AN, Nawchoo IA, Shafi S, Shameem N, Bandh SA. 2015. Fungal endophytes as prolific source of phytochemicals and other bioactive natural products: a review. *Microbial pathogenesis* 82:50-9
430. Pugh ND, Jackson CR, Pasco DS. 2013. Total bacterial load within Echinacea purpurea, determined using a new PCR-based quantification method, is correlated with LPS levels and in vitro macrophage activity. *Planta medica* 79:9-14
431. Todd DA, Gulledge TV, Britton ER, Oberhofer M, Leyte-Lugo M, et al. 2015. Ethanolic Echinacea purpurea extracts contain a mixture of cytokine-suppressive and cytokine-inducing compounds, including some that originate from endophytic bacteria. *PloS one* 10
432. Khare E, Mishra J, Arora NK. 2018. Multifaceted Interactions Between Endophytes and Plant: Developments and Prospects. *Frontiers in Microbiology* 9
433. Martinez-Klimova E, Rodríguez-Peña K, Sánchez S. 2017. Endophytes as sources of antibiotics. *Biochemical Pharmacology* 134:1-17
434. Ibrahim A, Tanney JB, Fei F, Seifert KA, Cutler GC, et al. 2020. Metabolomic-guided discovery of cyclic nonribosomal peptides from Xylaria ellisii sp. nov., a leaf and stem endophyte of Vaccinium angustifolium. *Scientific Reports* 10:4599
435. Yan J, Kline AD, Mo H, Shapiro MJ, Zartler ER. 2003. A Novel Method for the Determination of Stereochemistry in Six-Membered Chairlike Rings Using Residual Dipolar Couplings. *The Journal of Organic Chemistry* 68:1786-95
436. Kummerlöwe G, Luy B. 2009. CHAPTER 4 - Residual Dipolar Couplings for the Configurational and Conformational Analysis of Organic Molecules. In *Annual Reports on NMR Spectroscopy*, ed. GA Webb, 68:193-232: Academic Press. Number of 193-232 pp.
437. Gil RR. 2011. Constitutional, Configurational, and Conformational Analysis of Small Organic Molecules on the Basis of NMR Residual Dipolar Couplings. *Angewandte Chemie International Edition* 50:7222-4
438. Hallwass F, Schmidt M, Sun H, Mazur A, Kummerlöwe G, et al. 2011. Residual Chemical Shift Anisotropy (RCSA): A Tool for the Analysis of the Configuration of Small Molecules. *Angewandte Chemie International Edition* 50:9487-90

439. Kummerlöwe G, Grage SL, Thiele CM, Kuprov I, Ulrich AS, Luy B. 2011. Variable angle NMR spectroscopy and its application to the measurement of residual chemical shift anisotropy. *Journal of Magnetic Resonance* 209:19-30
440. Nath N, Schmidt M, Gil RR, Williamson RT, Martin GE, et al. 2016. Determination of Relative Configuration from Residual Chemical Shift Anisotropy. *Journal of the American Chemical Society* 138:9548-56
441. Liu Y, Sauri J, Mevers E, Peczuh MW, Hiemstra H, et al. 2017. Unequivocal determination of complex molecular structures using anisotropic NMR measurements. *Science* 356
442. Liu Y, Navarro-Vazquez A, Gil RR, Griesinger C, Martin GE, Williamson RT. 2019. Application of anisotropic NMR parameters to the confirmation of molecular structure. *Nature protocols* 14:217-47
443. Elyashberg M, Williams A, Blinov K. 2011. *Contemporary Computer-Assisted Approaches to Molecular Structure Elucidation*.
444. Elyashberg M, Williams AJ, Blinov K. 2010. Structural revisions of natural products by Computer-Assisted Structure Elucidation (CASE) systems. *Natural product reports* 27:1296-328
445. Burns DC, Mazzola EP, Reynolds WF. 2019. The role of computer-assisted structure elucidation (CASE) programs in the structure elucidation of complex natural products. *Natural product reports* 36:919-33
446. 2019. *Mnova StereoFitter*. https://mestrelab.com/software/mnova/mnova-stereofitter/
447. Linington RG, Kubanek J, Luesch H. 2019. New methods for isolation and structure determination of natural products. *Natural product reports* 36:942-3
448. Bisson J, Simmler C, Chen S-N, Friesen JB, Lankin DC, et al. 2016. Dissemination of original NMR data enhances reproducibility and integrity in chemical research. *Natural product reports* 33:1028-33
449. McAlpine JB, Chen SN, Kutateladze A, MacMillan JB, Appendino G, et al. 2019. The value of universally available raw NMR data for transparency, reproducibility, and integrity in natural product research. *Natural product reports* 36:35-107
450. Nannenga BL, Gonen T. 2016. MicroED opens a new era for biological structure determination. *Current opinion in structural biology* 40:128-35
451. Jones CG, Martynowycz MW, Hattne J, Fulton TJ, Stoltz BM, et al. 2018. The CryoEM Method MicroED as a Powerful Tool for Small Molecule Structure Determination. *ACS Central Science* 4:1587-92
452. Gruene T, Wennmacher JTC, Zaubitzer C, Holstein JJ, Heidler J, et al. 2018. Rapid Structure Determination of Microcrystalline Molecular Compounds Using Electron Diffraction. *Angewandte Chemie International Edition* 57:16313-7